

**THE ROLE OF BRAP-2 IN CAENORHABDITIS ELEGANS DNA
DAMAGE INDUCED GERMLINE APOPTOSIS,
DEVELOPMENT AND GERMLINE HEALTH**

DAYANA RITA D'AMORA

A DISSERTATION SUBMITTED TO
THE FACULTY OF GRADUATE STUDIES
IN PARTIAL FULFILLMENT OF THE REQUIREMENTS
FOR THE DEGREE OF
DOCTOR OF PHILOSOPHY

GRADUATE PROGRAM IN BIOLOGY
YORK UNIVERSITY
TORONTO, ONTARIO

© Dayana Rita D'Amora, August 2017

Abstract

The DNA damage response protects the genome by executing processes that prevent the disruption of normal cell physiology and the inheritance of mutations. BRCA1 is an essential tumor suppressor gene that facilitates DNA repair, transcription and plays a more complex role in apoptosis. A novel BRCA1 binding protein known as BRAP2/IMP has been characterized as a RAS effector with ubiquitin ligase activity and as a cytoplasmic retention protein. BRAP2 is conserved in *C. elegans*, and is known as BRAP-2. Previously, we have shown that BRAP-2 is a negative regulator of SKN-1/Nrf2 dependent detoxification gene expression. In addition, *brap-2* deletion mutants experience BRC-1 (BRCA1 ortholog) dependent larval arrest when exposed to oxidative stress. BRC-1 function in DNA repair is conserved in the germline, where a loss of *brc-1* increases apoptosis. Due to the conservation of BRC-1 function in *C. elegans* and the genetic link between BRC-1 and BRAP-2 upon oxidative stress, in this study we examined the role of BRAP-2 in DNA damage induced germline apoptosis, *C. elegans* development and germline health. We found that *brap-2* mutants display a reduction in DNA damage induced germline apoptosis and that apoptosis induced by loss of BRC-1 requires BRAP-2. We also found that a loss of PMK-1, SKN-1 and AKT-1 in *brap-2* mutants increases apoptosis, indicating that a loss of BRAP-2 limits DNA damage induced germline apoptosis and promotes cell survival through regulation of the PMK-1 activated SKN-1 oxidative stress response pathway and Insulin/Insulin-like growth factor signaling. In addition, *brap-2* mutants display defects in development, survival, brood size and germline morphology. Taken together, this suggests that BRAP-2 is required to promote DNA damage induced germline apoptosis by regulating pro-cell survival pathways and that BRAP-2 is required for proper *C. elegans* growth, development and germline health.

Co-Authorship

Chapter 2 & 3: Queenie Hu assisted with the preparation and provision of RNA samples, performed qRT-PCRs, and generated double mutant strains using standard protocols. Monica Pizzardi generated double mutants, and assisted in conducting the Dauer Defective Assay.

Dedication

I dedicate this work to my mother, **Concetta Russo**. Mami, thank you always being there for me and for everything you have done for me. Thank you for your friendship and for all of your love and kindness. Without your constant advice and support, this would not have been possible.

Acknowledgements

First and foremost, I would like to thank my friend, mentor and colleague **Dr. Queenie Hu**. You trained me in so many techniques and helped me solve any and every problem that came my way in the lab and in life. Thank you for taking the time to teach me and for being patient. I am confident in my skills as a researcher because of the foundation that you provided me with. Queenie Hu, thank you.

Jelena Brkic, thank you for your unwavering support and for being one of my greatest friends. You are truly one of a kind and helped me through so many obstacles. Thank you for always making time for me and being someone I can always count on.

Jyotsna Vinayak, I would like to thank you for being my friend, for your support and advice not just in research, but in life. Your smile and optimism is contagious. Thank you reminding me of all the good things around me, pushing me to be better, for always checking on me and being a shoulder to lean on.

Mohamed Salem, words cannot describe how thankful I am to have you as a friend. You have always been there to help me, to teach me new techniques, talk to me about literally anything, and help me find solutions to problems that I thought I could not solve.

Stefanie Bernaudo, thank you for all of your guidance and support as a colleague and friend. When I needed help, you were always there to listen to me and advise me. You are a constant source of motivation and an amazing role model.

Monica Pizzardi, you brought light and laughter to the lab, as well as dedication and care to your work. Thank you for all of your hard work, enthusiasm for learning but most of all for your amazing friendship.

Consuelo Perez, thank you for being my best friend, for always listening to me no matter what, for always believing in me, helping me through any problem, cheering me up and motivating me to be better.

Heyam Hayder, thank you for your constant kindness, warmth and advice. I could not have gone through this experience without your friendship.

Shaolong Zhu, I would like to thank you for your friendship and for always believing in me and for your constant encouragement.

Shahin Khazai, thank you for being a great friend and for always taking the time to listen to me, encourage me and for all of your advice.

Thank you to my wonderful friends for making time for me and for all of your support, advice, training and constant assistance inside the lab and out: **Gang Ye, Yara Zayed, Jake O'Brien, Uzma Nadeem, Ana Vakiloroyaei, Stefano Marrella, Marlee Ng, Adilya Rafikova, Muntasir Kamal, Ayat Yaseen, Irina Oganessian, Cristina Lento, Dr. Carol Bucking and Kristina Wantola.**

I would like to thank my brother **Jose D'Amora**. Jose, you are so generous and patient. You have always been there for me and never hesitated to help me when I asked, and even when I did not. Thank you for being the best brother in the world, for always making me laugh, giving me confidence and taking care of me. **Jillian Owens**, thank you for your constant support, for cheering me on and helping me get through so many difficult times. You are so wonderful and kind, thank you for always being there, for inspiring me and making me smile. Thank you to my father **Giuseppe D'Amora** for all of your love and understanding even in my most difficult days, for always driving me whenever and wherever I needed to go and for being there for me always.

Marianna y Raimundo Russo, gracias por siempre creer en mi y por todos tus consejos. Tuviste razon, yo tuve paciencia y logre me sueno.

I would like to thank Dr. Brent Derry and the entire Derry Lab from the University of Toronto for their help for the use of the Cs-137 source for the irradiation trials. I would personally like to thank members from the lab Madhavi Gunda, Mehran Haeri, Ben Lant, Abigail Mateo, Anh Tran and Mathew Hall. I would especially like to thank Bin Yu and Eric Chapman. I am truly grateful to you all for your kindness and friendship.

Dr. Nicola Silva and Dr. Anton Gartner, thank you for the time you spent speaking with me at *C. elegans* 2015 conference. Your advice and experimental suggestions helped me to broaden my understanding of this field and further my project.

I would like to thank my graduate advisory committee **Dr. Samuel Benchimol** and **Dr. Peter Cheung**. You always helped me to see the big picture and I am extremely grateful for the time you have taken to advise me on experiments, approaches and broadening my perspective on my research and the ways in which I analyze and interpret data. Your consistent encouragement and faith in my abilities fueled my passion for this project and for scientific research.

Lastly, I would like to thank **Dr. Terrance J. Kubiseski** for giving me the opportunity to work in this wonderful lab and “be my own boss”. Your support, guidance and encouragement made my experience and training extremely enjoyable. I could not have asked for a better environment and supervisor to complete my Ph.D. You allowed me to develop this investigation from the ground up and explore various techniques, all while keeping me on track.

Table of Contents

Abstract.....	ii
Co-authorship.....	iii
Dedication.....	iv
Acknowledgements.....	v
Table of Contents.....	vii
List of Tables.....	ix
List of Figures.....	x
List of <i>C. elegans</i> genes, their function and mammalian homologs.....	xii
List of Abbreviations.....	xv
Chapter 1: Introduction and Literature Review.....	1
1.1 General Introduction.....	1
1.2 Use of <i>Caenorhabditis elegans</i> as a model organism.....	4
1.2.1 Introduction to <i>C. elegans</i> as a model.....	4
1.2.2 Anatomy of the <i>C. elegans</i> germline.....	5
1.2.3 Brief overview of the <i>C. elegans</i> germline as a model for the DNA Damage Response.....	7
1.3 The intrinsic “mitochondrial dependent” pathway of apoptosis.....	10
1.3.1 Activation of the intrinsic pathway of apoptosis in mammalian systems.....	10
1.3.2 Intrinsic apoptosis is conserved in <i>C. elegans</i>	12
1.4 BRCA1 is a dynamic tumor suppressor of the DNA Damage Response.....	16
1.4.1 BRCA1 structure and function in mammalian systems.....	16
1.4.2 BRCA1 is conserved in <i>C. elegans</i> and is known as BRC-1.....	18
1.5 BRAP2 is a BRCA1 binding protein and potential scaffold for the regulation of cell signaling.....	20
1.5.1 BRAP2 is conserved in <i>C. elegans</i> and is known as BRAP-2.....	22
1.6 Conserved <i>C. elegans</i> cell signaling pathways relevant to this study.....	26
1.6.1 The RAS/MEK/ERK signaling pathway.....	26
1.6.2 The RAS/ERK signaling pathway is conserved in <i>C. elegans</i>	27
1.6.3 The stress activated p38 MAPK pathway is involved in the activation of apoptosis.....	28
1.6.4 The p38 MAPK pathway is conserved in <i>C. elegans</i>	29
1.6.5 The PI3K/AKT signaling pathway.....	32
1.6.6 The Insulin/Insulin-like growth factor signaling pathway in <i>C. elegans</i>	33
1.6.7 The SKN-1/Nrf2 oxidative stress response pathway.....	37
1.7 Rationale, hypotheses and objectives of this study.....	41
Chapter 2: BRAP-2 promotes DNA damage induced germline apoptosis through the regulation of SKN-1 and AKT-1 in <i>C. elegans</i>	43
2.1 Summary.....	45
2.2 Introduction.....	46
2.3 Materials & Methods.....	48
2.4 Results.....	56
2.5 Discussion.....	92

2.6 Supplementary Figures	97
2.7 Acknowledgements.....	102
Chapter 3: BRAP-2 is required for <i>C. elegans</i> development and germline health....	103
3.1 Summary.....	105
3.2 Introduction.....	106
3.3 Materials & Methods.....	108
3.4 Results.....	114
3.5 Discussion.....	137
3.6 Supplementary Figures.....	141
3.7 Acknowledgements.....	145
Chapter 4: General Discussion and Future Directions	146
4.1 Summary.....	146
4.2 Identification of BRAP-2 as a DNA damage response gene and regulator of the SKN-1/PMK-1 and IIS pathways reinforces the “intestine to germline” interaction during stress.....	146
4.3 Identification of BRAP-2 as a regulator of stress response pathways revealed its importance in <i>C. elegans</i> development, survival and germline health.....	149
4.4 Potential future studies for BRAP-2 in <i>C. elegans</i>	150
4.5 Future studies of BRAP2 should focus on the biological significance of its predicted interactions and potential conserved role in the DNA damage response.....	152
4.6 Conclusion.....	153
References.....	155
I. Chapter 1.....	155
II. Chapter 2.....	172
III. Chapter 3.....	177
IV. Chapter 4.....	181
Appendix	184
Additional publications.....	184
Worm strains and primers used in this study.....	186

List of Tables

Chapter 2

Table 2.1: *brap-2* mutants are dauer defective..... 84

Table 2.2: *brap-2* mutants have increased cytoplasmic DAF-16 localization..... 86

Chapter 3

Table S3.1: Number of sensory rays in *him-5* and *brap-2;him-5* mutants..... 143

Appendix

Table 1: Worm strains used in this study..... 186

Table 2: Forward and reverse primers for SW-PCR..... 188

Table 3: Forward and reverse primers for qRT-PCR..... 189

Table 4: Forward and reverse primers for cloning PHLP-2 into pCMV7.1 3xFLAG..... 190

Table 5: CRISPR-Cas9 primers used to generate BRAP-2::GFP strain..... 191

Table 6: Forward and reverse worm strain sequencing primers..... 192

Table 7: Antibodies and reagents for Western blot and immunostaining..... 193

List of Figures

Chapter 1

Figure 1.1: The cellular response to DNA damage.....	3
Figure 1.2: The <i>C. elegans</i> life cycle and adult germline anatomy.....	9
Figure 1.3: Pathway depicting DNA damage induced germline apoptosis in <i>C. elegans</i> and its conservation to mammalian intrinsic apoptosis.....	15
Figure 1.4: BRCA1 is functionally conserved in <i>C. elegans</i>	19
Figure 1.5: Protein domain structures of mammalian BRAP2 and <i>C. elegans</i> BRAP-2.....	24
Figure 1.6: The predicted role of BRAP2/IMP in RAS signaling.....	25
Figure 1.7: The RAS pathway can activate cell death and promote cell survival.....	31
Figure 1.8: The <i>C. elegans</i> DAF-2/IIS pathway and its high conservation to the mammalian IGF/Insulin signaling pathway.....	36
Figure 1.9: Regulation of SKN-1 by MPK-1/ERK, PMK-1/p38 MAPK and DAF-2/IIS pathways.....	40

Chapter 2

Figure 2.1: BRAP-2 promotes DNA damage induced germline apoptosis.....	59
Figure 2.2: One wild type <i>brap-2</i> allele restored apoptosis following DNA damage.....	60
Figure 2.3: BRAP-2 does not alter the rate of corpse appearance.....	61
Figure 2.4: BRAP-2 does not affect germ cell proliferation and is specific to germline apoptosis.....	63
Figure 2.5: <i>brap-2(ok1492)</i> induces robust mitotic arrest following DNA damage.....	64
Figure 2.6: <i>brap-2(ok1492)</i> increased apoptosis gene expression.....	68
Figure 2.7: Expression of <i>egl-1</i> and <i>ced-13</i> in <i>brap-2</i> mutants is dependent on CEP-1.....	70
Figure 2.8: Loss of <i>brap-2</i> did not reduce apoptosis in <i>ced-9</i> mutants.....	71
Figure 2.9: <i>skn-1</i> RNAi knockdown increases apoptosis in <i>brap-2;brc-1</i> double mutants following DNA damage.....	75
Figure 2.10: Loss of <i>pmk-1</i> increased germline apoptosis in <i>brap-2</i> mutants.....	79
Figure 2.11: Interaction between PHLPP1 and BRAP2 in <i>C. elegans</i> is conserved.....	81
Figure 2.12: <i>brap-2</i> mutants have increased <i>ins-7</i> and reduced <i>ctl-1</i> mRNA levels.....	85
Figure 2.13: Loss of <i>akt-1</i> increases apoptosis in <i>brap-2</i> mutants.....	89

Figure 2.14: AKT-1 is elevated in <i>brap-2(ok1492)</i> mutants.....	90
Figure 2.15: Loss of <i>phlp-2</i> reduced germline apoptosis in <i>akt-1</i> mutants.....	91
Figure 2.16: Proposed model for BRAP-2 regulation of DNA damage induced germline apoptosis.....	96
Figure S2.1: BRAP-2 is expressed in the germline cytoplasm following DNA damage.....	97
Figure S2.2: Genomic structure of <i>brap-2</i> and deletion mutant <i>ok1492</i>	98
Figure S2.3: <i>brap-2</i> mutants display reduced levels of germline apoptosis following DNA damage.....	99
Figure S2.4: A loss of <i>brc-1</i> extends <i>brap-2(ok1492)</i> mean survival.....	100
Figure S2.5: Loss of <i>mpk-1</i> did not increase apoptosis in <i>brap-2</i> mutants.....	101

Chapter 3

Figure 3.1: BRAP-2 localizes to the cytoplasm of mammalian 293T HEK cells.....	115
Figure 3.2: BRAP-2 is expressed in the cytoplasm of the germline.....	116
Figure 3.3: BRAP-2 expression is localized to the germline <i>in vivo</i>	117
Figure 3.4: <i>brap-2(ok1492)</i> worms possess reduced body length and width.....	120
Figure 3.5: <i>brap-2(ok1492)</i> causes a developmental delay and reduced survival.....	121
Figure 3.6: Brood size is reduced in <i>brap-2(ok1492)</i> mutants.....	125
Figure 3.7: <i>brap-2</i> mutants exhibit reduced gonad length and a shortened mitotic zone.....	126
Figure 3.8: <i>brap-2(ok1492)</i> reduces the number of nuclei to the transition zone.....	127
Figure 3.9: <i>brap-2(ok1492)</i> mutants display increased mRNA levels of <i>cki-1/2</i> and <i>cyb-1</i>	128
Figure 3.10: <i>brap-2(ok1492)</i> mutants are hypersensitive to IR during larval development....	131
Figure 3.11: <i>brap-2(ok1492)</i> mutants display abnormal chromosome phenotypes.....	132
Figure 3.12: <i>brap-2(ok1492)</i> decreases sperm quality.....	136
Figure S3.1: Brood size per day in <i>brap-2</i> mutant adults is reduced.....	141
Figure S3.2: Gonad length is reduced in <i>brap-2</i> mutants.....	142
Figure S3.3: Morphology of male sensory rays is altered in <i>brap-2</i> mutants.....	144

List of *C. elegans* genes, their function and mammalian homologs. Descriptions for genes of interest were adapted from Wormbase and references for each are cited in this study.

Mammalian	<i>C. elegans</i>	Function in <i>C. elegans</i>
Actin	<i>act-1</i>	Animal motility, body wall and pharyngeal muscle
AKT1	<i>akt-1</i>	Ser/thr kinase part of the IIS pathway that regulates dauer and chemotaxis
AKT2	<i>akt-2</i>	Ser/thr kinase part of the IIS pathway that regulates dauer and lifespan
APAF1	<i>ced-4</i>	Activation of apoptosis through binding to CED-9
BARD1	<i>brd-1</i>	Binds to and forms a heterodimer with BRC-1 to form an E3 ubiquitin ligase.
BCL2	<i>ced-9</i>	Prevents apoptosis through binding and suppression of CED-4
BH3	<i>egl-1</i>	Activator of apoptosis through direct interaction and inhibition of CED-9
BH3	<i>ced-13</i>	Promotes apoptosis through CED-9 inhibition
BRCA1	<i>brc-1</i>	Binds to and forms a heterodimer with BRD-1 to form an E3 ubiquitin ligase. Facilitates DNA double strand break repair through inter-sister recombination
BRAP2	<i>brap-2</i>	BRAP2/IMP ortholog linked to oxidative stress response
Caspase 3	<i>ced-3</i>	Executes programmed cell death through its protease activity
p21/p27	<i>cki-1/2</i>	Cyclin dependent kinase inhibitors involved in arresting cell division
CAT1	<i>ctl-1</i>	Antioxidant enzyme that protects against ROS. Activity contributes to lifespan extension. Negatively regulated by IIS pathway.

FOXO	<i>daf-16</i>	Transcription factor that is negatively regulated by IIS. Regulates dauer, longevity, stress responses and metabolism.
GST4	<i>gst-4</i>	Encodes a glutathione-requiring prostaglandin D synthase. Needed for response to oxidative stress.
-	<i>him-5</i>	Involved in X chromosome segregation
IGF	<i>daf-2</i>	Receptor tyrosine kinase. Involved in development, dauer, longevity, reproduction and fat storage.
ILP	<i>ins-7</i>	Insulin-like peptide, agonist of IIS
Nrf2	<i>skn-1</i>	Transcription factor involved in cell fate specification and initiates oxidative stress response.
ERK	<i>mpk-1</i>	MAP kinase involved in several cellular processes including cell migration, immunity, vulva development and germline progression for oogenesis.
p38	<i>pmk-1</i>	MAP Kinase involved in the innate immune response and activation of apoptosis in response to bacterial infection.
p53	<i>cep-1</i>	Transcription factor involved in activation of apoptosis and meiotic chromosome segregation.
PHLPP1/2	<i>phlp-2</i>	Ortholog of PHLPP1/2 with catalytic activity.
RAD51	<i>rad-51</i>	Required for meiotic recombination, chromosome morphology and resistance to radiation

RAS

let-60

Required for many processes including vulva development and germline meiotic progression

List of Abbreviations

ACT	Actin
AGE	Ageing alternation
AKAP	A-kinase anchor protein
AKT	Protein kinase B
APAF	Apoptotic peptidase activating factor
APOA	Apolipoprotein A
AO	Acridine orange
ARE	Antioxidant response element
ATM	Ataxia telangiectasia mutated
ATP	Adenosine triphosphate
ATR	Ataxia telangiectasia and Rad3 related
ATL	ATM (ataxia telangiectasia mutated)-Like
BARD	BRCA1 associated RING domain
BRAP2	BRCA1 associated binding protein 2
BRC	BRCA1 ortholog
BRCA	Breast cancer
BRCT	BRCA1 C-terminus
BRD	BARD1 homolog
BCL	B-cell CLL/lymphoma
BH	BCL2 homology
CDC	Cell division cycle
CDK	Cyclin dependent kinase
cDNA	Complementary DNA
<i>C. elegans</i>	<i>Caenorhabditis elegans</i>
CED	Cell death defective
CEP	<i>C. elegans</i> p53 like protein
CHK	Checkpoint kinase
CKI	Cyclin dependent kinase inhibitor
CLK	CDC like kinase
CO	Crossover
CUL	Cullin
CYB	Cyclin B
DAF	Abnormal dauer formation
DAPI	4', 6-diamidino-2-phenylindole
DDR	DNA damage response
DIC	Differential interference confocal

DNA	Deoxyribonucleic acid
DSB	Double strand break
DTC	Distal tip cell
E2	Ubiquitin conjugating enzyme
E3	Ubiquitin ligase
ECL	Enhanced chemiluminescence
<i>E. coli</i>	<i>Escherichia coli</i>
EGL	Egg laying
ERK	Extracellular signal-regulated kinases
EXO	EXOnuclease
FOXO	Forkhead box
G2	Gap 2
GAP	GTPase-activating protein
GCS	Glutamyl cysteine synthetase
GDP	Guanine diphosphate
GEF	Guanine nucleotide exchange factor
GEN	GEN endonuclease
GFP	Green fluorescent protein
GRB2	Growth factor receptor-bound protein 2
GSK	Glycogen synthase kinase
GST	Glutathione-S-Transferase
GTP	Guanine triphosphate
H2AX	Histone type 2A phosphorylated
HEK	Human embryonic kidney
HIM	High incidence of males
HPR	Homolog of <i>S. pombe</i> Rad
HMG20A	High mobility group 20A
HR	Homologous recombination
HUS	<i>S. pombe</i> checkpoint homolog
HUGO	Human genome organization
JNK	c-Jun N-terminal kinase
IGF	Insulin growth factor
ILP	Insulin-like peptide
IIS	Insulin/Insulin-like growth factor signaling
INS	Insulin related
IMP	Impedes mitogenic signal propagation
IR	Ionizing radiation
KEAP1	Kelch-like ECH-associated protein 1

KSR	Kinase suppressor of activated RAS
LCR	Low complexity region
LET	Lethal
LIN	Abnormal cell LINEage
LIP	Lateral-signal-induced phosphatase
MAPK/MPK	Mitogen-activated protein kinase
MAPKK	Mitogen-activated protein kinase kinase
MAPKKK	Mitogen-activated protein kinase kinase kinase
MDM	Mouse double minute
MEF	Mouse embryonic fibroblast
MEK	ERK kinase
modENCODE	Model organism encyclopedia of DNA elements
mRNA	messenger RNA
MRE	Meiotic recombination
MRN	MRE11/RAD51/NSB1
MRT	Mortal germline
MSH	mutS homolog
MZ	Mitotic zone
NES	Nuclear Export Signal
NF-κB	Nuclear factor kappa-light-chain-enhancer of activated B cells
NGM	Nematode growth media
NLS	Nuclear localization signal
NBS	Nijmegen breakage syndrome
NCO	Non-crossover
NSY	Neuronal symmetry
NRF2	Nuclear factor (erythroid-derived 2)-like 2
NUMA1	Nuclear mitotic apparatus protein 1
p38	Protein 38 MAPK
PAX	Paired box
PBS	Phosphate buffered saline
PCR	Polymerase chain reaction
PDK	Phosphoinositide dependent kinase
PHLPP	PH domain and leucine rich repeat protein phosphatase
PHLP	PH domain and leucine rich repeat protein phosphatase homolog
PI3K	Phosphatidylinositol 3-kinase
PMK	P38 MAP kinase family
PTEN	Phosphatidylinositol 3,4,5-trisphosphate 3-phosphatase and dual-specificity protein phosphatase

qRT-PCR	Quantitative real time polymerase chain reaction
RAF	Rapidly accelerated fibro sarcoma
RAD	Radiation
RAS	Rat sarcoma oncogene
RING	Really interesting new gene
RNA	Ribonucleic acid
RNAi	RNA interference
ROS	Reactive oxygen species
SAPK	Stress activated protein kinase
SDS	Sodium dodecyl sulfate
SEK	SAPK/ERK kinase
Ser/thr	Serine/Threonine
SGK	Serum- and glucocorticoid- inducible kinase homolog
sgRNA	Single-guide RNA
SIRT	Sirtuin
SKN	Skinhead
SLX	Synthetic lethal X
SOD	Superoxide dismutase
SPO	Meiotic protein covalently bound to DSB <i>S. cerevisiae</i> homolog
ssDNA	Single stranded DNA
SV	Simian virus
SW-PCR	Single Worm PCR
SYNE	Spectrin repeat containing nuclear envelope protein 2
TZ	Transition zone
WDR	WD repeat-containing protein
WT	Wild type
UBC	Ubiquitin conjugating enzyme
USP	Ubiquitin specific protease
UV	Ultraviolet
Y2H	Yeast 2 Hybrid
YF	Kubiseski Lab Strains

Chapter 1

Introduction and Literature Review

1.1 General Introduction

Programmed cell death (apoptosis), DNA repair and cell cycle arrest are vital pathways that protect the genome from the threat of DNA damage and mutations that lead to cellular dysfunction and disease (1). The DNA damage response (DDR) activates a network of tumour suppressors, enzymes and effector proteins to initiate intricate pathways that faithfully repair DNA and protect the cell (Figure 1.1) (2). Sensors, such as the DNA repair proteins RAD51 and BRCA1 (Breast cancer susceptibility gene 1) relay signals to downstream transducers (i.e. ATM, ATR kinases) and effectors (i.e. p53, CHK1) to coordinate events that determine the fate of a cell (2,3).

These surveillance mechanisms constantly monitor cellular health so that proper survival or death pathways are initiated to maintain physiological homeostasis when faced with exogenous (i.e. UV, chemicals, toxins) and endogenous forms (i.e. metabolism by-products, replication errors) of stress (1,3). However, when the balance of cell death factors outweighs those that signal for survival, apoptosis is triggered to eliminate malignancies (4). Without these protective measures, inherited or acquired mutations can wreak havoc, disrupting protein function and molecular signaling which can lead to apoptosis evasion, uncontrolled growth and cancer.

The genetic pathway for apoptosis activation was first discovered in *Caenorhabditis elegans*, and has since has been studied in models across phyla, including *Drosophila*, Zebrafish, *Xenopus*, mouse and human cell lines (1,5,6). In *C. elegans*, observation of apoptosis in both loss of function and gain of function mutants lead researchers to determine the conserved genetic order for apoptosis activated by CEP-1 (*C. elegans* p53-like protein 1) (7,8). *C. elegans*

possesses a high conservation of human disease genes, including those involved in DDR pathways (9,10). The *C. elegans* germline employs conserved mechanisms of cell cycle arrest, DNA repair and apoptosis in spatially distinct regions (11). Its simplicity, short life cycle and the ability to directly observe developmental and morphological defects caused by mutations, make it an ideal model to study gene function and cell signaling pathways (12). These studies provide us with a basis for investigation that can be translated to higher conserved model organisms.

BRCA1 facilitates DNA repair and is involved in transcription, cell cycle arrest and apoptosis (13). When BRC-1 (BRCA1 ortholog) function is lost in *C. elegans*, apoptosis increases in the germline (14). In mammalian systems, BRAP2/IMP (BRCA1-associated binding protein 2, or BRAP in the HUGO database) was found to bind to the nuclear localization signal (NLS) of BRCA1 and has since been characterized as a RAS effector and cytoplasmic retention protein (15,16). BRAP2/IMP is predicted to prevent BRCA1 from traveling to the nucleus, yet the biological significance of this interaction has not been explored extensively (15). Previous work from our lab revealed a genetic interaction between BRC-1 and BRAP-2 (BRAP2 ortholog) (17). *brap-2* mutant animals were found to be hypersensitive to oxidative stress and developmentally arrested at the first larval stage (L1), which was dependent on BRC-1 (17). Due to the identification of this genetic interaction during oxidative stress and conserved BRC-1 function, the objective of this project is to determine the role of BRAP-2 in DNA damage induced germline apoptosis, as well as determine its potential role in *C. elegans* development and germline health.

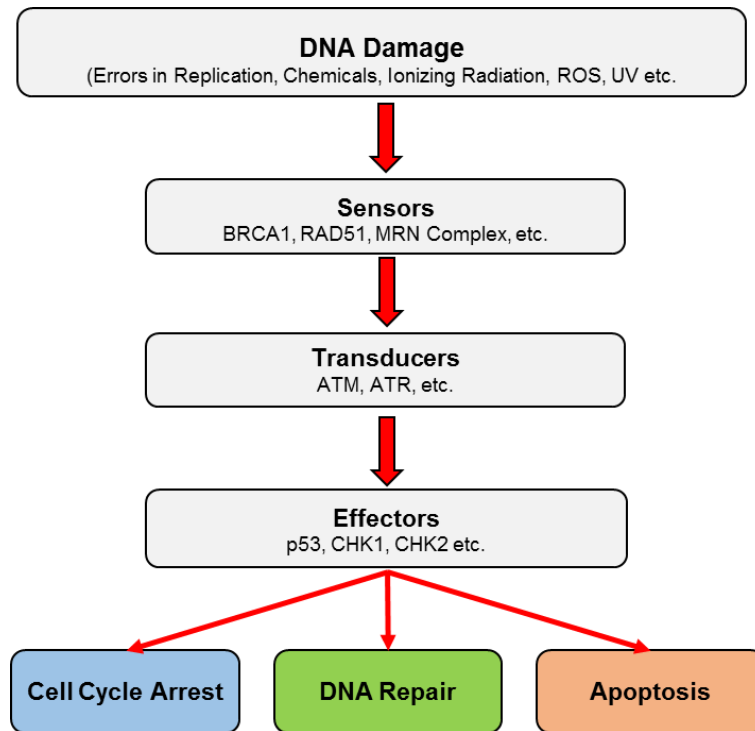


Figure 1.1: The cellular response to DNA damage

Although depicted as a linear pathway, the response to DNA damage is comprised of a network of interacting proteins that sense, transduce and relay signals, in order to execute an appropriate response that is dictated by the type and severity of damage sustained. This leads either to survival through cell cycle arrest and DNA repair for the resumption of normal cellular function, or activation of programmed cell death, all of which serves to preserve genomic stability. Image adapted and modified from (3).

1.2 Use of *Caenorhabditis elegans* as a model organism

1.2.1 Introduction to *C. elegans* as a model

C. elegans is a simple, non-parasitic invertebrate nematode (worm) advantageous for molecular genetics research and studies in development, aging, neurological disorders, innate immunity and stress response signaling (12,18,19). In 1998, it was the first multicellular organism to have its genome completed sequenced, revealing that 40% of human disease genes have a *C. elegans* ortholog (10). This also contributes to great functional similarity both in cellular metabolism and disease-related signal transduction cascades, allowing for the genetic order of complex pathways and novel genetic interactions to be identified.

As a hermaphroditic species, *C. elegans* can self-fertilize producing up to 300 offspring per worm, grow up to 1 mm in size and live up to 2 weeks (12). Although in low frequency, males can appear spontaneously in the wild type population (0.1-0.2%), due to X chromosome non-disjunction (20,21). The *C. elegans* life cycle is rapid and progresses from a hatched egg, through four larval stages (L1-L4) to reach adulthood in 3 days (Figure 1.2A) (12). When worms encounter dire stress that threatens their survival, a phase of developmental arrest (dauer) can be initiated (Figure 1.2A) (22,23). Worms lie dormant to survive harsh conditions such as an increase in temperature, overcrowding, or starvation and once the environment ameliorates, they can re-enter the life cycle and continue to develop normally (23). Extensive work has determined that inhibition of DAF-16 (the only FOXO ortholog in *C. elegans*) by the Insulin/Insulin like growth factor signaling pathway (IIS) prevents worm entry into dauer, while the sensing of pheromones and harsh environmental conditions activate DAF-16 and other parallel pathways for the transcription of dauer genes that prepare the worm for arrest and prolonged survival (22–26).

Forward and reverse genetic approaches including: inducing mutations using ionizing radiation (IR) or ethyl-methanesulfonate (EMS), or the gene knockdown technique of RNA interference (RNAi) respectively, can be employed to study gene function (27). Traditional crossing techniques allow for the generation of double mutants to study genetic interactions, while transgenic worms can be created to overexpress genes and produce strains with transcriptional or translational reporters (12). Genes of interest in *C. elegans* can now be more easily modified to create specific targeted genetic deletions, insertions or reporter tag fusions through CRISPR-Cas9 genome editing (28), which is highly advantageous as changes to gene and protein expression can be studied *in vivo*. However, limitations do exist for this model such as: it does not possess all the genes, molecular pathways or organ systems (respiratory and circulatory) present in mammals; it does not manifest all human disease pathologies; and *C. elegans* cell lines are difficult to maintain (29).

1.2.2 Anatomy of the *C. elegans* germline

In *C. elegans*, sex is determined by a XX/XO system where the hermaphrodite (viewed as female) has two X chromosomes and males have one X chromosome (30). For sexually reproducing organisms, meiosis I and II ensures the diploid state after fertilization is restored by producing haploid gametes (31). First, the hermaphrodite produces sperm late in larval development, which are pushed proximally to complete spermatogenesis and stored in the sperm sac (32). In adulthood, the hermaphrodite gonad focuses on oogenesis, where meiosis prophase I can be followed visually, progressing sequentially as stages are separated throughout the germline by location and can be identified by the changes in nuclear morphology (31).

The germline is a continuously proliferating, “bi-lobed” structure that develops in a spatial-temporal manner (33). Germ cells are held within a common cytoplasm with incomplete

cell membranes and each gonad arm empties into a common uterus where fertilized eggs are deposited. Proliferation of progenitor mitotic stem cells is maintained in the mitotic zone (MZ), due to their proximity to the distal tip cell (DTC) (Figure 1.2B) (34). As mitotic cells move away from the DTC, they begin meiosis and enter S phase in the transition zone (TZ) (35). In the TZ, chromosomes appear polarized or “crescent shaped” as they line up with their homologous partners (lepotene/zygotene stages), and synaptonemal complexes will then form between them to hold them together (33,35).

Germline nuclei then move on to pachytene, a stage that completes synapsis and meiotic recombination. Out of several DSBs induced between synapsed homologs by the topoisomerase II SPO-11 (SPO11 ortholog), repair by homologous recombination (HR) produces only one crossover (CO) between each pair of chromosomes, while the rest are repaired as non-crossovers (NCO) (33,36). One successful CO is needed for chiasmata to form between homologs, which is necessary for the subsequent condensation and structural changes chromosomes undergo later in diakinesis (37). Synaptonemal complexes disassemble in late pachytene located where the gonad bends, an area where physiological apoptosis occurs and is commonly referred to as the “death loop” (11,33). Here germ cells are at their most feeble and are thought to die if unable to survive recombination, or are purposely sacrificed to provide maternal and cytoplasmic factors to developing oocytes (11,38). Now at diakinesis, cells leave the common cytoplasm with 6 homologous chromosome pairs (bivalents) enclosed by their own membrane. Arrested oocytes are then fertilized by sperm and embryos are deposited in the uterus until they are ready to be expelled through the vulva (Figure 1.2B) (39).

1.2.3 Brief overview of the *C. elegans* germline as a model for the DNA Damage Response

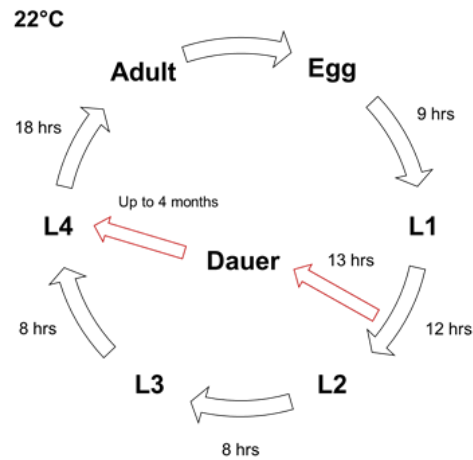
In addition to studies of meiosis, the *C. elegans* germline has become a valuable experimental system for study of the DDR as an adaptive response to cytotoxic and genotoxic insults (11). All three mechanisms for defense: cell cycle arrest, DNA repair and apoptosis are highly conserved, and occur in physically separated regions of the germline. Cell cycle arrest occurs in the MZ, DNA repair begins in the TZ and occurs throughout pachytene, while apoptosis is restricted to late pachytene just before and within the loop region (33). In response to DNA damage, arrest is dependent on the activation of the checkpoint genes, MRT-2, HUS-1 and CLK-2 (40–42). Although not upregulated in response to DNA damage of IR, regulators of cell cycle progression such as cyclin dependent kinases (CDKs), cyclin dependent kinase inhibitors CKI-1 and CKI-2 (p21 and p27 orthologs), as well as B-cyclins (i.e. *cyb-1*) are required during development (43). Mitotic cell cycle arrest following DNA damage exposure is transient, lasting up to 20 hours and is identified by the pronounced enlargement of nuclei which can be viewed with DAPI staining, or directly using differential interference contrast (DIC) microscopy (44,45).

DNA repair protects against mutation, genomic instability, chromosomal abnormalities, embryonic lethality, increased DNA damage sensitivity, and defects in development (46). In *C. elegans*, somatic cells use the highly error prone “better with errors than dead” approach, of non-homologous end joining (NHEJ) to repair DSBs, which ligates broken ends of DNA (47,48). In the germline, the dominant form of DNA repair is HR and is responsible for repairing DNA faithfully by locating a homologous template, to ensure at least one DSB in each of the worm’s six chromosomes is repaired to produce a CO for chiasmata formation (47).

Germline cells are constantly under threat from internal and external stressors that can compromise their resistance and genomic integrity. DNA damage caused by SPO-11 activity or stress exposure (i.e. IR) will activate the recruitment of conserved *C. elegans* DDR sensors to process and repair DSB sites. The MRN complex (MRE-11, RAD-50, NBS-1) first arrives to process the DSB, followed by nucleases like DNA-2 and EXO-1 that resect DNA strands to create single-stranded DNA (ssDNA) (49–51). ssDNA is coated with the replication protein RPA and then replaced by RAD-51, that together with structural maintenance proteins and BRC-1 search for and facilitate homologous template strand invasion (52–54). How exactly the broken DNA strand detects its homologous template is unclear, but it is thought that the ssDNA strand invades and binds to its nearest complement to complete DNA synthesis and repair (52–54). In the end, two outputs are possible: synthesis dependent strand annealing will produce NCOs, while the resolution of double Holliday junctions by resolvases such as GEN-1 and SLX-1 will generate both CO and NCO products (55,56). Mutations in genes involved in DNA repair can be identified by the morphology of oocyte chromosomes arrested in diakinesis (45). They have been found to exhibit a range of chromosomal abnormalities such as, increased chromosome number (up to 12) seen in *rad-51*, *mre-11* and *spo-11* mutants (57,58), chromosome fusions and entanglements (48), breaks or fragmentation, as well as bent chromosome axes (59).

Cell cycle arrest and DNA repair ensure that only cells with uncompromised genetic information are inherited, while apoptosis eliminates damaged cells to protect against transformation. Activation of intrinsic apoptosis in mammals and the conserved pathway of DNA damage induced germline apoptosis in *C. elegans* will be discussed in the following section.

A



B

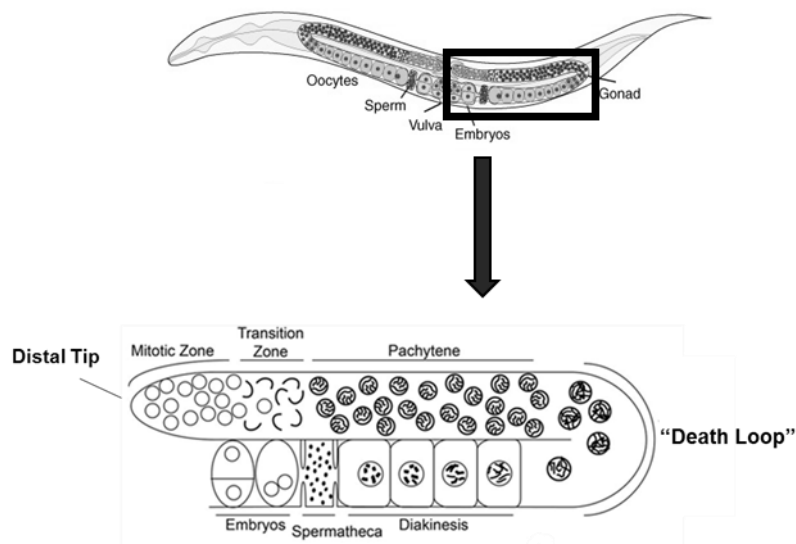


Figure 1.2: The *C. elegans* life cycle and adult germline anatomy

(A) Illustration of the stages of the *C. elegans* life cycle at 22°C, adapted and modified from WORMATLAS. (B) Diagram of adult *C. elegans* hermaphrodite anatomy. Image adapted and modified from (60). Illustration of one enlarged gonad arm with zones labelled to indicate stages of meiosis. The gonad bend, is known as the “death loop” where programmed cell death occurs. Image adapted and modified from (61).

1.3 The intrinsic “mitochondrial dependent” pathway of apoptosis

1.3.1 Activation of the intrinsic pathway of apoptosis in mammalian systems

Apoptosis is “cell suicide”, an essential event for tissue homeostasis, morphogenesis and the elimination of “self-reactive” or malignant cells that threaten the health an organism (1). Apoptosis activation was first discovered in cell fate studies of *C. elegans* embryogenesis, revealing conserved pro-apoptotic genes *egl-1* (BH3 ortholog), *ced-3* (Caspase 3 ortholog), *ced-4* (APAF1 ortholog), and anti-apoptotic gene *ced-9* (BCL2 ortholog) function to activate apoptosis in a simple linear genetic pathway (62,7). However, continued research in mammalian systems has shown that apoptosis is far more complex and while tightly controlled, is governed by fluctuations in the balance between pro-survival and pro-death factors (63).

Too much, or too little apoptosis can be detrimental and lead to autoimmune disorders, neurodegeneration and cancer (64). As a result, apoptosis has been found to be executed by one of two main mechanisms: The extrinsic pathway and the intrinsic pathway. The “death receptor” or extrinsic pathway of apoptosis, is activated when extracellular ligands such as Fas, TNF- α (Tumour necrosis factor), and TRAIL (TNF-related apoptosis-inducing ligand) bind to cell surface receptors for the activation and formation of DISC (Death inducing signaling complex) (65). DISC contains FADD (Fas associated protein with death domain), an adaptor protein which activates caspase 8 for the downstream activation of caspases 3/6/7, cysteine proteases that will execute cell death through the breakdown of vital organelles and structural proteins (66,67).

The “mitochondrial” or intrinsic pathway is governed by the abundance of either pro-death or pro-survival factors and is dependent on the type and severity of DNA damage (4). This pathway is activated in response to DNA damage exposure (i.e. IR, UV), oncogene activation, and growth factor removal, in order to eliminate the possibility of cellular transformation and

malignancy. The transcription factor p53 is one of the most important tumour suppressors that is most frequently mutated in cancer, preventing the transcription of genes that control cell cycle arrest, DNA repair and apoptosis (68). Although p53 can increase the expression of extrinsic pathway ligands to promote cell death through caspase 8 activation, the p53 transcriptional response shows preference for intrinsic apoptosis to eliminate cancer cells (65,69).

Checkpoint sensors ATM (Ataxia telangiectasia mutated), ATR (Ataxia telangiectasia mutated and Rad 3 related), and CHK1/2 (Checkpoint kinase 1/2) as well as prominent stress-activated protein kinases (SAPK) p38 MAPK and JNK (c-Jun N terminal Kinase), phosphorylate stabilize and activate p53 in response to stress (70–72). However, p53 must be able to respond to and interpret stimuli from a variety of stressors, and depending on severity must elicit an appropriate response of either survival or death, which is apparent by its complex regulation as it is also targeted for ubiquitination, sumoylation and neddylation (70). Once active, p53 enters the nucleus to increase the transcription of pro-apoptotic factors such as PIG3 (p53 induced gene 3) (73), and members of the BCL2 (B-cell CLL/lymphoma 2) family the BH3 domain containing genes: Bax, Bid, *Puma* and *Noxa* (64).

The increased production of these pro-apoptotic factors travel to and disrupt mitochondrial membranes through anti-apoptotic protein inhibition to facilitate the release of pro-death molecules such as AIF (Apoptosis inducing factor) for nuclear fragmentation, Smac and Diablo, and most notably cytochrome c from the intermembrane space (74–77). Once in the cytoplasm, cytochrome c binds to and interacts with the adaptor APAF1 (Apoptotic protease activation factor 1), and promotes its oligomerization (Figure 1.3). APAF1 and activated caspase 9 form an apoptosome complex which subsequently activates caspases 3 and 7, which will degrade cellular proteins (78).

In addition to increasing BH3 domain pro-apoptotic gene expression in response to stress, p53 also increases APAF1 transcription, which is believed to help drive apoptosis activation with cytochrome c release (79). At the same time, p53 can strengthen the apoptotic decision by increasing PTEN (Phosphatase and tensin homolog) gene expression, a PI3K (Phosphoinositide-3 kinase) phosphatase which can prevent the downstream activation of AKT (Protein kinase B) attenuating cell survival (80). To prevent prolonged p53 activation especially in healthy cells, the E3 ubiquitin ligase MDM2 (Mouse double minute 2) targets and ubiquitinates the p53 tumour suppressor, promoting its cytoplasmic localization and degradation (81). Thus, when a cell is faced with insurmountable DNA damage that cannot be overcome by survival associated pathways of DNA repair and cell cycle arrest, increased expression of pro-apoptotic factors will activate intrinsic apoptosis to prevent the accumulation of mutations and eliminate the threat of malignancy.

1.3.2 Intrinsic apoptosis is conserved in C. elegans

During *C. elegans* embryogenesis loss of function in *egl-1*, *ced-3* or *ced-4* genes prevents cell death. A loss of *ced-9* caused immense cell death leading to inviability, while *ced-9* gain of function mutants prevented cell death altogether (62,7). From this, *egl-1*, *ced-4* and *ced-3* were deemed executors of apoptosis while, *ced-9* is an essential anti-apoptotic gene. Epistatic studies established the conserved linear core apoptotic pathway, where *egl-1* inhibits *ced-9*, *ced-9* inhibits *ced-4*, and *ced-4* is required for *ced-3* activation (82).

Apoptosis in adult germlines follows the intrinsic pathway and removes approximately 50% of cells during development (11). There are two forms of apoptosis induction in *C. elegans* that occurs within the “death loop” region, which consists of late pachytene germ cells: (i) Physiological apoptosis is CEP-1 (p53-like protein) independent, and is necessary for oogenesis

and responds to cytoplasmic stressors such as the collapse of replication forks (11); (ii) DNA damage induced apoptosis which is CEP-1 dependent (11,83). In *C. elegans*, exposure to exogenous stressors such as chemicals, toxins and IR is first sensed by the 9-1-1 checkpoint proteins: MRT-2, HPR-9 and CLK-2 (40). These proteins are sensors that will relay signals to transducer proteins that decide based on damage type and severity whether cell cycle arrest, DNA repair, or apoptosis will be activated.

The 9-1-1 complex activates ATL-1 (ATR ortholog) and ATM-1 (ATM ortholog) transducer kinases to phosphorylate and activate CEP-1 (84,85). Upon activation of CEP-1, it increases the transcription of its BH3 only domain target *egl-1* and its paralog *ced-13*, where EGL-1 and CED-13 are believed to bind to and inhibit CED-9 to release its inhibition of CED-4 (86–89). CED-4 can then activate CED-3 to induce apoptosis (Figure 1.3), although recently there has been some debate whether CED-9 and CED-4 truly co-localize on mitochondria (90). In the “death loop”, cells programmed to die display a characteristic, highly refractive and raised “button-like” appearance that can be viewed directly using DIC microscopy (45). Dead cells will then express the CED-1 transmembrane protein marker for phagocytosis and are engulfed by neighbouring cells (91).

Similar to mammals, parallel pathways and independent factors can influence the core apoptosis pathway. Studies of individual *C. elegans* DDR related genes have also uncovered its own complex world of apoptosis activation, where DNA repair mutants tend to exhibit higher levels of germline apoptosis (i.e. *brc-1*), while DNA checkpoint mutants (i.e. *cep-1*) exhibit lower levels of apoptosis (45). Loss of the E3 ubiquitin ligase EEL-1 (Mule ortholog), KRI-1 (KRIT1/CCM1 ortholog), SIR-2.1 (SIRT1 ortholog), or meiosis CO genes MSH-4/5 reduce germline apoptosis in response to IR and were found to promote apoptosis independently of

CEP-1 (92–95). Germline P granule proteins PGL-1/3 have been found to act as apoptosis suppressors, where the loss of either *pgl-1* or *pgl-3* increased both SIR-2.1 and CED-4 co-localization outside of nuclei, and increased germline apoptosis before and after UV (ultraviolet) exposure (94,96).

In addition, the loss of either of the transcription factors EGL-38 and PAX-2 (Pax2/5/8 orthologs), reduced *ced-9* expression levels and increased germline apoptosis (97). The same was observed with a loss of LIN-35 (Retinoblastoma ortholog) in response to starvation stress, suggesting that these transcription factors regulate apoptosis apart from CEP-1, by regulating *ced-9* (98,99). Although an ortholog for the p53 inhibitor MDM2 is not known to be conserved, CEP-1 can be negatively regulated by the E3 ubiquitin ligase SCF^{FSN-1}, where *fsn-1* (F box protein 45 ortholog) mutants' display increased germline apoptosis induced by ENU (N-ethyl-N-nitrosourea), increased phosphorylation of CEP-1 and increased CEP-1 transcriptional activity (100,101). Also the loss of *akt-1* (AKT1 ortholog) of the IIS pathway increases *egl-1* and *ced-13* expression, while *akt-1* gain of function mutants suppress this enhancement in response to DNA damage, indicating that AKT-1 is another potential negative regulator of CEP-1 (102). This demonstrates that similar to mammalian systems, the complexity of apoptosis regulation in *C. elegans* is conserved, and in response to DNA damage can occur independently of CEP-1.

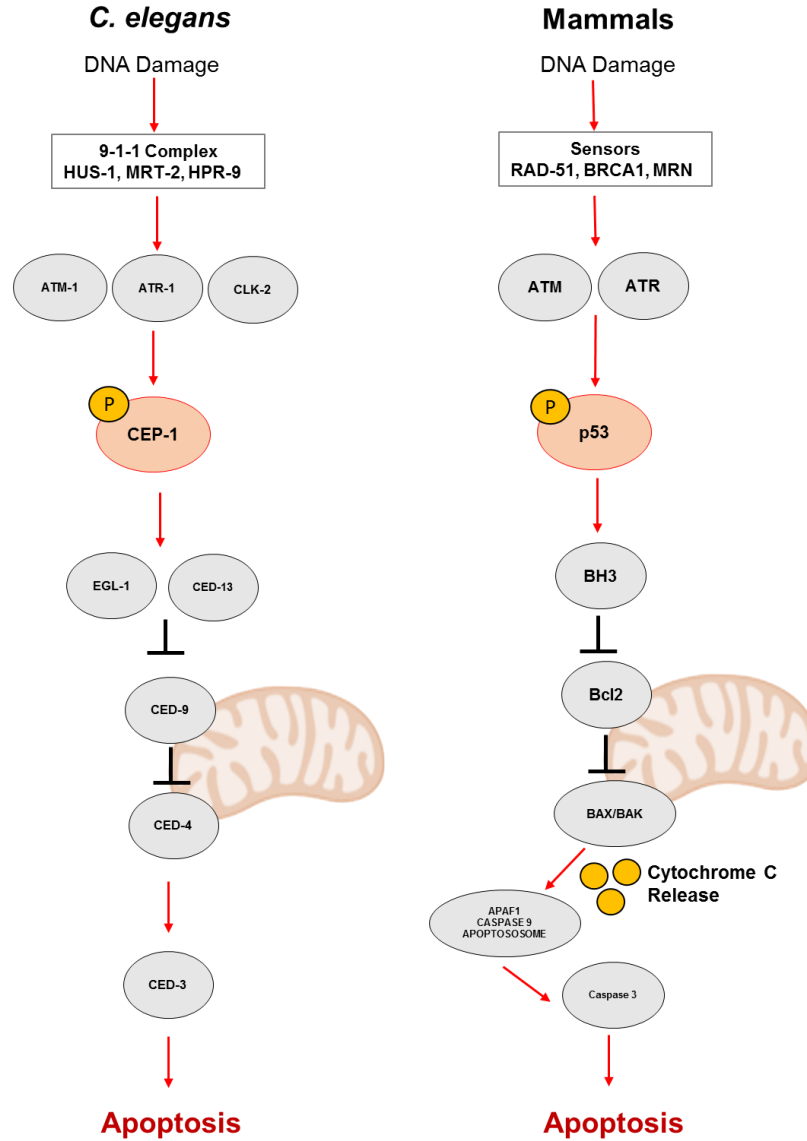


Figure 1.3: Pathways depicting DNA damage induced germline apoptosis in *C. elegans* and its conservation to mammalian intrinsic apoptosis.

The pathway for activation of DNA damage induced germline apoptosis in *C. elegans* is shown alongside its respective conserved components in mammalian intrinsic apoptosis. Adapted and modified from (78).

1.4 BRCA1 is a dynamic tumour suppressor of the DNA damage response

1.4.1 BRCA1 structure and function in mammalian systems

BRCA1 is a vital tumor suppressor that participates in several DDR mechanisms including DNA repair, transcriptional regulation, cell cycle control and ubiquitination in response to DNA damage (103–105). While somatic BRCA1 mutations are rare, loss of BRCA1 function through germline mutation accounts for 50% of all familial breast cancer cases, is associated with an 80% increased lifetime risk of developing ovarian cancer and has been linked to prostate cancer (106). The BRCA1 protein contains: a RING (Really Interesting New Gene) domain typical of E3 ubiquitin ligases, a NES (Nuclear export signal), a NLS, a coiled-coil, and two BRCT (BRCA1 C Terminus) domains which are typically found in proteins associated with DNA surveillance (Figure 1.4A) (13).

BRCA1 becomes a functional ubiquitin ligase when it binds to its heterodimeric binding partner and tumor suppressor BARD1 (BRCA1 RING-associated protein 1) (107). To preserve genomic integrity, BRCA1 can bind to several distinct complexes to regulate transcription, remodel chromatin, as well as participate in protein recruitment to facilitate DNA repair via HR, the least error-prone DNA repair system (Figure 1.4C) (108). BRCA1 shuttles into and out of the nucleus through the Importin- α / β pathway, and is most commonly detected at DNA replication sites (104). In response to DNA damage, BRCA1 is recruited to DSBs and will bind to larger functional protein complexes or dimerize with BARD1, which obscures the NES to keep BRCA1 in the nucleus (109).

Specifically, in response to IR, DSB sites are initially marked with H2AX (Histone type 2A phosphorylated) and kinases ATM and ATR are activated. CHK1/2 are direct downstream targets of these kinases, who in turn will phosphorylate and recruit BRCA1 and other DNA

repair proteins such as RAD51 and the MRN (MRE11, RAD50, NBS1) complex (110). Like p53, BRCA1 can be phosphorylated at different sites to direct its function and can be ubiquitinated and sumoylated (111). BRCA1 and MRN form a surveillance complex, where BRCA1 can regulate MRE11 ssDNA resection for subsequent homologous template invasion and repair. While the MRN complex is also involved in NHEJ, the presence of BRCA1 at these damage sites indicates a preference for HR (112). Therefore, BRCA1 mutations can lead to detrimental effects, ranging from genomic instability, formation of mammary gland tumours and cancer, to accelerated ageing (105,113,114).

Due to the various activities of BRCA1 during the DDR, it plays a more complex role in the regulation of apoptosis. Overexpression of BRCA1 is associated with increased apoptosis, while mutated BRCA1 has been linked to reduced apoptosis and tumorigenesis (15,115). BRCA1 expression can also stabilize p53 to facilitate the transcription of the cell cycle arrest gene p21, where a loss of BRCA1 can cause a switch from p53 targeted transcription of survival genes to increased expression of apoptosis genes (116,117). However, increased apoptosis has been associated with BRCA1 can be cleaved by caspase 3 in response to UV (118). In response to IR and growth factor removal, the presence of functional BRCA1 was associated with apoptosis induction, and less apoptosis was observed with a mutant form of BRCA1 (118,119). However, BRCA1 deficient cells have also been found to succumb to apoptosis more easily following IR exposure (120).

It is thought that the localization of BRCA1 also influences the cell death decision, as BARD1 binding and retention of BRCA1 in the nucleus is associated with reduced apoptosis (115). Interestingly, after IR exposure BRCA1 has been found to co-localize with BCL2 at

mitochondria and it is proposed that this interaction may repress DNA repair by depleting BRCA1 nuclear localization, to help facilitate intrinsic apoptosis (121).

1.4.2 BRCA1 is conserved in C. elegans and is known as BRC-1

In *C. elegans*, BRCA1 is functionally conserved and is known as BRC-1. It contains similar RING and BRCT domains and centrally located “low complexity regions” or LCR domains (Figure 1.4B). LCRs constitute amino acid sequences that contain single amino acids or short motif repeats (122). Abundant in eukaryotic proteins, proteins with LCRs tend to have many interacting binding partners and Gene Ontology analyses reveal both central and terminally located LCRs are common in proteins involved in stress response signaling (123). BARD1 is also conserved in *C. elegans* and is known as BRD-1. Using an Y2H (Yeast 2 Hybrid) assay (and subsequently verified *in vitro* with a pull down assay), the interaction between BRC-1 and BRD-1 was found to be conserved, where BRD-1 was also found to interact with UBC-9 (Ubiquitin conjugating enzyme 9) and RAD-51 (5).

BRC-1 is vital to the DDR, facilitating HR repair of DSBs during meiosis. A loss of *brc-1* causes an increase in RAD-51 foci persistence in pachytene nuclei, which is indicative of an inability to process DSBs (53). A loss of *brc-1* causes high levels of CEP-1 dependent germ cell death and X-chromosome non-disjunction, leading to an increased incidence of males (14). This high apoptosis phenotype has been linked to defective DNA repair in *brc-1* mutant animals following DNA damage, leaving DSBs unresolved during meiotic recombination which is also thought to lead to increased embryonic lethality (45).

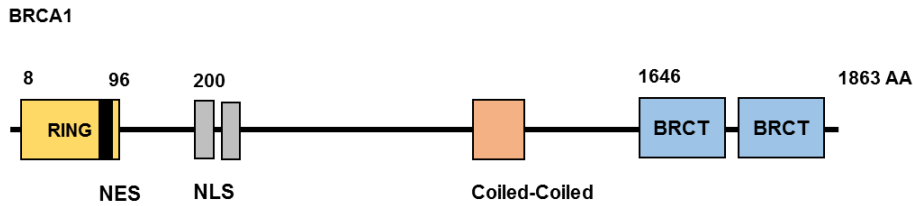
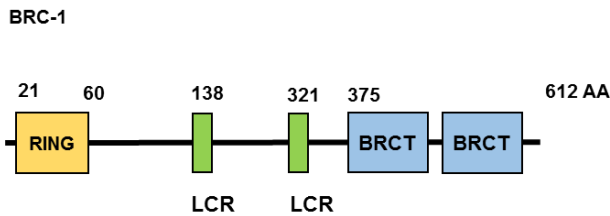
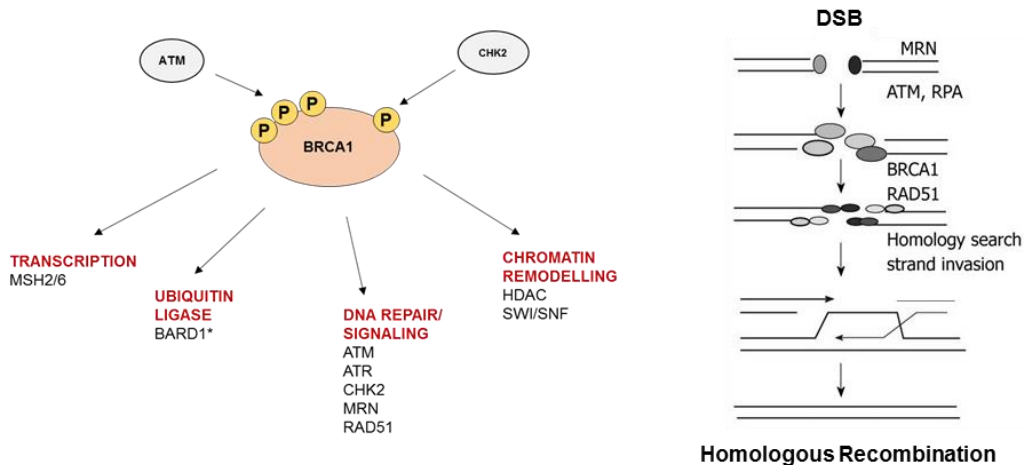
A**B****C**

Figure 1.4: BRCA1 is functionally conserved in *C. elegans*

(A) Mammalian BRCA1 is 1863 amino acids in length and has a RING (Really interesting new gene) domain. It has both a nuclear localization signal (NLS) and nuclear export signal (NES), a coiled-coil domain and two BRCT (BRCA1 C terminus) domains. Illustration of protein structure was adapted from (13). (B) In *C. elegans*, the BRCA1 ortholog known as BRC-1 also possesses a RING domain, and two “Low Complexity Regions” (LCR). It also has two BRCT domains at the C-terminal region but is much shorter in length at 612 amino acids. Protein domain structures are not to scale. Structure adapted from SMART. (C) BRCA1 is most well-known for facilitating DNA repair via HR and also participates in many process of the DDR by binding to several complexes. Image of the left adapted and modified from (108,124). Image on the right taken and modified from (125).

1.5 BRAP2 is a BRCA1 binding protein and potential scaffold for the regulation of cell signaling

BRAP2 was first discovered in a study using an Y2H screen searching for novel BRCA1 binding partners. The interaction between BRCA1 and BRAP2 was validated, and BRAP2 was found to bind to the NLS of BRCA1 (15). BRAP2 has been found to localize to the cytoplasm, a result that has been verified in every subsequent study of BRAP2 function. BRAP2 retains BRCA1 in the cytoplasm and impedes it from traveling to the nucleus, inferring that BRAP2 may prevent BRCA1 from performing its DDR associated functions (15). However, analysis of the biological implications of the BRCA1/BRAP2 interaction has not been extensively studied.

BRAP2 consists of 592 amino acids with the following characteristic domains: A RING domain, followed by a ZnF-UBP (Zinc Finger Ubiquitin Protease) domain. These two motifs comprise the enzymatic portion of BRAP2 as an E3 ubiquitin ligase. BRAP2 also contains a coiled-coiled domain made up of leucine heptad repeats, involved in protein-protein interactions (126). At the C-terminal end, a LCR domain is present, which suggests that BRAP2 may play a role in regulating stress responses (123) (Figure 1.5A). Following the discovery of the BRCA1/BRAP2 interaction, several studies emerged that while verifying its cytosolic localization and retention function, also revealed new BRAP2 protein binding partners. BRAP2 was found to bind to the NLS and prevented the nuclear translocation of viral proteins SV40 large tumour antigen and ppUL44 (Human Cytomegalovirus DNA Polymerase Processivity Factor) (126), as well as the cell cycle inhibitor p21 during monocyte differentiation (127). BRAP2 function as an E3 ubiquitin ligase was confirmed, seen with its ability to bind to and enhance Lys63 poly-ubiquitination of the protein phosphatase CDC14 (128). BRAP2 is also reported in literature as IMP (Impedes Mitogenic Propagation), and was found to bind to KSR1 (Kinase Suppressor of RAS). BRAP2 was also found to bind to RAS in a GTP dependent

manner. Thus in the absence of growth factor activated RAS, it is believed to act as an inhibitor of downstream ERK (Extracellular signal related kinase) activation (Figure 1.6) (16,129–131).

Upon activation of RAS, BRAP2 is auto-ubiquitinated, relieving KSR1 inhibition which allows KSR1 to translocate and mediate the formation of the RAF/MEK/ERK complex at the plasma membrane for terminal ERK1/2 activation (129). *In vivo*, BRAP2 was also found to be neddylated at Lys432 by the ubiquitin like protein Nedd8 (132). In the same study, in response to TNF- α stimulation BRAP2 was found to partly prohibit the nuclear translocation of NF- κ B (Nuclear factor kappa-light-chain-enhancer of activated B cells) *in vitro*, attenuating this pathway which is critical to survival, the inflammatory response and cell cycle regulation (132).

BRAP2 protein expression has been detected in many tissues including lung, kidney and brain but is most robustly expressed in mammalian heart and testes (133). This may indicate that BRAP2 is important for male germline development. An initial Y2H screen was performed using a human testis cDNA library and BRAP2 was found to bind to and inhibit the nuclear accumulation of the testis proteins HMG20A, NUMA1 and SYNE2 (134). Another group, Fatima et al. (2015) set out to build a BRAP2 interaction network, conducting a similar screen and detected another 24 potential testes specific protein binding candidates for BRAP2 including: APOA1, AKAP3, and the SWI/SNF-related matrix protein SMARCE1. They further validated BRAP2 interactions with DNMT1 (DNA Methyltransferase 1) and the AKT protein phosphatase PHLPP1 (PH Domain and Leucine Rich Repeat Protein Phosphatase 1). This reinforces the importance of BRAP2 as a binding protein and the potential distinct biological processes it may regulate. In the same study, when the interaction between BRAP2 and PHLPP1 in testes was further investigated, BRAP2 was found to act as a scaffold for PHLPP1 and retained it in the cytoplasm during spermatogenesis. Taken one step further, with this

PHLPP1/BRAP2 interaction it can be predicted that BRAP2 may also indirectly regulate the PI3K/AKT pathway, which is known to promote proliferation, cell survival and growth (135). Taken together, current literature characterizes BRAP2 as an E3 ubiquitin ligase, a RAS effector, as well as a cytoplasmic retention protein that prevents nuclear import.

1.5.1 BRAP2 is conserved in C. elegans and is known as BRAP-2

C. elegans possesses a BRAP2 ortholog known as BRAP-2 (Figure 1.5B). The *brap-2* gene is located on chromosome II next to PINK-1 (PINK1 PTEN-induced kinase ortholog). PINK1 is a ser/thr (serine/threonine) protein kinase that functions to protect cells from stress induced damage to mitochondria, where its loss can lead to a defective oxidative stress response and is associated with Parkinson's disease (136). In addition to its protein domain structure which alludes to its potential functional activity, the location of *brap-2* next to a gene that is involved in the oxidative stress response provides us with a clue to its potential physiological importance.

Previous work from our lab has shown that a mutant form of BRAP-2, the *brap-2(ok1492)* (Figure 1.5C) deletion mutant experienced L1 larval arrest that is dependent on BRC-1 when exposed to low concentrations of paraquat, an oxidative stress inducer (17). This indicates that a genetic interaction exists between these two genes during oxidative stress. Our lab has also confirmed that BRAP-2 physically interacts with the active form of LET-60 (*C. elegans* RAS ortholog) and KSR-2 (KSR2 ortholog). We also found that *brap-2(ok1492)* mutants exhibit increased levels of both MPK-1 and phosphorylated MPK-1 levels. This indicates that BRAP-2 may display conserved function as a RAS effector in *C. elegans*.

Extending previous work investigating the role of BRAP-2 during oxidative stress, our lab also demonstrated that *brap-2(ok1492)* mutants cause a 2.6-fold increase in SKN-1 (Nrf2

ortholog) import into intestinal nuclei, as well as increased expression of *gst-4* (GST4 ortholog) and other SKN-1 dependent phase II detoxification genes (137). This discovery led our lab to conduct a transcription factor specific RNAi screen, which uncovered 20 new potential candidates in the regulation of the *C. elegans* oxidative stress response and longevity. The SKN-1 transcription factor has been implicated in the regulation of lifespan, and is known as the master regulator of the oxidative stress response in *C. elegans* that upon phosphorylation enters intestinal nuclei to activate the transcription of detoxification genes (138). This suggests that BRAP-2 may act as a negative regulator of SKN-1, in order to prevent an inappropriate detoxification response (137). Yet, similar to the BRCA1/BRAP2 interaction in mammals, the role of BRAP-2 and its genetic link to BRC-1 in the DDR and its potential for the protection of germline genomic integrity have not yet been addressed.

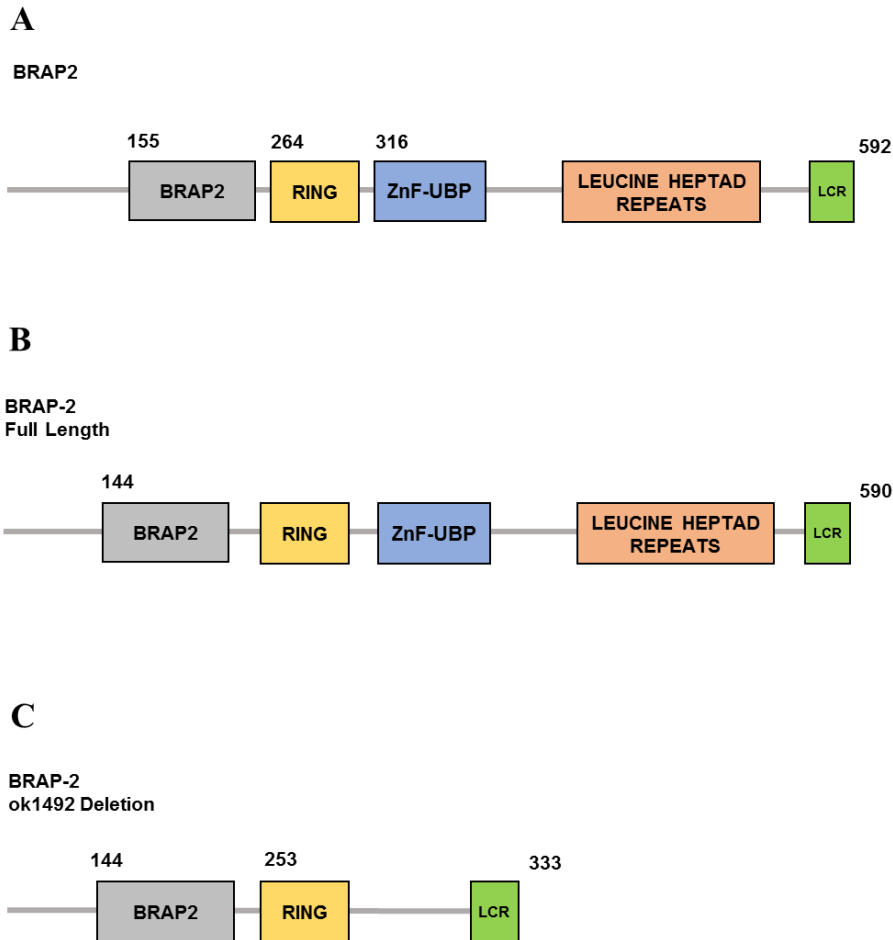


Figure 1.5: Protein domain structures of mammalian BRAP2 and *C. elegans* BRAP-2

(A) BRAP2 is a 592 amino acid protein with a RING domain, Zinc Finger Ubiquitin Protease (ZnF-UBP), leucine heptad repeats that constitute a coiled-coil domain, and a Low Complexity Region (LCR). LCR has been detected in proteins associated with stress responses. Domain structure adapted from SMART and (133). (B) Full length *C. elegans* BRAP-2 is conserved and possesses a BRAP2 domain, RING domain, ZnF-UBP and leucine heptad repeats (coiled-coil) that is predicted to be responsible for protein-protein interactions. It also retains the LCR, implicated in stress signaling (17). (C) In this study, we focus on the *brap-2(ok1492)* gene product, where exons 5-8 are deleted in the *ok1492* allele which results in the removal of 259 amino acids at the C-terminal end removing the ZnF-UBP and leucine heptad repeats (17).

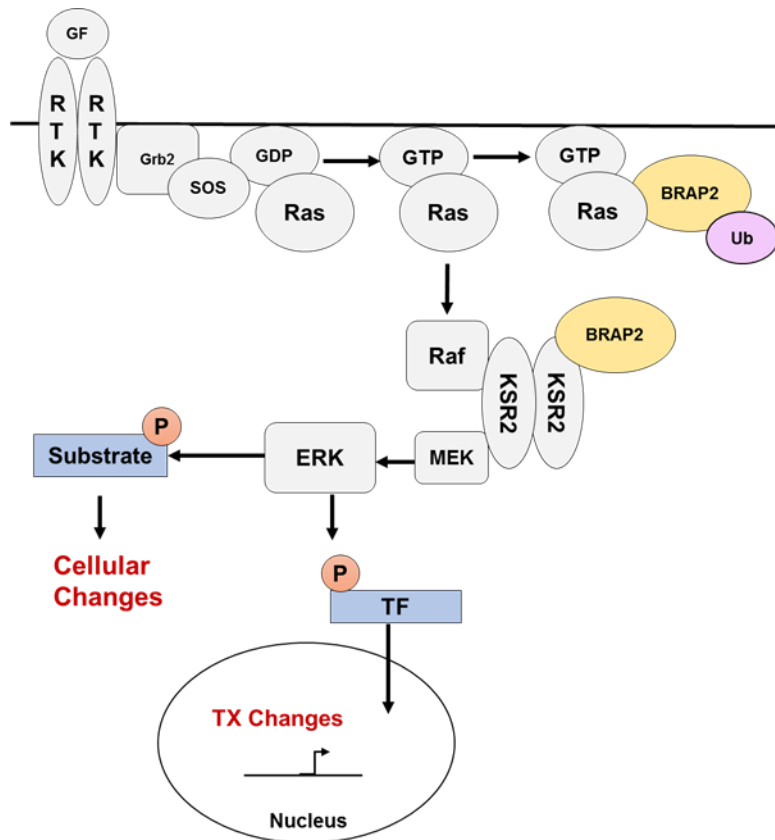


Figure 1.6: The predicted role of BRAP2/IMP in RAS signaling

When RAS is inactive, BRAP2/IMP remains bound to and inhibits KSR2, preventing the phosphorylation and thus activation of downstream kinases. When the pathway is activated, GDP-RAS will be converted to GTP-RAS and bind to BRAP2. BRAP2 degrades by auto-ubiquitination, releasing KSR2 from inhibition. This is followed by the activation of KSR2 by RAS-GTP. KSR2 facilitates the phosphorylation of MEK and ERK by RAF. Active ERK can then phosphorylate nuclear and cytoplasmic destined substrates to elicit both transcriptional and cellular changes, respectively. Image adapted and modified from (139).

1.6 Conserved *C. elegans* cell signaling pathways relevant to this study

1.6.1 The RAS/MEK/ERK signaling pathway

Mitogen activated protein kinase (MAPK) pathways are responsible for translating extracellular signals into cellular responses that regulate cell growth, proliferation, differentiation and death (140–142). Pathway activation follows sequential phosphorylation events in a cascade comprised of three kinases, MAP3K, MAP2K and MAPK (142,143). MAPK are ser/thr kinases that when active phosphorylate both cytoplasmic and nuclear bound targets, such as transcription factors to regulate tissue-specific transcription (141–143). With over 200 possible targets, structurally supportive proteins known as scaffolds increase the specificity and accuracy of MAPK activity (144,145). A scaffold can bind several proteins, keeping them in close proximity to control the location and duration of signaling to ensure the rapid propagation of phosphorylation (140).

The most well-studied MAPK pathway is RAS/MEK/ERK (Mitogen-activated protein kinase kinase/Extracellular signal related kinase), activated in response to stress and growth factor stimulation, where ligands bind to receptor tyrosine kinase (RTKs) to trigger cytoplasmic receptor dimerization and auto-phosphorylation (142,146). The SOS (Son of Sevenless) adaptor links RTKs to the cascade by activating RAS, a small GTPase, by converting the GDP (Guanosine diphosphate) bound to RAS to GTP (Guanosine triphosphate) (146). The downstream target of active RAS the MAP3K RAF will then phosphorylate the dual specificity kinase MEK for ERK activation (142). Catalytic ERK can target cytoplasmic, cytoskeletal and membrane proteins or enter the nucleus to phosphorylate transcription factors (140). Once the signal has been transmitted, GTP is hydrolyzed back to GDP by GAP (GTPase-activating protein) for inactivation (Figure 1.6).

RAS activation is needed for cell growth, proliferation and survival, and can indirectly regulate apoptosis by contributing to the flux between pro-survival and pro-cell death factor abundance. The prevailing view is that RAS plays a dual role in apoptosis regulation that is context dependent, and can be further complicated by cell type and damage severity. RAS activation can promote apoptosis to prevent the onset of cancer, by directly activating the tumour suppressors RASSF1 (RAS association domain-containing protein 1) and NORE1 (RASSF5). RASSF1 and NORE1 form a complex with MST1 (Macrophage stimulating 1), activator and cleavage target of caspase 3, to enhance apoptosis induction (147,148). However, the main role for RAS activation is to promote proliferation, apoptosis evasion and survival by phosphorylating PI3K for downstream AKT activation (149) (Figure 1.7). In addition, AKT and RAF activation by oncogenic RAS can also promote increased MDM2 activation, leading to p53 degradation and preventing pro-apoptotic gene expression (150).

1.6.2 The RAS/ERK signaling pathway is conserved in C. elegans

In *C. elegans*, downstream of two RTKs, LET-23 and EGL-15, lies the RAS ortholog LET-60. The most well-known downstream pathway activated by LET-60 is LIN-45/MEK-2/MPK-1, which similar to its mammalian counterpart (RAF/MEK/ERK) phosphorylates many targets to regulate survival, germline development and cell fate specification (151). Not all mutations in genes of this pathway are fatal, however they do cause a host of developmental problems. Loss of LET-60 produces vulva-less hermaphrodites (that die when progeny hatch and eat their way out of the mother), while LET-60 gain of function mutants possess multiple vulvas (152). Reduction in LET-60 signaling can also prevent male tail spicule specification leading to failures in mating, as males are unable to properly detect the hermaphrodite vulva for copulation and sperm transfer (153,151).

LET-60/MPK-1 signaling is also important for germline development and activation of both CEP-1 dependent and independent apoptosis. Activation of physiological apoptosis is CEP-1 independent and removes half of the developing germ cells in the “death loop”. Here, MPK-1 (ERK ortholog) activation assists the exit of germ cells from pachytene to become fully matured oocytes, and mutations in *mek-2* (MAP2K ortholog) or *mpk-1* can leave worms sterile, as germ cells are unable to exit and complete gametogenesis (154). Reduced MPK-1 activation is associated with reduced physiological apoptosis and an increase in phosphorylated MPK-1 has been found to increase apoptosis, potentially due to an associated reduction in *ced-9* transcription (38). LIP-1 (MKP3 ortholog) is a MPK-1 phosphatase and thus negative regulator of LET-60 signaling. In response to IR, similar to LET-60 gain of function mutants, loss of *lip-1* allowed for unimpeded MPK-1 activation, increased CEP-1 expression and caused a CEP-1 dependent increase in germline apoptosis (83).

1.6.3 The stress activated p38 MAPK pathway is involved in activation of apoptosis

The SAPK p38 MAPK is activated in response to inflammatory cytokines and various forms of stress including oxidative stress, UV and IR to promote cellular health and survival, as well as apoptosis (142,143,146,155). Activated p38 MAPK phosphorylates numerous nuclear (i.e. p53, MEF2) and cytosolic (i.e. Bax, Tau) targets, and its activity can be regulated through scaffold binding (144,156). Dysfunction of p38 MAPK signaling is implicated in various pathologies including inflammatory diseases (i.e. arthritis and psoriasis), heart disease, neurological disorders and cancer (157).

There are four p38 MAPK isoforms ($\alpha, \beta, \gamma, \delta$), where p38 α has been implicated in mediating both cell survival and apoptosis by influencing the abundance of pro-apoptotic factors (158). Studies in cardiac cells have shown that p38 α activation increases apoptosis by increasing

BCL2 phosphorylation, and increasing both the expression and translocation of pro-apoptotic factor Bax to mitochondria (159,160). p38 α can also target and phosphorylate p53 to initiate the transcription of pro-apoptotic genes (161). By contrast, a loss of p38 α in cardiomyocytes increases ERK and AKT activation enhancing cell survival, implying that p38 α may also act as a negative regulator of these pro-survival pathways (162). In addition, the prolonged activation and aberrant p38 α function in response to oxidative stress is associated with apoptosis in neurons and glial cells, a consequence of neurodegenerative diseases such as Parkinson's and Alzheimer's (163). However, in non-neuronal cells, in response to oxidative stress induced by hydrogen peroxide, p38 α activation increased the ATF2 (Activating transcription factor 2) dependent transcription of antioxidant gene SOD2 (Superoxide dismutase 2) to prolong cell survival (164).

1.6.4 The p38 MAPK pathway is conserved in C. elegans

In *C. elegans*, the SAPK p38 pathway is conserved and has been identified as a regulator of innate immune and oxidative stress responses, and recently has been implicated in germline apoptosis. In response to bacterial infection and oxidative stress caused by reactive oxygen species (ROS) (i.e. superoxide radicals and hydrogen peroxide) NSY-1 (ASK ortholog) activates SEK-1 (MAP2K3/6 ortholog) to phosphorylate the terminal kinase PMK-1 (p38 MAPK ortholog). PMK-1 is known to directly target and phosphorylate SKN-1, increasing its accumulation within intestinal nuclei to upregulate the transcription of phase II detoxification genes (Figure 1.9) (165). Worms treated with the oxidative stress inducer sodium arsenite had increased phosphorylated PMK-1 levels, while a loss of either *sek-1* or *pmk-1* prevented SKN-1 nuclear accumulation and increased lethality in these mutants (166).

In response to pathogen infection, such as exposure to *Yersinia pestis* and *Pseudomonas aeruginosa*, worms experience increased PMK-1 activation (167), increased PMK-1 dependent

SKN-1 nuclear import, as well as increased expression of SKN-1 target genes *gcs-1* (γ -Glutamyl Cysteine Synthetase 1 ortholog) and *gst-4* (168). PMK-1 has also been found to regulate the activity of ATF-7 (ATF2 ortholog), a transcription factor responsible for activation of host defense genes such as lysozymes and antimicrobial peptides (169). NSY-1 gain of function mutants increased PMK-1 activation and PMK-1 target immune effector gene expression, as well as enhanced resistance to *P. aeruginosa* (170). With these studies, it is thought that as a worm ages, they are more easily susceptible to bacterial infection and death due to reduced levels of PMK-1 and SKN-1 activity (171).

PMK-1 has also been linked to oxidative stress induced germline apoptosis. Following exposure to sodium arsenite, levels of apoptosis were found to be higher in *cep-1* and *egl-1* mutants. However, under the same conditions germline apoptosis in *mpk-1* and *pmk-1* mutants was lower (172). Reduced PMK-1 activity with *pmk-1* RNAi, saw reduced apoptosis levels when worms were exposed to *Salmonella* (173). This suggests that apoptosis caused by pathogen exposure is dependent on SAPK signaling and demonstrates that depending on stress type, pathways independent of the core apoptotic program are needed to activate apoptosis in the germline. The diverse functional role of PMK-1 in immunity, the oxidative stress response and apoptosis suggests that the intestine and germline, major worm stress response organs, may influence one another to promote cellular protection and health.

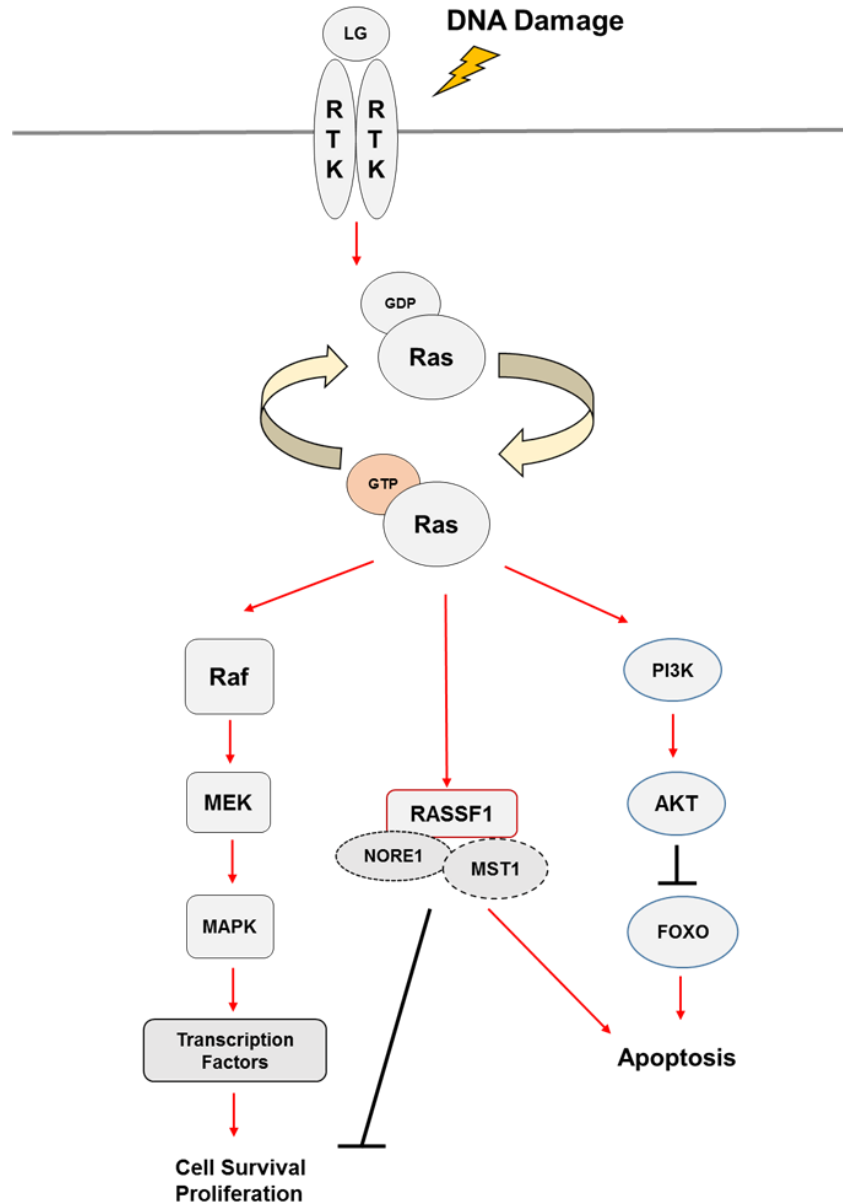


Figure 1.7: The RAS pathway can activate cell death and promote cell survival

The activation of RAS has been associated with the stimulation of many downstream pathways, particularly RAS has been found to promote cell survival by activation of transcription factors that lead to cell proliferation and at the same time activate PI3K for the prevention of apoptosis through AKT. RAS can also bind to RASSF1 for apoptosis activation to limit proliferation. LG indicates a ligand. Adapted and modified from (174).

1.6.5 The PI3K/AKT signaling pathway

AKT is a ser/thr kinase regulated by the PI3K/AKT signaling pathway, responsible for the regulation of metabolism, proliferation, cell growth and survival. AKT is phosphorylated in response to growth factors, cytokines and stress (175). Ligands bind to the IGF1 (Insulin-like growth factor 1) membrane receptor, stimulating the activity of the lipid enzyme PI3K (Phosphoinositide 3-kinase) which catalyzes PI(3,4)P₂ (PIP₂) conversion to PI(3,4,5)P₃ (PIP₃). This recruits and activates PDK1 (Phosphoinositide-dependent kinase 1) and AKT, where a conformational change in AKT allows PDK1 to access and phosphorylate Thr308 on AKT (176). Once active, AKT localizes to the inner cytosolic space to phosphorylate a variety of substrates (175) (Figure 1.8). A primary target of the AKT family (AKT1/2/3) is members of the FOXO (Forkhead Box O) transcription factor family, involved in regulating cell cycle arrest and apoptosis (177). When AKT phosphorylates FOXO, it is held in the cytoplasm and is unable to travel to the nucleus preventing the FOXO dependent transcription of pro-apoptotic BH3 domain genes such as Bax (Figure 1.8) (178).

Activated AKT can also promote cell survival by negatively regulating pro-apoptotic factors like Bad, and increase p53 degradation by activating MDM2 (179). However, constitutive AKT activation is detrimental and can lead to a cancerous state of increased cell proliferation and reduced apoptosis (180). AKT can be attenuated upstream, by the PTEN inhibition of PIP₂ conversion to PIP₃. However, AKT can be “turned off” directly in two steps. First, PP2A (Protein phosphatase 2A) removes a phosphate group on Thr308 (181), and then AKT inactivation is completed when the phosphate group on Ser473 is removed by the phosphatases PHLPP1/2 (182). PHLPP phosphatases are vital for the regulation of AKT, since a loss of either isoform causes the increased presence of phosphorylated FOXO, MDM2 and p27 (183).

1.6.6 The Insulin/Insulin-like growth factor signaling (IIS) pathway in C. elegans

In nematodes, DAF-16 is the sole FOXO ortholog that controls the transcription of genes which regulate lifespan, developmental arrest and participates in the oxidative stress response (184,185). The main components of the PI3K/AKT pathway are conserved in *C. elegans* and is commonly referred to as IIS or the DAF-2 pathway. IIS is controlled by the membrane bound receptor DAF-2 (IGF1 ortholog). In response to stress, or ligand binding DAF-2 is activated and the generation of PIP₃ by AGE-1 (PI3K ortholog) causes the translocation of PDK-1 (PDK1 ortholog), AKT-1 and AKT-2 (AKT1/2 orthologs) to the plasma membrane for phosphorylation (186–189). Activated AKT-1/2 then phosphorylate and negatively regulate DAF-16, preventing its entry into the nucleus (Figure 1.8) (190).

For activation, AKT-1 possesses conserved phosphorylation sites at Thr350 and Ser517, which are phosphorylated directly by PDK-1 (191). AKT-1 and AKT-2 are negatively regulated by DAF-18 (PTEN ortholog) inhibition of PIP₃ formation. When the phosphatase PPTR-1 (subunit of PP2A ortholog) is overexpressed, AKT-1 phosphorylation decreases, while DAF-16 nuclear localization is increased (192,193). A PHLPP1/2 ortholog exists in *C. elegans* and is known as PHLP-2 (F43C1.1). Although PHLP-2 has predicted enzymatic activity and is found expressed in neurons and around the pharynx, it has not yet been shown to directly inhibit either AKT isoform (194). When the IIS pathway is “off”, DAF-16 is free to enter intestinal nuclei and begin the transcription of genes involved in dauer, phase I detoxification, longevity and formation of germline associated nuclear pore complexes (185,195,196).

The IIS pathway and DAF-16 activation is most well-known for its regulation of worm lifespan, oxidative stress and dauer entry. When worms encounter stress in their environment such as overcrowding (usually accompanied with starvation), they can divert to an alternate

diapause stage known as dauer. Mutations in *daf-2* and *age-1* extend lifespan significantly, and these mutants were also found to be more resistant to stress (197,198). This increased longevity and dauer constitutive phenotype was found to be dependent on functional DAF-16, where *daf-16* mutants are unable to developmentally arrest and are thus dauer defective (23).

How do worms know when to enter dauer? Worms are able to sense changes in their environment in the form of pheromones, nutrients and temperature. Their amphid neurons then integrate, convert and relay these signals to parallel TGF- β (Transforming Growth Factor Beta) and IIS pathways, whose outputs will induce morphological changes including, producing a thickened cuticle and buccal plugs, constricting, elongating and slowing worm metabolism, all in an effort to enhance their resistance to stress (199,200,23). It is thought that in a healthy, stable environment the ample supply of hormones, nutrients and insulin-like peptides (ILPs) enable worms to continue with normal reproductive growth and development. There are approximately 40 predicted ILPs in *C. elegans* expressed in muscle, neurons and the intestine that can function as agonists (i.e. INS-7) or antagonists (i.e. INS-1) of the pathway in response to environmental cues and pheromones sensed by the worm (201).

The IIS pathway is also involved in regulating DNA damage induced germline apoptosis. In response to IR, a loss of *daf-2* causes a reduction in apoptosis dependent on activated MPK-1, yet a loss of *daf-16* produced similar levels of apoptosis to the wild type (101). Loss of *akt-1* or *akt-2* increases germline apoptosis but seem to function distinctly, where *akt-1* was found to negatively regulate CEP-1, while *akt-2* was found to inhibit DAF-16 (101,102). In addition, a novel *ced-3* target substrate CNT-1 (Arf GTPase ortholog), was found to move to the plasma membrane after being cleaved by *ced-3* to prevent AKT-1 activation (202,203). Interestingly, germline apoptosis induced by sodium arsenite increased apoptosis in *daf-2*, *age-1* and *akt-1*

mutants, while apoptosis was reduced with loss of *daf-16* function. However, in the same study the loss of *akt-2* demonstrated reduced apoptosis, which was increased with loss of *daf-16* (204). This demonstrates that in addition to development and longevity, the IIS pathway contributes to the regulation of stress induced germline apoptosis in distinct ways and can be independent of CEP-1.

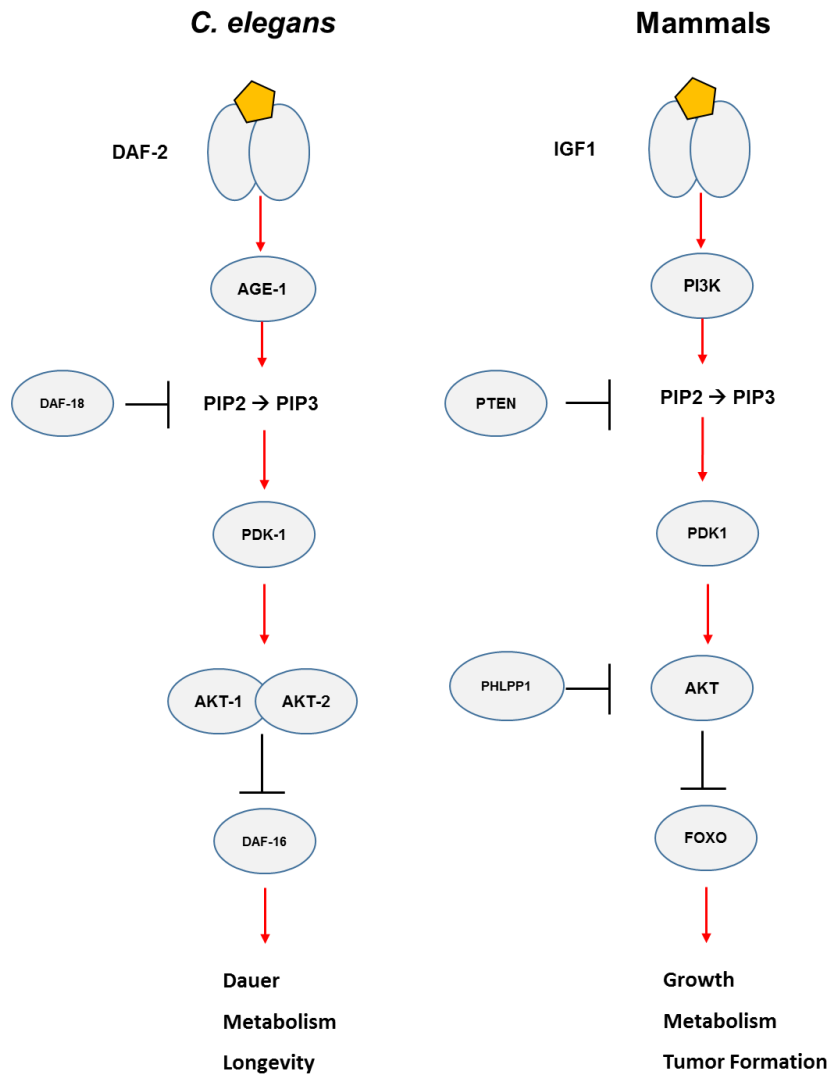


Figure 1.8: The *C. elegans* DAF-2/IIS pathway and its high conservation to the mammalian IGF/Insulin signaling pathway

The mammalian IGF/Insulin pathway is highly conserved in *C. elegans*, that when activated in addition to regulating entry into developmental arrest the DAF-2/IIS pathway is also responsible for metabolism and lifespan the regulation. Image adapted from (205).

1.6.7 The SKN-1/Nrf2 oxidative stress response pathway

The accumulation of ROS can lead to DNA damage, mitochondrial dysfunction, protein aggregation and contributes to the progression of neurodegenerative diseases such as Alzheimer's and Parkinson's. Organisms have developed the Nrf2 (Nuclear factor erythroid-derived 2-like 2) mediated oxidative stress response which eliminates ROS through the transcriptional upregulation of antioxidant genes to protect cells against aging and disease (206). Nrf2 is a Cap'n'Collar transcription factor activated and stabilized by phosphorylation, allowing it to break away from its inhibitor the Cul-Keap1-E3 ligase complex, that normally ubiquitinates and labels Nrf2 for degradation (138). Nrf2 then moves into the nucleus to bind to ARE (Antioxidant response element) promoter sites to induce the transcription of cytoprotective and notable antioxidants genes such as glutathione-synthesizing enzymes (207).

If highly reactive hydroxyl radicals come into contact with DNA it can destabilize the backbone, threatening its integrity. As a result, oxidative stress produced as by-products of radiation and other environmental stressors can contribute to tumor progression (208). Increased survival and expression of the Nrf2 target gene SOD1 (Superoxide dismutase 1) in human glioma cells and mouse hematopoietic myeloid progenitors was observed after exposure to radiation (209,210). Nrf2 has also been found to bind to the ARE of 53BP1 (p53-binding protein 1), a protein involved in NHEJ DNA repair (211). Interestingly, the DNA repair protein BRCA1 has also been linked to the regulation of the oxidative stress response. BRCA1 has been found to physically interact and promote Nrf2 stability, and loss of BRCA1 saw reduced antioxidant gene expression and an accumulation of ROS (212). Thus it can be inferred that increased Nrf2 activity plays a more expansive cytoprotective role to promote cell survival in response to stress (213).

The *C. elegans* Nrf2 ortholog is known as SKN-1, and is activated in response to oxidative stress, xenobiotics and bacterial infection. SKN-1 is a maternally expressed transcription factor that regulates the transcription of similar Nrf2 conserved target genes (214). Similar to Nrf2, SKN-1 possesses a conserved DNA binding DIDLID domain at the N-terminus, required for transcriptional activation and the ability to interact with its inhibitor WDR-23 (WD40 repeat protein) (214–216). SKN-1 is required for embryonic fate through maternal specification of the endomesoderm, giving rise to cells of body wall muscle and the pharynx, making SKN-1 mutations lethal (217). In adult worms, SKN-1 is expressed in amphid chemosensory neurons to regulate worm longevity and is highly active in the intestine, the major worm oxidative stress response organ (165).

In response to stress, SKN-1 is regulated positively by MPK-1 and PMK-1 phosphorylation and enters intestinal nuclei for the transcriptional activation of genes that promote longevity, initiates detoxification as well as the unfolded protein response (165). PMK-1 directly phosphorylates SKN-1 for its nuclear accumulation in response to oxidative stress and pathogen infection. Interestingly, a loss of *pmk-1* saw no change in lifespan, while RNAi knockdown of *mpk-1* reduced worm lifespan. Increased MPK-1 signaling with *lip-1* RNAi, increased lifespan and was found to be dependent on SKN-1. Thus specific MPK-1 phosphorylation may be the mechanism for SKN-1 dependent regulation of lifespan (165).

In addition to negative regulation by WDR-23, SKN-1 can also be inhibited through phosphorylation by IIS pathway terminal kinases. Inhibition of the IIS pathway with a *daf-2* mutation, increased *skn-1* expression levels (218). With a loss of *skn-1* function, the extended lifespan of long-lived *daf-2* mutants is also lost (218). AKT-1, AKT-2 and another IIS target kinase SGK-1 (Serum and glucocorticoid inducible kinase 1 ortholog) were found to

phosphorylate SKN-1. In the same study, RNAi knockdown of *akt-1*, *akt-2* and *sgk-1* all increased SKN-1 accumulation into intestinal nuclei (218). Thus IIS terminal kinase activation can phosphorylate SKN-1 to inhibit its function, while a reduction of IIS allows SKN-1 nuclear translocation for the transcription of phase II detoxification genes, to increase oxidative stress resistance and prolong longevity independently of DAF-16 (218).

EEL-1 is an E3 ubiquitin ligase that can bind to and target SKN-1. A loss of *eel-1* early in embryogenesis (2-cell stage) reduces the asymmetric expression of SKN-1 (219). Although EEL-1 has been found to promote DNA damage germline apoptosis, when examining the potential role of SKN-1 in apoptosis, it was found that *skn-1* RNAi knockdown produced similar levels of germline apoptosis to the wild type in response to IR and thus may not be necessary for germ cell death (33). SKN-1 is a maternal determinant, which in the germline is only present as an mRNA transcript, while SKN-1 protein is expressed following fertilization (220). In addition to regulating development, detoxification and longevity the IIS pathway has been implicated in the regulation of DNA damage induced germline apoptosis. In this way, it is possible that like Nrf2, SKN-1 may play a greater and more complex role in the regulation of cell survival in *C. elegans*.

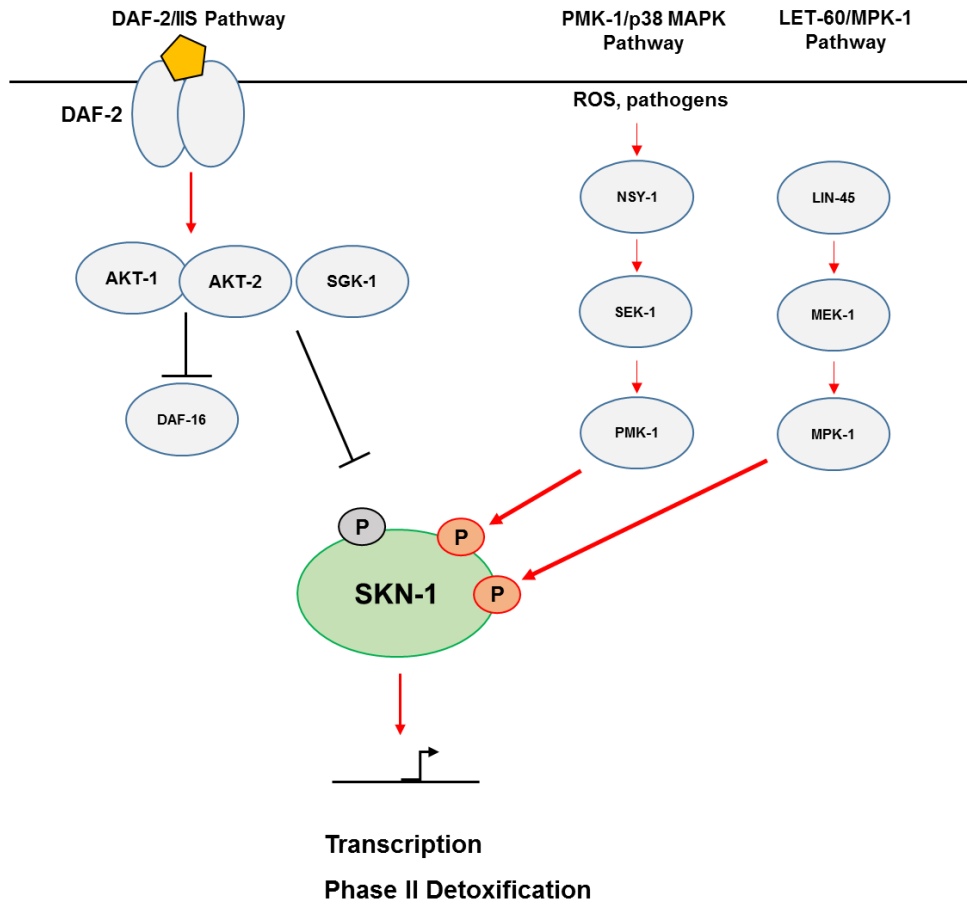


Figure 1.9: Regulation of SKN-1 by MPK-1/ERK, PMK-1/p38 MAPK and DAF-2/IIS pathways

SKN-1 is regulated by several highly conserved pathways in *C. elegans* in response to stress. Activation of SKN-1 occurs through phosphorylation by the effectors kinases MPK-1 and PMK-1, while SKN-1 inhibition can occur via activation of the DAF-2/IIS pathway again via phosphorylation by AKT1/2 and SGK-1. Adapted and modified from (19).

1.7 Rationale, hypotheses and objectives of this study

Current literature has characterized BRAP2 as an E3 ubiquitin ligase, a cytoplasmic retention protein and as an inhibitor of RAS (15,128,131,133). BRAP2 has been found to bind to a variety of proteins from diverse signaling pathways, and displays widespread tissue expression, most robustly in mammalian testes (133). Its function as a scaffold protein during sperm maturation indicates that it may be important for germline development and gametogenesis. However, although the role of BRAP2 as a binding protein has been verified in different contexts, the biological implications of these interactions have not yet all been interpreted. Particularly, the significance of its ability to bind to and prevent BRCA1 nuclear import and potentially its function, has not been extensively studied. BRCA1 is an essential tumor suppressor that regulates several cellular pathways of the DDR including DNA repair via HR, cell cycle arrest and plays a more complex role in apoptosis.

Previous work from our lab has characterized the conserved BRAP2 ortholog known as *brap-2* in *C. elegans*. Koon and Kubiseski (2010) found that the *brap-2(ok1492)* deletion mutant strain experienced L1 developmental arrest and lethality when exposed to the oxidative stress inducer paraquat. In addition, *brap-2(ok1492)* mutants exhibited increased expression of CKI-1 (p21 ortholog). The L1 stage developmental arrest, lethality and increased CKI-1 expression observed in *brap-2* mutants were all dependent on functional BRC-1. This revealed that in response to oxidative stress, a genetic link exists between BRC-1 and BRAP-2. Our lab also discovered that *brap-2(ok1492)* mutants increased intestinal SKN-1 nuclear accumulation and SKN-1 dependent phase II detoxification gene expression, revealing BRAP-2 as a potential regulator of SKN-1 and the oxidative stress response (137).

The ability of BRAP2 to bind to BRCA1, its involvement in RAS signaling, as well as its expression in germline tissue indicate that BRAP2 may be a potential candidate for DDR regulation. We have previously determined that BRAP-2 is involved in the regulation of SKN-1 dependent gene transcription, and identified that a genetic interaction exists between BRAP-2 and BRC-1 during oxidative stress. Furthermore, we detected a decrease in germ cell death in *brap-2(ok1492)* mutants following exposure to IR and qualitatively, we also observed that *brap-2* mutant animals were morphologically distinct to the wild type. Since BRC-1 function in the *C. elegans* DDR pathway of DNA repair is conserved, and *brc-1* mutants' exhibit increased germline apoptosis, we hypothesize that (1) BRAP-2 is a DNA damage response protein, (2) BRAP-2 is required to promote DNA damage induced germline apoptosis, and (3) BRAP-2 is required for *C. elegans* development and germline health. The objectives of this research project is to identify the biological role of BRAP-2 in the DDR, specifically germline apoptosis, and reveal the potential signaling mechanism through which it influences this event, as well as to determine the phenotypical consequences a mutation in *brap-2* has on worm morphology, survival and germline development.

Chapter 2

BRAP-2 promotes DNA damage induced germline apoptosis through the regulation of SKN-1 and AKT-1 in *C. elegans*

Dayana R. D'Amora¹, Queenie Hu^{1,2}, Monica Pizzardi¹ and Terrance J. Kubiseski¹

1. Department of Biology, York University, Toronto, Ontario, Canada

2. Sunnybrook Research Institute, Toronto, Ontario, Canada

Author Contributions

BRAP-2 promotes DNA damage induced germline apoptosis through the regulation of SKN-1 and AKT-1 in *C. elegans*

Dayana R. D'Amora¹, Queenie Hu^{1,2}, Monica Pizzardi¹ and Terrance J. Kubiseski¹

1. Department of Biology, York University, Toronto, Ontario, Canada

2. Sunnybrook Research Institute, Toronto, Ontario, Canada

MANUSCRIPT IN PREPARATION

Queenie Hu assisted in RNA isolation and performing qRT-PCRs in Figures 2.11, 2.13, and 2.15 and assisted in the generation of double mutants for experimentation using standard protocols.

Monica Pizzardi generated double mutants, and performed the Dauer Defective Assay presented in Table 2.1. Terrance J. Kubiseski and I prepared and revised the manuscript.

2.1 Summary

As part of the DNA damage response network, the tumour suppressor BRCA1 (Breast cancer susceptibility gene 1) is activated to facilitate DNA repair, transcription and cell cycle arrest. BRC-1, the *C. elegans* ortholog of BRCA1, has conserved function in DNA double strand break repair, wherein a loss of *brc-1* results in high levels of germline apoptosis (1).

BRAP2/IMP was initially identified as a BRCA1 associated binding protein and previously we have shown that the *C. elegans* *brap-2(ok1492)* deletion mutant experiences BRC-1 dependent larval arrest when exposed to low concentrations of paraquat (2). Since BRC-1 function in the germline is conserved, we wanted to determine the role of BRAP-2 in DNA damage induced germline apoptosis in *C. elegans*. We examined levels of germ cell death following DNA damage and found that *brap-2(ok1492)* mutants display reduced levels of germline apoptosis when compared to the wild type, and the loss of *brap-2* significantly reduced germ cell death in *brc-1* mutant animals. We also found increased mRNA levels of *skn-1* following DNA damage in *brap-2* mutants, where *skn-1* RNAi knockdown in *brap-2;brc-1* double mutants, and a loss of *pmk-1* in *brap-2* mutants increased apoptosis. This indicates that *brap-2* promotion of cell survival requires PMK-1 and SKN-1. Since mammalian BRAP2 has been shown to bind the AKT phosphatase PHLPP1, it suggests that BRAP2 could be involved in the PI3K/AKT pathway. We found that this interaction is conserved between the *C. elegans* homologs and that a loss of *akt-1* in *brap-2* mutants increased germline apoptosis. Thus in response to DNA damage, our findings suggest that BRAP-2 is required to attenuate the pro-cell survival signals of AKT-1 and PMK-1/SKN-1 to promote DNA damage induced germline apoptosis.

2.2 Introduction

Apoptosis is an essential process in development and as part of the DNA damage response ensures the elimination of abnormal cells that can lead to tumor formation and the onset of cancer (3). In *C. elegans*, apoptosis is genetically conserved and functions in the germline to provide cytoplasmic components and maternal determinants to growing oocytes, as well as remove cells whose DNA has been damaged beyond repair by exogenous stressors such as ionizing radiation (IR), chemicals and toxins (4).

Apoptosis activated by the p53-like protein CEP-1 occurs in the pachytene region of the germline, known as the “death loop” (4). DNA damage leads to the activation of upstream DNA damage sensors that phosphorylate and activate CEP-1 (5–7). CEP-1 transcriptional upregulation of pro-apoptotic factors EGL-1 and CED-13 release CED-9 inhibition of CED-4 to activate CED-3 for the execution of apoptosis (6). BRC-1 (BRCA1 ortholog) has been reported to facilitate the conserved repair of DNA double strand breaks through homologous recombination through inter-sister recombination (1). *brc-1* mutants exhibit increased levels of germline apoptosis, increased embryonic lethality and X-chromosome non-disjunction leading to an increase in males (8).

BRAP2 (BRCA1-binding protein 2 or BRAP as listed in the HUGO database) in mammalian systems has been characterized as a RAS-responsive effector protein, an E3 ubiquitin ligase and a cytoplasmic retention protein (9). BRAP2 was first found to bind to the nuclear localization signal (NLS) motifs of BRCA1 and retain BRCA1 in the cytoplasm, preventing its nuclear localization (10). BRAP2 has also been found to bind and prevent the nuclear import of other proteins such as SV40 T antigen, p21 and CDC14 (13–15). Recently,

BRAP2 has been found to bind to and act as a scaffold protein for PHLPP1, an AKT protein phosphatase, in mouse testes (11). The AKT pathway is also conserved in *C. elegans* and is known as the DAF-2 or Insulin/Insulin-like growth factor signaling (IIS) pathway, which regulates the oxidative stress response, longevity and developmental arrest (12,13).

In *C. elegans*, BRAP2 is conserved and is known as BRAP-2 (2). When exposed to oxidative stress induced by paraquat, *brap-2* mutants experience lethality and L1 developmental arrest due to high levels of CKI-1 (p21 ortholog) in seam cells (2). It was determined that a loss of BRC-1 in *brap-2* mutants prevented lethality and developmental arrest, as well as decreased CKI-1 levels, establishing a genetic link between BRAP-2 and BRC-1 in this context. In response to oxidative stress, the transcription factor SKN-1 (Nrf2 ortholog) is activated to initiate detoxification (14). Previously, we also found that a loss of *brap-2* increases SKN-1 target gene expression (15).

Due to the conservation of BRC-1 function in *C. elegans* and the genetic interaction between BRC-1 and BRAP-2 upon oxidative stress, we examined the role of BRAP-2 in DNA damage induced germline apoptosis. We found that *brap-2(ok1492)* mutants' exhibit a reduction in DNA damage induced germline apoptosis and that germline apoptosis induced by loss of BRC-1 requires BRAP-2. We also determined that *brap-2* mutants are dauer defective and the interaction between PHLP-2 (*C. elegans* homolog of AKT protein phosphatase PHLPP1/2) and BRAP-2 is conserved in *C. elegans*. We also found that a loss of PMK-1, SKN-1 and AKT-1 in *brap-2* mutants increased germline apoptosis, while *phlp-2* mutants have reduced apoptosis. Taken together, these observations suggest a model in which a loss of BRAP-2 limits DNA damage induced germline apoptosis and promotes cell survival through the regulation of the PMK-1 activated SKN-1/Nrf2 oxidative stress response pathway and the IIS Pathway.

2.3 Materials & Methods

2.3.1 *C. elegans* strains and genetics

All worm strains were cultured under standard conditions, as previously described (16). Strains were obtained from the *Caenorhabditis* Genetics Center located at the University of Minnesota and from the National Bioresource Project in Tokyo, Japan. Double mutant strains were generated according to standard protocols. The N2 Bristol strain was used as the wild type, and unless noted otherwise all experiments were conducted at 20°C. The following strains were used in this study: *akt-1(ok252)V* (YF198), *akt-2(ok393) X* (VC204), *brap-2(ok1492) II* (YF15), *brap-2(ok1492) II*; *akt-1(ok525) V* (YF198), *akt-1(ok252) V*; *phlp-2(tm7788) III* (YF193), *brap-2(ok1492) II*; *akt-2(ok393) X* (YF188), *brap-2(ok1492)/mIn 1 [MIs14dyp10(e128)] II* denoted as *brap-2(ok1492)/+* (YF104), *brc-1(tm1145) III* (DW102), *brap-2(ok1492) II*; *brc-1(tm1145) III* (YF64), *cep-1(gk138) I* (YF62), *brap-2(ok1492) II*; *cep-1(gk138) I* (YF63), bcIs39 [*lim-7p::ced-1::GFP + lin-15(+)*] (MD701), bcIs39; *brap-2(ok1492) II* (YF180), *ced-9(n2812) III/hT2 [bli-4(e937) let-?(q782) qIs48] (I;III)*; *nIs106 X* (PD9927), *brap-2(ok1492) II*; *ced-9(n2812) III/hT2 [bli-4(e937) let-?(q782) qIs48] (I;III)*; *nIs106 X* (YF179), *daf-16(mu86) I* (CF1038), *brap-2(ok1492) II*; *daf-16(mu86) I* (YF19), *brc-1(tm1145) III*; *daf-16(mu86) I* (YF189), *mpk-1(ga111) unc-79(e1068) III* (temperature sensitive, maintained at 15°C) (SD939), *brap-2(ok1492) II*; *mpk-1(ga111) unc-79(e1068) III* (YF94), *pmk-1(km25) IV* (KU25), *brap-2(ok1492) II*; *pmk-1 IV* (YF197), *phlp-2(tm7788) III* (YF200), *daf-16(mu86) I*; muIs61 (CF1139), *brap-2(ok1492) II*; *daf-16(mu86) I*; muIs61 (YF190).

2.3.2 Worm Synchronization

For all worm assays, worms were synchronized via egg lay as described by the Morimoto Lab (<http://groups.molbiosci.northwestern.edu/morimoto/research/Protocols>).

2.3.3 Irradiation

Worms were synchronized to the L4 stage and exposed to ionizing radiation using a ^{137}Cs sources (in coordination with the Derry Lab, McMaster Building & Sick Kids Peter Gilgan Research Tower) at indicated doses. Worms were left to recover for 18-24 hours on Nematode Growth Media (NGM) plates before visualization, apoptosis, RNA extraction and qRT-PCR, and mitotic arrest analyses.

2.3.4 Fluorescence Microscopy

Worms were picked and anesthetized using 2 mM Levamisole (Sigma L9756) and mounted on 2% agarose pads. Images of fluorescent worms were taken using a Zeiss LSM 700 confocal laser-scanning microscope with Zen 2010 Software.

2.3.5 Germline Apoptosis Assay

Worms were allowed to recover for 18-24 hours and corpses (apoptotic cells) were scored using Acridine Orange (AO) staining as previously described (17,18). Worms were paralyzed in 2 mM Levamisole and mounted on 2% agarose pads, where 15-20 gonad arms per genotype were scored per treatment. Apoptotic cells in developing embryos were scored in specific embryonic stages directly using the *ced-1p::GFP* strain.

2.3.6 DNA Staining

To quantify germline nuclei, whole worms were stained with DAPI as previously described (19). Z-stack images were taken and using the Zen 2010 Lite software free-form surface area measurement tool was used to measure gonad surface area of one representative slice. The ImageJ Cell Counter plugin was used to determine the total number of nuclei per zone in one gonad arm per worm in one representative slice.

2.3.7 Gonad Dissection

Gonad dissection and immunostaining was performed as previously described (20), with the following changes: Approximately 20-30 synchronized 1 day old adults were mounted onto 20 μ L of 2 mM Levamisole in M9 buffer on Superfrost Polylysine (Fisher 12-5550-15) coated slides in an area made with Immaedge Hydrophobic Pen (VECTOR Labs H-4000) and the heads or tails were removed with a “scissor-like” motion using 27G syringe needles. To this, 10 μ L 2% paraformaldehyde was added, coverslip mounted and were allowed to sit for 10 minutes and then frozen on an aluminum block on dry ice for 10 minutes. Slides were then freeze cracked using a razor blade and submerged in -20°C methanol for fixation for 1 minute.

2.3.8 Immunostaining

Dissected Germlines: Following methanol fixation, slides were washed with 1X PBST 3 times for 5 minutes. Incubated for 1 hour in 2% BSA for 1 hour in a humid chamber. Primary antibody was added and incubated overnight at room temperature. Slides were washed 3X with 1X PBST and then secondary antibody was added dropwise and incubated for 1 hour at room temperature in a humid chamber in the dark. Slides were washed 4X with 1X PBST for 5 minutes and in the third wash, 1 μ g/mL DAPI (Sigma D9542) was added. Before mounting, 3 μ L of Prolong Gold

Anti-Fade Reagent (ThermoFisher P36930) was added and coverslips were sealed using clear nail polish. Antibodies used were: rabbit anti-BRAP-2 (1:100) and Alexa Fluor 488 (1:1000) (ThermoFisher A11001) secondary antibody was used for fluorescent visualization. Rabbit polyclonal anti-sera against *C. elegans* BRAP-2 (EEED8.16) was generated by the Toronto Recombinant Antibody Centre of the University of Toronto using a GST fusion protein with BRAP-2 antigen corresponding to residues 108 to 134 which lie in the N terminus of the protein.

Worm Western Blot: Approximately 200 μ L of packed mixed-stage worms were washed 3X with M9 buffer and then re-suspended in worm lysis buffer [50 mM HEPES pH 7.5, 100 mM NaCl, 10% Glycerol, 1 mM EDTA, protease (EMD Millipore 539137) and phosphatase inhibitor cocktail II (Sigma P5726) and III (Sigma P0044)] followed by sonication (10s ON/10s OFF, 10% amplitude for 1.5 min). The lysates were cleared twice by centrifugation (15 minute at 13,000 x g) and the total protein lysate concentration was measured using the BCA assay according to the manufacturer's protocol (ThermoScientific 23227). Proteins (50 μ g of protein per genotype) were resolved using 10% SDS-PAGE gels and transferred to Millipore Immobilon-P PVDF (IPVH0010) membranes. Membranes were blocked with 5% skim milk and then probed with the following antibodies: anti-phospho p38 MAPK (Cell Signal 9211S), anti-AKT-1 527 (1:1000), anti-AKT-1 128 (1:1000) (Gift from the Derry Lab), and anti-tubulin (1:2000) (Cell Signal 3873). For visualization, proteins were detected using Luminata Crescendo Western HRP Substrate (EMD Millipore WBLURO100) and blots were imaged using the DNR Bio Imaging Systems Microchemi System. Band density was measured and normalized to their respective anti-tubulin protein levels using the Gel Analyzer in ImageJ.

2.3.9 RNA Interference (RNAi) Analysis

Worms were synchronized on RNAi plates (NGM containing 0.4 mM IPTG, 100 µg/mL Ampicillin and 12.5 µg/mL Tetracycline) and fed with *E. coli* HT115 (DE3), transcribing double stranded RNA (dsRNA) from fusion bacterial plasmids homologous to the target with pL4440 used the control. When animals reached the 1st day of adulthood they were then treated and assayed for germline corpse quantification. The *skn-1* RNAi plasmid was obtained from a transcription factor specific RNAi library, as described (41). The *akt-1* RNAi plasmid was purchased from GE Dharmacon (CeRNAi Feeder C12D8.10 10014-B-6). The *brap-2* RNAi construct was made by amplifying region 1-843 nucleotides of the *brap-2* ORF by PCR, using the EST yk1134a01 as template, and cloning into the KpnI site of pL4440. The *phlp-2* RNAi construct was made by amplifying region 2618-2800 nucleotides of the predicted *phlp-2* ORF (F43C1.1; Wormbase Version WS258) by PCR, using the EST yk1149d03 as template, and cloning into the KpnI site of pL4440.

2.3.10 RNA Isolation and Quantitative Real Time PCR (qRT-PCR)

Worm RNA Isolation, qRT-PCR and data analysis was performed as described previously (15). Approximately 100 µL of packed mixed-stage worms (IR treated and untreated controls) were collected and washed with M9 buffer 3X and unless extraction occurred immediately, samples were frozen at -80°C. RNA was extracted with TRI Reagent (Sigma 93289) as follows: Pelleted RNA was recovered with RNase-free water and residual DNA was digested using the DNA-Free Kit (Ambion AM1906). Total RNA concentration was measured using NanoDrop2000 and 0.5 µg of RNA was used to prepare cDNA following the manufacturer's protocol using the RNA to cDNA kit (Applied Biosystem 4387406). To quantify mRNA levels, qRT-PCR was performed

using SYBR green premix (Clontech 693676)/SensiFast SYBR Green (FroggaBio BIO-98005) and the Qiagen Rotor-Gene Q System (Qiagen R0511133). Data were derived from 3 biological replicates. Data analysis was performed using the Applied Biosystems Comparative CT Method ($\Delta\Delta$ CT Method). mRNA expression levels of each strain was compared relative to the wild type (N2) control, where the housekeeping gene *act-1* (Actin) was used as the endogenous control for normalization. To verify equal primer amplification efficiency a standard curve for each set of primers was constructed using a serial dilution of cDNA. Using the qPCR Efficiency Calculator (ThermoFisher), amplification efficiency (%) of the qPCR reaction was determined based on the R^2 value and the slope of the standard curve.

2.3.11 DAF-16 Localization Assay

DAF-16 expression was viewed *in vivo* using the reporter strain CF1139. To investigate DAF-16 expression in a *brap-2(ok1492)* mutant background, transgenic strains were generated using standard protocols and confirmed by Single Worm PCR (SW-PCR). Worms were synchronized to L4 stage and treated with 5 mM sodium arsenite (Sigma 35000-1L-R) in M9 Buffer for 1.5 hours to induce acute stress (21). For each genotype, worms were visualized and DAF-16::GFP expression was scored as cytoplasmic, intermediate or nuclear (22).

2.3.12 Dauer Defective Assay

The dauer defective assay was performed as previously described (23). Single adult worms from each strain were picked onto individual OP50 seeded NGM plates and allowed to grow for 2 weeks to enter dauer developmental arrest. Each plate was flooded with 1 mL of 1% SDS solution and allowed to sit for 30 minutes. Each plate was then observed under a stereomicroscope to assess the state of the worms. If worms were found to be thrashing on the

plate they were confirmed to have survived (proper entry into dauer). If worms were found to be motionless they were deemed dead (failed to enter dauer). For each genotype, a minimum of 40 starved plates were examined

2.3.13 Survival Analysis

Synchronized worms were raised at 20°C. Worms were exposed to 60 Gy IR at the L4 stage and survival was scored beginning on the first day of adulthood and compared to non-irradiated controls. Worm survival was scored every 2 days, with worms pronounced dead if no response to prodding at the head or tail was produced. Missing worms or those that developed “bag of worms” phenotype, were censored from the analysis. Worms were transferred to fresh NGM plates every 2 days.

2.3.14 Plasmid Construction

To construct 3xFLAG::PHLP-2, the C-terminal region of PHLP-2 (1428bp) was amplified from worm cDNA and the product was cloned in frame to a BamHI and EcoRI digested pCMV 7.1 (3xFLAG) vector. The N-terminal region (1682bp) of PHLP-2 was amplified from synthesized DNA (Biomatik) using the Wormbase F34C1.1 sequence into a NotI and BglI digested pCMV 7.1 (3xFLAG) vector containing the PHLP-2 C-terminal region, using the HI-FI Assembly Mix (NEB M5520A) following the manufacturer’s protocol.

2.3.15 GST Pull Down Assay and Western Blot Analysis

In this study, Human Embryonic Kidney (HEK) cells were used to assess physical interactions between our *C. elegans* proteins of interest. HEK cells were cultured in Dulbecco’s Modified Eagle’s Medium supplemented with 10% Fetal Bovine Serum. Cells were co-transfected for 48

hours, with 5 µg DNA of each mammalian expressing construct using polyethylenimine (PEI) (Sigma 408727-100 mL) and Optimem (Clontech 31985). The interaction between GST::BRAP-2 and 3xFLAG::PHLP-2, and GST::ΔCT-BRAP-2 and 3xFLAG::PHLP-2, was verified through co-transfection in HEK-293T cells and a GST pull-down assay. Cells were lysed in lysis buffer (1X TBS, 1% NP-40, 1% Glycerol, 150 mM NaCl, and complete protease inhibitor cocktail). The GST tagged protein was then pulled down from cell lysates using Glutathione Sepharose Beads (GE Healthcare 45000139), according to the manufacturer's protocol with a modification, washing of the beads was carried out 6X for 15 minutes before sample analysis. Samples were analyzed by standard SDS polyacrylamide gel, followed by Western Blot. The following antibodies were used: anti-FLAG M2 (1:5000) (Sigma F1804), anti-GST (1:5000) (Cell Signal 2625P). Proteins were then detected using SuperSignal West Femto Maximum Sensitivity Substrate (ThermoScientific 34095) and blots were imaged using the DNR Bio Imaging Systems Microchemi System.

2.3.16 Statistical Analysis

Statistical analysis was performed with GraphPad Prism 5 Software. Statistical significance was determined using Two-way ANOVA and Bonferroni post tests for comparison between different groups. Student's t-test was performed when comparing two means. P values of <0.05 were taken to indicate statistical significance. Error bars represent +/- standard error of the mean.

2.4 Results

2.4.1 BRAP-2 promotes DNA damage induced germline apoptosis

Since BRC-1 function in the DNA damage response is conserved in the germline, we used an anti-BRAP-2 antibody and immunostained wild type dissected germlines to identify the expression pattern of BRAP-2. We found BRAP-2 to be expressed in the cytoplasm of both wild type and *brap-2(ok1492)* mutant hermaphrodite germlines, surrounding germline nuclei creating a “honeycomb” effect, prior to and following exposure to DNA damage (Figure S2.1).

Localization of BRAP-2 in the germline suggests that it may be necessary for proper germline development and may also function to regulate other DNA damage response events including apoptosis, mitotic arrest and DNA repair.

This study focused on the *brap-2(ok1492)* mutant, which possesses a 1540 bp deletion in the C-terminal region (removing exons 5-8, ZnF-UBP and leucine heptad repeats domains) (Figure S2.2) (2). First, to determine whether BRAP-2 is necessary for the induction of germline apoptosis we scored the number of apoptotic cells (corpses) in *brap-2* mutants. Unlike *brc-1* mutants, we observed a decrease in apoptosis in *brap-2(ok1492)* mutants compared to the wild type following DNA damage (Figure 2.1A). When we introduced the *ced-1p::GFP* reporter strain in *brap-2(ok1492)*, allowing for both early and late phase apoptotic cells to be detected (18), a 50% reduction in corpse appearance following DNA damage was observed (Figure S2.3). However, physiological levels of apoptosis in *brap-2(ok1492)* mutants are similar to the wild type (Figure 2.1A), indicating that *brap-2* may specifically regulate DNA damage induced germline apoptosis.

Since we previously established a genetic link between BRC-1 and BRAP-2 during oxidative stress and observed that BRAP-2 may promote DNA damage induced germline

apoptosis, we hypothesized that *brap-2* is required for the high levels of germline apoptosis in *brc-1* mutants. To test this, we generated a *brap-2(ok1492);brc-1(tm1145)* double mutant and scored apoptosis levels following IR. At 60 Gy, we observed a significant reduction in germ cell death at both 60 and 120 Gy (Figure 2.1A). When both wild type and *brc-1(tm1145)* mutants were fed *brap-2* RNAi, a similar 2.5-fold reduction in apoptosis was observed (Figure 2.2A). This indicates that excessive apoptosis caused by a loss of *brc-1* is dependent on *brap-2*. Following DNA damage, heterozygous *brap-2(ok1492)* mutants [*brap-2(ok1492)/+*], which contain one wild type allele and one mutant allele (*ok1492*) for *brap-2*, display similar levels of apoptosis to the wild type (Figure 2.2B). This suggests that in this context, one wild type *brap-2* allele is able to restore apoptosis. Thus reduced cell death caused by *brap-2(ok1492)* may be a homozygous recessive trait. Even 48 hours after DNA damage exposure, *brap-2(ok1492)* mutants displayed low levels of apoptosis compared to the wild type (Figure 2.3). Therefore *brap-2* does not affect the timing or kinetics of corpse appearance.

To ensure that reduced apoptosis in *brap-2* mutants was not caused by a decrease in germ cell number, we scored the number of nuclei before and after DNA damage using whole worm DAPI staining (19). The number of germline nuclei per μm^2 in *brap-2(ok1492)* mutants at 0 and 60 Gy did not differ significantly compared to the wild type (Figure 2.4A). Although physiologically, we found *brap-2* mutants experienced a 20% reduction in total germline nuclei compared to the wild type (Figure 2.4B), we believe that this does account for the consistent and greater than 50% reduction in apoptosis seen in *brap-2* mutants following DNA damage. In order to determine whether BRAP-2 is involved in the regulation of apoptosis of somatic cells, we scored the number of apoptotic cells in developing embryos using a *ced-1p::GFP* reporter strain.

We found that in 5 distinct stages of embryonic development, *brap-2(ok1492)* mutants displayed no significant difference in the number of corpses when compared to the wild type (Figure 2.4C).

The 9-1-1 checkpoint (MRT-2, HUS-1, CLK-2) is a complex of protein sensors that interpret DNA damage signals and relay them to induce mitotic arrest in an attempt to repair DNA (8). If the damage is beyond repair, signals are sent to ATM-1 and ATL-1 kinases that can activate CEP-1 (p53 ortholog) for the induction of apoptosis (5,25). In the *C. elegans* germline, nuclei that have arrested in the mitotic zone can be viewed directly, enlarging transiently following DNA damage to enter G2 phase cell cycle arrest (19). Interestingly, *brap-2(ok1492)* mutants displayed an increase in mitotically arrested nuclei physiologically, and a more robust proportion of arrested nuclei following IR exposure (Figure 2.5). This suggests that while a loss of BRAP-2 may potentially enhance mitotic cell cycle arrest, BRAP-2 is not required for mitotic arrest induction and thus does not function as a DNA damage sensor upstream of CEP-1. Therefore, a loss of BRAP-2 does not (i) alter the timing of corpse appearance, (ii) inhibit germline proliferation, (iii) or prevent mitotic arrest. These results suggest that BRAP-2 specifically promotes DNA damaged induced germline apoptosis and is required for a *brc-1* mutant triggered activation of apoptosis.

Interestingly, when exposed to stressors such as paraquat and IR, DNA repair mutants like *brc-1* live longer than the wild type (26). We found that before and after DNA damage exposure, mean survival of *brap-2* mutant animals is reduced, living on average 2 days less than the wild type. However, with the loss of *brc-1* the mean survival of *brap-2(ok1492)* mutants was extended to resemble the wild type, both before and after DNA damage. Therefore, this suggests that reduced survival caused by a loss of *brap-2* is dependent on BRC-1 (Figure S2.4).

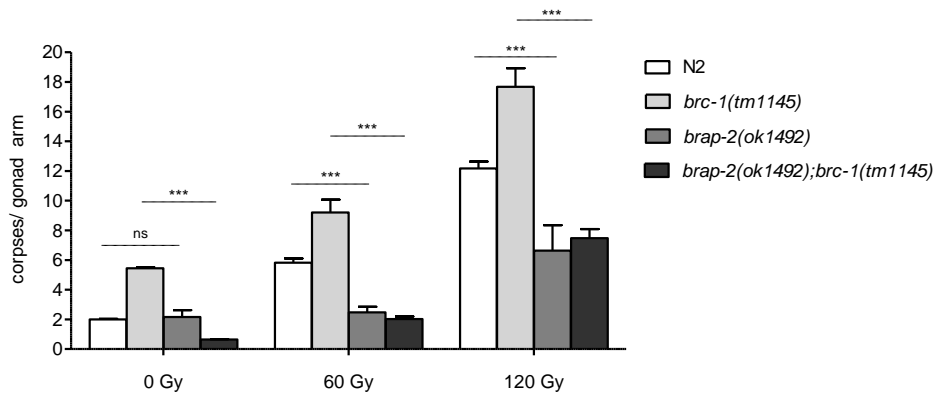
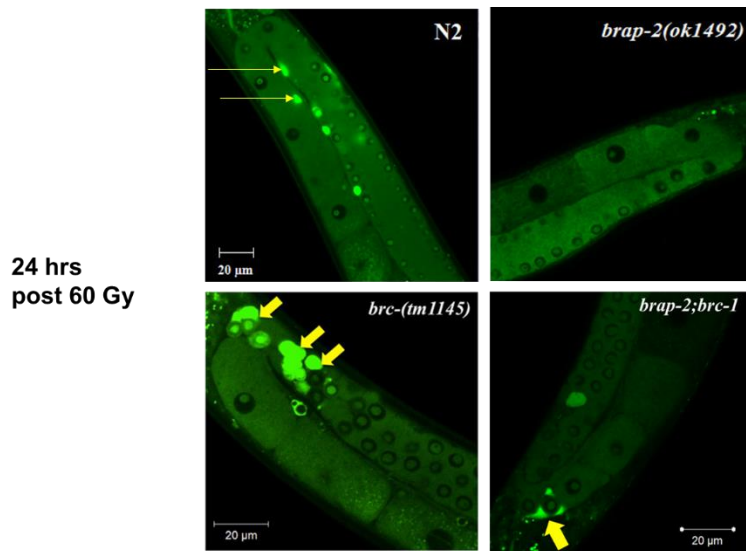
A**B**

Figure 2.1: BRAP-2 promotes DNA damage induced germline apoptosis

(A) Following IR *brap-2(ok1492)* mutants displayed a significant reduction in apoptosis compared to the wild type (N2). At 60 Gy, *brc-1(tm1145)* mutants have an incidence of 9.20 ± 0.90 corpses, while *brap-2;brc-1* double mutants exhibit a 4.5-fold decrease in apoptosis with 2.02 ± 0.17 corpses. A reduction in apoptosis with a loss of *brap-2* is also observed at 120 Gy. (B) Representative images of germline corpses (indicated with yellow arrows) 24 hours post IR. A significant reduction of apoptosis was observed in *brap-2* and *brap-2;brc-1* double mutants compared to N2 and *brc-1* mutants. Results represent 3 independent trials. Two trials were completed at 120 Gy. Corpses were scored 24 hours post IR using Acridine Orange (AO). $p < 0.001$ ***.

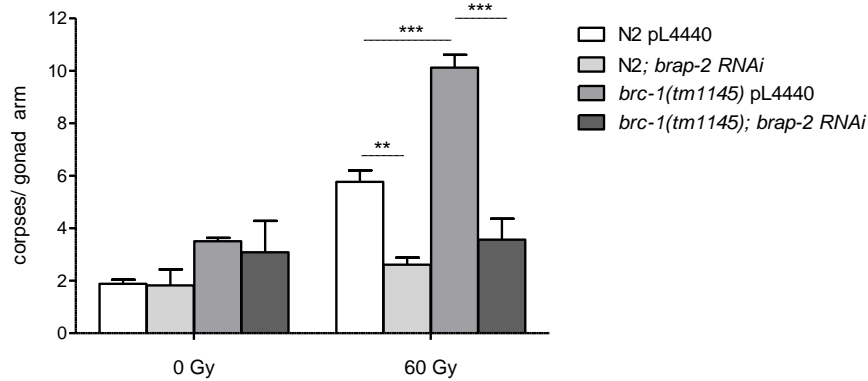
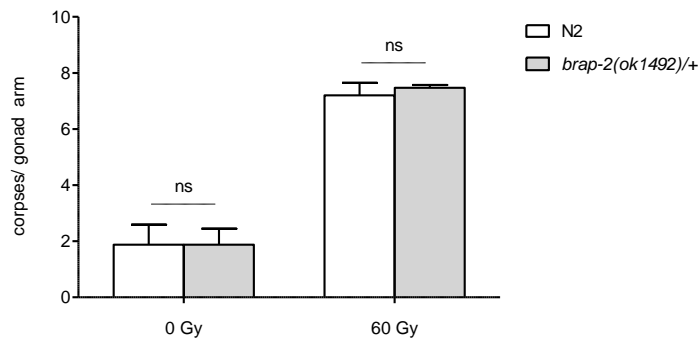
A**B**

Figure 2.2: One wild type *brap-2* allele restored apoptosis following DNA damage

(A) Using *brap-2* RNAi to knockdown *brap-2* expression, a 2.5-fold reduction in apoptosis was observed in wildtype (N2) and *brc-1* mutant animals. Worms were grown on *brap-2* RNAi bacteria or control pL4440, irradiated at the L4 stage and corpses were scored 24 hours post IR using AO. (B) Heterozygous *brap-2* [*brap-2(ok1492)/+*] worms displayed similar levels of apoptosis to N2, indicating that one wild type *brap-2* allele restores apoptosis to wild type levels. Corpses were scored 24 hours post IR using AO. Results represent 3 independent trials. $p < 0.001$ ***, $p < 0.01$ **.

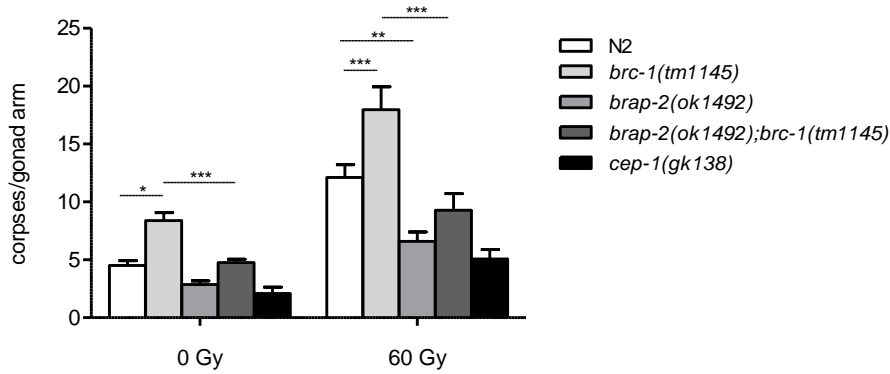
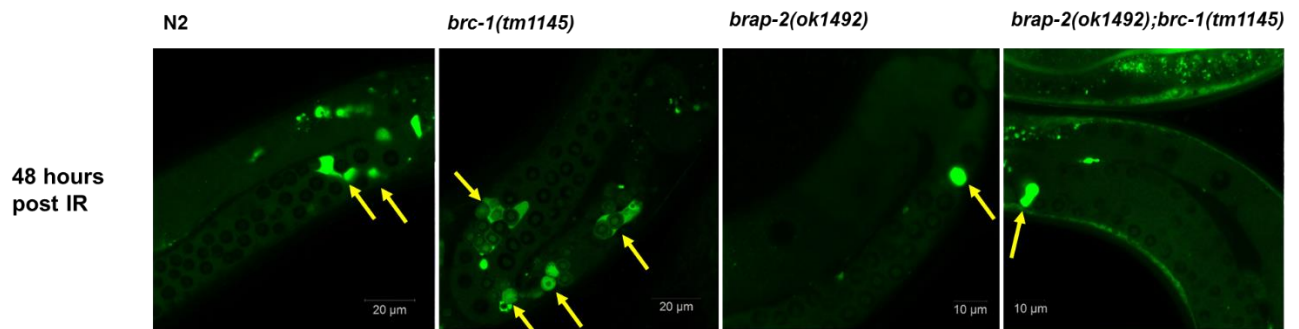
A**B**

Figure 2.3: BRAP-2 does not alter the rate of corpse appearance

(A) Reduced apoptosis in *brap-2(ok1492)* mutants was maintained 48 hours after IR exposure. This indicates that a loss of BRAP-2 does not delay corpse appearance. (B) Representative confocal images taken of germlines 48 hours post 60 Gy of IR. Worms were stained with AO and corpses were scored after 48 hours, following 0 and 60 Gy. Results represent 3 independent trials. Yellow arrows indicate apoptotic cells. Two independent trials at 60 Gy were completed for *cep-1(gk138)*. $p < 0.001$ ***, $p < 0.01$ ** , $p < 0.05$ *.

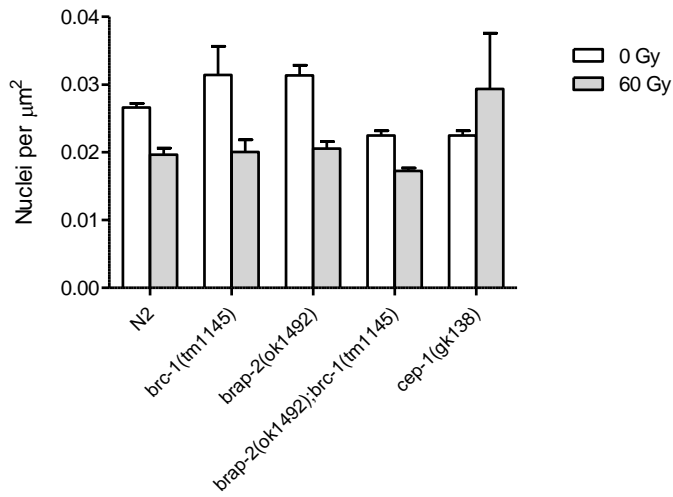
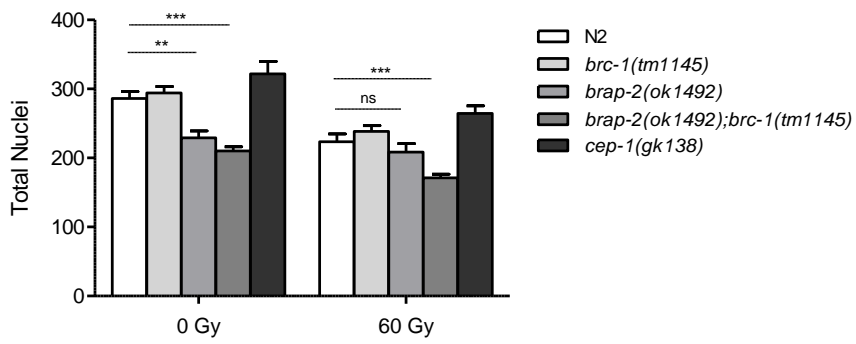
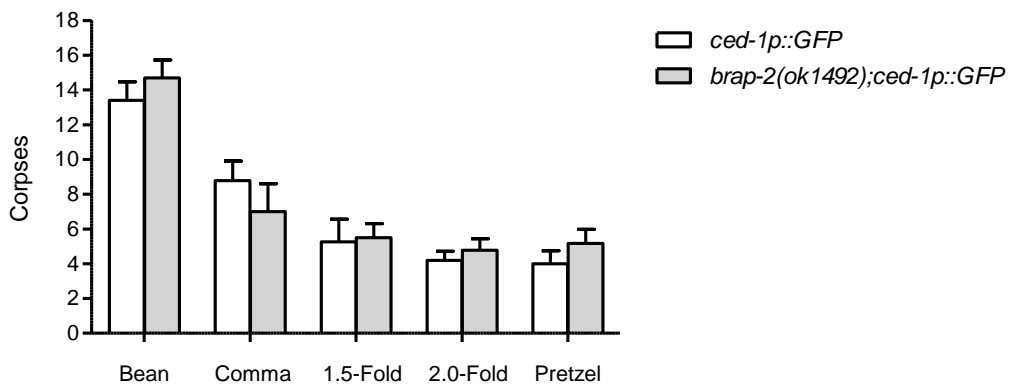
A**B****C**

Figure caption on next page.

Figure 2.4: BRAP-2 does not affect germ cell proliferation and is specific to germline apoptosis

(A) The number of germline nuclei per μm^2 at 0 and 60 Gy in these mutants did not differ significantly from each other and were similar to the wild type (N2). Thus a mutation in *brap-2* does not alter germ cell number. Results represent N = 40 per genotype. (B) Total germline nuclei at 0 and 60 Gy were counted in these mutants. An approximately 20% reduction is seen in *brap-2* mutants compared to the wild type at 0 Gy, but no difference is observed at 60 Gy. Results represent N = 14-31 per genotype. One day old whole worms were fixed and stained with DAPI. The surface area was measured using Zen 2010 Lite Software and the total number germline nuclei were scored in 1 slice of each Z-stack using ImageJ. (C) The number of corpses detected in each embryonic stage in *brap-2(ok1492)* mutants is similar to the wild type. This suggests that BRAP-2 is specific to germline cell death regulation and is not involved in somatic or developmental programmed cell death. Z-stack images were taken and corpses were counted manually in each embryonic stage using a *ced-1p::GFP* reporter strain. Results represent N = 8-12, per embryonic stage per genotype. $p < 0.001^{***}$, $p < 0.01^{**}$.

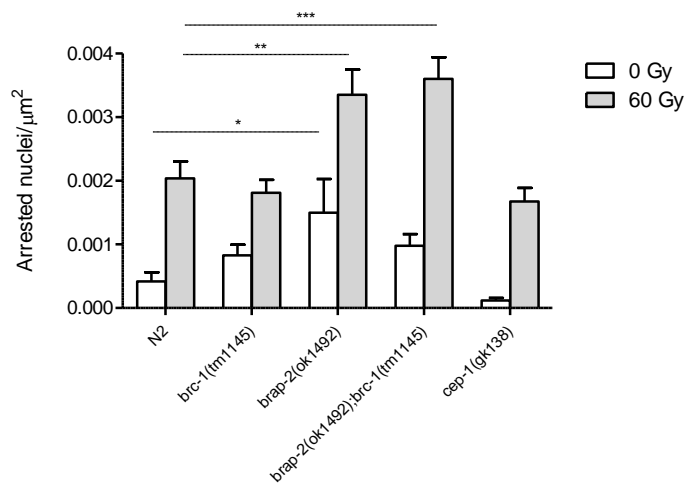
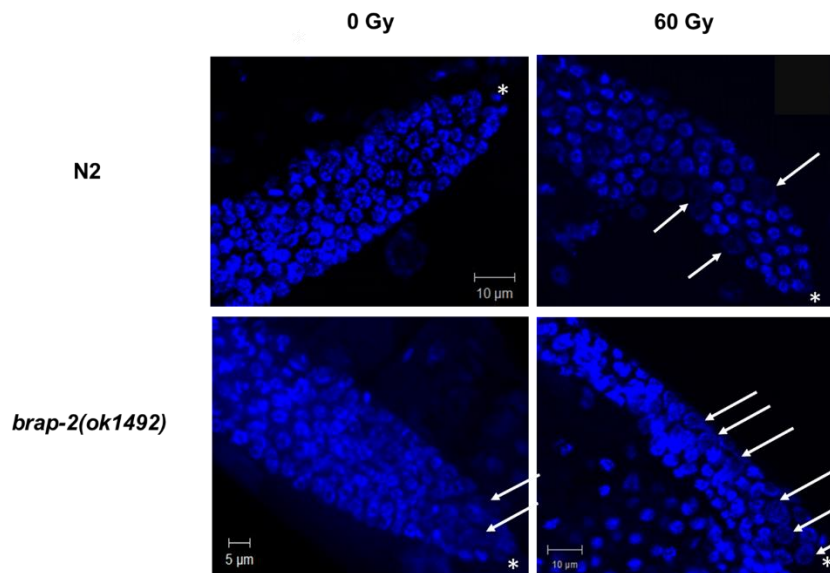
A**B**

Figure 2.5: *brap-2(ok1492)* induces robust mitotic arrest following DNA damage

(A) *brap-2(ok1492)* mutants displayed an increase in the number of arrested nuclei (per μm^2) in the mitotic zone (MZ) compared to the wild type (N2). (B) Representative confocal images of the MZ for each genotype at 0 and 60 Gy. One day old whole worms were stained with DAPI. Arrested nuclei transiently enlarge (indicated by white arrows) and were scored manually using Zen 2010 Software. White asterisk indicates distal tip of the gonad. Results represent N= 15-40 per genotype. $p < 0.001$ ***, $p < 0.01$ ** , $p < 0.05$ *.

2.4.2 BRAP-2 functions upstream or independently of the CEP-1 activated programmed cell death pathway

DNA damage induced germline apoptosis is activated by a conserved canonical signaling pathway initiated by CEP-1, the *C. elegans* p53-like protein that activates cell death through the transcriptional up-regulation of *egl-1* and *ced-13* (BH3 orthologs) (27–29). EGL-1 and CED-13 proteins bind to and inhibit CED-9 (BCL2 ortholog), an anti-apoptotic protein that normally impedes apoptosis by inhibiting CED-4 (APAF1 ortholog) from activating the downstream caspase CED-3 (28–30). To determine whether a loss of *brap-2* affects the expression of *egl-1* and *ced-13*, we performed qRT-PCR before and after DNA damage exposure. *brap-2* mutants displayed a significant increase in both *egl-1* and *ced-13* mRNA expression levels both prior to and following DNA damage induction (Figure 2.6A,B). This increased expression of *egl-1* and *ced-13* indicates that *brap-2(ok1492)* mutants may have increased CEP-1 activity, where BRAP-2 may act as a potential negative regulator of CEP-1.

Following DNA damage, *cep-1* mutants display a resistance to apoptosis, which is associated with the failure to activate the transcription of *egl-1* and *ced-13* (Figure 2.7) (31). *brap-2(ok1492)* mutants display reduced apoptosis similar to *cep-1* mutants following DNA damage exposure (Figure 2.7A). We also found that increased *egl-1* and *ced-13* expression levels in *brap-2* mutants is abolished with a loss of *cep-1* (Figure 2.7B). Thus *egl-1* and *ced-13* expression in *brap-2* mutants is dependent on CEP-1. CED-9 (BCL2 ortholog) is a “pro-survival” gene that prevents apoptosis, and its ablation leads to immense germ cell death and inviability (32). Interestingly, *brap-2* mutants also displayed elevated *ced-9* mRNA levels following DNA damage (Figure 2.6C). To investigate the potential interaction between BRAP-2 and CED-9, we generated *brap-2;ced-9* double mutants and assessed apoptosis levels. We observed that a loss of *brap-2* in *ced-9* mutants failed to reduce the high levels of apoptosis seen

in *ced-9* mutants (Figure 2.8), indicating that the decreased apoptosis seen in *brap-2* mutants probably requires CED-9. Together, this suggests that BRAP-2 may function upstream or independently of the CEP-1 activated pathway of DNA damage induced germline apoptosis.

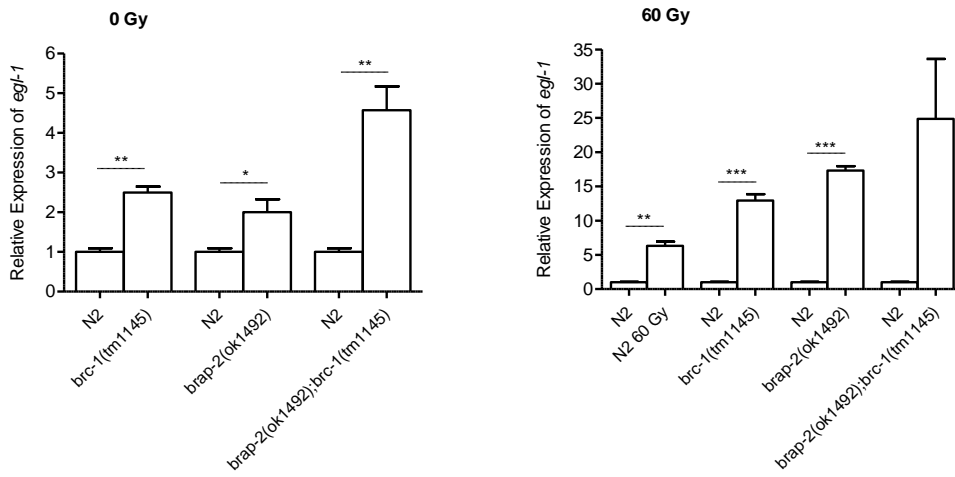
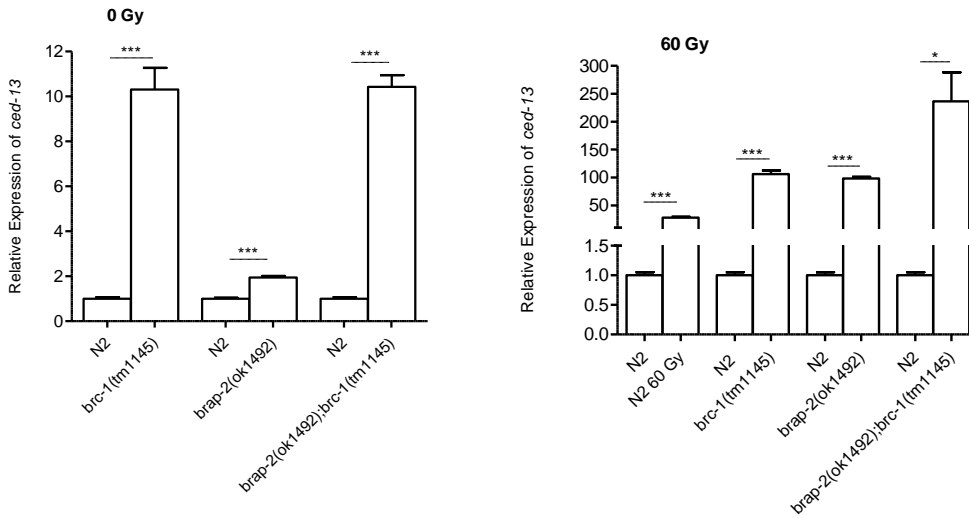
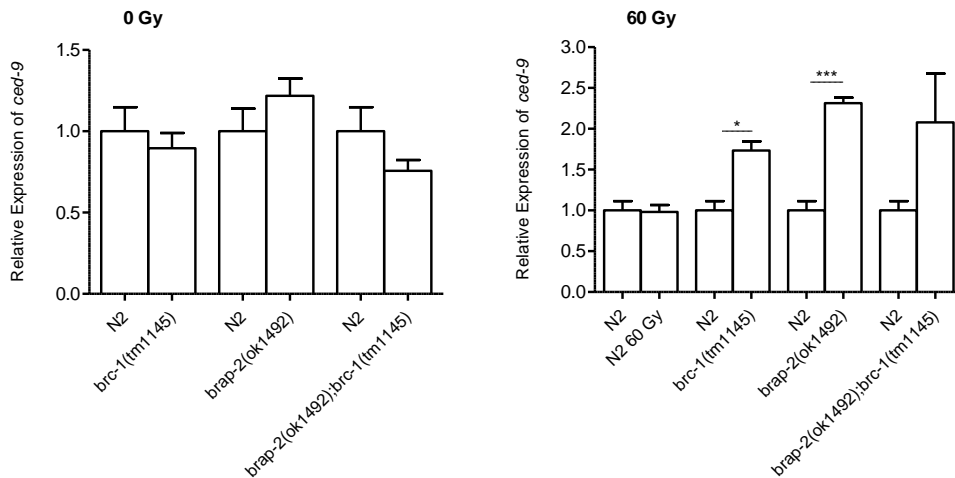
A**B****C****Figure caption on next page.**

Figure 2.6: *brap-2(ok1492)* increased apoptosis gene expression

Using qRT-PCR, mRNA levels of (A) *egl-1*, (B) *ced-13* (pro-apoptotic) and (C) *ced-9* (anti-apoptotic) were quantified at 0 Gy and following 60 Gy of DNA damage. Following IR, levels of *egl-1*, *ced-13* and *ced-9* are enhanced in *brap-2(ok1492)* mutants. Results represent 3 independent trials, normalized to *act-1* of the wild type (N2) 0 Gy. $p < 0.001$ ***, $p < 0.01$ **, $p < 0.05$ *.

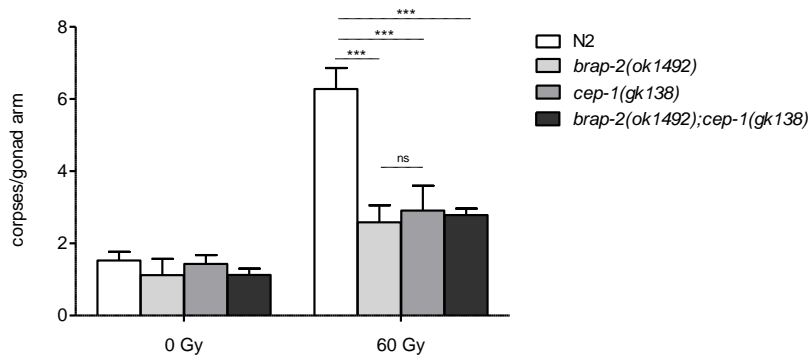
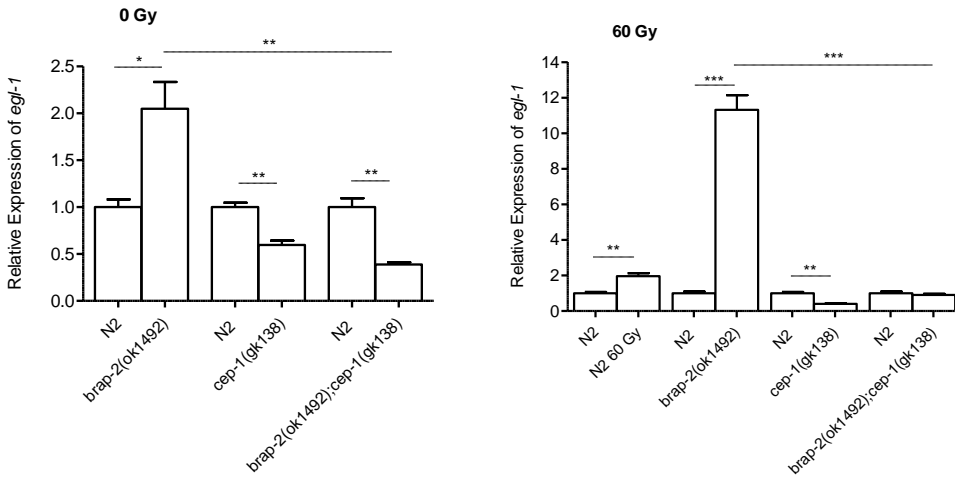
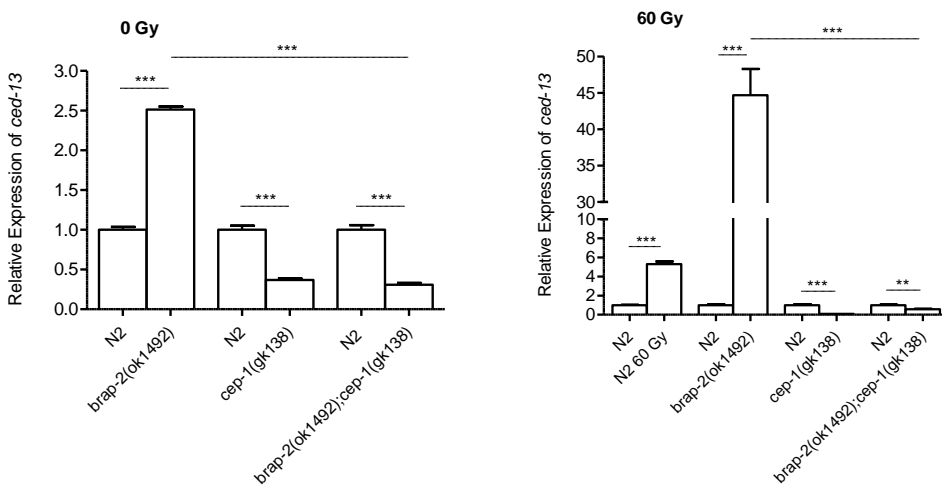
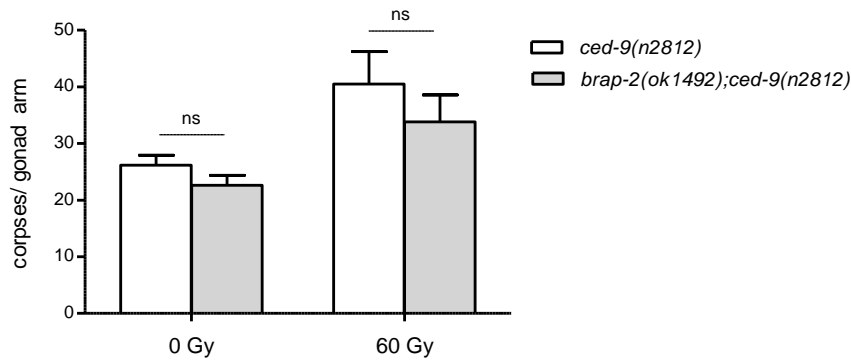
A**B****C****Figure caption on next page.**

Figure 2.7: Expression of *egl-1* and *ced-13* in *brap-2* mutants is dependent on CEP-1

(A) Levels of apoptosis in *brap-2(ok1492)* mutants is similar to that of *cep-1(gk138)* mutants. Results represent 3 independent trials. Corpses were scored and visualized 24 hours post IR using AO. (B) *brap-2(ok1492)* displayed increased *egl-1* and (C) *ced-13* expression levels that were reduced with the loss of *cep-1*. This indicates that the potential increased CEP-1 activity in *brap-2* mutants is dependent on CEP-1. Transcript levels were quantified using qRT-PCR prior to and following DNA damage. Results represent 3 independent trials, normalized to *act-1* of the wild type (N2) at 0 Gy. $p < 0.001$ ***, $p < 0.01$ ** , $p < 0.05$ *.

A



B

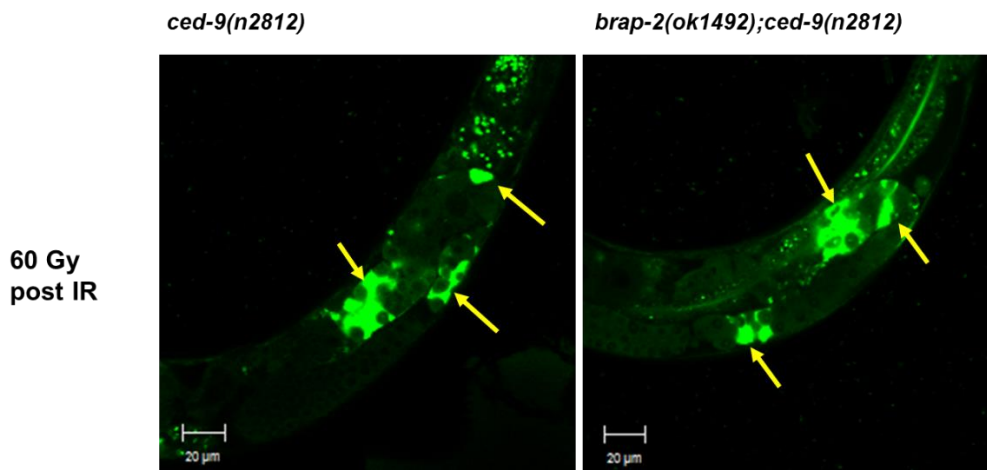


Figure 2.8: Loss of *brap-2* did not reduce apoptosis in *ced-9* mutants

(A) Loss of CED-9 causes massive germline cell death and inviability. A loss of *brap-2* in *ced-9* mutants produced no significant difference in apoptosis prior to or following DNA damage.

(B) Representative images of irradiated mutant gonads for comparison 24 hours post IR. Worms were irradiated at the L4 stage and corpses were scored using AO 24 hours post IR. Yellow arrows indicate apoptotic cells. Results represent N= 31-41 and N= 11-12 gonads at 0 Gy and 60 Gy, respectively.

2.4.3 Loss of SKN-1/Nrf2 increases apoptosis in *brap-2; brc-1* mutants

SKN-1 is an essential transcription factor for the initiation of gene expression to protect against harmful reactive oxygen species (ROS), and serves as an embryonic precursor for intestinal and mesoendodermal development (14,33). Overexpression of SKN-1 leads to extension of the *C. elegans* lifespan that may be attributed to ROS removal maintaining cellular homeostasis, helping to promote health and survival (34,35). IR can directly harm cells by inducing double-strand breaks (DSBs) in DNA and indirectly, through ‘radiolysis’, the hydrolysis of water molecules leading to ROS production and possible disruption of nucleic acids, proteins and lipids (50).

Previously, we have found that a loss of *brap-2* increased *skn-1* mRNA levels, and increased SKN-1 intestinal nuclear localization and phase II detoxification gene expression (15). This prompted us to determine whether SKN-1 is involved in the regulation of DNA damage induced germline apoptosis. We found that *brap-2* mutants experience a 2-fold increase in *skn-1* mRNA levels after IR (Figure 2.9A). Thus we hypothesized that SKN-1 acts as a transcriptional regulator of apoptosis. To determine if core apoptosis gene expression requires SKN-1, we fed wild type worms with *skn-1* RNAi and measured *cep-1*, *egl-1*, *ced-13* and *ced-9* mRNA levels. *skn-1* RNAi produced significant reductions in all genes tested (Figure 2.9B), indicating that at least at physiologically, SKN-1 may be required for apoptosis gene expression.

We then asked whether the reduction of apoptosis in *brap-2* mutants was dependent on SKN-1. Using RNAi, we knocked down *skn-1* in *brap-2* mutants and scored germline apoptosis before and after IR. As previously reported, we also observed that *skn-1* RNAi knockdown does not affect apoptosis levels in wild type worms (31). Although *skn-1* RNAi also did not increase apoptosis in single *brap-2* mutants, *skn-1* RNAi increased apoptosis in *brap-2; brc-1* double

mutants to levels similar to the wild type (Figure 2.9C). This suggests that a loss of *brap-2* may promote cell survival in *brc-1* mutants, in part through SKN-1 activation.

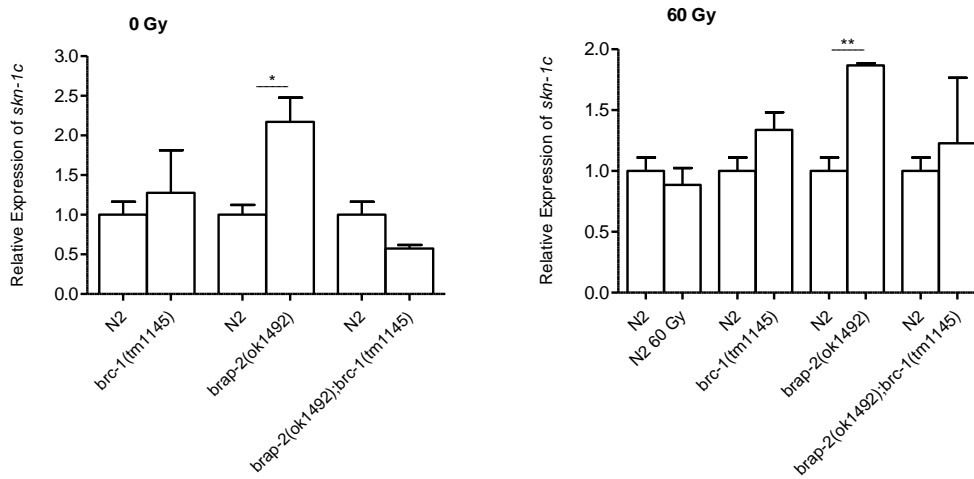
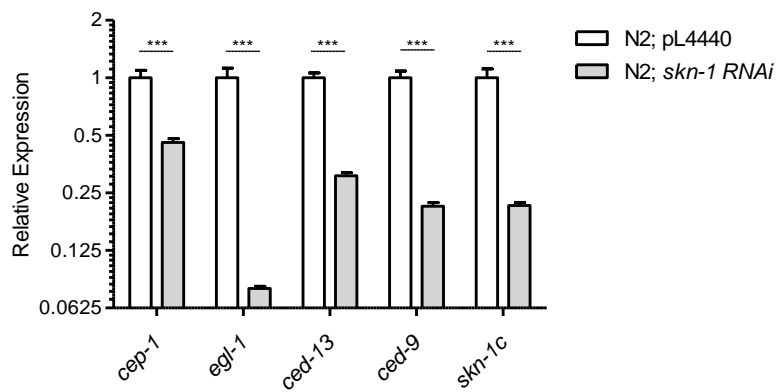
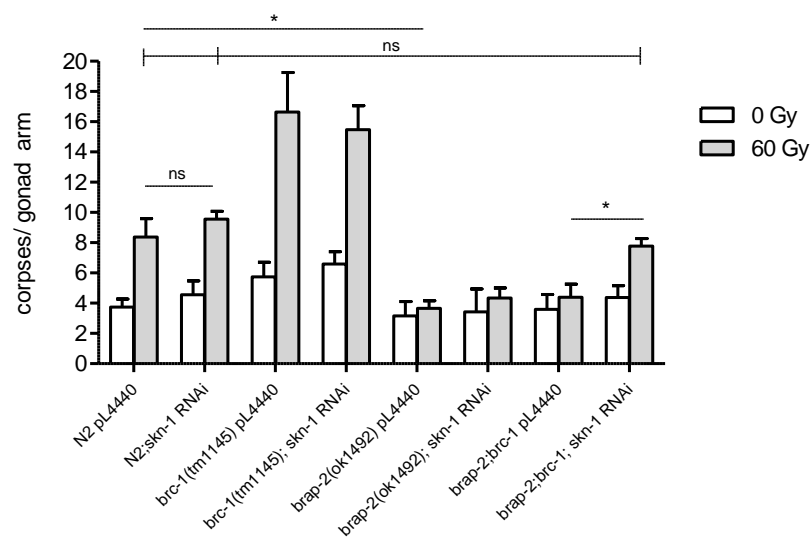
A**B****C**

Figure caption on next page.

Figure 2.9: *skn-1* RNAi knockdown increases apoptosis in *brap-2*;*brc-1* double mutants following DNA damage

(A) qRT-PCR was performed before and after DNA damage. Levels of *skn-1c* are elevated in *brap-2* mutants following IR. Results represent 3 independent trials, normalized to *act-1* of the wild type (N2). (B) Expression levels of apoptosis genes were measured in N2 worms fed with *skn-1* RNAi. *skn-1* knockdown was confirmed by quantifying *skn-1c* transcripts. A reduction in *cep-1*, *egl-1*, *ced-13* and *ced-9* levels was observed. Results represent 3 independent trials, normalized to *act-1* of N2 (log2 scale). (C) Although *skn-1* RNAi in the wild type does not affect apoptosis levels, *skn-1* knockdown in *brap-2*;*brc-1* increased apoptosis to levels similar to the wild type. Results represent 3-7 trials. Two trials were completed for *brc-1(tm1145)* and *brap-2(ok1492)* on pL4440 at 0 Gy. Apoptotic cells were scored 24 hours post IR using AO. p<0.001***, p<0.01**, p<0.05*.

2.4.4 Loss of *pmk-1* increases germline apoptosis in *brap-2(ok1492)* mutants

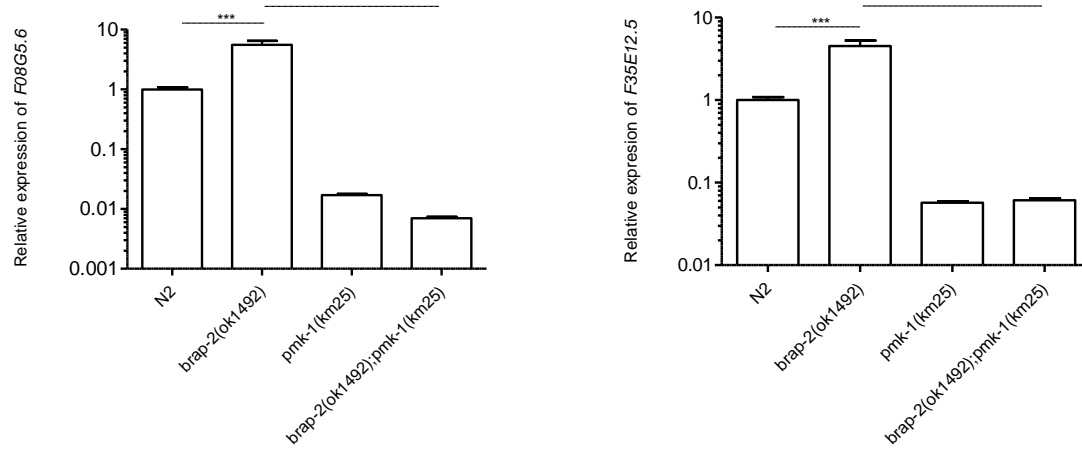
Phosphorylation of SKN-1 by MPK-1 (ERK ortholog) and PMK-1 (p38 MAPK ortholog) kinases promote SKN-1 entry into intestinal nuclei and transcription of target detoxification genes to mount a defence against oxidative stress (36,37). Phosphorylated MPK-1 has been found to be required for apoptosis activation and the progression of pachytene nuclei to oogenesis (4,38). We previously found that *brap-2(ok1492)* mutants display a 1.5-fold increase in phosphorylated MPK-1. However, in *brap-2(ok1492)* mutants a loss of *mpk-1* did not increase apoptosis after DNA damage exposure, and only reduced *egl-1* mRNA levels (Figure S2.5).

In addition to SKN-1 activation, a loss of PMK-1 has been found to prevent arsenite induced germline apoptosis independently of CEP-1 (39). We next asked if PMK-1 was required for BRAP-2 regulation of DNA damage induced germline apoptosis. To determine whether PMK-1 activity is elevated in *brap-2* mutants we measured the mRNA expression levels of two known PMK-1 target genes *F35E12.5* (40) and *F08G5.6* (41), expressed as part of the innate immune response to defend against bacterial pathogens (41–43). We found that *brap-2* mutants have a significant PMK-1 dependent 4.5-fold and 5.3-fold ($p < 0.001$) increased expression of *F08G5.6* and *F35E12.5* respectively (Figure 2.10A).

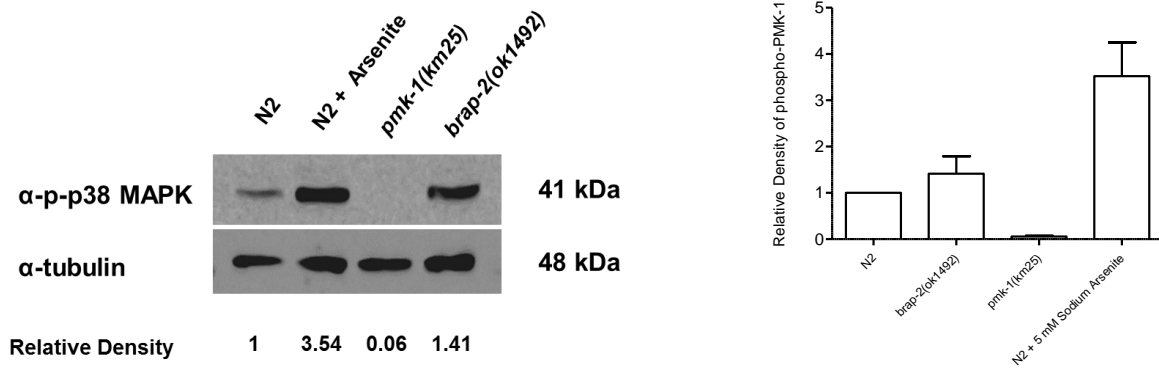
We performed Western blot of worm lysates to quantify the levels of phosphorylated PMK-1 in *brap-2* mutants. *brap-2* mutants displayed a 1.41-fold increase in phospho-PMK-1 compared to the wild type, indicating that *brap-2* mutants may have an increase in activated PMK-1 (Figure 2.10B). Although a loss of *pmk-1* reduced *egl-1* and *ced-13* mRNA levels by half, loss of *pmk-1* in *brap-2(ok1492)* did not decrease the levels of these apoptotic genes (Figure S2.5B). We then asked if increased PMK-1 activity contributes to the reduced apoptosis in *brap-2* mutants following DNA damage exposure. To verify this, we scored apoptosis levels in *brap-*

2;pmk-1 double mutants and found that a loss of *pmk-1* in *brap-2(ok1492)* mutants elevated apoptosis to wild type levels (Figure 2.10C). Together, these results suggest that the reduction in apoptosis in *brap-2(ok1492)* mutants is dependent on PMK-1 activity and indicates that reduced levels of apoptosis previously seen in *brap-2;brc-1* mutants, may be mediated in part by SKN-1 through PMK-1 activation.

A



B



C

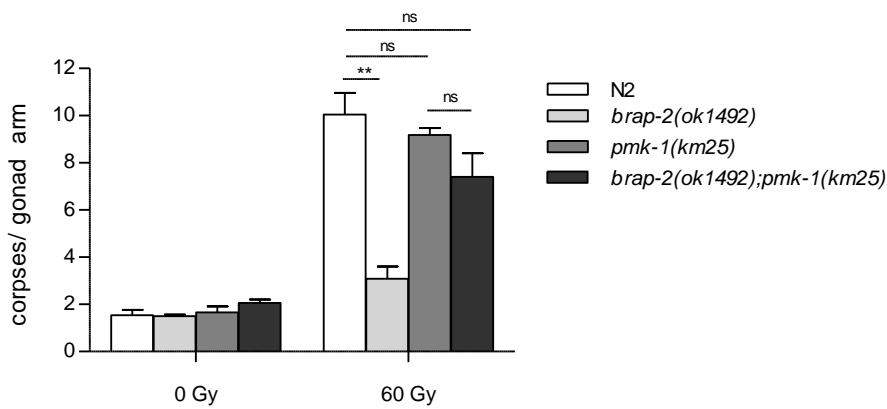


Figure caption on next page.

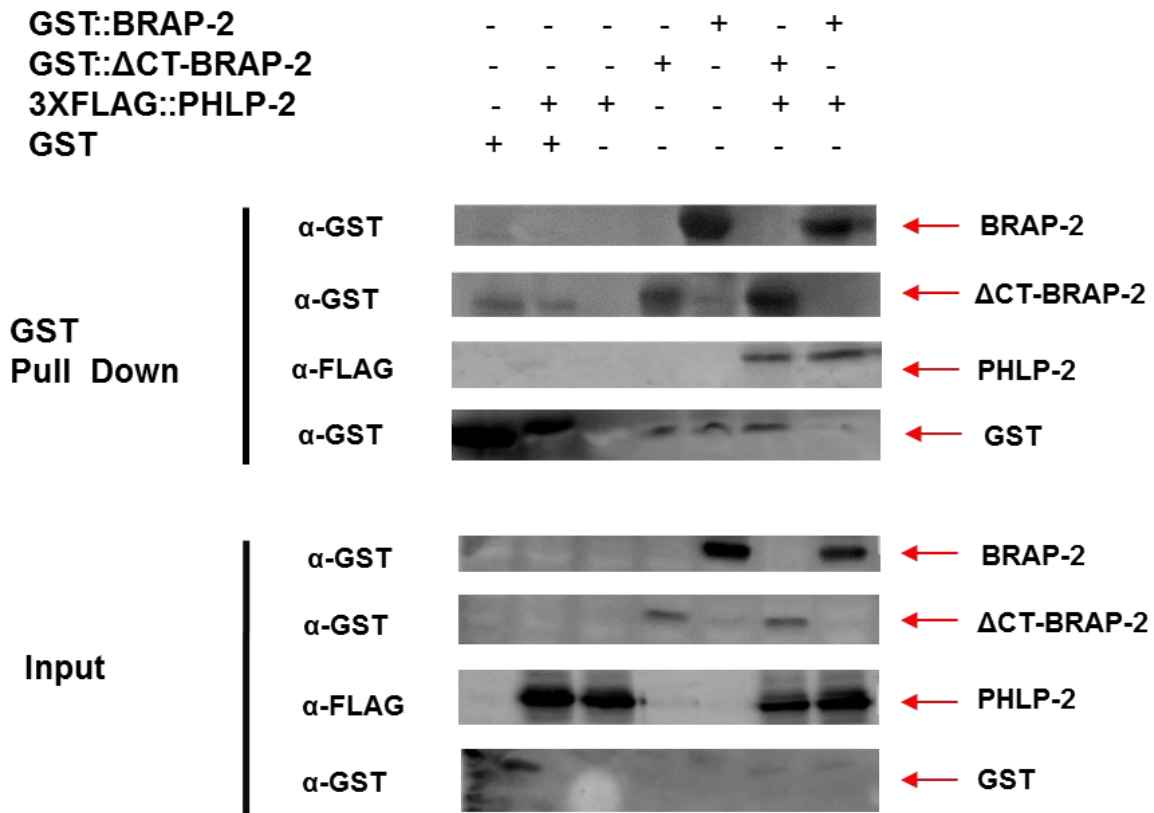
Figure 2.10: Loss of *pmk-1* increased germline apoptosis in *brap-2* mutants

(A) qRT-PCR was used to measure PMK-1 activity by quantifying the levels of PMK-1 targets *F08G5.6* and *F35E12.5* (log10 scale). Transcript levels of both genes increased significantly in *brap-2* mutants and was dependent on PMK-1. Results represent 3 independent trials, normalized to *act-1* of the wild type (N2). (B) A 1.41-fold increase in phospho-p38 MAPK/PMK-1 intensity is seen in *brap-2(ok1492)* mutants compared to N2. N2 treated with 5 mM sodium arsenite was used as a positive control, while the *pmk-1(km25)* mutant was used as a negative control. Results represent 3 independent trials. Band intensity was measured in ImageJ, normalized to their respective α -tubulin levels and then compared to N2. Graph represents the average relative density of phosphorylated PMK-1 for each genotype. (C) Loss of *pmk-1* in *brap-2* mutants increased apoptosis to levels comparable to N2. Corpses were scored before and after IR using AO. Results represent 3 independent trials. $p < 0.001$ ***, $p < 0.01$ **.

2.4.5 Interaction between PHLPP1 and BRAP2 in *C. elegans* is conserved

BRAP2 is expressed in many tissues but is most enriched in mammalian testes (11). An Y2H (Yeast 2 Hybrid) screen using a human testes specific cDNA library uncovered several potential BRAP2 binding partners, and one protein uncovered was the AKT protein phosphatase PHLPP1 (11). AKT is a serine/threonine kinase responsible for promoting cell survival, growth and proliferation (44). AKT is inactivated by the removal of phosphate groups at two sites, Thr308 and Ser473 (45). PHLPP1 dephosphorylates AKT at Ser473 (46,47) and as a result completes AKT inactivation, preventing the inhibition of FOXO and other targets which promote cell death (48). The interaction between BRAP2 and PHLPP1 was determined to prevent PHLPP1 from reaching spermatocyte nuclei, indicating that BRAP2 may act as a PHLPP1 binding protein (11).

This was of interest to us since we found that BRAP-2 expression is conserved in the cytoplasm of the *C. elegans* hermaphrodite germline (Figure S2.1). In *C. elegans*, PHLP-2 (F43C1.1) is orthologous to PHLPP1 and PHLPP2. Using a GST pull down assay and Western blot we found that BRAP-2 physically binds to PHLP-2, indicating that this interaction is conserved (Figure 2.11). We also found that a truncated form of BRAP-2, denoted as Δ CT-BRAP-2 which mimics the *ok1492* mutant protein and lacks the C-terminal region (removing the RING, Zinc Finger and coiled-coil domains) was also able to bind to PHLP-2. This indicates that the C-terminal portion of BRAP-2 is not necessary for this interaction. Therefore, it is possible that BRAP-2 may function to regulate the activation of the IIS/AKT pathway in *C. elegans*.



2.4.6 *brap-2* mutants are dauer defective

Developmental arrest (dauer) is initiated by inactivation of IIS leading to inhibition of AKT-1 and AKT-2 (AKT orthologs), allowing DAF-16 (FOXO ortholog) to enter the nucleus for the transcriptional upregulation of pro-survival and dauer genes (49–51). Mutants of the IIS pathway can leave worms dauer constitutive and in a constant state of developmental arrest, or dauer defective where they are unable to initiate the arrested state for survival (50). While maintaining our *brap-2(ok1492)* strain, we observed that they did not appear to enter dauer when starved and previous work from our lab showed that *brap-2(ok1492)* mutants displayed no change in the expression levels of *sod-3* (SOD3 ortholog), a DAF-16 target gene involved in phase I ROS detoxification (15). Thus we hypothesized that *brap-2* mutants may increase IIS signaling leading to DAF-16 inactivation.

To test this we performed a dauer defective assay (23), where following nutrient deprivation dauer worms were isolated with 1% Sodium Dodecyl Sulfate (SDS) treatment. We found that similar to *daf-16(mu86)* mutants, *brap-2(ok1492)* mutants were unable to survive SDS treatment (Table 2.1), indicating that the *brap-2(ok1492)* mutation may inhibit DAF-16, preventing worms from entering the dauer state. We also tested the effect of removing MPK-1, PMK-1, and AKT-1 and found that they rescued the *brap-2* mutants and allowed them to enter dauer (Table 2.1). Interestingly, unlike AKT-1, a loss of AKT-2 in *brap-2* mutants did not restore dauer entry. This suggests that BRAP-2 may function specifically through AKT-1, and not AKT-2 to inhibit DAF-16.

Increased IIS signaling causes phosphorylation of DAF-16 preventing its nuclear accumulation in the intestine and targeted gene transcription (51). Since we observed *brap-2*

mutants to be dauer defective, we hypothesized IIS signaling is enhanced in *brap-2* mutants, decreasing DAF-16 activity. To verify whether a loss of *brap-2* causes increased IIS signaling, we used qRT-PCR to measure the mRNA expression levels of known targets of this pathway. INS-7 is an insulin/IGF-1 –like peptide (ILP) whose expression is elevated with increased IIS stimulation (52). Similar to *daf-16* mutants, which exhibited increased *ins-7* levels, *brap-2* mutants displayed a 2-fold increase in *ins-7* expression (Figure 2.12A). We also measured the levels of the antioxidant enzyme and DAF-16 target, *ctl-1* (CAT1 ortholog) and found that in *brap-2* mutants *ctl-1* mRNA levels were reduced 167-fold ($p < 0.01$) (Figure 2.12B) (53).

We also examined the localization of DAF-16 *in vivo*, using a DAF-16::GFP reporter strain in a *brap-2(ok1492)* mutant background. As a positive control for DAF-16 activation and nuclear accumulation, worms were treated with 5 mM sodium arsenite. We scored DAF-16::GFP expression in the intestine as cytoplasmic, intermediate or nuclear. We found that both before and following arsenite treatment, *brap-2(ok1492)* mutants displayed a reduction in nuclear accumulation and greater intermediate and cytoplasmic localization of DAF-16 in the intestine (Table 2.2). In addition, we also saw a modest increase in cytoplasmic DAF-16 localization in *brap-2* mutants following 60 Gy of IR. Taken together these results suggest that BRAP-2 may regulate IIS signaling, where a loss of BRAP-2 may lead to increased DAF-16 inhibition by AKT-1, both physiologically and when exposed to exogenous stressors.

Table 2.1: *brap-2* mutants are dauer defective

brap-2(ok1492) mutants were unable to survive SDS treatment following starvation. Loss of *mpk-1*, *pmk-1* and *akt-1* but *akt-2* allowed *brap-2* mutants to enter dauer and survive SDS treatment. Plates were viewed under a dissection microscope and scored as “Thrashing” if worms were alive and moving in solution. This demonstrates selection for dauers due to their ability to resist SDS. Plates were scored as “Dead” if no worm movement in solution was observed.

Strain	N (Number of Plates)	Thrashing (% N)	Dead (% N)
N2	70	100	0
<i>akt-1(ok525)</i>	46	82.61	17.39
<i>akt-2(ok393)</i>	46	65.22	34.78
<i>brap-2(ok1492)</i>	61	0	100
<i>daf-16(mu86)</i>	69	0	100
<i>mpk-1(ga111)</i>	40	95	5
<i>pmk-1(km25)</i>	48	100	0
<i>akt-1(ok525);brap-2(ok1492)</i>	41	65.85	34.15
<i>akt-2(ok393);brap-2(ok1492)</i>	42	4.76	95.24
<i>brap-2(ok1492);mpk-1(ga111)</i>	44	90.91	9.10
<i>brap-2(ok1492);pmk-1(km25)</i>	37	70.27	29.73

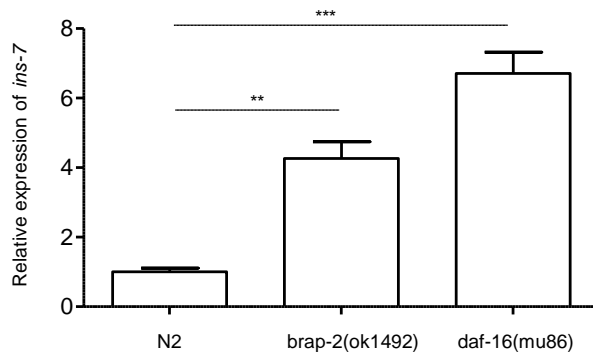
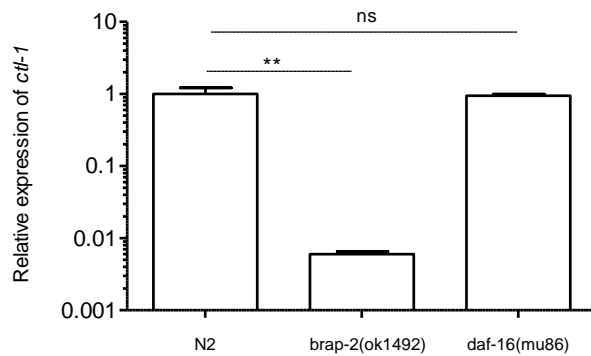
A**B**

Figure 2.12: *brap-2* mutants have increased *ins-7* and reduced *ctl-1* mRNA levels

(A) Using qRT-PCR we found that similar to *daf-16(mu86)* mutants, *brap-2(ok1492)* mutants expressed increased mRNA levels of *ins-7*, an insulin-like signaling peptide whose expression increases with increased IIS pathway stimulation. (B) *ctl-1* (DAF-16 target gene) mRNA expression is significantly reduced in *brap-2* mutants (log10 scale). Results represent 3 independent trials, normalized to *act-1* of the wild type (N2). $p < 0.001$ ***, $p < 0.01$ **.

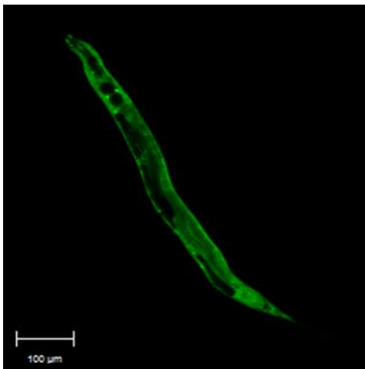
Table 2.2: *brap-2* mutants have increased cytoplasmic DAF-16 localization

Using a DAF-16::GFP reporter, we found that *brap-2(ok1492)* mutants displayed reduced nuclear accumulation, and increased cytoplasmic and intermediate distributions of DAF-16. Worms were scored as having either cytoplasmic, intermediate or nuclear distributions of DAF-16. Representative images of wild type worms depicting cytoplasmic, intermediate and nuclear expression of DAF-16 in the intestine.

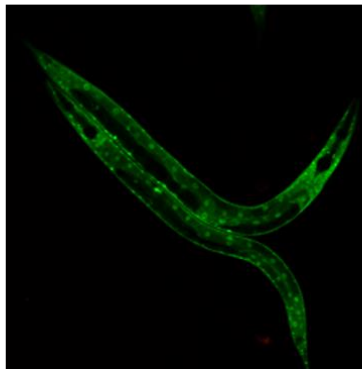
DAF-16::GFP worms (%)

	WT			<i>brap-2(ok1492)</i>		
	0 Gy/ 0 mM Sodium Arsenite	5 mM Sodium Arsenite	60 Gy	0 Gy/ 0 mM Sodium Arsenite	5 mM Sodium Arsenite	60 Gy
Cytoplasmic	23 (15.54)	0 (0)	4 (9.09)	46 (36.80)	31 (36.05)	10 (30.30)
Intermediate	77 (52.03)	28 (28.28)	26 (59.09)	59 (47.20)	33 (38.37)	14 (42.42)
Nuclear	48 (32.43)	71 (71.72)	14 (31.82)	20 (16.00)	22 (25.58)	9 (27.27)
Total	148 (100)	99 (100)	44 (100)	125 (100)	86 (100)	33 (100)

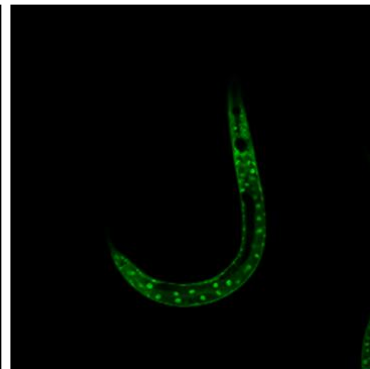
Cytoplasmic



Intermediate



Nuclear



2.4.7 Loss of *akt-1* increased apoptosis in *brap-2* mutants

akt-1 and *akt-2* gain of function mutants have been found to suppress DNA damage induced germline apoptosis (54). Thus the promotion of cell survival through AKT activation in *C. elegans* is conserved. However, in this context AKT isoforms are predicted to function in distinct ways. AKT-1 is thought to inhibit CEP-1 transcriptional activation of *egl-1* and *ced-13*, while AKT-2 functions to inhibit DAF-16 (55). Having found *brap-2* mutants to be dauer defective and inhibit DAF-16 function, we hypothesized that BRAP-2 may function through AKT-1 to regulate DNA damage induced germline apoptosis.

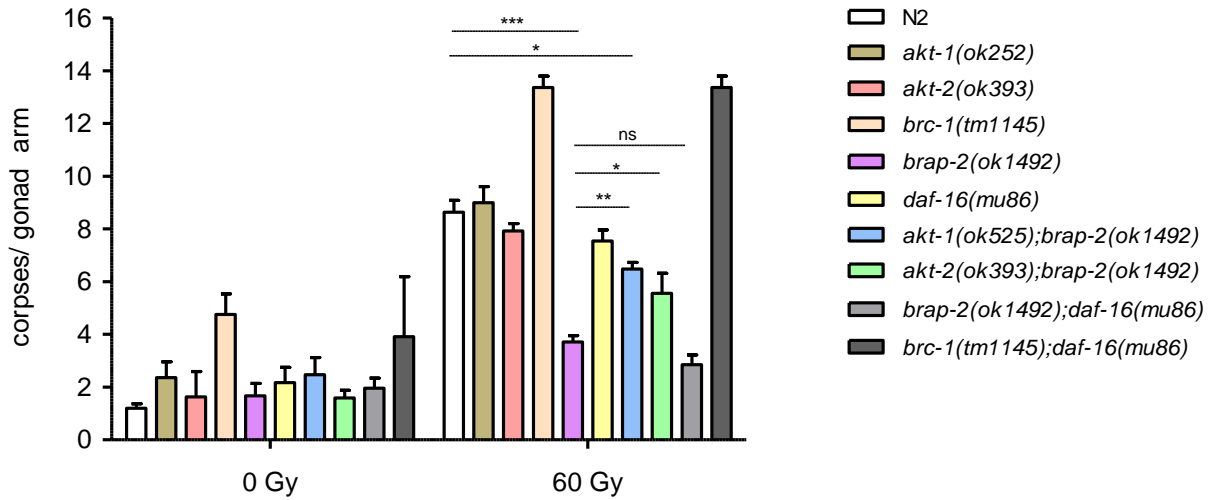
We generated an *akt-1(ok525);brap-2(ok1492)* double mutant strain and scored apoptosis following IR. We found that a loss of *akt-1* in *brap-2* mutants increased apoptosis to wild type levels (Figure 2.13A). Interestingly, although a loss of *akt-2* in *brap-2* mutants increased apoptosis, it was not as significant as a loss of *akt-1*. Knockdown of *akt-1* using RNAi in both *brap-2* and *brap-2;brc-1* double mutants also increased apoptosis to wild type levels following DNA damage (Figure 2.13B). However, removal of DAF-16 did not increase apoptosis in *brap-2(ok1492)* mutants indicating that DAF-16 was not required. Together, these results indicate that AKT-1 is at least partially required for the decrease in germline apoptosis seen in *brap-2* mutants upon IR, in a *daf-16* independent manner.

Having observed that *brap-2* mutants reduced DAF-16 nuclear accumulation and require AKT-1 for reduced levels of germline apoptosis following DNA damage, we predicted AKT-1 protein would be increased in *brap-2(ok1492)* mutants. We quantified *akt-1* mRNA expression levels in *brap-2* mutants and found that *akt-1* levels in *brap-2* mutants increased 2.2-fold (Figure 2.14A). We also found that the levels of endogenous AKT-1 in *brap-2* mutants increased 1.43-fold, while *phlp-2* mutants produced no change in AKT-1 levels (Figure 2.14B).

De-phosphorylation of AKT by PHLPP1 inactivates AKT preventing downstream AKT function that leads to cell survival, growth and proliferation (47). We hypothesized that a loss of PHLP-2 would allow for persistent AKT-1 activation and cause a reduction in germline apoptosis following DNA damage exposure. We found that *phlp-2(tm7788)* mutants displayed a 4.5-fold reduction in apoptosis following IR compared to the wild type (Figure 2.15A). At the same time, apoptosis levels in *phlp-2* mutants were also lower than the wild type physiologically, indicating that PHLP-2 is required for the general activation of apoptosis. We also found that *phlp-2* RNAi knockdown moderately reduced apoptosis in *brc-1* mutants (Figure 2.15B). To determine whether PHLP-2 is required for the activation of apoptosis in *akt-1* mutants we generated an *akt-1(ok525);phlp-2(tm7788)* double mutant strain and found that again a loss of *phlp-2* significantly reduced apoptosis following IR (Figure 2.15A).

Reduced apoptosis in PHLP-2 mutants indicates that like BRAP-2, PHLP-2 is required to promote germline apoptosis. However, these findings also suggest that PHLP-2 may be required to regulate other proteins besides AKT-1 in this context. Therefore, these findings suggest that BRAP-2 may function through AKT-1 to regulate DNA damage induced germline apoptosis, where increased AKT-1 activation caused by a loss of *brap-2* may promote cell survival.

A



B

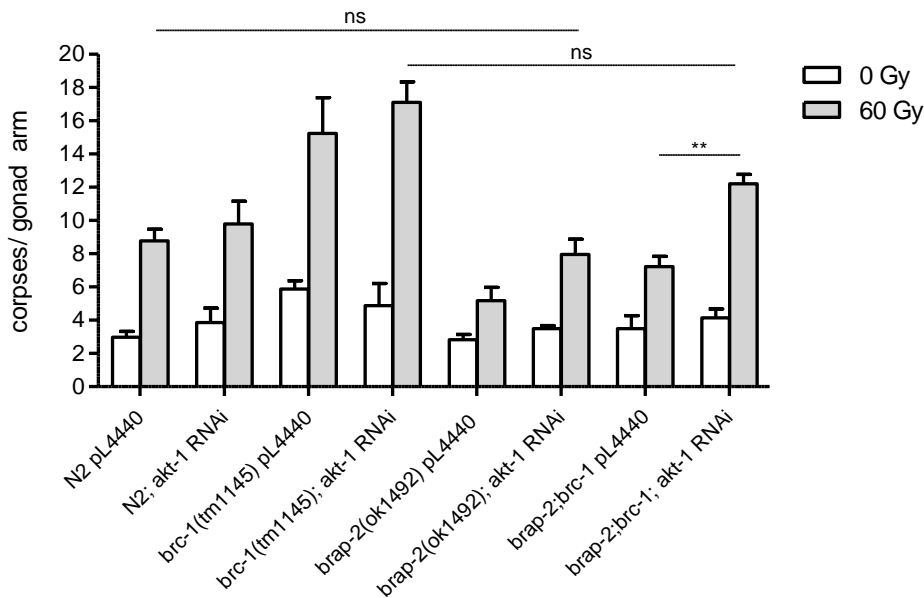


Figure 2.13: Loss of *akt-1* increases apoptosis in *brap-2* mutants

(A) Loss of *akt-1* significantly increased apoptosis in *brap-2* mutants to levels similar to the wild type (N2), following IR. While no change in apoptosis levels was observed in *brap-2* mutants with the loss of *daf-16*. Results represent 3 independent trials. (B) *akt-1* RNAi in *brap-2;brc-1* mutants increased apoptosis to levels similar to N2 following IR. Results represent 3 independent trials. Two independent trials were completed for *brc-1;daf-16* mutants. Germline corpses were scored using AO. $p < 0.01$ **, $p < 0.05$ *.

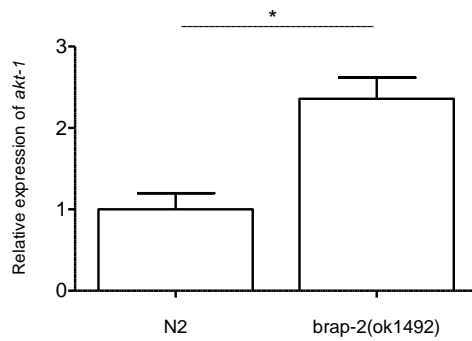
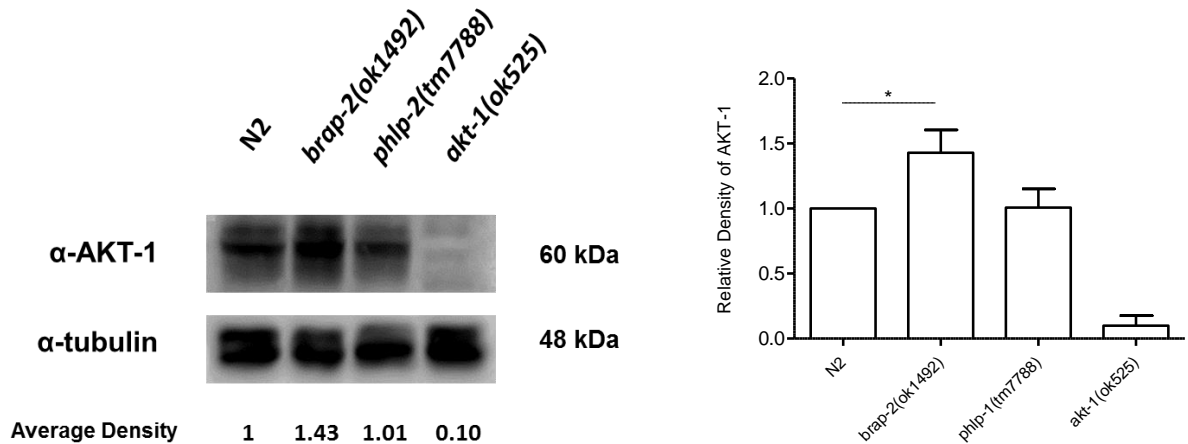
A**B**

Figure 2.14: AKT-1 is elevated in *brap-2(ok1492)* mutants

(A) Using qRT-PCR *brap-2* mutants display a 2.2-fold increase in *akt-1* mRNA expression. Results represent 3 independent trials, normalized to *act-1* of the wild type (N2). (B) *brap-2(ok1492)* mutants displayed a 1.43-fold increase in AKT-1 protein levels. Endogenous AKT-1 levels were detected using α -AKT-1 128 and α -AKT-1 527 antibodies, recognizing the C-terminal region. Band intensity was measured using ImageJ and normalized to their respective α -tubulin levels and then to N2. Graph represents the average relative density of endogenous AKT-1 levels for each genotype. Result represents 3 independent trials. $p < 0.05^*$.

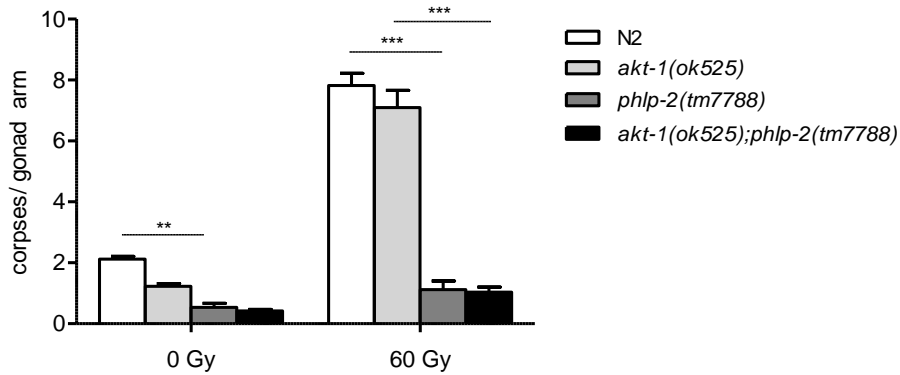
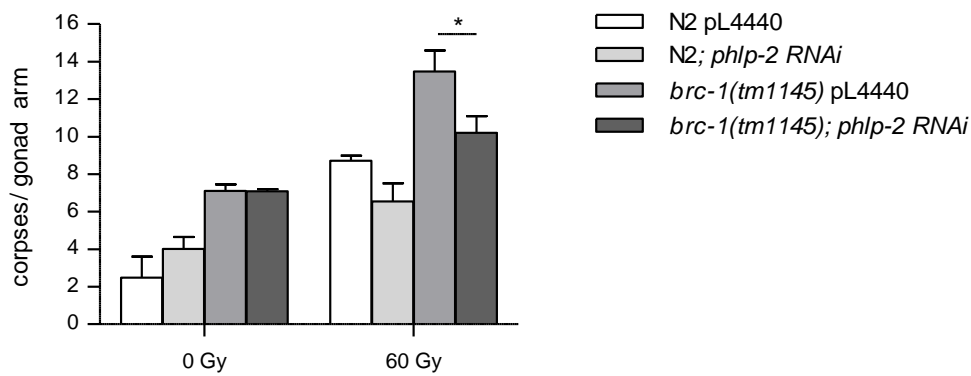
A**B**

Figure 2.15: Loss of *phlp-2* reduced germline apoptosis in *akt-1* mutants

(A) *phlp-2* mutants displayed a significant reduction in apoptosis before and after IR. Loss of *phlp-2* also significantly reduced apoptosis in *akt-1* mutants following IR. (B) *phlp-2* RNAi caused a modest reduction in apoptosis in the wild type and *brc-1* mutants. Two independent trials were completed for pL4440 and 3 independent trials for *phlp-2* RNAi. Germline corpses were scored using AO. $p < 0.001$ ***, $p < 0.05$ *.

2.5 Discussion

The work presented here identifies a new role for BRAP-2 in DNA damage induced germline apoptosis through the regulation of the transcription factor SKN-1 and the protein kinase AKT-1. The *C. elegans* germline possesses highly conserved mechanisms of the DNA damage response, where a loss of BRC-1 leads to a failure in DNA repair and increased germline apoptosis (8). We have shown that *brap-2(ok1492)* mutants cause a reduction in germline apoptosis in response to DNA damage induced by IR, and high levels of germline apoptosis in *brc-1* mutants is dependent on BRAP-2.

Previously, we found that *brap-2(ok1492)* mutants increased SKN-1/Nrf2 localization into intestinal nuclei and increased SKN-1 dependent phase II detoxification gene expression (15). Here we have shown that *skn-1* mRNA levels remain elevated in *brap-2* mutants after DNA damage, and *skn-1* RNAi reduced the expression levels of apoptosis genes. ChIP (Chromatin Immunoprecipitation) of SKN-1 binding sites conducted by the Snyder Lab, has predicted that SKN-1 binds to the promoters of *egl-1* and *ced-13*, and is most enriched at the promoter of *mev-1*, which is upstream and part of the operon that regulates *ced-9* transcription (modENCODE). This indicates that SKN-1 may have the potential to act as a transcriptional regulator of the core apoptotic pathway.

SKN-1 is provided maternally during embryogenesis, yet SKN-1 protein has not yet been detected in adult hermaphrodite germlines, nor does the loss of SKN-1 alter the levels of apoptosis in wild type worms (31,56). We found that *skn-1* RNAi increased apoptosis only in *brap-2;brc-1* double mutants, and although we did not detect any defects in the germline directly, we cannot rule out that increased apoptosis in these double mutants may be due to germline instability with a loss of both *brc-1* and *skn-1*. However, in this context it may be

possible for an intestine-germline interaction in which SKN-1 has a cell survival role in the germline apart from it responding to oxidative stress that may be similar to Nrf2, which has been shown to have a pro-survival role in cancer development through its upregulation of anti-apoptotic genes, promotion of an unaltered metabolism and changes to ubiquitin-proteasome protein turnover (57).

A loss of *brap-2* caused a CEP-1 dependent increase in expression of pro-apoptotic genes *egl-1* and *ced-13*, which were even greater when exposed to DNA damage, suggesting a potential role for BRAP-2 as a negative regulator of CEP-1. Several genes have been found to regulate apoptosis such as *eel-1*, *sir-2.1* and *kri-1*, all of which display pro-apoptotic function independent of CEP-1 (31,58,59). We determined that *brap-2* mutants displayed elevated PMK-1 activity, and a loss of *pmk-1* (but not *mpk-1*) increased apoptosis in *brap-2* mutants to wild type levels following IR. Interestingly, while a loss of both these kinases decreased *egl-1* and *ced-13* expression, a loss of *mpk-1* was only able to reduce *egl-1* levels in *brap-2* mutants. This indicates that PMK-1 and MPK-1 may influence CEP-1 activity, but increased levels of these apoptotic genes in *brap-2* mutants does not directly dictate apoptosis induction. Thus we predict that *brap-2* may also act as a pro-apoptotic gene that regulates DNA damage induced apoptosis through pathways parallel to the core apoptotic program. We believe that BRAP-2 regulates apoptosis in part through the PMK-1/p38 MAPK pathway which is known to activate SKN-1 and is associated with oxidative stress and immune responses (36,39,60).

AKT-1 and AKT-2 regulate apoptosis through two distinct mechanisms, and dimerize to phosphorylate and inhibit DAF-16 preventing dauer formation (54). We found that a loss of *akt-1* more significantly increased apoptosis in *brap-2* mutants than a loss of *akt-2*, in a *daf-16* independent manner. Although we were unable to test phosphorylated AKT-1 levels to verify

whether increased endogenous AKT-1 protein levels in *brap-2(ok1492)* mutants corresponded to increased AKT-1 activation, we have found that a loss of *brap-2* enhanced IIS stimulation and DAF-16 attenuation, seen with the increased intermediate and cytoplasmic distribution of DAF-16 in the intestine and a reduction in DAF-16 target expression.

We also confirmed that BRAP-2 interacts with PHLP-2 *in vitro*, placing BRAP-2 as a potential regulator of the IIS pathway. We have shown that *phlp-2* is required for apoptosis activation in *akt-1* mutants, and that *phlp-2* mutants display a significant reduction in germline apoptosis. Although we did not see elevated levels of endogenous AKT-1 in *phlp-2* mutants, we cannot assume levels of activated AKT-1 are not increased with *phlp-2* inactivation. Therefore, we postulate that AKT-1 and SKN-1 activity are modulated by BRAP-2 for regulation of DNA damage induced germline apoptosis. Similar to *brap-2*, further investigation is required to determine whether the IIS or an alternative pathway is activated in *phlp-2* mutants. However, we were able to show that *phlp-2* mutants displayed a significant and general reduction in apoptosis, and thus have identified a potential novel role for PHLP-2 in germline apoptosis.

Previous studies have determined that ubiquitin ligases SCF^{FSN-1} and EEL-1 are also regulators of germline apoptosis (31,61). Like its mammalian ortholog, BRAP-2 possesses conserved functional domains of an E3 ubiquitin ligase. We did not verify whether functionally this enzymatic activity is conserved however, it cannot be ruled out as a possible mechanism to post translationally modify proteins such as PHLP-2 to regulate their activity and affect the downstream signaling of these pathways. Our findings suggest that BRAP-2 regulates DNA damage induced germline apoptosis, wherein BRAP-2 blocks the activation of pro-cell survival pathways to promote apoptosis, by inhibiting SKN-1 and AKT-1 through the p38 MAPK pathway and PHLP-2 respectively (Figure 2.16).

Programmed cell death is vital for shaping organs and limbs, eliminating self-reactive cells and for protection against malignant transformation that can lead to tumor formation and cancer. Here we have uncovered a new role for BRAP-2 and its potential for regulating both SKN-1 through the PMK-1/p38 MAPK pathway, and AKT-1 to regulate *C. elegans* germline apoptosis. Although further investigation is needed, we also revealed a potential novel role for PHLP-2, where it may be necessary for the general induction of *C. elegans* germline apoptosis. We did not detect a conserved physical interaction between BRC-1 and BRAP-2, and thus do not know if BRAP2 functions to promote apoptosis in higher organisms in the same way as we have observed with BRAP-2 in the *C. elegans* germline. Although to our knowledge a role for BRAP2 has not been identified for the regulation of programmed cell death, our previous findings that BRAP-2 acts as a regulator of the oxidative stress response through regulation of SKN-1/Nrf2, and our work presented here reveals BRAP-2 as a potential conserved binding protein for PHLP-2 and regulator of AKT-1. We would predict that if enhancement of these pathways is observed with BRAP2 inactivation they could function together to prevent apoptosis and enhance cell survival. The evasion of programmed cell death is a hallmark of cancerous cells, and this has provided us with a genetic tool that will allow us to better understand the complex and intricate regulation of signaling pathways that govern the balance between pro-death and pro-cell survival factors that lead to apoptosis activation, while discovering potential new targets that regulate apoptosis for future study and therapeutic development.

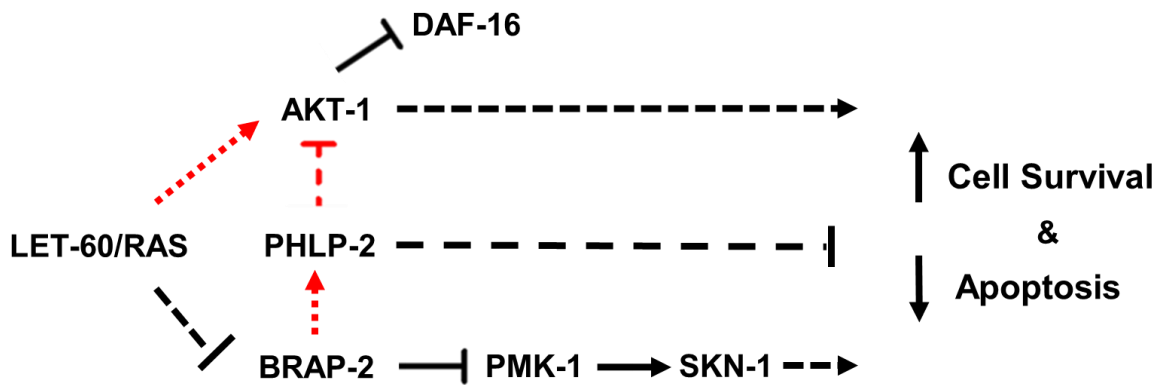
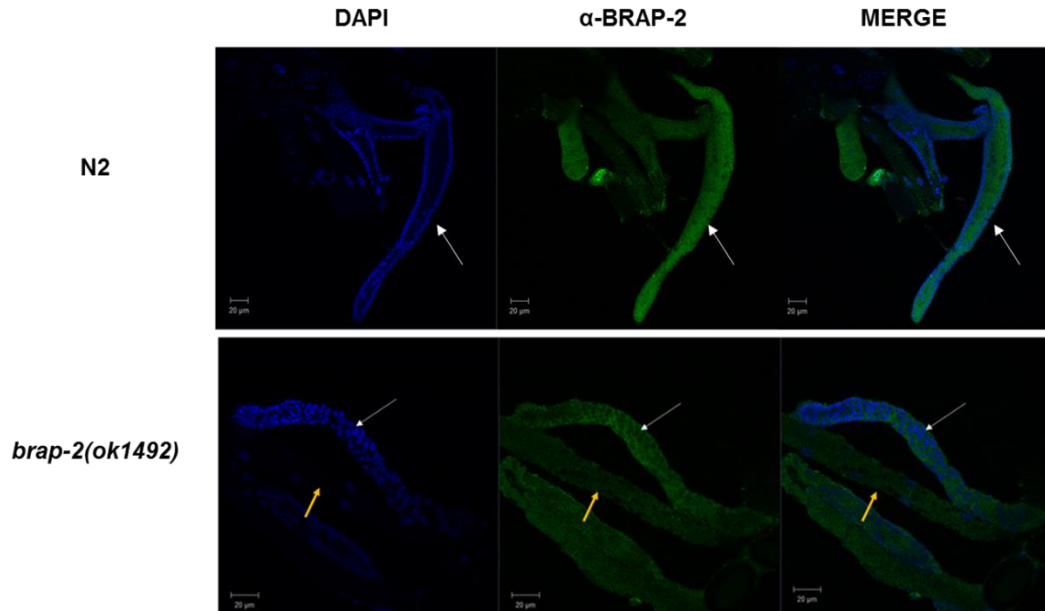


Figure 2.16: Proposed model for BRAP-2 regulation of DNA damage induced germline apoptosis.

Schematic diagram depicting a proposed mechanism for BRAP-2 regulation of DNA damage induced germline apoptosis. Our findings suggest that BRAP-2 regulates DNA damage induced germline apoptosis through a non-canonical signaling mechanism, regulating pro-cell survival pathways to promote apoptosis by inhibiting SKN-1 and AKT-1, through the PMK-1/p38 MAPK pathway and potentially PHLP-2, respectively. Dashed lines represent hypothesized interactions.

2.6. Supplementary Figures

A



B

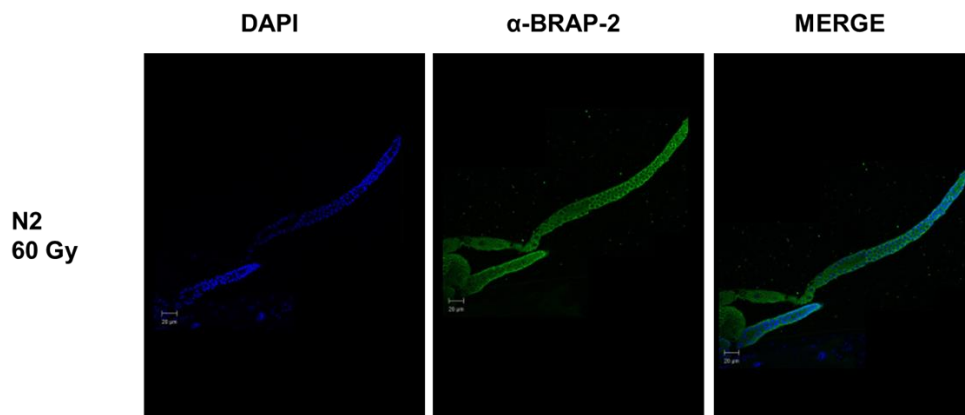


Figure S2.1: BRAP-2 is expressed in the germline cytoplasm following DNA damage

(A) Adult wild type (N2) and *brap-2(ok1492)* mutant germlines were immunostained with α -BRAP-2 antibody. We found BRAP-2 to be expressed in the cytoplasm of the germline, surrounding nuclei in both N2 and *brap-2* mutants. (B) Following 60 Gy, BRAP-2 is still found to be expressed in the N2 germline cytoplasm. Representative images of 10 extruded germlines. Due to the large size, image presented is a composite of two images taken of the same gonad. White arrows indicate germline. Yellow arrows indicate intestine.

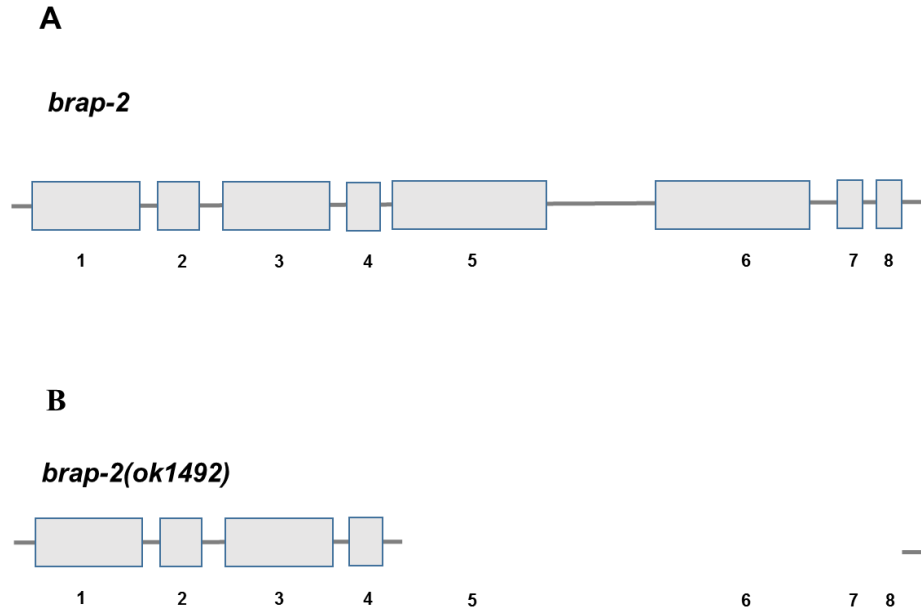


Figure S2.2: Genomic structure of *brap-2* and deletion mutant *ok1492*

(A) Located on Chromosome II, the *brap-2* gene is comprised of 8 exons with a total length of 2693 bp. Its coding sequence is 1773 bp. (B) This study focused on the *brap-2(ok1492)* mutant that possesses a 1540 bp deletion in the C-terminal end which removes exons 5-8 but leaves 15 bp untouched at the end. Gene depictions are not to scale. Genomic structures were adapted from Wormbase and Koon and Kubiseski (2).

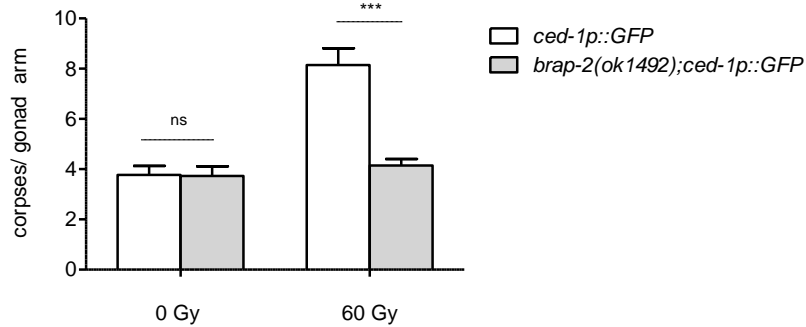
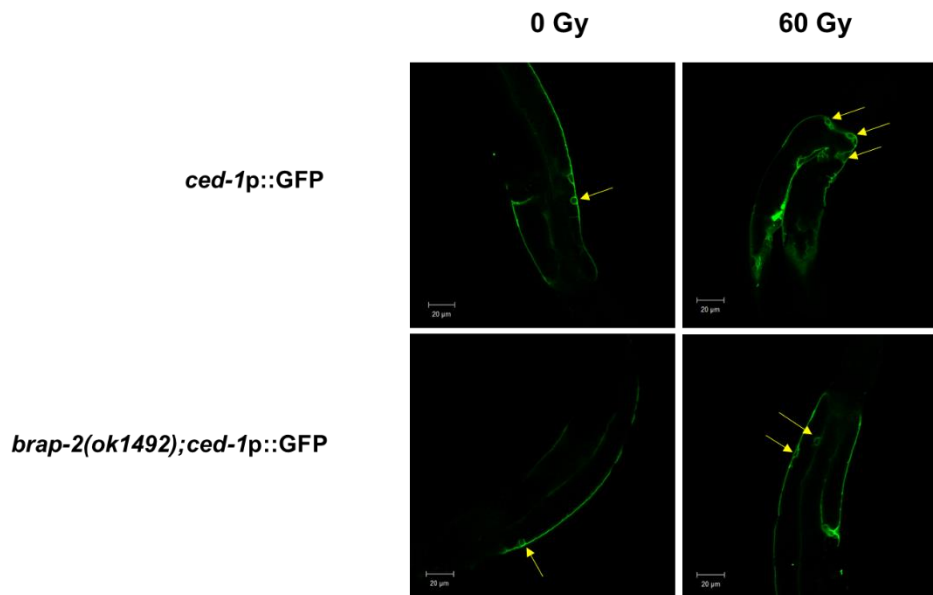
A**B**

Figure S2.3: *brap-2* mutants display reduced levels of germline apoptosis following DNA damage

(A) We scored the levels of apoptosis using a *ced-1p::GFP* reporter strain in a *brap-2(ok1492)* mutant background. We found that following DNA damage, *brap-2* mutants experience a 50% reduction in germline apoptosis. (B) Representative images of the *ced-1p::GFP* reporter strain 24 hours post IR. A significant reduction of apoptosis was observed in *brap-2(ok1492)* mutants compared to the wild type. Yellow arrows indicate apoptotic cells (outlined by GFP halo). Results represent 3 independent trials. $p < 0.001$ ***.

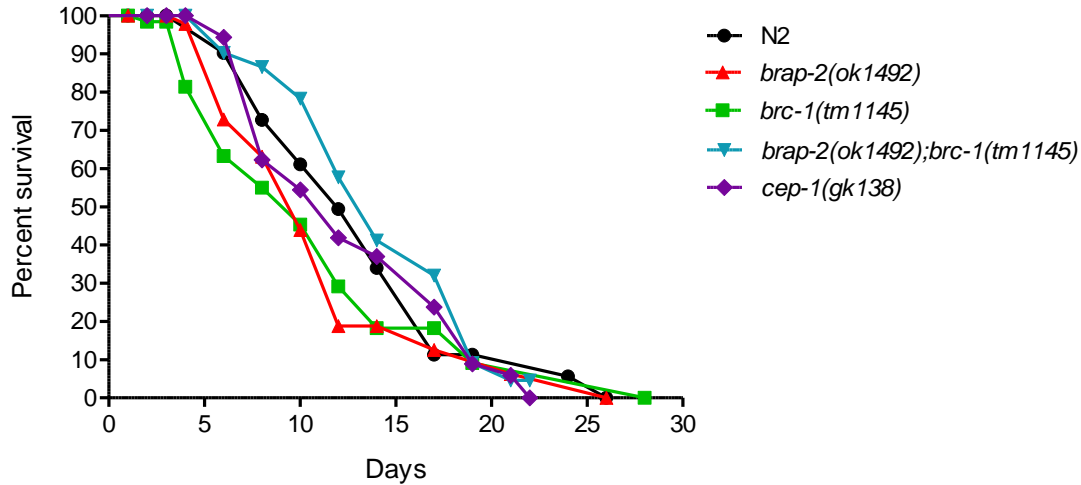
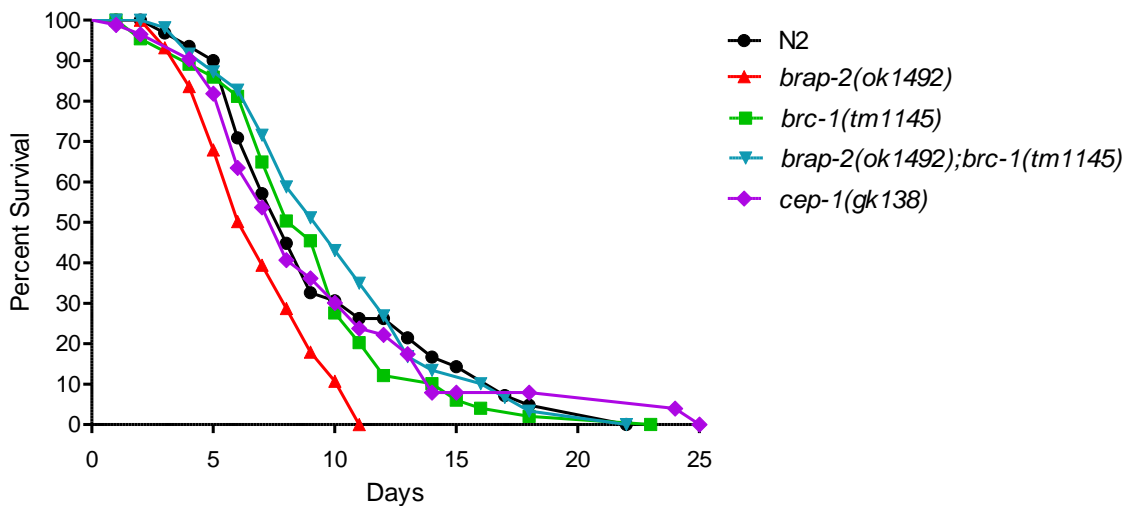
A**B**

Figure S2.4: A loss of *brc-1* extends *brap-2(ok1492)* mean survival

(A) At 0 Gy *brap-2(ok1492)* experiences a mean survival of 11.67 ± 1.67 days compared to the wild type (N2) wildtype of 13.3 ± 0.67 days. *brap-2* mutant survival was extended to 13.0 ± 1.0 days with the loss of *brc-1*. (B) Following 60 Gy, *brap-2(ok1492)* experiences a mean survival of 8.33 ± 0.67 days compared to N2 of 9 ± 0.57 days. Survival of *brap-2(ok1492)* mutants is extended with the loss of *brc-1* to 10 days. Synchronized worms of each genotype were plated in quadruplicates, 15-20 worms were followed from the 1st day of adulthood to their death. Graph represents one of 3 independent trials.

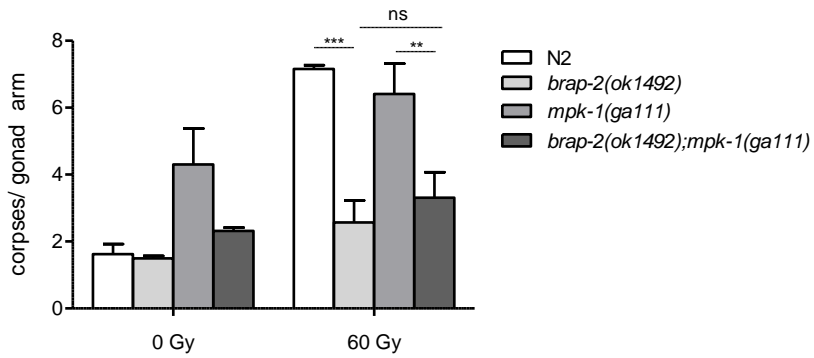
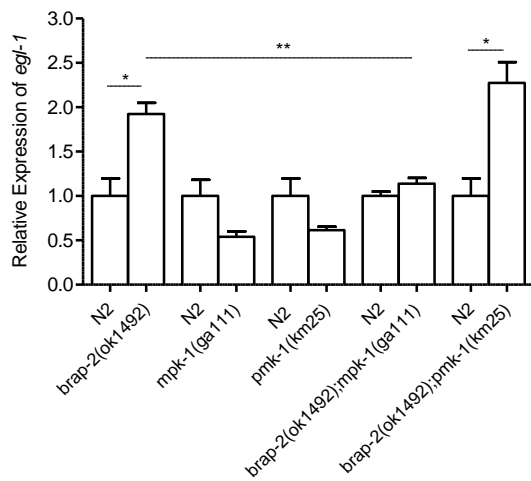
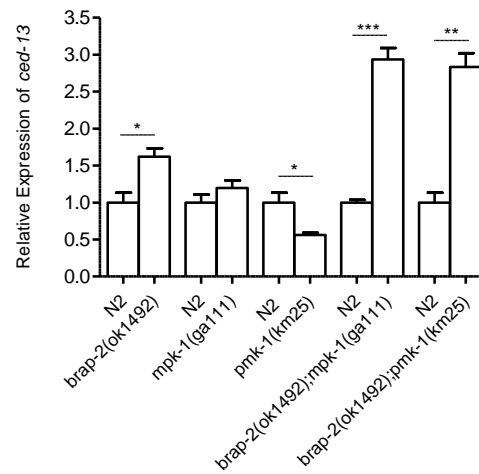
A**B****C**

Figure S2.5: Loss of *mpk-1* did not increase apoptosis in *brap-2* mutants

(A) Loss of *mpk-1* in *brap-2(ok1492)* mutants did not increase apoptosis following DNA damage. Result represents 3 independent trials. (B) *mpk-1* and *pmk-1* mutants displayed a reduction in *egl-1* mRNA levels. A loss of *mpk-1*, but not *pmk-1*, reduced *egl-1* mRNA expression levels in *brap-2(ok1492)* mutants. (C) A loss of either *mpk-1* or *pmk-1* did not reduce *ced-13* mRNA levels in *brap-2(ok1492)* mutants. Results represent 3 independent trials, normalized to *act-1* of the wild type (N2). p < 0.001***, p < 0.01**, p < 0.05*.

2.7 Acknowledgements

A number of strains were provided by the CGC, which is funded by NIH Office of Research Infrastructure Programs (P40 OD010440) and the National BioResource Project. AKT antibodies were a kind gift from W.B. Derry of Hospital for Sick Children, Toronto. We thank also members of the Derry Lab (E. Chapman, B. Yu, B. Lant, A. Mateo, M. Hall, A. Tran, M. Gunda & M. Haeri) for their assistance with the irradiation. D.R.D. is a recipient of the Ontario Graduate Scholarship. M.P. is a recipient of the Dean's Award from the Faculty of Science, York University and a Natural Sciences and Engineering Research Council of Canada (NSERC) undergraduate studentship. D.R.D., Q.H., M.P. and T.J.K were supported by a grant from NSERC.

Chapter 3

BRAP-2 is required for *Caenorhabditis elegans* survival, development and germline health

Dayana R. D'Amora¹, Queenie Hu^{1,2}, Monica Pizzardi¹ and Terrance J. Kubiseski¹

1. Department of Biology, York University, Toronto, Ontario, Canada
2. Sunnybrook Research Institute, Toronto, Ontario, Canada

Authors Contributions

BRAP-2 is required for *Caenorhabditis elegans* survival, development and germline health

Dayana R. D'Amora¹, Queenie Hu^{1,2}, Monica Pizzardi¹ and Terrance J. Kubiseski¹

1. Department of Biology, York University, Toronto, Ontario, Canada

2. Sunnybrook Research Institute, Toronto, Ontario, Canada

MANUSCRIPT IN PREPARATION

Queenie Hu assisted in RNA isolation and performed qRT-PCR in Figure 3.9. Queenie Hu and Monica Pizzardi assisted in the generation of double mutants for experimentation using standard protocols. Terrance J. Kubiseski generated the BRAP-2::GFP transgenic strain using CRISPR-Cas9 shown in Figure 3.3. Terrance J. Kubiseski and I prepared the manuscript.

3.1 Summary

Mutations in *C. elegans* can produce visible and quantifiable defects in morphology, lifespan and development. Along with its high genetic conservation, it provides us with an exceptionally useful model for the study of human disease-related gene function. BRC-1 (BRCA1 ortholog) mutant animals look and develop similar to the wild type, but possess defective DNA repair, increased germline apoptosis and greater embryonic lethality (1). BRAP2/IMP (BRCA1-associated binding protein 2) has been characterized as an E3 ubiquitin ligase and as a cytoplasmic retention protein (2–4). It has also been found to be widely expressed throughout various mammalian tissues, most highly in testes (4). However, its role in the development or health of these tissues has not been addressed. The focus of this study is to determine the role of BRAP-2 in *C. elegans* morphology, development and germline integrity. Previously, we have found that the *C. elegans* BRAP2 ortholog BRAP-2, is involved in the regulation of oxidative and DNA damage stress responses. We have determined that *brap-2* mutants display defects in morphology, delayed life cycle progression, and a reduction in brood size and survival. Furthermore, embryonic lethality and sterility is elevated in *brap-2* mutants following DNA damage, suggesting a potential role for BRAP-2 in facilitating DNA repair. We have also found that a loss of *brap-2* reduced sperm quality and reduced male production in *him-5* (High incidence of males) mutants. Our findings suggest that BRAP-2 is required for *C. elegans* development, survival and overall germline health.

3.2 Introduction

C. elegans is a powerful model organism due to its simplicity and high genetic conservation with mammalian disease genes and subsequently many cell signaling pathways. It is a tiny, transparent hermaphroditic nematode that possesses an invariant number of somatic cells (5). One of the many benefits of this model is that it has a short generation time, reaching adulthood in 3 days, produces a large number of progeny (~300) in every generation and can live up to 2 weeks (5). Genetic screens have uncovered the involvement and function of many conserved human genes, dissecting the genetic order of signaling cascades that execute stress responses, programmed cell death and control development (6). Novel gene mutations can alter *C. elegans* development or produce visible phenotypes in morphology, which can implicate their involvement in disease-associated signaling pathways.

The germline is the only continuously proliferative tissue in *C. elegans*, where mitotically proliferating cells eventually become oocytes after meiosis prophase I progression which begins at the transition zone (TZ), followed by meiotic recombination in pachytene and diakinesis (7). The germline also employs mitotic arrest, DNA repair and apoptosis in spatially distinct areas to protect nuclei from the threat of external and internal stressors for successful meiotic progression, gametogenesis and self-fertilization (8,9). Mutations in genes involved in coordinating and executing the DNA damage response (DDR) can exhibit defects in embryonic lethality, chromosome morphology and radiation sensitivity (9). BRCA1 (Breast cancer susceptibility gene 1) is a tumor suppressor that participates in several DNA damage surveillance mechanisms including DNA repair, transcription and cell cycle arrest (10). Although worms appear normal, loss of BRC-1 (BRCA1 ortholog) causes an increase in germline apoptosis, increased RAD-51 (RAD51 ortholog) foci formation at double strand break (DSBs) sites,

increased embryonic lethality, as well as X chromosome non-disjunction increasing the incidence of males (1,11). Thus the continued maintenance and protection of the germline is vital for *C. elegans* development and survival.

BRAP2 (BRCA1-associated binding protein 2 or BRAP according to the HUGO database) is an E3 ubiquitin ligase and is characterized as a cytoplasmic retention protein due to its ability to prevent BRCA1 nuclear import (12). BRAP2 has been found to interact with other proteins and prevent their nuclear localization, most notably p21, CDC14 and PHLPP1 (3,2,13,4). BRAP2 has also been identified as a RAS effector that upon activation of RAS, is auto-ubiquitinated, releasing KSR for increased ERK activation (14–16). Previously, we characterized the *C. elegans* BRAP2 ortholog BRAP-2, and found that *brap-2* mutants experience BRC-1 dependent L1 developmental arrest when exposed to oxidative stress (17). In addition, we found that BRAP-2 is a potential negative regulator of SKN-1 (*C. elegans* Nrf2 ortholog), master regulator of the phase II detoxification response (18). We also determined that BRAP-2 promotes DNA damage induced germline apoptosis, a vital component of the DDR.

We previously confirmed that *brap-2(ok1492)* mutants are dauer defective, and while maintaining the *brap-2* mutant strain we also observed that they grew more slowly and their morphology was distinct to the wild type. The focus of this study was to determine the effects a loss of BRAP-2 has on *C. elegans* morphology, development and survival as well as examine the potential importance of BRAP-2 in maintaining germline integrity. We have found that *brap-2* mutant animals are shorter in length, possess a developmental delay and have reduced mean survival. *brap-2* mutants also have reduced brood size and sperm quality, and following DNA damage induced by ionizing radiation (IR), have increased radiation sensitivity in mitotic nuclei. This suggests that BRAP-2 is required for proper *C. elegans* development and germline health.

3.3 Materials & Methods

3.3.1 *C. elegans* strains and genetics

All worm strains were cultured under standard conditions, as previously described (19). All strains were obtained from the *Caenorhabditis* Genetics Center located at the University of Minnesota and double mutant strains were generated using standard protocols. The N2 Bristol strain was used as the wild type, and unless noted otherwise all experiments were conducted at 20°C. Strains were sequenced at Sick Kids TCAG for the presence of *him-5(e1490)*. The following strains were used in this study: N2, *brap-2(ok1492) II* (YF15), *brc-1(tm1145) III* (DW102), *brap-2(ok1492) II; brc-1(tm1145) III* (YF64), *brap-2(ok1492)/mIn 1 [MIs14dyp10(e128)] II* [denoted as *brap-2(ok1492)/+*] (YF104), *him-5(e1490) V* (DR466), *brap-2(ok1492) II; him-5(e1490)* (YF195), BRAP-2::GFP (YF199).

3.3.2 Brood size and embryonic lethality

To assess brood size, 5 adult worms for each genotype were plated per Nematode Growth Media (NGM) plate in triplicate. Adult worms were allowed to lay eggs for 5 hours at 3 permissive temperatures (16°C, 20°C and 25°C) and then removed. Eggs were scored, and the following day the number of unhatched eggs and L1 larvae were counted to assess both brood size, number of males and embryonic lethality.

3.3.3 Developmental timing to adulthood

Five adult worms for each genotype were plated per NGM plate in triplicate, allowed to lay eggs and then removed. For each strain, development to each larval stage was recorded every day

post-hatching on NGM plates (denoted as Day 0). Progression to each larval stage was recorded until the first day of adulthood was reached.

3.3.4 Fluorescence Microscopy

For each genotype, worms were synchronized and when they reached the first day of adulthood were mounted on 2% agarose in 2 mM Levamisole (Sigma L9756) in M9 Buffer. To examine worm length, width, male sensory rays and the BRAP-2::GFP reporter strain images were taken using a Zeiss LSM 700 Confocal Laser-Scanning Microscope with Zen 2010 Software. Length and width were measured using the line measurement tool in Zen 2010 Lite Software.

3.3.5 Survival Analysis

Synchronized worms were raised at 20°C and survival was scored beginning on the first day of adulthood and compared to non-irradiated controls. Worm survival was scored every 2 days, with worms pronounced dead using the “poke test”, if no response at the head or tail was produced to gentle prodding. Missing worms or those that developed “bag of worms” phenotype, were censored from the analysis. Worms were transferred to fresh NGM plates every 2 days.

3.3.6 DNA Staining

To quantify germline nuclei, whole worms were stained with DAPI as previously described (9). Z-stack images were taken at 63X and the Zen 2010 Lite software free-form surface area measurement tool was used to measure gonad surface area of one representative slice. To compare meiotic progression, germlines were dissected and stained with DAPI (VECTOR Labs H-1200). The ImageJ Cell Counter plugin was used to determine the total number of nuclei per zone in one gonad arm per worm per genotype imaged and scored. For chromosomal

fragmentation, Z-stack images of terminal oocytes at the -2 and -1 positions at the proximal end where examined for manual counting of condensed chromosome bodies.

3.3.7 Gonad dissection and immunofluorescence in worms

Gonad dissection and immunostaining was performed as previously described by (20), with the following changes: Approximately 20-30 synchronized 1 day old adults were mounted onto 20 μ L of 2mM Levamisole in M9 buffer on Superfrost Polylysine (Fisher 12-55505-15) coated slides in an area made with Immaedge Hydrophobic Pen (VECTOR Labs H-4000). The heads or tails were removed using 27G syringe needles in a “scissor-like motion”. Then 2% paraformaldehyde was added, coverslip was mounted and slides were allowed to sit for 10 minutes and then frozen on an aluminum block on dry ice for 10 minutes. Slides were then freeze cracked using a razor blade and submerged in -20°C methanol for fixation for 1 minute. Following methanol fixation, slides were washed with 1X PBST (PBS, 0.1% Triton X-100) 3X for 5 minutes, followed by incubation for 1 hour in 2% BSA for 1 hour in a humid chamber. Primary antibody (prepared in 2% BSA) was added overnight at room temperature. Slides were washed 3X with 1X PBST and then secondary antibody was added dropwise and incubated for 1 hour at room temperature in a humid chamber in the dark. Slides were washed 4X with 1X PBST for 5 minutes and in the third wash 1 μ g/ml DAPI was added. Before mounting, 3 μ L of Prolong Gold Anti-Fade Reagent (Life P36930) was added and coverslips were sealed using clear nail polish. Images of 10 fluorescent worms per genotype were taken. Antibodies used were: rabbit anti-BRAP-2 (1:100) and DAPI. Alexa Fluor 488 (1:1000) (Invitrogen A11001) secondary antibody was used. Rabbit polyclonal anti-sera against *C. elegans* BRAP-2 (EEED8.16) was generated by the Toronto Recombinant Antibody Centre of the University of Toronto using a

GST fusion protein with BRAP-2 antigen corresponding to residues 108 to 134, which lie in the N terminus of the protein.

3.3.8 Generation of BRAP::GFP transgenic strain

The transgenic strain BRAP-2::GFP was generated as described previously (21). The 5'HR arm was amplified using a fosmid template and sub-cloned into NaeI/SalI site of pDD282 (Addgene) using the HiFi Assembly Kit (NEB). 3'HR arm, using the fosmid template was then sub-cloned into pDD282 in SpeI and AvrII site to create the final plasmid. The single guide RNA (sgRNA) was designed manually and used to mutate the pDD162 (Addgene) vector.

3.3.9 Cell transfection and immunofluorescence

Human Embryonic Kidney (HEK) cells were used to examine BRAP-2 cellular localization. HEK cells were cultured in Dulbecco's Modified Eagle's Medium supplemented with 10% Fetal Bovine Serum. Cells were co-transfected for 24 hours, with 1 μ g DNA of mammalian expressing constructs using polyethylenimine (PEI) (Sigma 408727-100 mL) and Optimem (Clontech 31985). Cells were washed with PBS and then fixed with 4% paraformaldehyde for 15 minutes. Cells were permeabilized with 0.1 % Triton-X 100 for 5 minutes and then washed 3X with 1X PBST. Cells were incubated with 4% BSA for 1 hour in a humid chamber at room temperature. Cells were then incubated with primary antibody (in 4% BSA) for 1 hour at room temperature, and then washed 3X with 1X PBST. Secondary antibody (in 4% BSA) was then added for 1 hour at room temperature in the dark and then wash 3X with 1X PBST. In the third wash, 1 μ g/mL DAPI was added. Coverslips were mounted onto plain glass slides with 3 μ L of Pro-long Gold Anti-Fade Reagent and edges were sealed with clear nail polish. Z-stack images of cells were

taken using at 40X. The following antibodies were used: rabbit anti-GST (1:100), and Alexa Fluor 555 (1:200) for fluorescence visualization.

3.3.10 RNA Isolation and Quantitative Real Time PCR (qRT-PCR)

Worm RNA Isolation and qRT-PCR was performed as previously described (18). For each genotype, 100 μ L of packed mixed-stage worms (IR treated and untreated controls) were collected and washed with M9 buffer 3X unless extraction occurred immediately, samples were frozen at -80°C . RNA was extracted with TRI Reagent (Sigma #93289) as follows: Pelleted RNA was recovered with RNase-free water and residual DNA was digested using the DNA-Free Kit (Ambion AM1906). Total RNA concentration was measured using NanoDrop2000 and 0.5 μ g of RNA was used to prepare cDNA following the manufacturer's protocol using the RNA to cDNA kit (Applied Biosystem #4387406). To quantify mRNA levels, qRT-PCR was performed using SYBR green premix (Clontech #693676)/SensiFast SYBR Green (FroggaBio BIO-98005) and the Qiagen Rotor-Gene Q System (Qiagen R0511133). Data were derived from 3 biological replicates. Data analysis was performed using the Applied Biosystems Comparative CT Method ($\Delta\Delta\text{CT}$ Method). mRNA expression levels of each strain was compared relative to the wild type (N2) control, where the housekeeping gene *act-1* (Actin) was used as the endogenous control for normalization. To verify equal primer amplification efficiency a standard curve for each set of primers was constructed using a serial dilution of cDNA. Using the qPCR Efficiency Calculator (ThermoFisher), amplification efficiency (%) of the qPCR reaction was determined based on the R^2 value and the slope of the standard curve.

2.3.11 Radiation Sensitivity

Synchronized L4 worms were irradiated at 60 and 120 Gy. Approximately 18-20 hours later, five 1 day old hermaphrodites were transferred to NGM plates and allowed to lay eggs for 5 hours (with eggs laid corresponding to nuclei in the pachytene region) and were counted. The following day the number of unhatched eggs were scored. To determine L1 sterility, L1 stage worms were irradiated at 60 Gy, embryonic lethality of F1 adult progeny was assessed to determine sterility of these IR treated animals (22).

3.3.12 Mating Assay

To determine sperm quality, we performed a mating assay as previously described (23) with the following changes: 3 males and one L4 stage wildtype hermaphrodite were placed on NGM plates with a small spot of OP50 in the center and allowed to mate for 48 hours. Adult worms were then removed and brood size was quantified. Embryonic lethality was scored the following day. Two days later, the number of males and XXX hermaphrodites were scored. XXX hermaphrodites were identified due to their “dumpy” appearance. Assays were completed in triplicate and plates that produced zero male progeny were excluded from analyses.

3.3.13 Statistical Analysis

Statistical analysis was performed with GraphPad Prism 5 Software. Student’s t-test was performed when comparing two means. P values of <0.05 were taken to indicate statistical significance. Error bars represent +/- standard error of the mean.

3.4 Results

3.4.1 BRAP-2 is expressed in the *C. elegans* germline

Previous functional studies of BRAP2 in mammalian cell culture have determined that BRAP2 is localized to the cytoplasm, interacting with a variety of proteins where it has been found to generally retain and prevent their nuclear localization (3,4,13). One study found that BRAP2 is expressed in liver, heart and lung tissues but is most highly expressed in testes (4). We wished to determine whether localization and expression of BRAP-2 (BRAP2 ortholog) is conserved in *C. elegans*. To determine BRAP-2 subcellular localization *in vitro* we transfected a mammalian expressing construct with BRAP-2 in 293T HEK cells and found that like BRAP2, BRAP-2 exhibited a cytoplasmic localization (Figure 3.1).

Previously, using α -BRAP-2 antibody we performed whole-worm antibody staining and detected a high level of BRAP-2 expression in the gonad of wild type worms. We took this one step further and immuno-stained wild type extruded germlines with α -BRAP-2 and found BRAP-2 to be localized in the cytoplasm surrounding germline nuclei, producing a “honeycomb effect” (Figure 3.2A). While examining BRAP-2 expression, we detected few germlines with BRAP-2 expression in the sperm sac (part of the somatic gonad, at the most proximal end of the germline before the uterus) (Figure 3.2B). Using the CRISPR-Cas9 system as previously described (21), we generated a BRAP-2::GFP transgenic strain to examine BRAP-2 expression *in vivo*. Again, we found BRAP-2 to be expressed throughout the germline, as well as in the sperm sac, and within embryos held in the uterus (Figure 3.3). Therefore, the cytoplasmic localization and high expression within the germline is conserved in *C. elegans*. Therefore it is possible that BRAP-2 function may be necessary for germline protection and development.

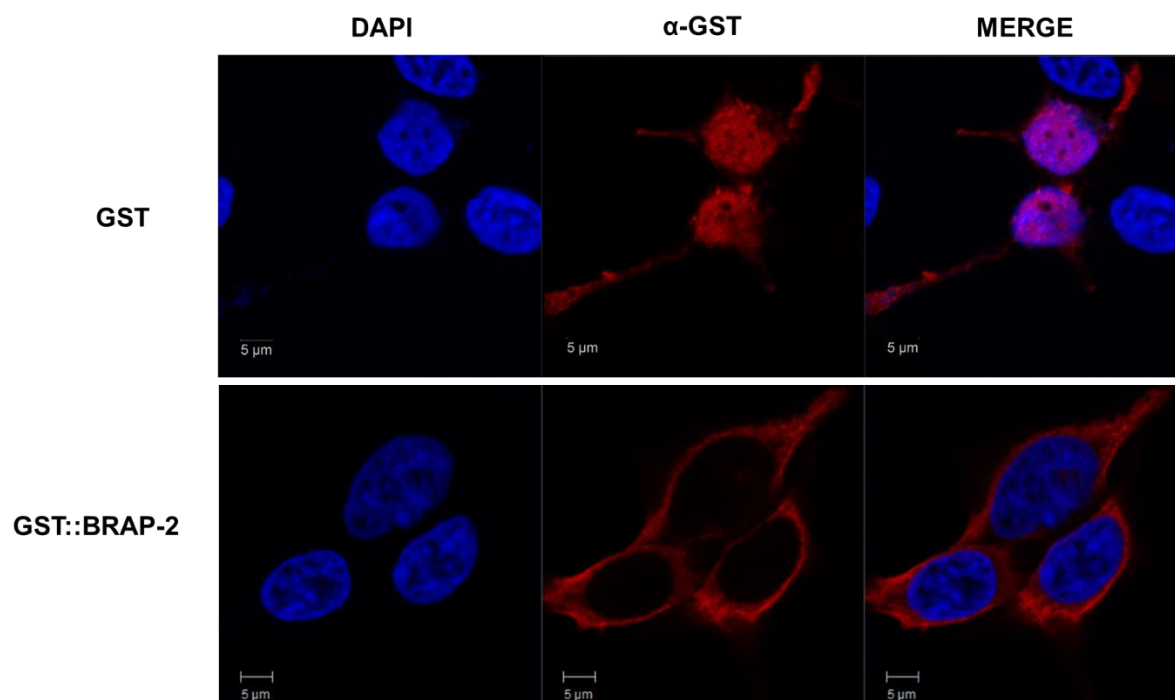


Figure 3.1: BRAP-2 localizes to the cytoplasm of mammalian 293T HEK cells

GST::BRAP-2 was transfected into 293T HEK cells for 24 hours, fixed, probed with α -GST and stained with DAPI to detect BRAP-2 expression. Cells transfected with GST alone was used as a negative control. Representative images represent 3 independent trials.

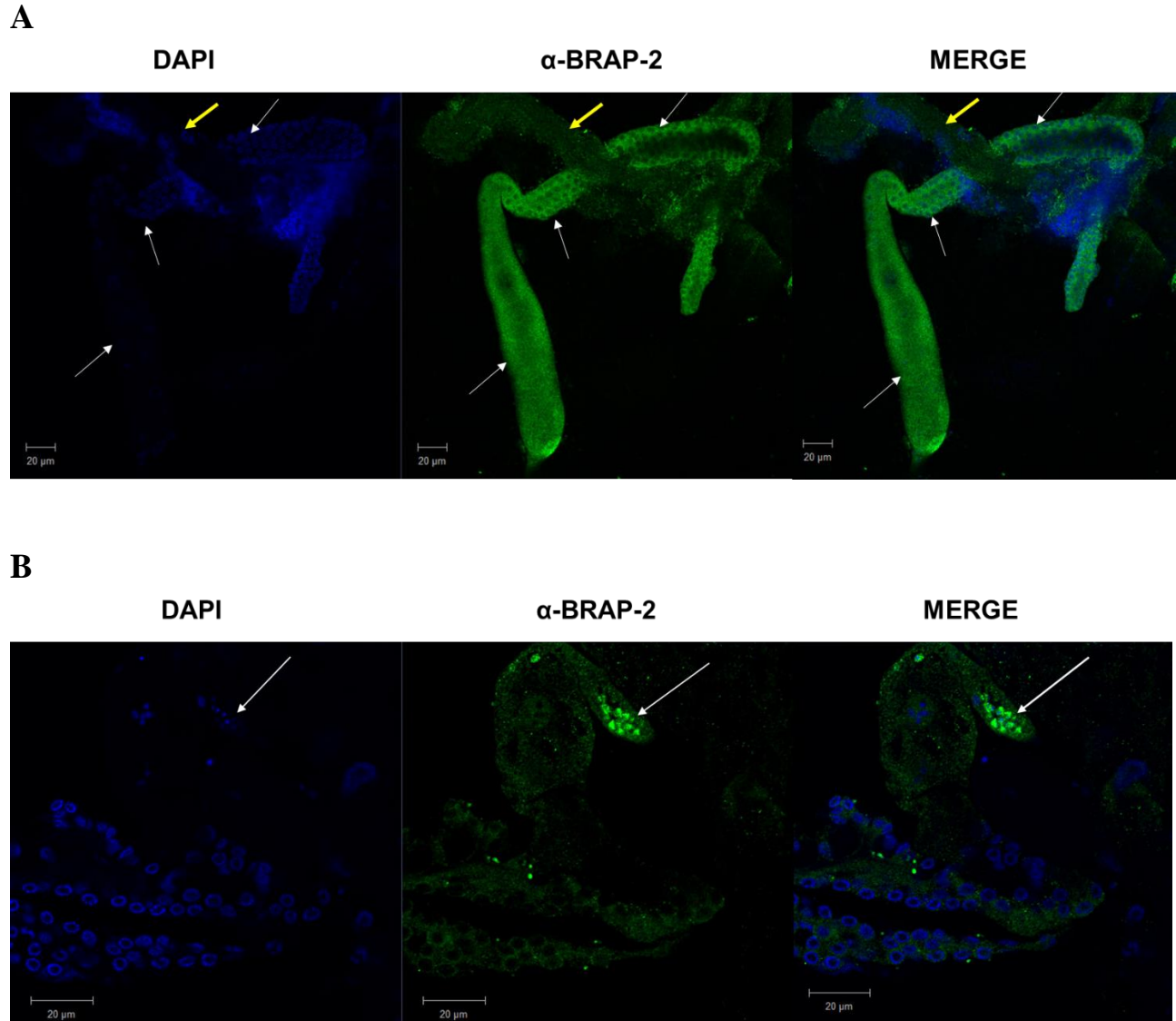


Figure 3.2: BRAP-2 is expressed in the cytoplasm of the germline

(A) Representative image of extruded wild type adult germlines stained with α -BRAP-2 antibody, found BRAP-2 to be highly expressed in the cytoplasm of the germline, exhibiting a “honeycomb” effect with BRAP-2 expression surrounding germline nuclei. Ten one day old wild type adult worms were dissected and extruded germlines were examined. White arrows indicate the germline, while yellow arrows indicate the intestine of the worm. (B) BRAP-2 is expressed in the sperm sac of wild type hermaphrodite germlines. Representative image depicting BRAP-2 expression in the sperm sac overlying nuclei in the wild type germline. BRAP-2 was detected in the sperm sacs of three extruded wild type adult germlines. White arrows indicate the sperm sac located at the proximal end of the gonad.

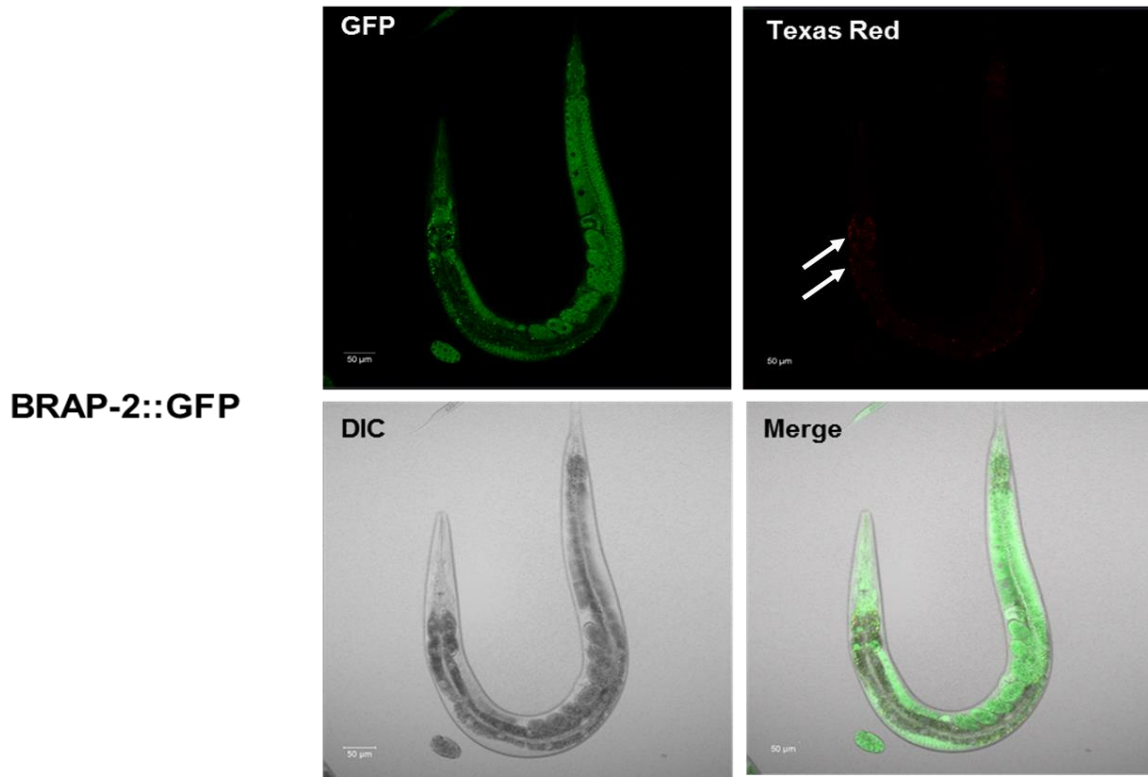


Figure 3.3: BRAP-2 expression is localized to the germline *in vivo*

BRAP-2 expression was examined *in vivo* using a BRAP-2::GFP transgenic strain, generated using CRISPR-Cas9 (21). Representative image of exhibiting BRAP-2 expression in the germline of an adult worm. White arrows indicate Texas Red auto-fluorescence of the intestine that does not overlap BRAP-2::GFP expression. Ten one-day old adults were examined.

3.4.2 BRAP-2 is required for *C. elegans* survival and development

C. elegans is a small, transparent roundworm ideal for genetic studies as defective phenotypes caused by mutation can be visualized directly. We examined whether *brap-2* mutants possessed any developmental or morphological defects. Upon inspection it was apparent that the morphology of *brap-2(ok1492)* mutant worms differed from the wildtype. First, we found that *brap-2(ok1492)* mutants exhibited reductions in worm body length and width, of 100 μm and 10 μm respectively (Figure 3.3).

The *C. elegans* life cycle is short, reaching adulthood after 3 days at 20°C after progressing through four larval stages (L1-L4), distinguished by increasing size. If worms encounter stress in their environment they can exit the life cycle and enter an alternative L3 stage of developmental arrest (dauer), and survive harsh conditions for months (24). When environmental conditions become favorable, worms can re-enter the active life cycle and continue their development normally (25). Previously, we found that *brap-2(ok1492)* mutants are dauer defective and unable to developmentally arrest when starved. First, we examined the timing of development through each larval stage of *brap-2* mutants and found that compared to the wild type, *brap-2(ok1492)* mutants experienced a developmental delay. Only 10% of *brap-2* mutants reached adulthood after 3 days, and 63% reaching adulthood after 4 days compared to the wild type (Figure 3.5).

The average wild type *C. elegans* lifespan typically lasts up to 2 weeks. Long lived *daf-2* mutants of the IIS pathway can prolong worm lifespan 2-fold, while *skn-1* mutant animals reduce mean survival 25-50% (26–28). Since we previously determined that in the context of DNA damage induced germline apoptosis BRAP-2 may act as a regulator of both IIS and the SKN-1/Nrf2 oxidative stress pathway through p38 MAPK/PMK-1, we sought to determine whether a

loss of BRAP-2 affects worm survival. We found that *brap-2(ok1492)* mutants displayed a modest reduction in mean survival, and lived to an average of 11 days compared to the wild type of 13 days (Figure 3.5C). However, we previously found that with the loss of BRC-1 *brap-2(ok1492)* survival can be extended to resemble the wild type. Taken together these results suggest that BRAP-2 is required for normal worm morphology, development and survival.

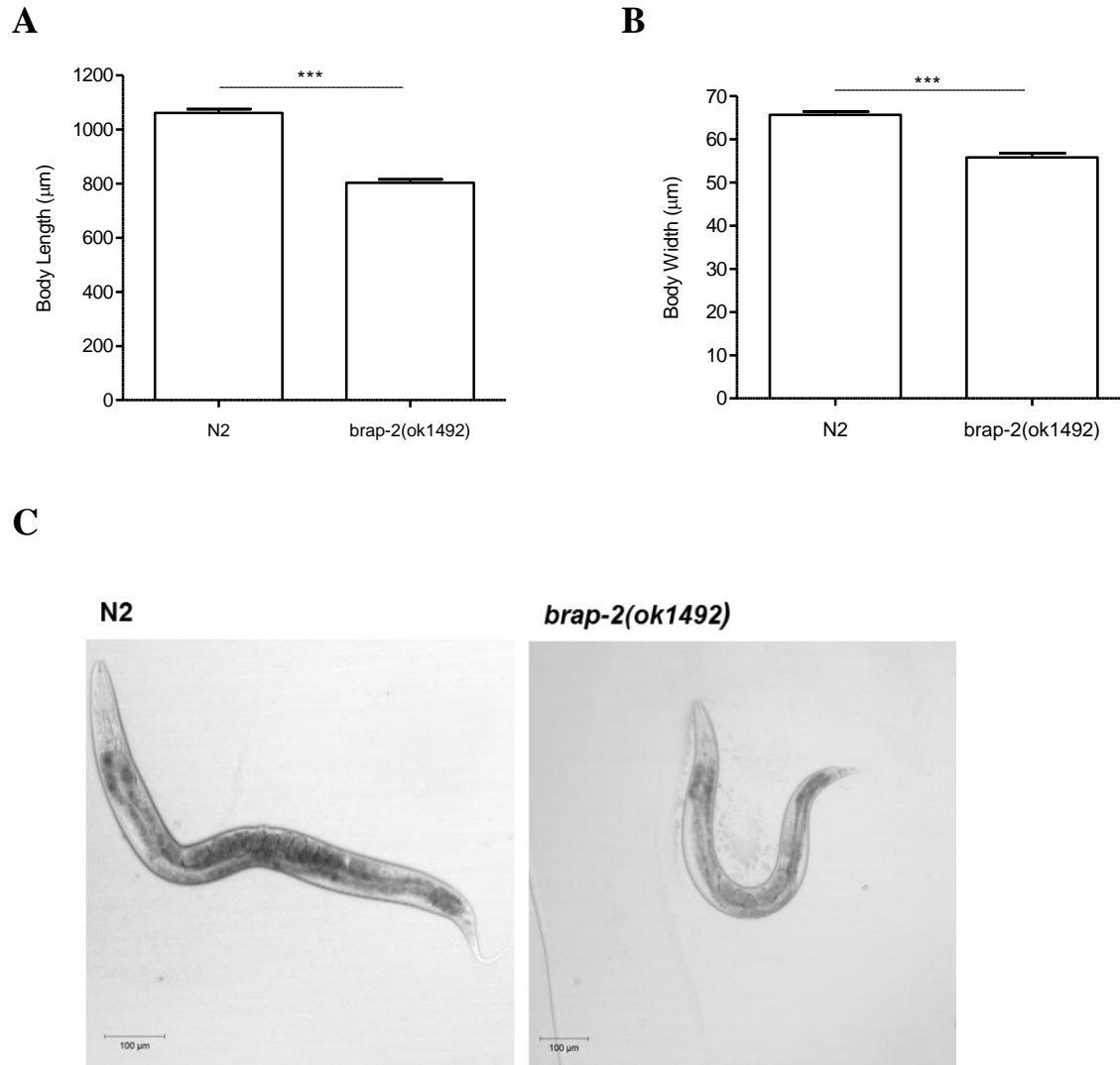


Figure 3.4: *brap-2(ok1492)* worms possess reduced body length and width

brap-2(ok1492) mutants exhibit a significant reduction in (A) body length and (B) body width compared to the wild type (N2). (C) Representative images comparing one day old N2 and *brap-2(ok1492)* mutant animals. Worms were visualized with DIC and total worm length and width was measured [from the anterior-most portion (head) to the posterior tail] using Zen Lite 2010 Software. Results represent N= 30-40 worms per genotype. $p < 0.001$ ***.

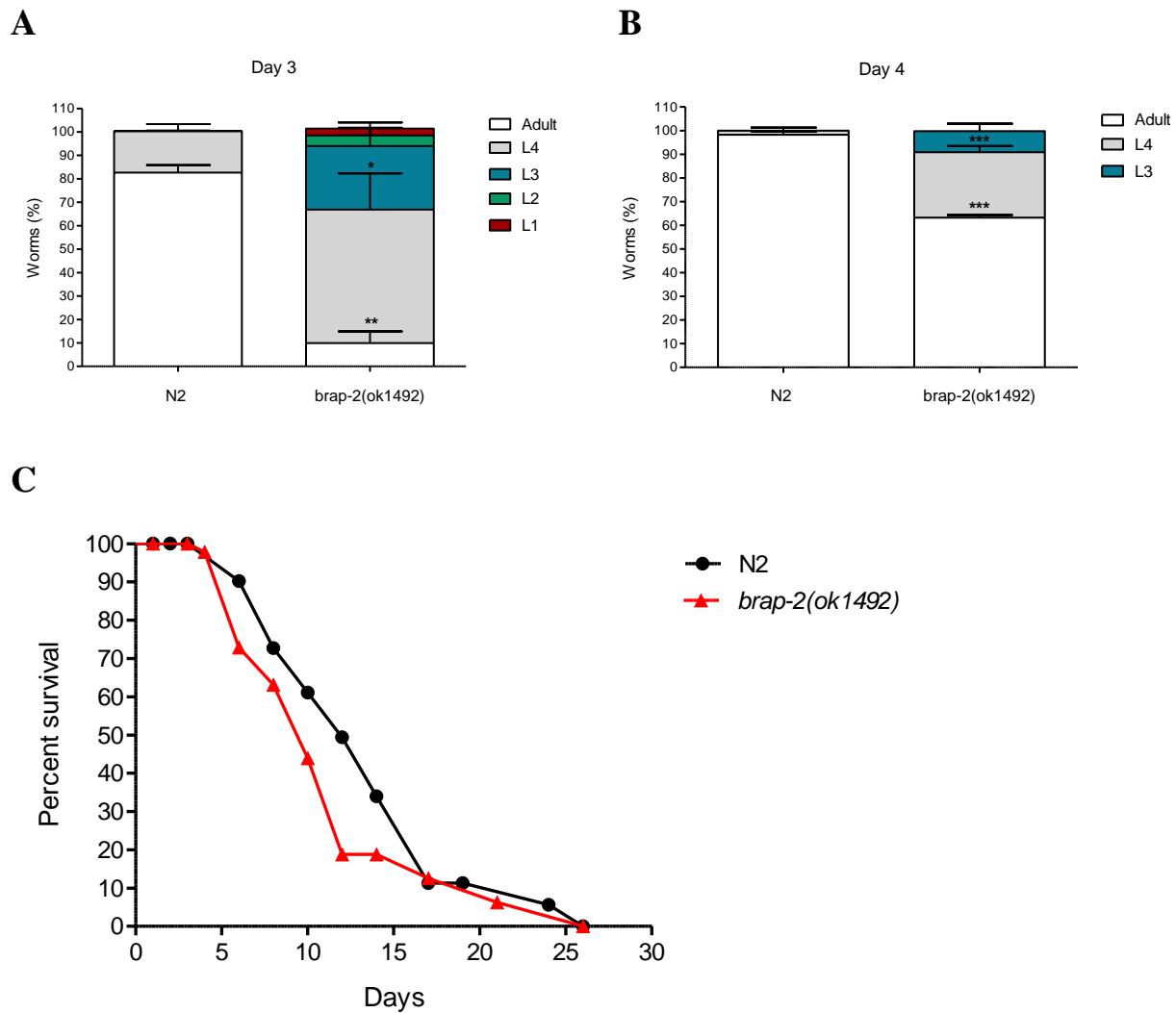


Figure 3.5: *brap-2(ok1492)* causes a developmental delay and reduced survival

(A) After 3 days only 9.9% of *brap-2(ok1492)* worms reach adulthood compared to 72.3% in the wild type (N2). Only 63% of *brap-2(ok1492)* worms reach adulthood after (B) 4 days, compared to N2 at 20°C, resulting in a developmental delay of ~24 hours. Development and larval stages reached were scored each day for 4 days. Results represent 4 independent trials. (C) *brap-2(ok1492)* experiences a mean survival of 11.67 ± 1.67 days compared to the wild type N2 of 13.3 ± 0.67 days. Graph represents one of 3 independent trials. $p < 0.001$ ***, $p < 0.01$ ** , $p < 0.05$ *

3.4.3 BRAP-2 is required for brood size and germline development

The growth rate for *C. elegans* changes with temperature and next we examined brood size and embryonic lethality in *brap-2* mutants at three temperatures: 16°C, 20°C and 25°C. At all 3 temperatures, *brap-2(ok1492)* mutants displayed a 50% decrease in brood size compared to the wild type (Figure 3.6). Over 5 days of adulthood, in *brap-2* mutants we found brood size to be most significantly reduced on the second day of adulthood (Figure S3.1). While embryonic lethality appeared elevated in *brap-2* mutants at 20°C, it was observed to be most significantly increased at 16°C (Figure 3.6A,B). At 20°C, brood size in worms heterozygous for *brap-2* [*brap-2(ok1492)/+*] was similar to the wild type yet the presence of one *ok1492* mutant allele was sufficient to elevate embryonic lethality (Figure 3.6E).

Having observed an overall reduction in brood size and elevated embryonic lethality, we examined *brap-2(ok1492)* mutant germlines for the presence of any abnormalities. Similar to the overall decrease in body size, when we measured gonad length in *brap-2(ok1492)* mutants they displayed a 100 µm decrease compared to the wild type (Figure S3.2). Dissecting intact germlines of *brap-2(ok1492)* mutants followed by DAPI staining, revealed that *brap-2* mutants exhibited shortened mitotic and transition zones compared to the wild type (Figure 3.7). When we scored the number of nuclei diameters from the distal tip of the mitotic zone (MZ) to the beginning of the transition zone (TZ), we saw a more significant reduction at 0 Gy in *brap-2* mutants with an average of 16 mitotic nuclei compared to 23 in the wild type (Figure 3.8A,C).

This suggests that *brap-2* mutants may have reduced number of germline progenitor cells in the MZ. Specifically, we found *brap-2* mutants display similar numbers of germline nuclei in all zones except the MZ, with a 50% reduction at 0 Gy and only a 20% reduction at 60 Gy (Figure 3.8B). This reduction in the number of mitotic nuclei may contribute to the 20% reduction in total germ cell number we observed previously in *brap-2* mutants. Interestingly, in

addition to finding that *brap-2* mutants display similar distribution of germline nuclei over surface area compared to the wild type, we also found that *brap-2* mutants displayed an increase in mitotically arrested nuclei, which may contribute to this reduction in cells in the MZ due to an interruption in cell cycle progression.

Previous work from our lab found that the levels of CKI-1 (p21 ortholog) *in vivo* in *brap-2* mutants increased in seam cells of the hypodermis, cells responsible for growth and development (17). Using qRT-PCR, we measured the mRNA levels of the cyclin dependent kinase inhibitors *cki-1* and *cki-2* (p27 ortholog), and found that they increased 2-fold in *brap-2* mutants (Figure 3.9A) (29). We also found that the G2 mitotic phase arrest associated gene *cyb-1* (Cyclin B1 ortholog) also increased 2-fold in *brap-2(ok1492)* (Figure 3.9B) (30). Interestingly, increased expression of all these genes in *brap-2* mutants was dependent on BRC-1 (Figure 3.9B). This indicates that there may be an increase in cell cycle arrest in the MZ, which may contribute to the increased mitotic arrest and reduction of mitotic cells in *brap-2* mutants. Taken together these results suggest that BRAP-2 is required for normal brood size, embryonic survival, as well as proper germline development.

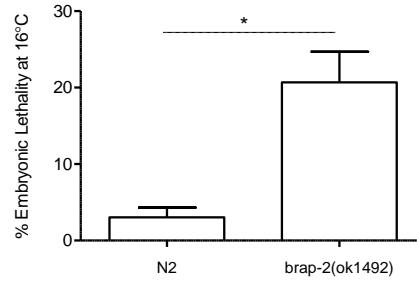
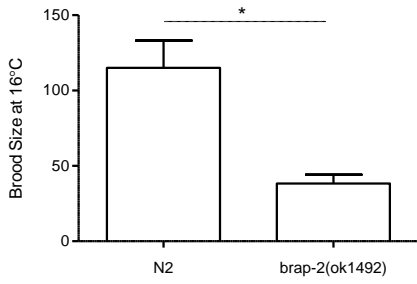
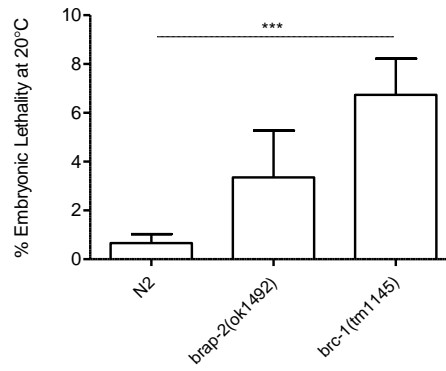
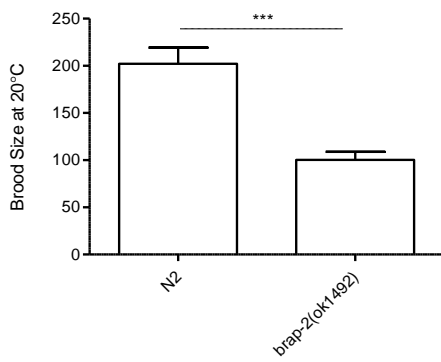
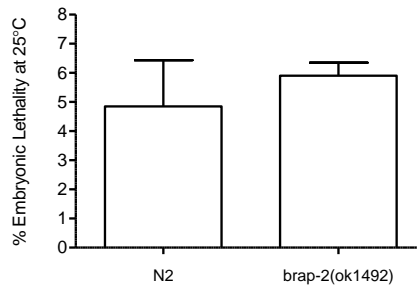
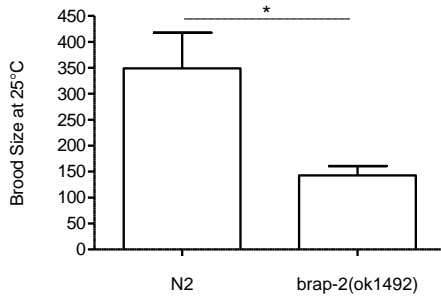
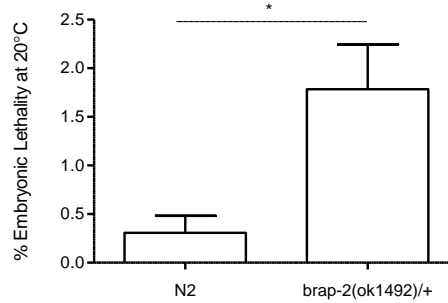
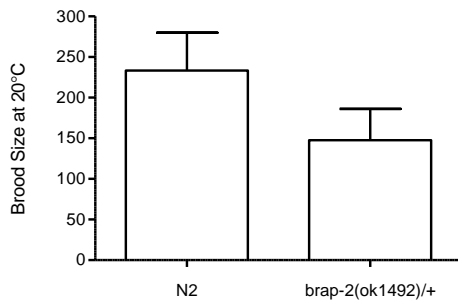
A**B****C****D****Figure caption on next page.**

Figure 3.6: Brood size is reduced in *brap-2(ok1492)* mutants

Brood size and embryonic lethality (%) were scored at (A) 16°C (B) 20°C and (C) 25°C. At all temperatures, *brap-2(ok1492)* mutants displayed a 50% reduction in brood size compared to the wild type (N2). Elevated embryonic lethality was also observed in *brap-2(ok1492)*, except at 25°C. At 20°C, *brc-1(tm1145)* was used a positive control for embryonic lethality. (B) Brood size in worms heterozygous for *brap-2* [*brap-2(ok1492)/+*] is not affected. However, the presence of one *ok1492* mutant allele was sufficient to elevate embryonic lethality. Results represent 3 independent trials. $p < 0.001$ ***, $p < 0.05$ *.

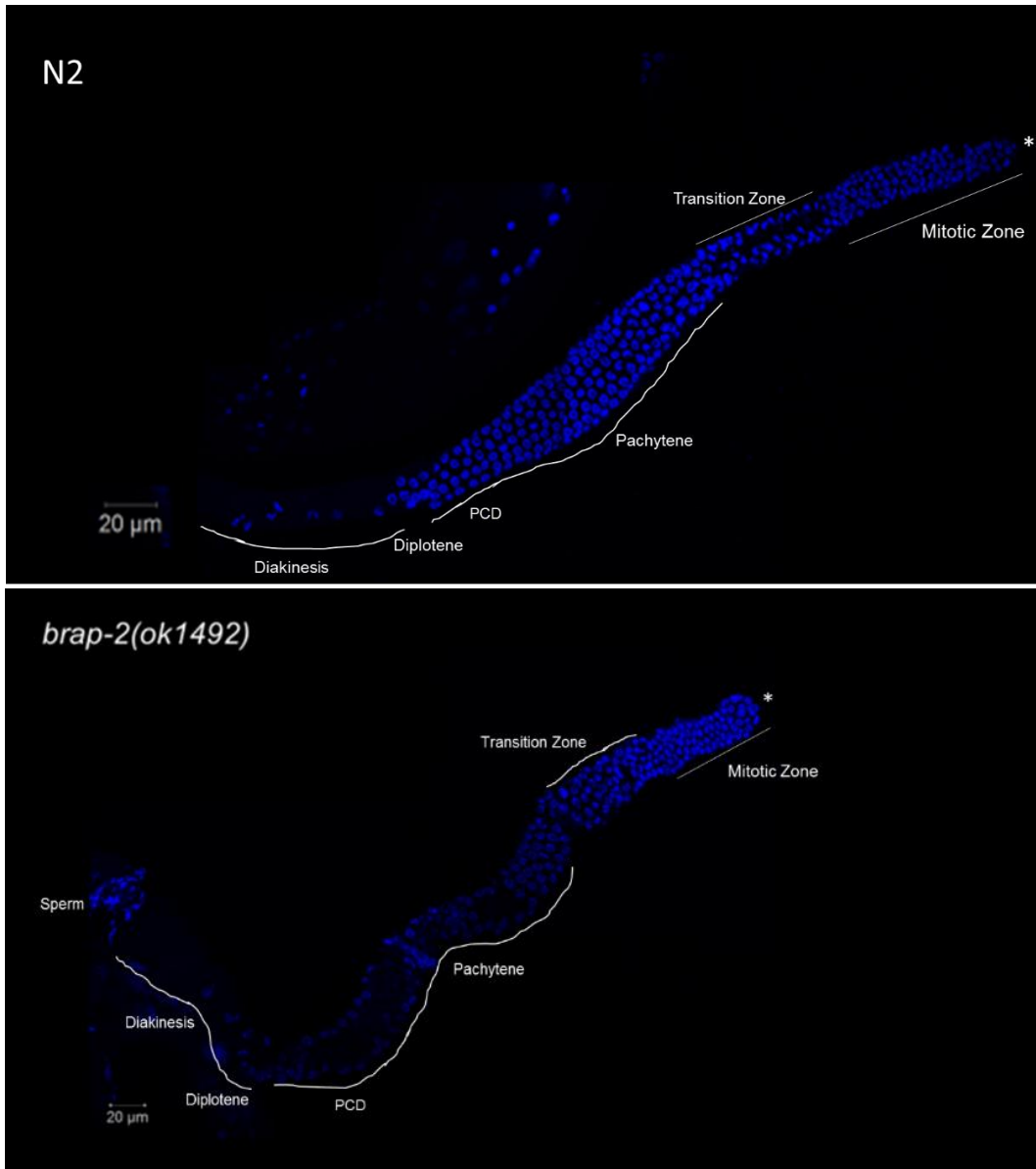


Figure 3.7: *brap-2* mutants exhibit reduced gonad length and a shortened mitotic zone

Representative images comparing DAPI-stained extruded wild type (N2) germline nuclei progression to that of *brap-2(ok1492)* mutants. Z-stack images were taken. Due to the large size, images presented are a composite of two images taken at the same gonad. N=10 per genotype. Asterisk indicates the distal tip. PCD (Programmed Cell Death) labels the loop region of the gonad where apoptosis occurs.

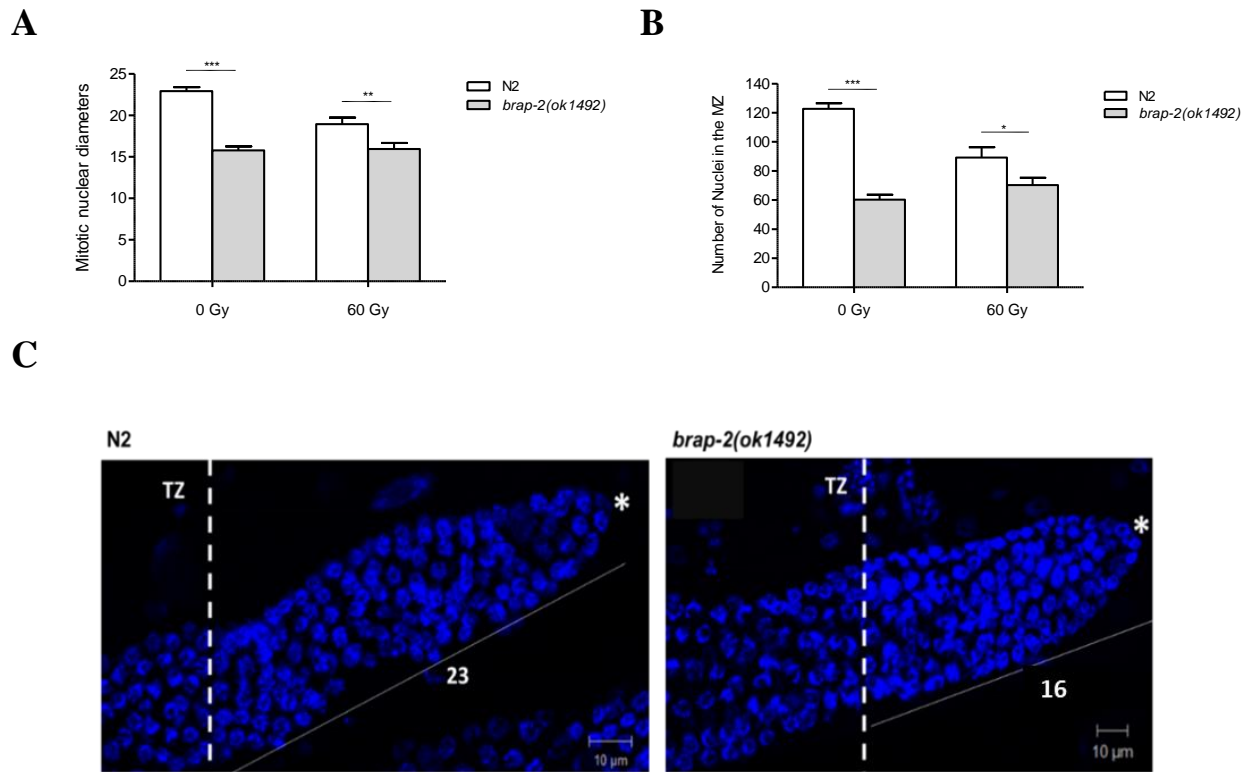


Figure 3.8: *brap-2(ok1492)* reduces the number of nuclei to the transition zone

(A) The number of nuclei diameters [scored from the distal tip of the mitotic zone (MZ) to the beginning of the transition zone (TZ)] are reduced in *brap-2* mutants before and after IR. (B) *brap-2(ok1492)* mutants displayed a more significant reduction in the number of mitotic nuclei in the MZ at 0 Gy, than at 60 Gy. (C) Representative images of the MZ for each genotype. Rows of nuclei were manually counted in whole worms stained with DAPI from the distal tip (marked by asterisk) to the beginning of the TZ (marked by the dotted line). White number represents the average length of the mitotic zone in nuclear diameters from the distal tip of the germline to the TZ. Whole worms were fixed and stained with DAPI. Z-stack images were taken. Nuclei of the MZ were counted from one slice of the Z-stack using ImageJ. Results represent N= 15-40 worms per genotype. $p < 0.001$ ***, $p < 0.01$ ** , $p < 0.05$ *.

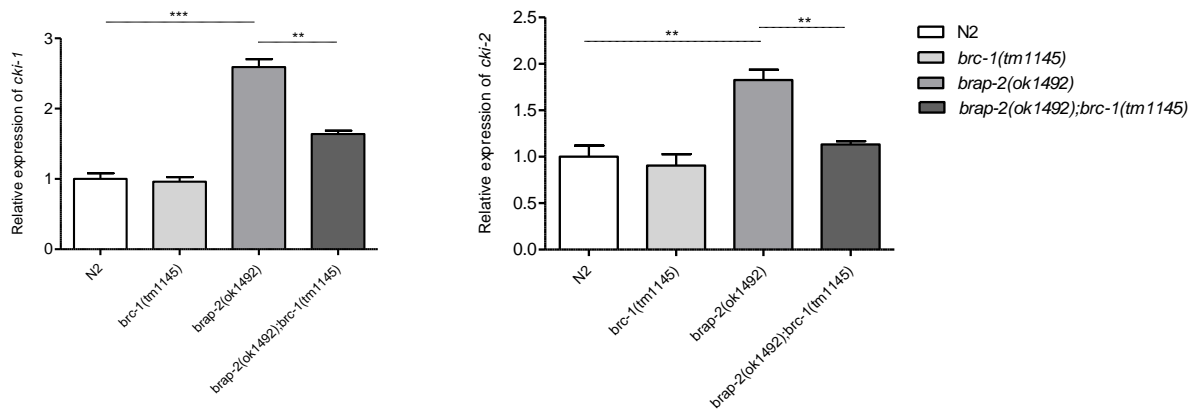
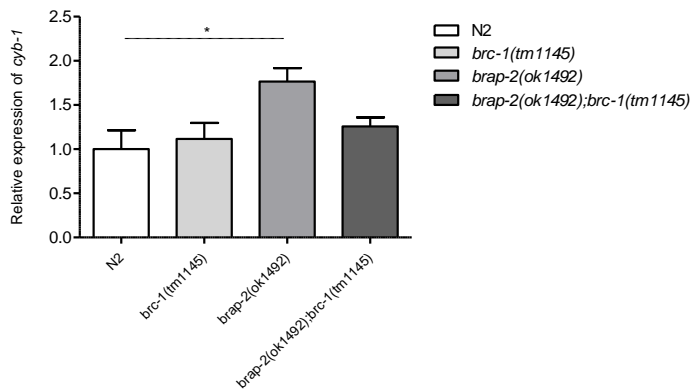
A**B**

Figure 3.9: *brap-2(ok1492)* mutants display increased mRNA levels of *cki-1/2* and *cyb-1*

Using qRT-PCR, mRNA levels of (A) *cki-1* and *cki-2*, as well as (B) *cyb-1* were quantified. Levels of *cki-1*, *cki-2*, and *cyb-1* (one day old adults) all increased 2-fold with a loss of *brap-2*. Results represent 3 independent trials, normalized to *act-1* of N2. $p < 0.001$ ***, $p < 0.01$ **, $p < 0.05$ *

3.4.4 *brap-2* mutants possess increased mitotic radiation sensitivity and chromosomal abnormalities

Having determined that BRAP-2 is required for DNA damage induced germline apoptosis in *brc-1* mutants, and detected BRAP-2 expression in the germline we asked whether BRAP-2 like BRC-1 is involved in DNA repair. To test this, we assessed whether *brap-2* mutants are sensitive to DNA damage using two radiation sensitivity survival assays (9,22). First, sensitivity of meiotic pachytene nuclei was determined by scoring lethality of the progeny produced by L4 stage animals subjected to DNA damage. Following increasing doses of IR, *brap-2* mutants displayed similar sensitivity to DNA damage to that of the wild type (Figure 3.10A). We next examined the sensitivity of mitotic nuclei by scoring embryonic lethality of progeny produced by adult animals that were irradiated at the L1 stage. We found that *brap-2(ok1492)* mutants displayed a 20% increase in embryonic lethality following IR (Figure 3.10B). This indicates that BRAP-2 may be necessary to protect mitotic nuclei from DNA damage, but is dispensable for nuclei at the pachytene stage.

Following late pachytene, nuclei exit the loop region and move on to complete gametogenesis to become large oocytes arresting in diakinesis. Wild type oocytes possess 6 condensed bivalents, representing pairs of homologous chromosomes held together by chiasmata, the physical manifestation of DNA cross-over recombination (7). We scored the number of bivalents in *brap-2(ok1492)* oocytes and found that they possessed a similar number of bivalents to the wild type. However, following IR *brap-2* mutants exhibited a small increase in nuclei with greater than 6 bivalents compared to the wild type (Figure 3.11A). Overall, while examining the oocytes in *brap-2(ok1492)* mutants we also observed that approximately 30% of oocytes displayed chromosomes that appeared in very close proximity to each other or “aggregated”, making it more difficult to score (Figure 3.11B). These results indicate that

BRAP-2 may be required to protect germline integrity, as a loss of *brap-2* increases mitotic nuclei sensitivity to radiation and the appearance of abnormal oocyte chromosome morphology.

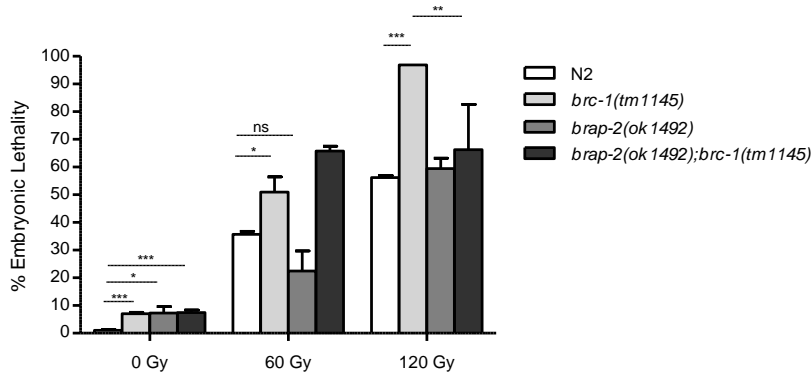
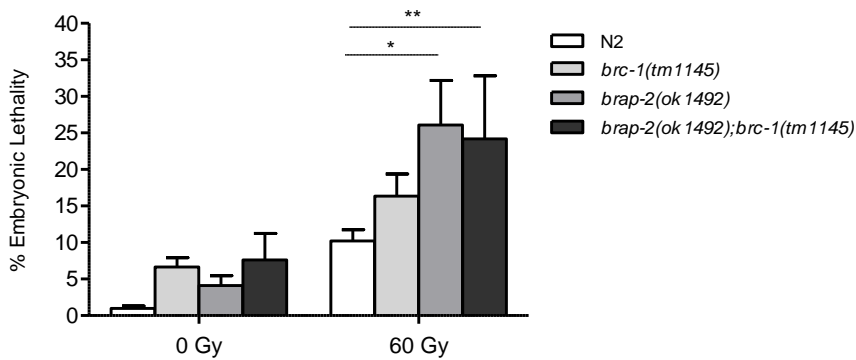
A**B**

Figure 3.10: *brap-2(ok1492)* mutants are hypersensitive to IR during larval development

(A) At increasing doses of IR, embryonic lethality in *brap-2(ok1492)* mutants is similar to the wild type (N2), suggesting that a loss of *brap-2* does not affect radiation sensitivity of pachytene nuclei. Results represent 3-6 independent trials. (B) An increase in embryonic lethality of progeny arising from mitotic nuclei is observed with the loss of *brap-2* indicating that BRAP-2 is required by mitotic nuclei to resist DNA damage. Results represent 3 independent trials. $p < 0.001$ ***, $p < 0.01$ **, $p < 0.05$ *.

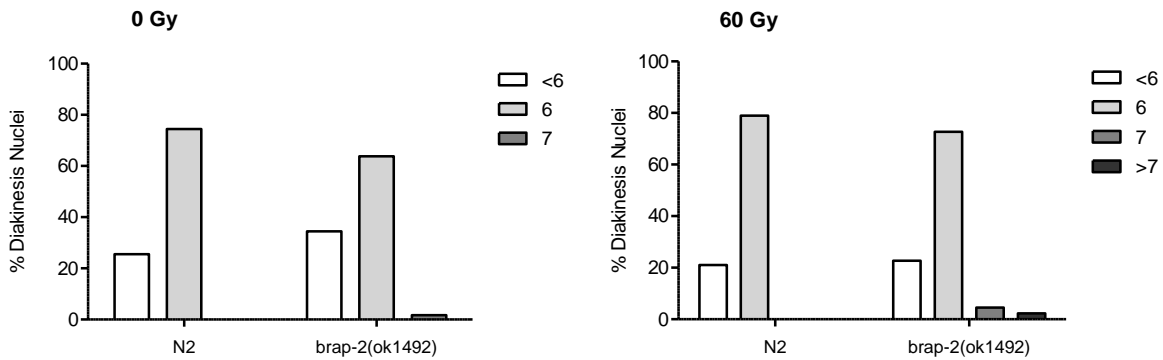
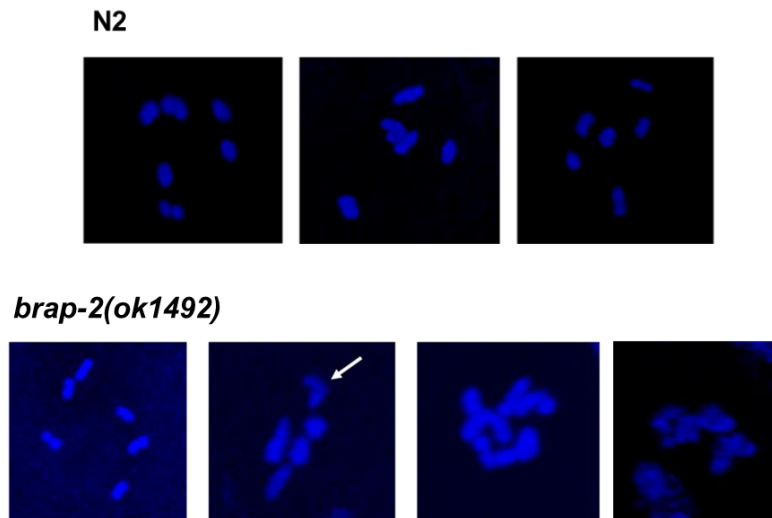
A**B**

Figure 3.11: *brap-2(ok1492)* mutants display abnormal chromosome phenotypes

(A) We observed that *brap-2* mutants possess a small proportion of oocytes with greater than 6 bivalents before and after DNA damage (60 Gy) compared to the wild type (N2). (B) *brap-2(ok1492)* mutants also displayed oocytes that appeared aggregated or abnormal compared to N2. Representative images of N2 and *brap-2(ok1492)* diakinesis nuclei. Z-stack images were taken, where N= 40 oocytes per genotype. The number of DAPI bodies were counted manually in -1 and -2 position oocytes at the proximal end of the gonad using Zen 2010 Lite Software.

3.4.5 Loss of BRAP-2 reduces sperm quality

Previously, it was determined that BRAP2 is a binding protein for testis specific proteins and binds to PHLPP1 during spermatogenesis (31,4). Since we found the expression of BRAP-2 in both female and male portions of the germline to be conserved, this led us to hypothesize that a loss of BRAP-2 may decrease sperm efficiency and their capacity for fertilization, contributing to the reduction in brood size observed in *brap-2(ok1492)* mutants.

The incidence of males in the *C. elegans* population occurs at a frequency of 0.01 to 0.1% and is attributed to the spontaneous non-disjunction of sex chromosomes during meiosis (5). However, a mutation known as “high incidence of males” (HIM) significantly increases embryonic lethality and increases the frequency of males and XXX hermaphrodites due to a reduction in the number of crossovers and defective segregation of the X chromosome (32,33). Unlike *brc-1* mutants, that display both increased embryonic lethality and increased male progeny, *brap-2(ok1492)* mutants do not display an increase in the number of males. To test the effect *brap-2(ok1492)* has on the frequency of males produced by *him-5* mutants, we generated a *brap-2(ok1492);him-5(e1490)* double mutant strain. While embryonic lethality was not significantly affected, we found that compared to single *him-5* mutants, a loss of *brap-2* reduced brood size by half (Figure 3.12A), reduced XXX progeny (identified due to their “dumpy” phenotype) and reduced the incidence of males by 15% (Figure 3.12B,C).

Sex is determined by a XX/XO system, thus when a male worm mates with a hermaphrodite, male sperm will outcompete hermaphrodite sperm and approximately 50% of progeny produced by this mating are expected to be male (34). To determine the quality (ability to fertilize oocytes) of *brap-2(ok1492)* mutant sperm, three young *brap-2;him-5* males were mated with one virgin L4 wild type hermaphrodite. We found that *brap-2(ok1492);him-5(e1490)*

males produced a modest decrease of 13% less male progeny and thus were partly less able to outcompete hermaphrodite sperm (Figure 3.12E). Males have nine paired sensory rays along their hooked tail that allows them to search for and penetrate the hermaphrodite vulva for sperm transfer and fertilization (34). Although we did not observe a difference in the number of sensory rays (Table S3.1), we did observe qualitatively that similar to *brap-2* hermaphrodites, *brap-2;him-5* mutant males compared to single *him-5* mutants appeared smaller in size, and their tails and the morphology of their sensory rays appeared slightly smaller and shorter, respectively (Figure S3.3). These results indicate that BRAP-2 may play a role for proper development of sperm and may in part reduce X chromosome mis-segregation in *him-5* mutants.

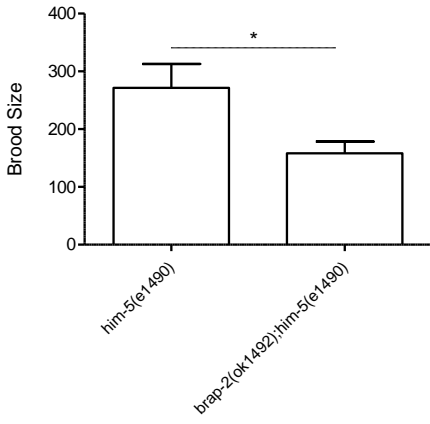
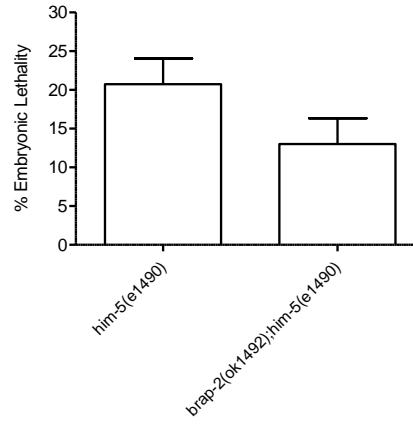
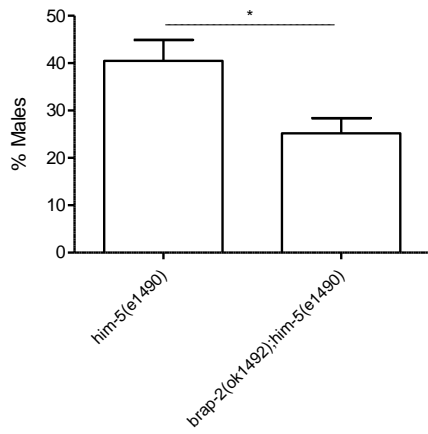
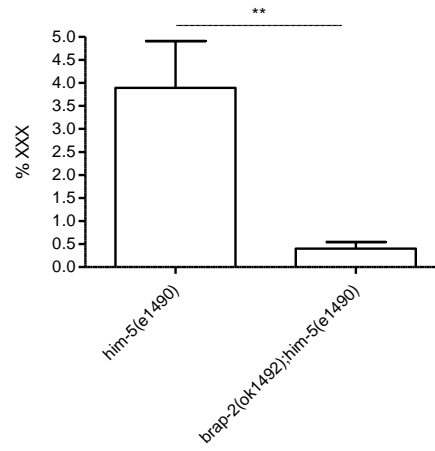
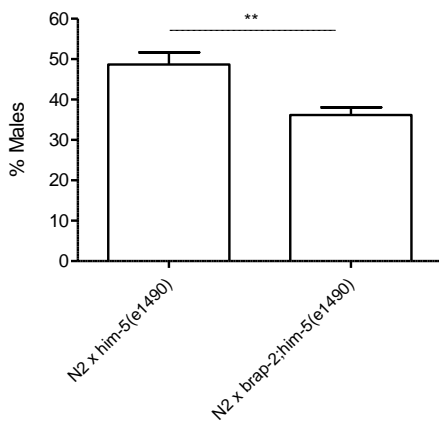
A**B****C****D****E**

Figure caption on next page.

Figure 3.12: *brap-2(ok1492)* decreases sperm quality

(A) *brap-2(ok1492)* mutants decreased brood size in *him-5* mutants by 50%. (B) A loss of *brap-2* reduced embryonic lethality but not significantly in *him-5* mutants. (C) Male progeny (%) in *him-5(e1490)* was reduced by 15 % with a loss of *brap-2*. (D) XXX progeny was significantly reduced in *him-5(e1490)* mutants with a loss of *brap-2*. (E) *brap-2;him-5* males were less able to outcompete hermaphrodite sperm and produced an average of 12% less male progeny. On the x-axis, “N2 x *him-5*” and “N2 x *him-5;brap-2*” represent matings set up between a virgin wild type hermaphrodite and 3 male worms. Results represent 3 independent trials. $p < 0.01^{**}$, $p < 0.05^{*}$.

3.5 Discussion

Here we have shown that *brap-2* mutant animals are shorter in length and width, possess a 24 hour developmental delay to adulthood and exhibit a reduced mean survival compared to the wild type. We previously determined that *brap-2(ok1492)* mutants are dauer defective and unable to enter developmental arrest in response to starvation due to increased DAF-2/Insulin-like signaling and attenuation of DAF-16 (FOXO ortholog). In *C. elegans*, SKN-1/Nrf2 activation contributes to increased lifespan (35). A mutation in *daf-2* (IGF1 ortholog) significantly increases *C. elegans* lifespan due to DAF-16 activation (27). We have previously found that *brap-2* mutants display increased SKN-1 activity (18). This contradiction wherein *brap-2* mutants experience a reduction in mean survival, while possibly possessing over activation of SKN-1, may be due in part to the potential increase in IIS and DAF-16 inhibition occurring in parallel. At the same time, a loss of *brap-2* may influence several others pathways which converge and have an overall negative affect on lifespan.

We have shown that BRAP-2 expression is conserved and localized to the cytoplasm of the wild type hermaphrodite germline surrounding germline nuclei. Using CRISPR-Cas9, we were able to confirm BRAP-2 expression in both the meiotic and somatic (sperm sac, uterus) portions of the germline *in vivo*. Expression of BRAP-2 in the germline suggests that it may be required for its proper development and preservation of genetic integrity. First, we found that *brap-2* mutants displayed a 50% reduction in brood size across three different temperatures. However, in a strain heterozygous for *brap-2(ok1492)* one wild type *brap-2* allele was able to restore brood size to levels more similar to the wild type. Due to the overall reduction in body size in *brap-2* mutants, we expected and observed a reduction in gonad length. Although *brap-2* mutant germlines were shorter, we previously determined that the number of nuclei per surface

area were similar to the wild type. We also found that *brap-2* mutants exhibit a significant reduction of nuclei in the MZ, as well as a reduction in the number of nuclei diameters from the distal tip of the MZ to the TZ, indicating that entry in the TZ may occur earlier in *brap-2* mutants.

Age-related loss of mitotic nuclei has been observed in aging worms and has been associated with defective mitotic cell cycle arrest, a decrease in mitotic index and IIS pathway activation, where elimination of IIS through *daf-2* knockdown or mutation elevated the number of stem cell progenitors in these older worms (36). We previously observed that *brap-2(ok1492)* mutants display enhanced mitotic arrest and potential attenuation of DAF-16, a downstream target of the IIS pathway. In addition, we observed a 2-fold increased expression of cycle arrest associated genes *cki-1*, *cki-2* and *cyb-1* in *brap-2* mutants. It is possible that enhanced IIS and robust mitotic arrest could contribute to the reduction of mitotic nuclei in *brap-2* mutant germlines, as well as contribute to their reduction in brood size. However, it is also possible that a loss of *brap-2* adversely affects other pathways that control meiotic progression, or entry of pachytene nuclei into oogenesis such as the LET-60/MPK-1 (Ras/ERK orthologs) pathway that could decrease oocyte production and therefore lead to an overall reduction in brood size.

DNA repair mutants like *brc-1*, tend to display higher levels of embryonic lethality due to an accumulation of unrepaired DSBs induced during recombination (9). Although not as high as *brc-1* mutants, *brap-2* mutants also display elevated levels of embryonic lethality. After testing the radiation sensitivity of mitotic and pachytene nuclei, we found that a loss of *brap-2* reduced the resistance of only mitotic nuclei to IR. So far it has been observed that DDR mutants tend to increase damage sensitivity in either mitotic or pachytene nuclei, not both, a trend consistent in *brap-2* mutants, indicating it may be involved in DNA repair (9). However, further work such as

examining RAD-51 foci formation following DNA damage and careful classification of chromosome abnormalities, as well as how they can be rescued is required to determine if BRAP-2 is involved in facilitating DNA repair or if a loss of *brap-2* produces these defects indirectly, by affecting the proteins or pathways involved in DNA repair or the conformational changes and packaging of chromosomes prior to fertilization (37).

BRAP2 is conserved in the model flowering plant *Arabidopsis thaliana* which possesses conserved RING domain BRAP2 protein homologs BRIZ1 and BRIZ2 (BRAP2 RING ZnF-UBP domain-containing protein) that dimerize and exhibit conserved functional E3 ubiquitin ligase activity, that is required for seed germination and growth (38). BRAP2 was also found to be highly expressed in mouse testis, acting as a potential scaffold protein for the AKT protein phosphatase PHLPP1 during sperm maturation (4). Since we previously confirmed the conserved interaction between PHLPP-2 (PHLPP1/2 ortholog) and BRAP-2, and observed conserved expression of BRAP-2 in the sperm sac, we examined the affect a loss of *brap-2* has on sperm quality and determined if it is genetically linked to *him-5*, a mutation that increases male production (32). We found that a loss of *brap-2* modestly reduced the number of males in *him-5* mutants and that *brap-2* mutant males were less able to outcompete hermaphrodite sperm, producing a modest reduction in male progeny. Although further work is required, these initial studies indicate that BRAP-2 may in part be required for the production of males in *him-5* mutants and may also play a potential conserved functional role in proper sperm maturation that affects their capacity for fertilization.

Here we have uncovered a novel role for BRAP-2 in *C. elegans* and have found that it is required for normal morphology, development and survival. We also determined that BRAP-2 is involved in germline development and protection where its loss compromises brood size,

embryonic viability, and affects germline development and morphology. Particularly, we found that BRAP-2 is required for the health and protection of the mitotic progenitor stem cell pool. However, although we have uncovered a potential novel role for BRAP-2 further investigation is required to determine the mechanisms through which BRAP-2 may regulate meiotic germline development, DNA repair, as well as other possible signaling cascades such as the Sma/Mab TGF- β (Small/Male Abnormal Transforming Growth Factor β) pathway that governs *C. elegans* development and worm size (39,40).

Protection of genomic integrity in the germline from both endogenous and exogenous stressors is essential, as DNA damage left unfaithfully repaired can lead to an accumulation of mutations, abnormal cells, compromised gametes, dysfunction and disease (41). Although it is unknown whether BRAP2 is directly involved in regulating development, DNA repair or meiosis, due to BRAP-2's high genetic, functional and tissue expression conservation to its mammalian counterpart, this work can be used as a starting point to determine whether the role of BRAP-2 in *C. elegans* morphology, development, survival and germline health is conserved in higher organisms.

3.6 Supplementary Figures

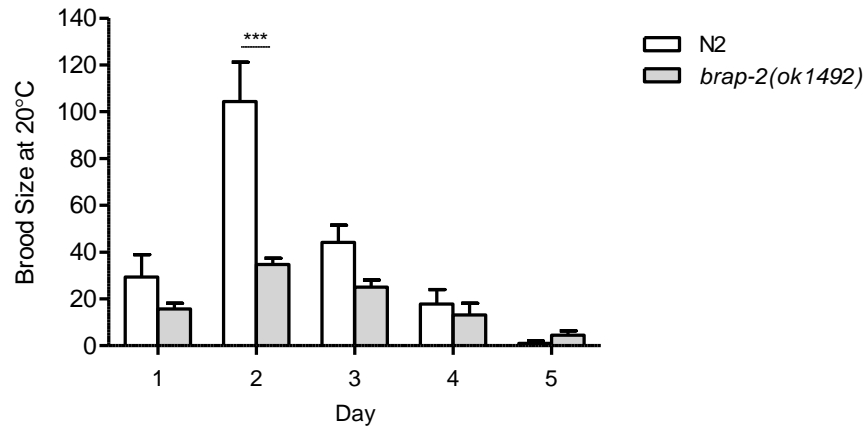


Figure S3.1: Brood size per day in *brap-2* mutant adults is reduced

Compared to the wild type (N2), the number of progeny (brood size) was scored over 5 days of adulthood and was found to be significantly reduced in *brap-2(ok1492)* mutants on the second day of adulthood by 60%. The number of progeny was scored each day for 5 worms placed individually on NGM plates. Results represent 3 independent trials. $p < 0.001$ ***.

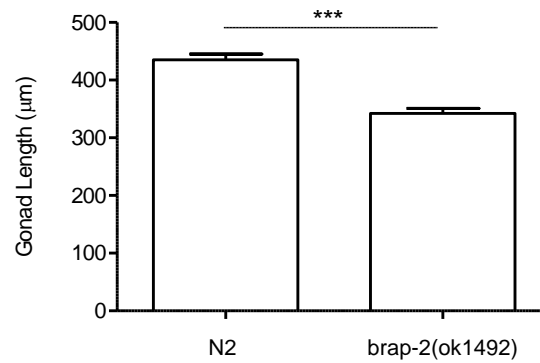


Figure S3.2: Gonad length is reduced in *brap-2* mutants

brap-2 mutants exhibit a reduction in gonad length compared to the wild type (N2). One day old adult worms were fixed and stained with DAPI and images of whole worms were taken for analyses. The line measurement tool in Zen 2010 Software was used to measure the length of one gonad per worm from the distal tip to terminal oocyte at the -1 position. Results represent N= 50 per genotype. $p < 0.001$ ***.

Table S3.1: Number of sensory rays in *him-5* and *brap-2;him-5* mutants

With a loss of *brap-2*, the number of sensory rays was not significantly different to single *him-5* mutant males. Numbers represent the number of rays on one side of the male tail fan. DIC images of young males for each genotype were taken and counted manually in Zen 2010 Lite software.

Strain	N	Number of Sensory Rays (%)		
		9	8	7
<i>him-5(e1490)</i>	49	93.88	4.08	2.04
<i>brap-2(ok1492);him-5(e1490)</i>	56	89.29	10.71	0

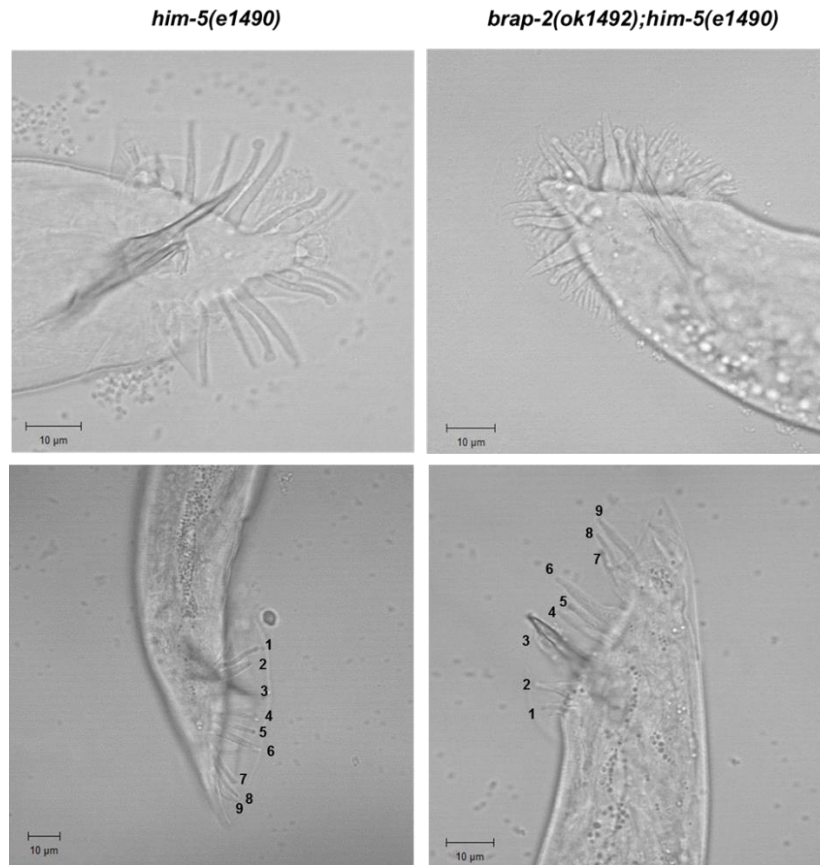


Figure S3.3: Morphology of male sensory rays is altered in *brap-2* mutants

Representative images of young *him-5(e1490)* and *brap-2(ok1492);him-5(e1490)* males. While a loss of *brap-2* did not alter the number of sensory rays in *him-5* mutants, we observed that a small proportion of *brap-2;him-5* mutant males were smaller in size and displayed shorter sensory rays as seen in the top panel. Z-stack images were taken and rays were counted manually in Zen Lite 2010 Software. Black numbers on bottom panel label the sensory rays on one half of each male tail fan. N=49 for *him-5(e1490)* and N=56 for *brap-2(ok1492);him-5(e1490)*.

3.7 Acknowledgements

A number of strains were provided by the CGC, which is funded by NIH Office of Research Infrastructure Programs (P40 OD010440) and the National BioResource Project. We thank also members of the Derry Lab (E. Chapman, B. Yu, B. Lant, A. Mateo, M. Hall, A. Tran, M. Gunda & M. Haeri) for their assistance with the irradiation. D.R.D. is a recipient of the Ontario Graduate Scholarship. M.P. is a recipient of the Dean's Award from the Faculty of Science, York University and a Natural Sciences and Engineering Research Council of Canada (NSERC) undergraduate studentship. D.R.D., Q.H., M.P. and T.J.K were supported by a grant from NSERC.

\

Chapter 4

General Discussion and Future Directions

4.1 Summary

The objective of this study was to characterize the role of BRAP-2 in the DDR and determine its importance in *C. elegans* survival and development. In this study, we have identified the potential mechanism through which BRAP-2 promotes DNA damage induced germline apoptosis and shown that BRAP-2 is required for normal *C. elegans* morphology and development. We have (i) identified *brap-2* as a DNA damage response gene; (ii) determined BRAP-2 specifically promotes DNA damage induced germline apoptosis through the regulation of SKN-1 through p38 MAPK/PMK-1 and IIS pro-survival pathways, and (iii) shown that BRAP-2 is required for *C. elegans* survival, development and germline health.

4.2 Identification of BRAP-2 as a DNA damage response gene and regulator of the SKN-1/PMK-1 and IIS pathways reinforces the “intestine to germline” interaction during stress

Our lab focused its interest on BRAP2/IMP, a BRCA1 binding protein and cytoplasmic retention protein involved in cell signaling pathway regulation (1). Using *C. elegans* as a model, our lab first identified a genetic interaction between BRAP-2 and BRC-1 during oxidative stress (2). Study of BRAP-2 in the oxidative stress response continued and it was determined that a loss of *brap-2* increased SKN-1/Nrf2 nuclear accumulation, and significantly increased the expression of SKN-1 target genes (3). This revealed a novel role for BRAP-2 as a possible negative regulator of SKN-1, a primary activator of the *C. elegans* phase II detoxification response whose function is localized to the intestine (major detoxification organ) for protection against stress, and within neurons to influence longevity (4).

Since BRCA1 and its function in DNA HR repair is conserved in *C. elegans*, in this study we sought to further explore the genetic interaction between *brap-2* and *brc-1* in response to

DNA damage and determine whether BRAP-2 is a potential DDR gene. Using the *C. elegans* germline as an experimental system, the work conducted here provides the first evidence of a role for BRAP-2 in the DDR, where it is required to specifically promote DNA damage induced germline apoptosis and is required for high levels of germline apoptosis incurred by a loss of *brc-1*. We determined that BRAP-2 is required to promote apoptosis in response to IR and that it does so by regulating pathways parallel to the CEP-1 core apoptotic program.

The RAS signaling pathway and p38 MAPK have been implicated in the regulation of apoptosis, and this is conserved in *C. elegans*. MPK-1 is required for germline progression and activation of CEP-1 (5), while PMK-1/p38 MAPK function has been linked to germline apoptosis induced by arsenite exposure, bacterial infection and IR (6). Having observed increased SKN-1 activation in *brap-2* mutants, we found that *skn-1* RNAi knockdown decreased pro-apoptotic gene expression, but only elevated apoptosis in *brap-2;brc-1* double mutants. We also determined that activity of the SKN-1 activator PMK-1 is elevated in *brap-2* mutants.

Previously, in response to IR, *pmk-1(km25)* mutants were found to display reduced levels of apoptosis compared to the wild type (7). However, in this study we observed that *pmk-1* mutants produced similar levels of apoptosis to the wild type and increased apoptosis in *brap-2* mutants, while a loss of *mpk-1* did not. We found that the loss of *mpk-1* or *pmk-1* both decreased the expression of pro-apoptotic CEP-1 target genes *egl-1* and *ced-13*. However, in *brap-2* mutants increased *egl-1* expression levels were dependent on CEP-1 and MPK-1. This suggests that the reduction in germline apoptosis caused by a loss of *brap-2* is dependent on PMK-1, but pro-apoptotic *egl-1* expression in this context may be dependent on increased MPK-1 activation of CEP-1. Although complex, activated PMK-1 observed with a loss of *brap-2* may function

either independently or through the downstream activation of SKN-1 to induce the transcription of genes that prolong cellular health and survival to antagonize CEP-1 activity.

A Y2H screen using a human testis cDNA library has identified novel BRAP2 protein binding candidates (8,9). In addition to the validation of BRAP2 interacting with testis specific proteins, Fatima et al. (2015) confirmed BRAP2 interactions with three additional proteins, including the AKT protein phosphatase PHLPP1. We identified that this interaction is conserved in *C. elegans* and we further postulated that BRAP-2 may act as a potential regulator of AKT-1, and its downstream target DAF-16. We determined that not only does a loss of *brap-2* elevate PMK-1 activity, it increases AKT-1 protein levels and may also cause increased IIS activation.

Although we were not able to test for levels of phosphorylated AKT-1 in *brap-2* mutants to confirm elevated AKT-1 activity as a marker for IIS activation, we believe that (i) the inability of *brap-2* mutants to enter dauer, (ii) reduced DAF-16 intestinal nuclear accumulation, and (iii) reduced DAF-16 target gene expression indicates elevated IIS and partial attenuation of DAF-16. We also saw that a loss of *akt-1* more significantly restored apoptosis to wild type levels than *akt-2* in *brap-2* mutants, suggesting the potential for AKT-1 activation promoting cell survival in the absence of *brap-2*. At the same time, we also uncovered a possible new role for PHLP-2 as being required for the general activation of apoptosis.

Extensive research has shown that the choice for cell survival and homeostasis is governed by many pathways that respond differently, depending on stress and cell type as well as severity. The interpretation of these stimuli, and the subsequent outputs of stress signaling and repair pathways are dependent on one another, and eventually can all influence the balance between pro-apoptotic and anti-apoptotic factors that decide the fate of a cell. Taken together, in addition to regulation of SKN-1/Nrf2 and PMK-1/p38 MAPK, we have determined that BRAP-2

is also a potential regulator of the IIS pathway, a major regulator of *C. elegans* development, longevity and developmental arrest, whose function is also localized to the intestine. This indicates that BRAP-2 may act as an anchor, linking the intestine and germline for parallel regulation and potential cross talk of these pathways in response to stress that converge and influence cell survival or death decisions. When BRAP-2 is lost, it may tip the balance of these signals toward cell survival and evasion of cell death in the germline, simulating a hallmark of cancer.

4.3 Identification of BRAP-2 as a regulator of stress response pathways revealed its importance in *C. elegans* development, survival and germline health.

Working with *brap-2* mutant animals, qualitatively we observed that they were shorter and grew more slowly compared to the wild type. Our identification of the involvement of BRAP-2 in regulating DNA damage induced germline apoptosis, as well as IIS and SKN-1/Nrf2 pathways which are known to regulate oxidative stress, longevity and worm development prompted us to further examine the effects that a loss of BRAP-2 has on the worm overall. We found that in addition to the inability for *brap-2* mutants to enter dauer, worms are shorter, have reduced mean survival, a reduction in brood size and delayed development.

The conserved expression of BRAP-2 in germline tissue led us to further inspect the germline in *brap-2* mutant animals and we found that a loss of *brap-2* modestly reduced the ability for sperm to outcompete and fertilize oocytes, while also reducing the number of males produced in *him-5* mutants. We also determined that BRAP-2 may be specifically needed to protect the mitotic germ cell population from DNA damage. Since shortcomings in several aspects of worm development were observed, it demonstrates that a diverse array of detrimental effects can be caused by pathway mis-regulation incited by a loss of BRAP-2. Phenotypes caused by a loss of *brap-2* is comparable to other previously identified DDR as well as aging

mutants, which can also display defects in *C. elegans* development, longevity and germline protection. Although further work is needed to examine the potential pathways BRAP-2 may regulate in this context, we have revealed that a loss of BRAP-2 produces defective phenotypes in worm anatomy, development and survival, as well as disrupts germline morphology and integrity.

4.4 Potential future studies for BRAP-2 in *C. elegans*

In this study, since BRC-1 is a conserved DNA repair protein that facilitates HR, we focused on determining the role of BRAP-2 in the DDR when exposed to IR, which induces DSBs and activates HR repair pathways. We did not expose *brap-2* mutants to other direct forms of DNA damage such as UV and ENU, known to activate other DNA repair pathways such as nucleotide excision repair and NHEJ) (10) or indirect forms of damage that may arise from exposure to oxidative stress inducers such as paraquat or arsenite (11). It would be interesting to determine whether BRAP-2 is necessary or produces a similar resistance to apoptosis through a comparable stress response mechanism to different forms of DNA damage, or if it is specific to stress caused by DSBs due to its genetic link to BRC-1.

Our study has demonstrated the expansive influence BRAP-2 has on stress signaling cascades involved in detoxification and cell death, as well as on the outcome of *C. elegans* morphology, development and survival. We have also determined that BRAP-2 expression, localization and potential function as a binding protein is conserved. BRAP-2 also possesses conserved RING and ZnF-UBP domains, suggesting that it may function as E3 ubiquitin ligase. However, we did not determine whether BRAP-2 displays intrinsic E3 ligase activity to target itself or other proteins it interacts with, such as PHLP-2 for degradation. Ubiquitination allows for targeted stabilization and degradation of many proteins as a means for cell signaling

regulation and feedback loops (12). RING-type E3 ubiquitin ligases transfer ubiquitin (Ub) from E2-Ub (Ubiquitin conjugating enzymes) to target substrates (13), and in *C. elegans* 20 ubiquitin conjugating enzymes (UBCs) have been identified (14). It will be important to determine if BRAP-2 binds to any of the conserved UBCs, and verify whether BRAP-2 elicits this enzymatic activity for the potential ubiquitination of its targets as a means of regulating oxidative stress and DDR pathways other than by acting as a general binding protein.

We have shown that *brap-2* mutants exhibit defects in development, morphological abnormalities in overall anatomy and within the germline. The IIS pathway is primarily involved in the regulation of lifespan, developmental arrest and participates in the oxidative stress response through DAF-16 activation (15). With these observed defects in *brap-2* mutants, and BRAP-2 functioning as a potential regulator of the IIS pathway, it hints at a possible regulatory role of BRAP-2 in size determination controlled by the Sma/Mab TGF- β pathway (16). The effects a mutation in *brap-2* has on the MZ in the germline could also associate BRAP-2 with the regulation of Notch signaling, localized at the distal tip cell of the germline and functions to renew mitotic stem cells (17). Due to their extensive downstream reach and control of several substrates, there is a possibility that the morphological, developmental and survival defects seen in *brap-2* mutants are a by-product of the dysregulation of the pathways regulated by BRAP-2. However, it would be interesting to explore the potential involvement of BRAP-2 as a regulator of pathways that are not necessarily associated with stress responses, and if BRAP-2 acts as a bridge between them.

One of the ways in which we can further illuminate the role of BRAP-2 in *C. elegans* is using the BRAP-2::GFP transgenic strain generated in this study. An interaction network for BRAP-2 can be built using this strain to conduct mass spectrometry and proteomics to identify

novel protein candidates for BRAP-2 (18,19). Using this high throughput approach, it may reveal novel interactions and pathways that BRAP-2 may be part of which may or may not mimic its mammalian counterpart. In this way, it will establish a more comprehensive view of the role of BRAP-2 in *C. elegans*.

4.5 Future studies of BRAP2 should focus on the biological significance of its predicted interactions and potential conserved role in the DNA damage response

Due to the high expression of BRAP2 in mammalian testes, a testis-specific human cDNA Y2H screen produced a list of 30 candidate proteins that BRAP2 is predicted to interact with (8,9). While these studies have validated a few candidates and reinforced the idea that BRAP2 acts as a general cytoplasmic retention protein seen with its interaction several proteins including PHLPP1 during spermatogenesis, it will be important to continue the validation of other proteins in the screen to help further elucidate the role and influence BRAP2 has on other cellular mechanisms. For example, BRAP2 was found to bind to the DNA methyltransferase DNMT1, necessary for methylation and implicated in cancer, as tumors display aberrant methylation patterns (20). BRAP2 was also predicted to bind to SMARCE1, which encodes one subunit of the SWI/SNF chromatin remodeling complex required for transcription (21). This, in addition to the ability of BRAP2 to bind to BRCA1, which is an important DNA repair and tumour suppressor protein, indicates that BRAP2 may be needed for the maintenance and protection of genomic integrity for the prevention of cancer, and thus these BRAP2 interactions should be further explored.

BRAP2 was also found to be highly expressed in heart tissue (9). A reduction in BRAP2 expression has been linked to myocardial hypertrophy (22), and BRAP2 polymorphisms have been associated with coronary artery disease and metabolic syndromes (23–25). This association

with heart disease suggests the importance of conducting a more in depth investigation into the role of BRAP2 in cardiovascular health, reveal potential heart specific proteins it may associate with as well determine if its role in the regulation of RAS signaling is important in this context. Recently, BRAP2 has also been associated with CCDC178 (Coiled-coil domain-containing protein 178), that is frequently mutated in hepatocellular carcinoma. CCDC178 promotes BRAP2 degradation for increased ERK signaling, and a loss of CCDC178 caused a BRAP2 dependent inactivation of ERK (26).

This provides evidence that functional BRAP2 is linked to several disease states, and due to the high prevalence of cancer caused by BRCA1 mutations, BRAP2 should also be considered as a disease biomarker. However, although BRAP2 is linked to disease we do not know if a mutation in BRAP2 will reveal a similar mechanism of p38 MAPK, Nrf2 and AKT pathway regulation, or confer resistance to apoptosis in response to IR in the same way as we have observed in *C. elegans*. Due to the high genetic similarity between humans and *C. elegans*, our investigation does provide a basis for future studies to investigate the potential role and mechanism of BRAP2 in apoptosis in response to DNA damage, and its potential interaction with BRCA1 in this context.

4.6 Conclusion

BRCA1 is a tumor suppressor involved in transcription, cell cycle arrest and apoptosis and when its function is lost due to mutation it results in the increased risk of breast and ovarian cancer (27). The biological implications of its interaction with BRAP2 have only be inferred, as preventing BRCA1 nuclear translocation thereby prohibiting its functions that protect genomic integrity (1). This study has uncovered the role of *C. elegans* BRAP-2, where a mutation in BRAP-2 tips the balance towards activating cell survival pathways mediated by SKN-1/Nrf2 and

AKT-1/AKT, evading cell death which is necessary for the removal of genetically compromised cells. With approximately 40% of human disease genes having a homolog in *C. elegans*, this study reinforces the power of this organism and its germline as a model to study gene function in DDR pathways to predict their involvement in diseases such as cancer (28). Although further study is needed to determine the clinical importance of BRAP2, the work presented here has identified a previously unknown role for BRAP-2 in *C. elegans* in the regulation of pro-cell survival signaling pathways, presenting a potential intestine to germline interaction for the regulation of DNA damage induced germline apoptosis. We have also uncovered a role for BRAP-2 in *C. elegans* development and germline health. Studies such as this, illustrate the importance of exploring the biological significance of novel proteins involved in physical interactions between established disease-related genes such as BRCA1. What may at first appear as a simple binding event, may have profound effects and present potential therapeutic targets if they influence essential cellular pathways, that when disrupted lead to aberrant signaling, cellular disarray and the onset of diseases such as cancer.

References

I. Chapter 1

1. Fuchs Y, Steller H. Programmed Cell Death in Animal Development and Disease. *Cell*. 2011 Nov 11;147(4):742–58.
2. Liang Y, Lin S-Y, Brunicardi FC, Goss J, Li K. DNA Damage Response Pathways in Tumor Suppression and Cancer Treatment. *World J Surg*. 2009 Apr 1;33(4):661–6.
3. Li L, Zhu T, Gao Y-F, Zheng W, Wang C-J, Xiao L, et al. Targeting DNA Damage Response in the Radio(Chemo)therapy of Non-Small Cell Lung Cancer. *Int J Mol Sci*. 2016 May 31;17(6):839.
4. Tsujimoto Y, Shimizu S. Bcl-2 family: Life-or-death switch. *FEBS Lett*. 2000 Jan 21;466(1):6–10.
5. Eroglu M, Derry WB. Your neighbours matter - non-autonomous control of apoptosis in development and disease. *Cell Death Differ*. 2016 Jul;23(7):1110–8.
6. Cupello S, Richardson C, Yan S. Cell-free *Xenopus* egg extracts for studying DNA damage response pathways. *Int J Dev Biol*. 2016;60(7-8-9):229–36.
7. Ellis HM, Horvitz HR. Genetic control of programmed cell death in the nematode *C. elegans*. *Cell*. 1986 Mar 28;44(6):817–29.
8. Schumacher B, Hofmann K, Boulton S, Gartner A. The *C. elegans* homolog of the p53 tumor suppressor is required for DNA damage-induced apoptosis. *Curr Biol* CB. 2001 Oct 30;11(21):1722–7.
9. Shaye DD, Greenwald I. OrthoList: A Compendium of *C. elegans* Genes with Human Orthologs. *PLoS ONE* [Internet]. 2011 May 25;6(5). Available from: <http://www.ncbi.nlm.nih.gov/pmc/articles/PMC3102077/>
10. Culetto E, Sattelle DB. A role for *Caenorhabditis elegans* in understanding the function and interactions of human disease genes. *Hum Mol Genet*. 2000 Apr 12;9(6):869–77.
11. Gartner A, Boag, Peter, Blackwell TK. Germline survival and apoptosis. *WormBook*. 2008;1–20.
12. Corsi AK, Wightman B, Chalfie M. A Transparent Window into Biology: A Primer on *Caenorhabditis elegans*. *Genetics*. 2015 Jun;200(2):387–407.
13. Jiang Q, Greenberg RA. Deciphering the BRCA1 Tumor Suppressor Network. *J Biol Chem*. 2015 Jul 17;290(29):17724–32.

14. Boulton SJ, Martin JS, Polanowska J, Hill DE, Gartner A, Vidal M. BRCA1/BARD1 Orthologs Required for DNA Repair in *Caenorhabditis elegans*. *Curr Biol*. 2004 Jan;14(1):33–9.
15. Li S, Ku C-Y, Farmer AA, Cong Y-S, Chen C-F, Lee W-H. Identification of a novel cytoplasmic protein that specifically binds to nuclear localization signal motifs. *J Biol Chem*. 1998;273(11):6183–6189.
16. Matheny SA, Chen C, Kortum RL, Razidlo GL, Lewis RE, White MA. Ras regulates assembly of mitogenic signalling complexes through the effector protein IMP. *Nature*. 2004 Jan 15;427(6971):256–60.
17. Koon JC, Kubiseski TJ. Developmental Arrest of *Caenorhabditis elegans* BRAP-2 Mutant Exposed to Oxidative Stress Is Dependent on BRC-1. *J Biol Chem*. 2010 Apr 30;285(18):13437–43.
18. Honnen S. *Caenorhabditis elegans* as a powerful alternative model organism to promote research in genetic toxicology and biomedicine. *Arch Toxicol*. 2017 May;91(5):2029–44.
19. Moreno-Arriola E, Cerdas-Rodríguez N, Coballase-Urrutia E, Pedraza-Chaverri J, et al. *Caenorhabditis elegans*: A Useful Model for Studying Metabolic Disorders in Which Oxidative Stress Is a Contributing Factor. *Oxid Med Cell Longev*. 2014 May 18;2014:e705253.
20. Hodgkin J. Male Phenotypes and Mating Efficiency in *Caenorhabditis elegans*. *Genetics*. 1983 Jan;103(1):43–64.
21. Anderson JL, Morran LT, Phillips PC. Outcrossing and the Maintenance of Males within *C. elegans* Populations. *J Hered*. 2010;101(Suppl 1):S62–74.
22. Gottlieb S, Ruvkun G. *daf-2*, *daf-16* and *daf-23*: genetically interacting genes controlling Dauer formation in *Caenorhabditis elegans*. *Genetics*. 1994 May;137(1):107–20.
23. Hu PJ. Dauer. *Wormbook*. 2007 Aug 8;1–19.
24. Mukhopadhyay A, Oh SW, Tissenbaum HA. Worming pathways to and from DAF-16/FOXO. *Exp Gerontol*. 2006 Oct;41(10):928–34.
25. Paradis S, Ruvkun G. *Caenorhabditis elegans* Akt/PKB transduces insulin receptor-like signals from AGE-1 PI3 kinase to the DAF-16 transcription factor. *Genes Dev*. 1998 Aug 15;12(16):2488–98.
26. Dorman JB, Albinder B, Shroyer T, Kenyon C. The *age-1* and *daf-2* genes function in a common pathway to control the lifespan of *Caenorhabditis elegans*. *Genetics*. 1995 Dec;141(4):1399–406.
27. Ahringer J. Reverse genetics. *WormBook* [Internet]. 2006; Available from: http://www.wormbook.org/chapters/www_introreversegenetics/introreversegenetics.html

28. Dickinson DJ, Goldstein B. CRISPR-Based Methods for *Caenorhabditis elegans* Genome Engineering. *Genetics*. 2016 Mar;202(3):885–901.
29. Kaletta T, Hengartner MO. Finding function in novel targets: *C. elegans* as a model organism. *Nat Rev Drug Discov*. 2006 May;5(5):387–99.
30. Doniach T. Activity of the Sex-Determining Gene *tra-2* Is Modulated to Allow Spermatogenesis in the *C. ELEGANS* Hermaphrodite. *Genetics*. 1986 Sep;114(1):53–76.
31. Colaiácovo MP. The many facets of SC function during *C. elegans* meiosis. *Chromosoma*. 2006 Jun;115(3):195–211.
32. Hodgkin J. Sex determination in the nematode *C. elegans*: analysis of *tra-3* suppressors and characterization of *fem* genes. *Genetics*. 1986 Sep;114(1):15–52.
33. Lui DY, Colaiácovo MP. Meiotic development in *Caenorhabditis elegans*. *Adv Exp Med Biol*. 2013;757:133–70.
34. Kimble JE, White JG. On the control of germ cell development in *Caenorhabditis elegans*. *Dev Biol*. 1981 Jan 30;81(2):208–19.
35. Hillers KJ, Jantsch V, Martinez-Perez E, Yanowitz JL. Meiosis. *WormBook Online Rev C Elegans Biol*. 2017 May 4;1–43.
36. Hayashi M, Chin GM, Villeneuve AM. *C. elegans* germ cells switch between distinct modes of double-strand break repair during meiotic prophase progression. *PLoS Genet*. 2007 Nov;3(11):e191.
37. Villeneuve AM. A cis-acting locus that promotes crossing over between X chromosomes in *Caenorhabditis elegans*. *Genetics*. 1994 Mar;136(3):887–902.
38. Gumienny TL, Lambie E, Hartweg E, Horvitz HR, Hengartner MO. Genetic control of programmed cell death in the *Caenorhabditis elegans* hermaphrodite germline. *Dev Camb Engl*. 1999 Feb;126(5):1011–22.
39. Hubbard EJ. Introduction to the germ line. *WormBook* [Internet]. 2005; Available from: http://www.wormbook.org/chapters/www_introgermline/introgermline.html
40. Jolliffe AK, Derry WB. The TP53 signaling network in mammals and worms. *Brief Funct Genomics*. 2013 Mar;12(2):129–41.
41. Ahmed S, Alpi A, Hengartner MO, Gartner A. *C. elegans* RAD-5/CLK-2 defines a new DNA damage checkpoint protein. *Curr Biol CB*. 2001 Dec 11;11(24):1934–44.
42. Harris J, Lowden M, Clejan I, Tzoneva M, Thomas JH, Hodgkin J, et al. Mutator phenotype of *Caenorhabditis elegans* DNA damage checkpoint mutants. *Genetics*. 2006 Oct;174(2):601–16.

43. Heuvel S van den. Cell-cycle regulation [Internet]. WormBook; 2005 [cited 2017 May 31]. Available from: <https://www.ncbi.nlm.nih.gov/books/NBK19719/>
44. Gartner A, Milstein S, Ahmed S, Hodgkin J, Hengartner MO. A conserved checkpoint pathway mediates DNA damage--induced apoptosis and cell cycle arrest in *C. elegans*. *Mol Cell*. 2000 Mar;5(3):435–43.
45. Craig AL, Moser SC, Bailly AP, Gartner A. Methods for studying the DNA damage response in the *Caenorhabditis elegans* germ line. *Methods Cell Biol*. 2012;107:321–52.
46. Lemmens BBLG, Tijsterman M. DNA double-strand break repair in *Caenorhabditis elegans*. *Chromosoma*. 2011 Feb;120(1):1–21.
47. O'Neil N, Rose A. DNA repair. *WormBook Online Rev C Elegans Biol*. 2006 Jan 13;1–12.
48. Lemmens BBLG, Johnson NM, Tijsterman M. COM-1 promotes homologous recombination during *Caenorhabditis elegans* meiosis by antagonizing Ku-mediated non-homologous end joining. *PLoS Genet*. 2013;9(2):e1003276.
49. Yin Y, Smolikove S. Impaired resection of meiotic double-strand breaks channels repair to nonhomologous end joining in *Caenorhabditis elegans*. *Mol Cell Biol*. 2013 Jul;33(14):2732–47.
50. Lee M-H, Hollis SE, Yoo BH, Nykamp K. *Caenorhabditis elegans* DNA-2 helicase/endonuclease plays a vital role in maintaining genome stability, morphogenesis, and life span. *Biochem Biophys Res Commun*. 2011 Apr 15;407(3):495–500.
51. Lee MH, Han SM, Han JW, Kim YM, Ahnn J, Koo H-S. *Caenorhabditis elegans* dna-2 is involved in DNA repair and is essential for germ-line development. *FEBS Lett*. 2003 Dec 4;555(2):250–6.
52. Bickel JS, Chen L, Hayward J, Yeap SL, Alkers AE, Chan RC. Structural maintenance of chromosomes (SMC) proteins promote homolog-independent recombination repair in meiosis crucial for germ cell genomic stability. *PLoS Genet*. 2010 Jul 22;6(7):e1001028.
53. Adamo A, Montemauri P, Silva N, Ward JD, Boulton SJ, La Volpe A. BRC-1 acts in the inter-sister pathway of meiotic double-strand break repair. *EMBO Rep*. 2008 Mar;9(3):287–92.
54. Bailly A, Gartner A. Germ cell apoptosis and DNA damage responses. *Adv Exp Med Biol*. 2013;757:249–76.
55. Bailly AP, Freeman A, Hall J, Déclais A-C, Alpi A, Lilley DMJ, et al. The *Caenorhabditis elegans* homolog of Gen1/Yen1 resolvases links DNA damage signaling to DNA double-strand break repair. *PLoS Genet*. 2010 Jul 15;6(7):e1001025.

56. Agostinho A, Meier B, Sonnevile R, Jagut M, Woglar A, Blow J, et al. Combinatorial regulation of meiotic holliday junction resolution in *C. elegans* by HIM-6 (BLM) helicase, SLX-4, and the SLX-1, MUS-81 and XPF-1 nucleases. *PLoS Genet.* 2013;9(7):e1003591.
57. Baudrimont A, Penkner A, Woglar A, Mamnun YM, Hulek M, Struck C, et al. A New Thermosensitive smc-3 Allele Reveals Involvement of Cohesin in Homologous Recombination in *C. elegans*. *PLOS ONE.* 2011 Sep 21;6(9):e24799.
58. Martin JS, Winkelmann N, Petalcorin MIR, McIlwraith MJ, Boulton SJ. RAD-51-Dependent and -Independent Roles of a *Caenorhabditis elegans* BRCA2-Related Protein during DNA Double-Strand Break Repair. *Mol Cell Biol.* 2005 Apr 15;25(8):3127–39.
59. Clemons AM, Brockway HM, Yin Y, Kasinathan B, Butterfield YS, Jones SJM, et al. akirin is required for diakinesis bivalent structure and synaptonemal complex disassembly at meiotic prophase I. *Mol Biol Cell.* 2013 Apr;24(7):1053–67.
60. Hansen D, Hubbard EJ, Schedl T. Multi-pathway control of the proliferation versus meiotic development decision in the *Caenorhabditis elegans* germline. *Dev Biol.* 2004 Apr 15;268(2):342–57.
61. VanGompel MJW, Nguyen KCQ, Hall DH, Dauer WT, Rose LS. A novel function for the *Caenorhabditis elegans* torsin OOC-5 in nucleoporin localization and nuclear import. *Mol Biol Cell.* 2015 May 1;26(9):1752–63.
62. Sulston JE, Horvitz HR. Post-embryonic cell lineages of the nematode, *Caenorhabditis elegans*. *Dev Biol.* 1977 Mar;56(1):110–56.
63. Fulda S. Shifting the balance of mitochondrial apoptosis: therapeutic perspectives. *Front Oncol* [Internet]. 2012 Oct 8;2. Available from: <http://www.ncbi.nlm.nih.gov/pmc/articles/PMC3465793/>
64. Vousden KH, Prives C. Blinded by the Light: The Growing Complexity of p53. *Cell.* 2009 May 1;137(3):413–31.
65. Bennett M, Macdonald K, Chan SW, Luzio JP, Simari R, Weissberg P. Cell surface trafficking of Fas: a rapid mechanism of p53-mediated apoptosis. *Science.* 1998 Oct 9;282(5387):290–3.
66. Strasser A, Cory S, Adams JM. Deciphering the rules of programmed cell death to improve therapy of cancer and other diseases. *EMBO J.* 2011 Sep 14;30(18):3667–83.
67. Parcellier A, Tintignac LA, Zhuravleva E, Hemmings BA. PKB and the mitochondria: AKTing on apoptosis. *Cell Signal.* 2008 Jan;20(1):21–30.
68. Haupt S, Berger M, Goldberg Z, Haupt Y. Apoptosis - the p53 network. *J Cell Sci.* 2003 Oct 15;116(Pt 20):4077–85.

69. Wu GS, Burns TF, McDonald ER, Jiang W, Meng R, Krantz ID, et al. KILLER/DR5 is a DNA damage-inducible p53-regulated death receptor gene. *Nat Genet.* 1997 Oct;17(2):141–3.
70. Amaral JD, Xavier JM, Steer CJ, Rodrigues CM. The Role of p53 in Apoptosis. *Discov Med.* 2010 Feb 20;9(45):145–52.
71. Canman CE, Lim DS, Cimprich KA, Taya Y, Tamai K, Sakaguchi K, et al. Activation of the ATM kinase by ionizing radiation and phosphorylation of p53. *Science.* 1998 Sep 11;281(5383):1677–9.
72. Shieh SY, Ahn J, Tamai K, Taya Y, Prives C. The human homologs of checkpoint kinases Chk1 and Cds1 (Chk2) phosphorylate p53 at multiple DNA damage-inducible sites. *Genes Dev.* 2000 Feb 1;14(3):289–300.
73. Zhang W, Luo J, Chen F, Yang F, Song W, Zhu A, et al. BRCA1 regulates PIG3-mediated apoptosis in a p53-dependent manner. *Oncotarget.* 2015 Feb 18;6(10):7608–18.
74. Daugas E, Susin SA, Zamzami N, Ferri KF, Irinopoulou T, Larochette N, et al. Mitochondrio-nuclear translocation of AIF in apoptosis and necrosis. *FASEB J Off Publ Fed Am Soc Exp Biol.* 2000 Apr;14(5):729–39.
75. Du C, Fang M, Li Y, Li L, Wang X. Smac, a mitochondrial protein that promotes cytochrome c-dependent caspase activation by eliminating IAP inhibition. *Cell.* 2000 Jul 7;102(1):33–42.
76. Kaufmann T, Strasser A, Jost PJ. Fas death receptor signalling: roles of Bid and XIAP. *Cell Death Differ.* 2012 Jan;19(1):42–50.
77. Verhagen AM, Ekert PG, Pakusch M, Silke J, Connolly LM, Reid GE, et al. Identification of DIABLO, a mammalian protein that promotes apoptosis by binding to and antagonizing IAP proteins. *Cell.* 2000 Jul 7;102(1):43–53.
78. Degtarev A, Yuan J. Expansion and evolution of cell death programmes. *Nat Rev Mol Cell Biol.* 2008 May;9(5):378–90.
79. Fridman JS, Lowe SW. Control of apoptosis by p53. *Oncogene.* 2003;22(56):9030–40.
80. Stambolic V, MacPherson D, Sas D, Lin Y, Snow B, Jang Y, et al. Regulation of PTEN Transcription by p53. *Mol Cell.* 2001 Aug 1;8(2):317–25.
81. Horn HF, Vousden KH. Coping with stress: multiple ways to activate p53. *Oncogene.* 2007;26(9):1306–16.
82. Blum ES, Driscoll M, Shaham S. Noncanonical cell death programs in the nematode *Caenorhabditis elegans*. *Cell Death Differ.* 2008 Jul;15(7):1124–31.

83. Rutkowski R, Dickinson R, Stewart G, Craig A, Schimpl M, Keyse SM, et al. Regulation of *Caenorhabditis elegans* p53/CEP-1-dependent germ cell apoptosis by Ras/MAPK signaling. *PLoS Genet*. 2011 Aug;7(8):e1002238.
84. Garcia-Muse T, Boulton SJ. Distinct modes of ATR activation after replication stress and DNA double-strand breaks in *Caenorhabditis elegans*. *EMBO J*. 2005 Dec 21;24(24):4345–55.
85. Suetomi K, Mereiter S, Mori C, Takanami T, Higashitani A. *Caenorhabditis elegans* ATR checkpoint kinase ATL-1 influences life span through mitochondrial maintenance. *Mitochondrion*. 2013 Nov;13(6):729–35.
86. Derry WB, Putzke AP, Rothman JH. *Caenorhabditis elegans* p53: role in apoptosis, meiosis, and stress resistance. *Science*. 2001 Oct 19;294(5542):591–5.
87. Nehme R, Conradt B. *egl-1*: a key activator of apoptotic cell death in *C. elegans*. *Oncogene*. 2008 Dec;27 Suppl 1:S30-40.
88. Schumacher B, Schertel C, Wittenburg N, Tuck S, Mitani S, Gartner A, et al. *C. elegans* *ced-13* can promote apoptosis and is induced in response to DNA damage. *Cell Death Differ*. 2005 Feb;12(2):153–61.
89. Fairlie WD, Perugini MA, Kvangsakul M, Chen L, Huang DCS, Colman PM. CED-4 forms a 2 : 2 heterotetrameric complex with CED-9 until specifically displaced by EGL-1 or CED-13. *Cell Death Differ*. 2006 Mar;13(3):426–34.
90. Modi V, Sankararamakrishnan R. Antiapoptotic Bcl-2 homolog CED-9 in *Caenorhabditis elegans*: dynamics of BH3 and CED-4 binding regions and comparison with mammalian antiapoptotic Bcl-2 proteins. *Proteins*. 2014 Jun;82(6):1035–47.
91. Zhou Z, Hartweg E, Horvitz HR. CED-1 is a transmembrane receptor that mediates cell corpse engulfment in *C. elegans*. *Cell*. 2001 Jan 12;104(1):43–56.
92. Ross AJ, Li M, Yu B, Gao MX, Derry WB. The EEL-1 ubiquitin ligase promotes DNA damage-induced germ cell apoptosis in *C. elegans*. *Cell Death Differ*. 2011 Jul;18(7):1140–9.
93. Ito S, Greiss S, Gartner A, Derry WB. Cell-nonautonomous regulation of *C. elegans* germ cell death by *kri-1*. *Curr Biol CB*. 2010 Feb 23;20(4):333–8.
94. Greiss S, Hall J, Ahmed S, Gartner A. *C. elegans* SIR-2.1 translocation is linked to a proapoptotic pathway parallel to *cep-1/p53* during DNA damage-induced apoptosis. *Genes Dev*. 2008 Oct 15;22(20):2831–42.
95. Silva N, Adamo A, Santonicola P, Martinez-Perez E, La Volpe A. Pro-crossover factors regulate damage-dependent apoptosis in the *Caenorhabditis elegans* germ line. *Cell Death Differ*. 2013 Sep;20(9):1209–18.

96. Min H, Shim Y-H, Kawasaki I. Loss of PGL-1 and PGL-3, members of a family of constitutive germ-granule components, promotes germline apoptosis in *C. elegans*. *J Cell Sci*. 2016 Jan 15;129(2):341–53.
97. Park D, Jia H, Rajakumar V, Chamberlin HM. Pax2/5/8 proteins promote cell survival in *C. elegans*. *Dev Camb Engl*. 2006 Nov;133(21):4193–202.
98. Schertel C, Conradt B. *C. elegans* orthologs of components of the RB tumor suppressor complex have distinct pro-apoptotic functions. *Dev Camb Engl*. 2007 Oct;134(20):3691–701.
99. Láscares-Lagunas LI, Silva-García CG, Dinkova TD, Navarro RE. LIN-35/Rb causes starvation-induced germ cell apoptosis via CED-9/Bcl2 downregulation in *Caenorhabditis elegans*. *Mol Cell Biol*. 2014 Jul;34(13):2499–516.
100. Gao MX, Liao EH, Yu B, Wang Y, Zhen M, Derry WB. The SCF FSN-1 ubiquitin ligase controls germline apoptosis through CEP-1/p53 in *C. elegans*. *Cell Death Differ*. 2008 Jun;15(6):1054–62.
101. Perrin AJ, Gunda M, Yu B, Yen K, Ito S, Forster S, et al. Noncanonical control of *C. elegans* germline apoptosis by the insulin/IGF-1 and Ras/MAPK signaling pathways. *Cell Death Differ*. 2013 Jan;20(1):97–107.
102. Quevedo C, Kaplan DR, Derry WB. AKT-1 regulates DNA-damage-induced germline apoptosis in *C. elegans*. *Curr Biol CB*. 2007 Feb 6;17(3):286–92.
103. Wang Q, Zhang H, Fishel R, Greene MI. BRCA1 and cell signaling. *Oncogene*. 2000 Dec 11;19(53):6152–8.
104. Henderson BR. The BRCA1 Breast Cancer Suppressor: Regulation of Transport, Dynamics, and Function at Multiple Subcellular Locations. *Scientifica*. 2012;2012:796808.
105. Polanowska J, Martin JS, Garcia-Muse T, Petalcorin MIR, Boulton SJ. A conserved pathway to activate BRCA1-dependent ubiquitylation at DNA damage sites. *EMBO J*. 2006 May 17;25(10):2178–88.
106. Walsh CS. Two decades beyond BRCA1/2: Homologous recombination, hereditary cancer risk and a target for ovarian cancer therapy. *Gynecol Oncol*. 2015 May;137(2):343–50.
107. Westermarck UK, Reyngold M, Olshen AB, Baer R, Jasin M, Moynahan ME. BARD1 participates with BRCA1 in homology-directed repair of chromosome breaks. *Mol Cell Biol*. 2003 Nov;23(21):7926–36.
108. Li ML, Greenberg RA. Links between genome integrity and BRCA1 tumor suppression. *Trends Biochem Sci*. 2012 Oct 1;37(10):418–24.

109. Fabbro M, Rodriguez JA, Baer R, Henderson BR. BARD1 induces BRCA1 intranuclear foci formation by increasing RING-dependent BRCA1 nuclear import and inhibiting BRCA1 nuclear export. *J Biol Chem*. 2002 Jun 14;277(24):21315–24.
110. Wu J, Lu L-Y, Yu X. The role of BRCA1 in DNA damage response. *Protein Cell*. 2010 Feb;1(2):117–23.
111. Thomson TM, Guerra-Rebollo M. Ubiquitin and SUMO signalling in DNA repair. *Biochem Soc Trans*. 2010 Feb;38(Pt 1):116–31.
112. Zhang J, Powell SN. The Role of the BRCA1 Tumor Suppressor in DNA Double-Strand Break Repair. *Mol Cancer Res*. 2005 Oct 1;3(10):531–9.
113. Michalak EM, Jonkers J. Studying therapy response and resistance in mouse models for BRCA1-deficient breast cancer. *J Mammary Gland Biol Neoplasia*. 2011 Apr;16(1):41–50.
114. Thompson ME. BRCA1 16 years later: nuclear import and export processes. *FEBS J*. 2010 Aug;277(15):3072–8.
115. Fabbro M, Schuechener S, Au WWY, Henderson BR. BARD1 regulates BRCA1 apoptotic function by a mechanism involving nuclear retention. *Exp Cell Res*. 2004 Aug 15;298(2):661–73.
116. MacLachlan TK, Takimoto R, El-Deiry WS. BRCA1 Directs a Selective p53-Dependent Transcriptional Response towards Growth Arrest and DNA Repair Targets. *Mol Cell Biol*. 2002 Jun 15;22(12):4280–92.
117. MacLachlan TK, Somasundaram K, Sgagias M, Shifman Y, Muschel RJ, Cowan KH, et al. BRCA1 Effects on the Cell Cycle and the DNA Damage Response Are Linked to Altered Gene Expression. *J Biol Chem*. 2000 Jan 28;275(4):2777–85.
118. Caspase-3 mediated cleavage of BRCA1 during UV-induced apoptosis. *Publ Online 02 August 2002 Doi101038sjonc1205665* [Internet]. 2002 Aug 2 [cited 2017 May 25];21(34). Available from: <http://www.nature.com/onc/journal/v21/n34/full/1205665a.html>
119. Thangaraju M, Kaufmann SH, Couch FJ. BRCA1 facilitates stress-induced apoptosis in breast and ovarian cancer cell lines. *J Biol Chem*. 2000 Oct 27;275(43):33487–96.
120. Foray N, Randrianarison V, Marot D, Perricaudet M, Lenoir G, Feunteun J. Gamma-rays-induced death of human cells carrying mutations of BRCA1 or BRCA2. *Oncogene*. 1999 Dec 2;18(51):7334–42.
121. Laulier C, Barascu A, Guirouilh-Barbat J, Pennarun G, Chalony CL, Chevalier F, et al. Bcl-2 Inhibits Nuclear Homologous Recombination by Localizing BRCA1 to the Endomembranes. *Cancer Res*. 2011 May 15;71(10):3590–602.

122. Toll-Riera M, Radó-Trilla N, Martys F, Albà MM. Role of Low-Complexity Sequences in the Formation of Novel Protein Coding Sequences. *Mol Biol Evol.* 2012 Mar 1;29(3):883–6.
123. Coletta A, Pinney JW, Solís DYW, Marsh J, Pettifer SR, Attwood TK. Low-complexity regions within protein sequences have position-dependent roles. *BMC Syst Biol.* 2010;4:43.
124. Jang ER, Lee J-S. DNA Damage Response Mediated through BRCA1. *Cancer Res Treat* *Cancer Res Treat.* 2004 Aug 31;36(4):214–21.
125. Peng G. Exploiting the homologous recombination DNA repair network for targeted cancer therapy. *World J Clin Oncol.* 2011;2(2):73.
126. Fulcher AJ, Roth DM, Fatima S, Alvisi G, Jans DA. The BRCA-1 binding protein BRAP2 is a novel, negative regulator of nuclear import of viral proteins, dependent on phosphorylation flanking the nuclear localization signal. *FASEB J.* 2010 May 1;24(5):1454–66.
127. Asada M, Ohmi K, Delia D, Enosawa S, Suzuki S, Yuo A, et al. Brap2 Functions as a Cytoplasmic Retention Protein for p21 during Monocyte Differentiation. *Mol Cell Biol.* 2004 Sep 15;24(18):8236–43.
128. Chen J-S, Hu H-Y, Zhang S, He M, Hu R-M. Brap2 facilitates HsCdc14A Lys-63 linked ubiquitin modification. *Biotechnol Lett.* 2009 May;31(5):615–21.
129. Chen C, Lewis RE, White MA. IMP modulates KSR1-dependent multivalent complex formation to specify ERK1/2 pathway activation and response thresholds. *J Biol Chem.* 2008 May 9;283(19):12789–96.
130. Matheny SA, White MA. Ras-sensitive IMP modulation of the Raf/MEK/ERK cascade through KSR1. *Methods Enzymol.* 2006;407:237–47.
131. Matheny SA, White MA. Signaling threshold regulation by the Ras effector IMP. *J Biol Chem.* 2009 Apr 24;284(17):11007–11.
132. Takashima O, Tsuruta F, Kigoshi Y, Nakamura S, Kim J, Katoh MC, et al. Brap2 Regulates Temporal Control of NF- κ B Localization Mediated by Inflammatory Response. Srinivasula SM, editor. *PLoS ONE.* 2013 Mar 15;8(3):e58911.
133. Fatima S, Wagstaff KM, Loveland KL, Jans DA. Interactome of the negative regulator of nuclear import BRCA1-binding protein 2. *Sci Rep.* 2015 Mar 30;5:9459.
134. Davies RG, Wagstaff KM, McLaughlin EA, Loveland KL, Jans DA. The BRCA1-binding protein BRAP2 can act as a cytoplasmic retention factor for nuclear and nuclear envelope-localizing testicular proteins. *Biochim Biophys Acta BBA - Mol Cell Res.* 2013 Dec;1833(12):3436–44.

135. Lien EC, Dibble CC, Toker A. PI3K signaling in cancer: beyond AKT. *Curr Opin Cell Biol.* 2017 Mar 23;45:62–71.
136. Zhuang N, Li L, Chen S, Wang T. PINK1-dependent phosphorylation of PINK1 and Parkin is essential for mitochondrial quality control. *Cell Death Dis.* 2016 Dec;7(12):e2501.
137. Hu Q, D'Amora DR, MacNeil LT, Walhout AJM, Kubiseski TJ. The Oxidative Stress Response in *Caenorhabditis elegans* requires the GATA Transcription Factor ELT-3 and SKN-1/Nrf2. *Genetics.* 2017 Jun 9; doi: 10.1534/genetics.116.198788.
138. An JH, Vranas K, Lucke M, Inoue H, Hisamoto N, Matsumoto K, et al. Regulation of the *Caenorhabditis elegans* oxidative stress defense protein SKN-1 by glycogen synthase kinase-3. *Proc Natl Acad Sci U S A.* 2005 Nov 8;102(45):16275–80.
139. Kolch W. Coordinating ERK/MAPK signalling through scaffolds and inhibitors. *Nat Rev Mol Cell Biol.* 2005 Nov;6(11):827–37.
140. Brown MD, Sacks DB. Protein scaffolds in MAP kinase signalling. *Cell Signal.* 2009 Apr;21(4):462–9.
141. Dickinson RJ, Keyse SM. Diverse physiological functions for dual-specificity MAP kinase phosphatases. *J Cell Sci.* 2006 Nov 15;119(Pt 22):4607–15.
142. Cargnello M, Roux PP. Activation and function of the MAPKs and their substrates, the MAPK-activated protein kinases. *Microbiol Mol Biol Rev MMBR.* 2011 Mar;75(1):50–83.
143. Krens SFG, Spaink HP, Snaar-Jagalska BE. Functions of the MAPK family in vertebrate-development. *FEBS Lett.* 2006 Sep 18;580(21):4984–90.
144. Cuadrado A, Nebreda AR. Mechanisms and functions of p38 MAPK signalling. *Biochem J.* 2010 Aug 1;429(3):403–17.
145. Wilkinson MG, Millar JB. Control of the eukaryotic cell cycle by MAP kinase signaling pathways. *FASEB J Off Publ Fed Am Soc Exp Biol.* 2000 Nov;14(14):2147–57.
146. Pearson G, Robinson F, Beers Gibson T, Xu BE, Karandikar M, Berman K, et al. Mitogen-activated protein (MAP) kinase pathways: regulation and physiological functions. *Endocr Rev.* 2001 Apr;22(2):153–83.
147. Khokhlatchev A, Rabizadeh S, Xavier R, Nedwidek M, Chen T, Zhang X, et al. Identification of a novel Ras-regulated proapoptotic pathway. *Curr Biol CB.* 2002 Feb 19;12(4):253–65.
148. Avruch J, Praskova M, Ortiz-Vega S, Liu M, Zhang X-F. Nore1 and RASSF1 regulation of cell proliferation and of the MST1/2 kinases. *Methods Enzymol.* 2006;407:290–310.
149. Cox AD, Der CJ. The dark side of Ras: regulation of apoptosis. *Oncogene.* 2003 Dec 8;22(56):8999–9006.

150. Ries S, Biederer C, Woods D, Shifman O, Shirasawa S, Sasazuki T, et al. Opposing effects of Ras on p53: transcriptional activation of mdm2 and induction of p19ARF. *Cell*. 2000 Oct 13;103(2):321–30.
151. Sundaram M. RTK/Ras/MAPK signaling. WormBook [Internet]. 2006; Available from: http://www.wormbook.org/chapters/www_RTKRasMAPKsignaling/RTKRasMAPKsignaling.html
152. Han M, Sternberg PW. let-60, a gene that specifies cell fates during *C. elegans* vulval induction, encodes a ras protein. *Cell*. 1990 Nov 30;63(5):921–31.
153. Chamberlin HM, Sternberg PW. The lin-3/let-23 pathway mediates inductive signalling during male spicule development in *Caenorhabditis elegans*. *Dev Camb Engl*. 1994 Oct;120(10):2713–21.
154. Church DL, Guan KL, Lambie EJ. Three genes of the MAP kinase cascade, mek-2, mpk-1/sur-1 and let-60 ras, are required for meiotic cell cycle progression in *Caenorhabditis elegans*. *Dev Camb Engl*. 1995 Aug;121(8):2525–35.
155. Lopez-Illasaca M. Signaling from G-protein-coupled receptors to mitogen-activated protein (MAP)-kinase cascades. *Biochem Pharmacol*. 1998 Aug 1;56(3):269–77.
156. Takaesu G, Kang J-S, Bae G-U, Yi M-J, Lee CM, Reddy EP, et al. Activation of p38alpha/beta MAPK in myogenesis via binding of the scaffold protein JLP to the cell surface protein Cdo. *J Cell Biol*. 2006 Nov 6;175(3):383–8.
157. Gehart H, Kumpf S, Ittner A, Ricci R. MAPK signalling in cellular metabolism: stress or wellness? *EMBO Rep*. 2010 Nov;11(11):834–40.
158. Wada T, Penninger JM. Mitogen-activated protein kinases in apoptosis regulation. *Oncogene*. 2004 Apr 12;23(16):2838–49.
159. Capano M, Crompton M. Bax translocates to mitochondria of heart cells during simulated ischaemia: involvement of AMP-activated and p38 mitogen-activated protein kinases. *Biochem J*. 2006 Apr 1;395(1):57–64.
160. Markou T, Dowling AA, Kelly T, Lazou A. Regulation of Bcl-2 phosphorylation in response to oxidative stress in cardiac myocytes. *Free Radic Res*. 2009 Sep;43(9):809–16.
161. Bragado P, Armesilla A, Silva A, Porras A. Apoptosis by cisplatin requires p53 mediated p38alpha MAPK activation through ROS generation. *Apoptosis Int J Program Cell Death*. 2007 Sep;12(9):1733–42.
162. Porras A, Zuluaga S, Black E, Valladares A, Alvarez AM, Ambrosino C, et al. p38alpha Mitogen-activated Protein Kinase Sensitizes Cells to Apoptosis Induced by Different Stimuli. *Mol Biol Cell*. 2004 Feb;15(2):922–33.

163. Jha SK, Jha NK, Kar R, Ambasta RK, Kumar P. p38 MAPK and PI3K/AKT Signalling Cascades in Parkinson's Disease. *Int J Mol Cell Med*. 2015;4(2):67–86.
164. Gutiérrez-Uzquiza Á, Arechederra M, Bragado P, Aguirre-Ghiso JA, Porras A. p38 α Mediates Cell Survival in Response to Oxidative Stress via Induction of Antioxidant Genes EFFECT ON THE p70S6K PATHWAY. *J Biol Chem*. 2012 Jan 20;287(4):2632–42.
165. Okuyama T, Inoue H, Ookuma S, Satoh T, Kano K, Honjoh S, et al. The ERK-MAPK pathway regulates longevity through SKN-1 and insulin-like signaling in *Caenorhabditis elegans*. *J Biol Chem*. 2010 Sep 24;285(39):30274–81.
166. Andrusiak MG, Jin Y. Context Specificity of Stress-activated Mitogen-activated Protein (MAP) Kinase Signaling: The Story as Told by *Caenorhabditis elegans*. *J Biol Chem*. 2016 Apr 8;291(15):7796–804.
167. Bolz DD, Tenor JL, Aballay A. A Conserved PMK-1/p38 MAPK Is Required in *Caenorhabditis elegans* Tissue-specific Immune Response to *Yersinia pestis* Infection. *J Biol Chem*. 2010 Apr 2;285(14):10832–40.
168. Papp D, Csermely P, Söti C. A role for SKN-1/Nrf in pathogen resistance and immunosenescence in *Caenorhabditis elegans*. *PLoS Pathog*. 2012;8(4):e1002673.
169. Shivers RP, Pagano DJ, Kooistra T, Richardson CE, Reddy KC, Whitney JK, et al. Phosphorylation of the Conserved Transcription Factor ATF-7 by PMK-1 p38 MAPK Regulates Innate Immunity in *Caenorhabditis elegans*. *PLoS Genet* [Internet]. 2010 Apr 1;6(4). Available from: <http://www.ncbi.nlm.nih.gov/pmc/articles/PMC2848548/>
170. Cheesman HK, Feinbaum RL, Thekkiniath J, Downen RH, Conery AL, Pukkila-Worley R. Aberrant Activation of p38 MAP Kinase-Dependent Innate Immune Responses Is Toxic to *Caenorhabditis elegans*. *G3 GenesGenomesGenetics*. 2016 Jan 27;6(3):541–9.
171. Youngman MJ, Rogers ZN, Kim DH. A Decline in p38 MAPK Signaling Underlies Immunosenescence in *Caenorhabditis elegans*. *PLoS Genet* [Internet]. 2011 May 19;7(5). Available from: <http://www.ncbi.nlm.nih.gov/pmc/articles/PMC3098197/>
172. Pei B, Wang S, Guo X, Wang J, Yang G, Hang H, et al. Arsenite-induced germline apoptosis through a MAPK-dependent, p53-independent pathway in *Caenorhabditis elegans*. *Chem Res Toxicol*. 2008 Aug;21(8):1530–5.
173. Aballay A, Drenkard E, Hilbun LR, Ausubel FM. *Caenorhabditis elegans* innate immune response triggered by *Salmonella enterica* requires intact LPS and is mediated by a MAPK signaling pathway. *Curr Biol CB*. 2003 Jan 8;13(1):47–52.
174. van der Weyden L, Adams DJ. The Ras-association domain family (RASSF) members and their role in human tumorigenesis. *Biochim Biophys Acta*. 2007 Sep;1776(1):58–85.
175. Hers I, Vincent EE, Tavaré JM. Akt signalling in health and disease. *Cell Signal*. 2011 Oct;23(10):1515–27.

176. Newton AC, Trotman LC. Turning off AKT: PHLPP as a drug target. *Annu Rev Pharmacol Toxicol.* 2014;54:537–58.
177. Webb AE, Brunet A. FOXO flips the longevity SWitch. *Nat Cell Biol.* 2013 May;15(5):444–6.
178. Zhang X, Tang N, Hadden TJ, Rishi AK. Akt, FoxO and regulation of apoptosis. *Biochim Biophys Acta.* 2011 Nov;1813(11):1978–86.
179. Duronio V. The life of a cell: apoptosis regulation by the PI3K/PKB pathway. *Biochem J.* 2008 Nov 1;415(3):333–44.
180. Toker A, Marmiroli S. Signaling specificity in the Akt pathway in biology and disease. *Adv Biol Regul.* 2014 May;55:28–38.
181. Narasimhan SD, Mukhopadhyay A, Tissenbaum HA. InAKTivation of insulin/IGF-1 signaling by dephosphorylation. *Cell Cycle Georget Tex.* 2009 Dec;8(23):3878–84.
182. Gao T, Brognard J, Newton AC. The phosphatase PHLPP controls the cellular levels of protein kinase C. *J Biol Chem.* 2008 Mar 7;283(10):6300–11.
183. Brognard J, Sierecki E, Gao T, Newton AC. PHLPP and a second isoform, PHLPP2, differentially attenuate the amplitude of Akt signaling by regulating distinct Akt isoforms. *Mol Cell.* 2007 Mar 23;25(6):917–31.
184. Ogg S, Paradis S, Gottlieb S, Patterson GI, Lee L, Tissenbaum HA, et al. The Fork head transcription factor DAF-16 transduces insulin-like metabolic and longevity signals in *C. elegans*. *Nature.* 1997 Oct 30;389(6654):994–9.
185. Bansal A, Kwon E-S, Conte D, Liu H, Gilchrist MJ, MacNeil LT, et al. Transcriptional regulation of *Caenorhabditis elegans* FOXO/DAF-16 modulates lifespan. *Longev Heal.* 2014;3:5.
186. Paradis S, Ruvkun G. *Caenorhabditis elegans* Akt/PKB transduces insulin receptor-like signals from AGE-1 PI3 kinase to the DAF-16 transcription factor. *Genes Dev.* 1998 Aug 15;12(16):2488–98.
187. Paradis S, Ailion M, Toker A, Thomas JH, Ruvkun G. A PDK1 homolog is necessary and sufficient to transduce AGE-1 PI3 kinase signals that regulate diapause in *Caenorhabditis elegans*. *Genes Dev.* 1999 Jun 1;13(11):1438–52.
188. Hung WL, Wang Y, Chitturi J, Zhen M. A *Caenorhabditis elegans* developmental decision requires insulin signaling-mediated neuron-intestine communication. *Dev Camb Engl.* 2014 Apr;141(8):1767–79.
189. Tissenbaum HA, Ruvkun G. An insulin-like signaling pathway affects both longevity and reproduction in *Caenorhabditis elegans*. *Genetics.* 1998 Feb;148(2):703–17.

190. Hesp K, Smant G, Kammenga JE. *Caenorhabditis elegans* DAF-16/FOXO transcription factor and its mammalian homologs associate with age-related disease. *Exp Gerontol.* 2015 Dec;72:1–7.
191. Padmanabhan S, Mukhopadhyay A, Narasimhan SD, Tesz G, Czech MP, Tissenbaum HA. A PP2A regulatory subunit regulates *C. elegans* insulin/IGF-1 signaling by modulating AKT-1 phosphorylation. *Cell.* 2009 Mar 6;136(5):939–51.
192. Shaw R, Dillin A. PPTR-1 counteracts insulin signaling. *Cell.* 2009 Mar 6;136(5):816–8.
193. Padmanabhan S, Mukhopadhyay A, Narasimhan SD, Tesz G, Czech MP, Tissenbaum HA. A PP2A regulatory subunit PPTR-1 regulates the *C. elegans* Insulin/IGF-1 signaling pathway by modulating AKT-1 phosphorylation. *Cell.* 2009 Mar 6;136(5):939–51.
194. Mounsey A, Bauer P, Hope IA. Evidence suggesting that a fifth of annotated *Caenorhabditis elegans* genes may be pseudogenes. *Genome Res.* 2002 May;12(5):770–5.
195. Pinkston-Gosse J, Kenyon C. DAF-16/FOXO targets genes that regulate tumor growth in *Caenorhabditis elegans*. *Nat Genet.* 2007 Nov;39(11):1403–9.
196. Jensen VL, Gallo M, Riddle DL. Targets of DAF-16 involved in *Caenorhabditis elegans* adult longevity and dauer formation. *Exp Gerontol.* 2006 Oct;41(10):922–7.
197. Kenyon C, Chang J, Gensch E, Rudner A, Tabtiang R. A *C. elegans* mutant that lives twice as long as wild type. *Nature.* 1993 Dec 2;366(6454):461–4.
198. Dorman JB, Albinder B, Shroyer T, Kenyon C. The *age-1* and *daf-2* genes function in a common pathway to control the lifespan of *Caenorhabditis elegans*. *Genetics.* 1995 Dec;141(4):1399–406.
199. Liu T, Zimmerman KK, Patterson GI. Regulation of signaling genes by TGFbeta during entry into dauer diapause in *C. elegans*. *BMC Dev Biol.* 2004 Sep 20;4:11.
200. Gumienny TL, Savage-Dunn C. TGF- β signaling in *C. elegans*. *WormBook Online Rev C Elegans Biol.* 2013 Jul 10;1–34.
201. Pierce SB, Costa M, Wisotzkey R, Devadhar S, Homburger SA, Buchman AR, et al. Regulation of DAF-2 receptor signaling by human insulin and *ins-1*, a member of the unusually large and diverse *C. elegans* insulin gene family. *Genes Dev.* 2001 Mar 15;15(6):672–86.
202. Nakagawa A, Sullivan KD, Xue D. Caspase-activated phosphoinositide binding by CNT-1 promotes apoptosis by inhibiting the AKT pathway. *Nat Struct Mol Biol.* 2014 Dec;21(12):1082–90.
203. Sullivan KD, Nakagawa A, Xue D, Espinosa JM. Human ACAP2 is a homolog of *C. elegans* CNT-1 that promotes apoptosis in cancer cells. *Cell Cycle Georget Tex.* 2015;14(12):1771–8.

204. Wang S, Teng X, Wang Y, Yu H-Q, Luo X, Xu A, et al. Molecular control of arsenite-induced apoptosis in *Caenorhabditis elegans*: roles of insulin-like growth factor-1 signaling pathway. *Chemosphere*. 2014 Oct;112:248–55.
205. van Heemst D. Insulin, IGF-1 and longevity. *Aging Dis*. 2010;1(2):147–57.
206. Villeneuve NF, Tian W, Wu T, Sun Z, Lau A, Chapman E, et al. USP15 negatively regulates Nrf2 through deubiquitination of Keap1. *Mol Cell*. 2013 Jul 11;51(1):68–79.
207. Staab TA, Griffen TC, Corcoran C, Evgrafov O, Knowles JA, Sieburth D. The Conserved SKN-1/Nrf2 Stress Response Pathway Regulates Synaptic Function in *Caenorhabditis elegans*. *PLoS Genet* [Internet]. 2013 Mar 21;9(3). Available from: <http://www.ncbi.nlm.nih.gov/pmc/articles/PMC3605294/>
208. Kang HJ, Hong YB, Kim HJ, Wang A, Bae I. Bioactive food components prevent carcinogenic stress via Nrf2 activation in BRCA1 deficient breast epithelial cells. *Toxicol Lett*. 2012 Mar 7;209(2):154–60.
209. Gao Z, Sarsour EH, Kalen AL, Li L, Kumar MG, Goswami PC. Late ROS accumulation and radiosensitivity in SOD1-overexpressing human glioma cells. *Free Radic Biol Med*. 2008 Dec 1;45(11):1501–9.
210. Petkau A. Protection of bone marrow progenitor cells by superoxide dismutase. *Mol Cell Biochem*. 1988 Dec;84(2):133–40.
211. Kim SB, Pandita RK, Eskiocak U, Ly P, Kaisani A, Kumar R, et al. Targeting of Nrf2 induces DNA damage signaling and protects colonic epithelial cells from ionizing radiation. *Proc Natl Acad Sci U S A*. 2012 Oct 23;109(43):E2949-2955.
212. Gorrini C, Baniasadi PS, Harris IS, Silvester J, Inoue S, Snow B, et al. BRCA1 interacts with Nrf2 to regulate antioxidant signaling and cell survival. *J Exp Med*. 2013 Jul 29;210(8):1529–44.
213. Sekhar KR, Freeman ML. NRF2 promotes survival following exposure to ionizing radiation. *Free Radic Biol Med*. 2015 Nov;88(0 0):268–74.
214. Blackwell TK, Steinbaugh MJ, Hourihan JM, Ewald CY, Isik M. SKN-1/Nrf, stress responses, and aging in *Caenorhabditis elegans*. *Free Radic Biol Med*. 2015 Nov;88(Pt B):290–301.
215. Sykiotis GP, Bohmann D. Stress-activated cap'n'collar transcription factors in aging and human disease. *Sci Signal*. 2010 Mar 9;3(112):re3.
216. Choe KP, Przybysz AJ, Strange K. The WD40 repeat protein WDR-23 functions with the CUL4/DDB1 ubiquitin ligase to regulate nuclear abundance and activity of SKN-1 in *Caenorhabditis elegans*. *Mol Cell Biol*. 2009 May;29(10):2704–15.

217. Lin KT-H, Broitman-Maduro G, Hung WWK, Cervantes S, Maduro MF. Knockdown of SKN-1 and the Wnt effector TCF/POP-1 reveals differences in endomesoderm specification in *C. briggsae* as compared with *C. elegans*. *Dev Biol*. 2009 Jan 1;325(1):296–306.
218. Tullet JMA, Hertweck M, An JH, Baker J, Hwang JY, Liu S, et al. Direct inhibition of the longevity-promoting factor SKN-1 by insulin-like signaling in *C. elegans*. *Cell*. 2008 Mar 21;132(6):1025–38.
219. Page BD, Diede SJ, Tenlen JR, Ferguson EL. EEL-1, a Hect E3 ubiquitin ligase, controls asymmetry and persistence of the SKN-1 transcription factor in the early *C. elegans* embryo. *Dev Camb Engl*. 2007 Jun;134(12):2303–14.
220. Bowerman B, Draper BW, Mello CC, Priess JR. The maternal gene *skn-1* encodes a protein that is distributed unequally in early *C. elegans* embryos. *Cell*. 1993 Aug 13;74(3):443–52.

II. Chapter 2

1. Adamo A, Montemauri P, Silva N, Ward JD, Boulton SJ, La Volpe A. BRC-1 acts in the inter-sister pathway of meiotic double-strand break repair. *EMBO Rep.* 2008 Mar;9(3):287–92.
2. Koon JC, Kubiseski TJ. Developmental Arrest of *Caenorhabditis elegans* BRAP-2 Mutant Exposed to Oxidative Stress Is Dependent on BRC-1. *J Biol Chem.* 2010 Apr 30;285(18):13437–43.
3. Fuchs Y, Steller H. Programmed cell death in animal development and disease. *Cell.* 2011 Nov 11;147(4):742–58.
4. Gartner A, Boag, Peter, Blackwell TK. Germline survival and apoptosis. *WormBook.* 2008;1–20.
5. Jolliffe AK, Derry WB. The TP53 signaling network in mammals and worms. *Brief Funct Genomics.* 2013 Mar;12(2):129–41.
6. Ahmed S, Alpi A, Hengartner MO, Gartner A. *C. elegans* RAD-5/CLK-2 defines a new DNA damage checkpoint protein. *Curr Biol CB.* 2001 Dec 11;11(24):1934–44.
7. Harris J, Lowden M, Clejan I, Tzoneva M, Thomas JH, Hodgkin J, et al. Mutator phenotype of *Caenorhabditis elegans* DNA damage checkpoint mutants. *Genetics.* 2006 Oct;174(2):601–16.
8. Boulton SJ, Martin JS, Polanowska J, Hill DE, Gartner A, Vidal M. BRCA1/BARD1 Orthologs Required for DNA Repair in *Caenorhabditis elegans*. *Curr Biol.* 2004 Jan;14(1):33–9.
9. Chen C, Lewis RE, White MA. IMP modulates KSR1-dependent multivalent complex formation to specify ERK1/2 pathway activation and response thresholds. *J Biol Chem.* 2008 May 9;283(19):12789–96.
10. Li S, Ku C-Y, Farmer AA, Cong Y-S, Chen C-F, Lee W-H. Identification of a novel cytoplasmic protein that specifically binds to nuclear localization signal motifs. *J Biol Chem.* 1998;273(11):6183–6189.
11. Fatima S, Wagstaff KM, Loveland KL, Jans DA. Interactome of the negative regulator of nuclear import BRCA1-binding protein 2. *Sci Rep.* 2015 Mar 30;5:9459.
12. Gami MS, Iser WB, Hanselman KB, Wolkow CA. Activated AKT/PKB signaling in *C. elegans* uncouples temporally distinct outputs of DAF-2/insulin-like signaling. *BMC Dev Biol.* 2006 Oct 4;6:45.
13. Jensen VL, Simonsen KT, Lee Y-H, Park D, Riddle DL. RNAi screen of DAF-16/FOXO target genes in *C. elegans* links pathogenesis and dauer formation. *PloS One.* 2010 Dec 31;5(12):e15902.

14. Park S-K, Tedesco PM, Johnson TE. Oxidative stress and longevity in *Caenorhabditis elegans* as mediated by SKN-1. *Aging Cell*. 2009 Jun;8(3):258–69.
15. Hu Q, D’Amora DR, MacNeil LT, Walhout AJM, Kubiseski TJ. The Oxidative Stress Response in *Caenorhabditis elegans* Requires the GATA Transcription Factor ELT-3 and SKN-1/Nrf2. *Genetics*. 2017 Jun 9; doi: 10.1534/genetics.116.198788.
16. Brenner S. The genetics of *Caenorhabditis elegans*. *Genetics*. 1974 May;77(1):71–94.
17. Kelly KO, Dernburg AF, Stanfield GM, Villeneuve AM. *Caenorhabditis elegans* msh-5 is required for both normal and radiation-induced meiotic crossing over but not for completion of meiosis. *Genetics*. 2000 Oct;156(2):617–30.
18. Lant B, Derry WB. Methods for detection and analysis of apoptosis signaling in the *C. elegans* germline. *Methods San Diego Calif*. 2013 Jun 1;61(2):174–82.
19. Craig AL, Moser SC, Bailly AP, Gartner A. Methods for studying the DNA damage response in the *Caenorhabditis elegans* germ line. *Methods Cell Biol*. 2012;107:321–52.
20. Lawrence KS, Chau T, Engebrecht J. DNA damage response and spindle assembly checkpoint function throughout the cell cycle to ensure genomic integrity. *PLoS Genet*. 2015 Apr;11(4):e1005150.
21. Wang S, Teng X, Wang Y, Yu H-Q, Luo X, Xu A, et al. Molecular control of arsenite-induced apoptosis in *Caenorhabditis elegans*: roles of insulin-like growth factor-1 signaling pathway. *Chemosphere*. 2014 Oct;112:248–55.
22. Schafer JC, Winkelbauer ME, Williams CL, Haycraft CJ, Desmond RA, Yoder BK. IFTA-2 is a conserved cilia protein involved in pathways regulating longevity and dauer formation in *Caenorhabditis elegans*. *J Cell Sci*. 2006 Oct 1;119(19):4088–100.
23. Malone EA, Inoue T, Thomas JH. Genetic analysis of the roles of daf-28 and age-1 in regulating *Caenorhabditis elegans* dauer formation. *Genetics*. 1996 Jul;143(3):1193–205.
24. Yang J-S, Nam H-J, Seo M, Han SK, Choi Y, Nam HG, et al. OASIS: online application for the survival analysis of lifespan assays performed in aging research. *PloS One*. 2011;6(8):e23525.
25. Garcia-Muse T, Boulton SJ. Distinct modes of ATR activation after replication stress and DNA double-strand breaks in *Caenorhabditis elegans*. *EMBO J*. 2005 Dec 21;24(24):4345–55.
26. Ermolaeva MA, Segref A, Dakhovnik A, Ou H-L, Schneider JI, Utermöhlen O, et al. DNA damage in germ cells induces an innate immune response that triggers systemic stress resistance. *Nature*. 2013 Sep 19;501(7467):416–20.

27. Salinas LS, Maldonado E, Navarro RE. Stress-induced germ cell apoptosis by a p53 independent pathway in *Caenorhabditis elegans*. *Cell Death Differ*. 2006 Dec;13(12):2129–39.
28. Conradt B, Horvitz HR. The *C. elegans* protein EGL-1 is required for programmed cell death and interacts with the Bcl-2-like protein CED-9. *Cell*. 1998 May 15;93(4):519–29.
29. Schumacher B, Schertel C, Wittenburg N, Tuck S, Mitani S, Gartner A, et al. *C. elegans* ced-13 can promote apoptosis and is induced in response to DNA damage. *Cell Death Differ*. 2005 Feb;12(2):153–61.
30. Bailly A, Gartner A. Germ cell apoptosis and DNA damage responses. *Adv Exp Med Biol*. 2013;757:249–76.
31. Ross AJ, Li M, Yu B, Gao MX, Derry WB. The EEL-1 ubiquitin ligase promotes DNA damage-induced germ cell apoptosis in *C. elegans*. *Cell Death Differ*. 2011 Jul;18(7):1140–9.
32. Malin JZ, Shaham S. Cell Death in *C. elegans* Development. *Curr Top Dev Biol*. 2015;114:1–42.
33. An JH, Blackwell TK. SKN-1 links *C. elegans* mesendodermal specification to a conserved oxidative stress response. *Genes Dev*. 2003 Aug 1;17(15):1882–93.
34. Wang J, Robida-Stubbs S, Tullet JMA, Rual J-F, Vidal M, Blackwell TK. RNAi screening implicates a SKN-1-dependent transcriptional response in stress resistance and longevity deriving from translation inhibition. *PLoS Genet*. 2010 Aug 5;6(8).
35. Holmström KM, Kostov RV, Dinkova-Kostova AT. The multifaceted role of Nrf2 in mitochondrial function. *Curr Opin Toxicol*. 2016 Dec;1:80–91.
36. Inoue H, Hisamoto N, An JH, Oliveira RP, Nishida E, Blackwell TK, et al. The *C. elegans* p38 MAPK pathway regulates nuclear localization of the transcription factor SKN-1 in oxidative stress response. *Genes Dev*. 2005 Oct 1;19(19):2278–83.
37. Kell A, Ventura N, Kahn N, Johnson TE. Activation of SKN-1 by novel kinases in *Caenorhabditis elegans*. *Free Radic Biol Med*. 2007 Dec 1;43(11):1560–6.
38. Rutkowski R, Dickinson R, Stewart G, Craig A, Schimpl M, Keyse SM, et al. Regulation of *Caenorhabditis elegans* p53/CEP-1-dependent germ cell apoptosis by Ras/MAPK signaling. *PLoS Genet*. 2011 Aug;7(8):e1002238.
39. Pei B, Wang S, Guo X, Wang J, Yang G, Hang H, et al. Arsenite-induced germline apoptosis through a MAPK-dependent, p53-independent pathway in *Caenorhabditis elegans*. *Chem Res Toxicol*. 2008 Aug;21(8):1530–5.
40. Jakobsen H, Bojer MS, Marinus MG, Xu T, Struve C, Krogfelt KA, et al. The Alkaloid Compound Harmane Increases the Lifespan of *Caenorhabditis elegans* during Bacterial

Infection, by Modulating the Nematode's Innate Immune Response. PLoS ONE [Internet]. 2013 Mar 27;8(3). Available from: <http://www.ncbi.nlm.nih.gov/pmc/articles/PMC3609739/>

41. Shivers RP, Pagano DJ, Kooistra T, Richardson CE, Reddy KC, Whitney JK, et al. Phosphorylation of the Conserved Transcription Factor ATF-7 by PMK-1 p38 MAPK Regulates Innate Immunity in *Caenorhabditis elegans*. PLoS Genet [Internet]. 2010 Apr 1;6(4). Available from: <http://www.ncbi.nlm.nih.gov/pmc/articles/PMC2848548/>
42. JebaMercy G, Vigneshwari L, Balamurugan K. A MAP Kinase pathway in *Caenorhabditis elegans* is required for defense against infection by opportunistic *Proteus* species. *Microbes Infect*. 2013 Aug;15(8–9):550–68.
43. Head BP, Olaitan AO, Aballay A. Role of GATA transcription factor ELT-2 and p38 MAPK PMK-1 in recovery from acute *P. aeruginosa* infection in *C. elegans*. *Virulence*. 2016 Aug 11;8(3):261–74.
44. Toker A, Marmiroli S. Signaling specificity in the Akt pathway in biology and disease. *Adv Biol Regul*. 2014 May;55:28–38.
45. Newton AC, Trotman LC. Turning off AKT: PHLPP as a drug target. *Annu Rev Pharmacol Toxicol*. 2014;54:537–58.
46. Gao T, Furnari F, Newton AC. PHLPP: a phosphatase that directly dephosphorylates Akt, promotes apoptosis, and suppresses tumor growth. *Mol Cell*. 2005 Apr 1;18(1):13–24.
47. Grzechnik AT, Newton AC. PHLPPing through history: a decade in the life of PHLPP phosphatases. *Biochem Soc Trans*. 2016 Dec 15;44(6):1675–82.
48. Narasimhan SD, Mukhopadhyay A, Tissenbaum HA. InAKTivation of insulin/IGF-1 signaling by dephosphorylation. *Cell Cycle Georget Tex*. 2009 Dec;8(23):3878–84.
49. Jensen VL, Gallo M, Riddle DL. Targets of DAF-16 involved in *Caenorhabditis elegans* adult longevity and dauer formation. *Exp Gerontol*. 2006 Oct;41(10):922–7.
50. Hu PJ. Dauer. *Wormbook*. 2007 Aug 8;1–19.
51. Hesp K, Smant G, Kammenga JE. *Caenorhabditis elegans* DAF-16/FOXO transcription factor and its mammalian homologs associate with age-related disease. *Exp Gerontol*. 2015 Dec;72:1–7.
52. Zheng S, Liao S, Zou Y, Qu Z, Liu F. *ins-7* Gene expression is partially regulated by the DAF-16/IIS signaling pathway in *Caenorhabditis elegans* under celecoxib intervention. *PLoS One*. 2014;9(6):e100320.
53. Lu L, Zhao X, Zhang J, Li M, Qi Y, Zhou L. Calycosin promotes lifespan in *Caenorhabditis elegans* through insulin signaling pathway via *daf-16*, *age-1* and *daf-2*. *J Biosci Bioeng*. 2017 Apr 20;

54. Quevedo C, Kaplan DR, Derry WB. AKT-1 regulates DNA-damage-induced germline apoptosis in *C. elegans*. *Curr Biol CB*. 2007 Feb 6;17(3):286–92.
55. Perrin AJ, Gunda M, Yu B, Yen K, Ito S, Forster S, et al. Noncanonical control of *C. elegans* germline apoptosis by the insulin/IGF-1 and Ras/MAPK signaling pathways. *Cell Death Differ*. 2013 Jan;20(1):97–107.
56. Page BD, Diede SJ, Tenlen JR, Ferguson EL. EEL-1, a Hect E3 ubiquitin ligase, controls asymmetry and persistence of the SKN-1 transcription factor in the early *C. elegans* embryo. *Dev Camb Engl*. 2007 Jun;134(12):2303–14.
57. Geismann C, Arlt A, Sebens S, Schäfer H. Cytoprotection “gone astray”: Nrf2 and its role in cancer. *OncoTargets Ther*. 2014;7:1497–518.
58. Greiss S, Hall J, Ahmed S, Gartner A. *C. elegans* SIR-2.1 translocation is linked to a proapoptotic pathway parallel to cep-1/p53 during DNA damage-induced apoptosis. *Genes Dev*. 2008 Oct 15;22(20):2831–42.
59. Ito S, Greiss S, Gartner A, Derry WB. Cell-nonautonomous regulation of *C. elegans* germ cell death by kri-1. *Curr Biol CB*. 2010 Feb 23;20(4):333–8.
60. Bolz DD, Tenor JL, Aballay A. A Conserved PMK-1/p38 MAPK Is Required in *Caenorhabditis elegans* Tissue-specific Immune Response to *Yersinia pestis* Infection. *J Biol Chem*. 2010 Apr 2;285(14):10832–40.
61. Gao MX, Liao EH, Yu B, Wang Y, Zhen M, Derry WB. The SCF FSN-1 ubiquitin ligase controls germline apoptosis through CEP-1/p53 in *C. elegans*. *Cell Death Differ*. 2008 Jun;15(6):1054–62.
62. Savage KI, Harkin DP. BRCA1, a “complex” protein involved in the maintenance of genomic stability. *FEBS J*. 2015 Feb;282(4):630–46.

III. Chapter 3

1. Boulton SJ, Martin JS, Polanowska J, Hill DE, Gartner A, Vidal M. BRCA1/BARD1 Orthologs Required for DNA Repair in *Caenorhabditis elegans*. *Curr Biol*. 2004 Jan;14(1):33–9.
2. Chen J-S, Hu H-Y, Zhang S, He M, Hu R-M. Brap2 facilitates HsCdc14A Lys-63 linked ubiquitin modification. *Biotechnol Lett*. 2009 May;31(5):615–21.
3. Asada M, Ohmi K, Delia D, Enosawa S, Suzuki S, Yuo A, et al. Brap2 Functions as a Cytoplasmic Retention Protein for p21 during Monocyte Differentiation. *Mol Cell Biol*. 2004 Sep 15;24(18):8236–43.
4. Fatima S, Wagstaff KM, Loveland KL, Jans DA. Interactome of the negative regulator of nuclear import BRCA1-binding protein 2. *Sci Rep*. 2015 Mar 30;5:9459.
5. Corsi AK, Wightman B, Chalfie M. A Transparent Window into Biology: A Primer on *Caenorhabditis elegans*. *Genetics*. 2015 Jun;200(2):387–407.
6. Ahringer J. Reverse genetics. *WormBook* [Internet]. 2006; Available from: http://www.wormbook.org/chapters/www_introreversegenetics/introreversegenetics.html
7. Lui DY, Colaiácovo MP. Meiotic development in *Caenorhabditis elegans*. *Adv Exp Med Biol*. 2013;757:133–70.
8. Gartner A, Boag, Peter, Blackwell TK. Germline survival and apoptosis. *WormBook*. 2008;1–20.
9. Craig AL, Moser SC, Bailly AP, Gartner A. Methods for studying the DNA damage response in the *Caenorhabditis elegans* germ line. *Methods Cell Biol*. 2012;107:321–52.
10. Jang ER, Lee J-S. DNA Damage Response Mediated through BRCA1. *Cancer Res Treat*. 2004 Aug 31;36(4):214–21.
11. Adamo A, Montemauri P, Silva N, Ward JD, Boulton SJ, La Volpe A. BRC-1 acts in the inter-sister pathway of meiotic double-strand break repair. *EMBO Rep*. 2008 Mar;9(3):287–92.
12. Li S, Ku C-Y, Farmer AA, Cong Y-S, Chen C-F, Lee W-H. Identification of a novel cytoplasmic protein that specifically binds to nuclear localization signal motifs. *J Biol Chem*. 1998;273(11):6183–6189.
13. Davies RG, Wagstaff KM, McLaughlin EA, Loveland KL, Jans DA. The BRCA1-binding protein BRAP2 can act as a cytoplasmic retention factor for nuclear and nuclear envelope-localizing testicular proteins. *Biochim Biophys Acta BBA - Mol Cell Res*. 2013 Dec;1833(12):3436–44.

14. Chen C, Lewis RE, White MA. IMP modulates KSR1-dependent multivalent complex formation to specify ERK1/2 pathway activation and response thresholds. *J Biol Chem*. 2008 May 9;283(19):12789–96.
15. Matheny SA, Chen C, Kortum RL, Razidlo GL, Lewis RE, White MA. Ras regulates assembly of mitogenic signalling complexes through the effector protein IMP. *Nature*. 2004 Jan 15;427(6971):256–60.
16. Matheny SA, White MA. Ras-sensitive IMP modulation of the Raf/MEK/ERK cascade through KSR1. *Methods Enzymol*. 2006;407:237–47.
17. Koon JC, Kubiseski TJ. Developmental Arrest of *Caenorhabditis elegans* BRAP-2 Mutant Exposed to Oxidative Stress Is Dependent on BRC-1. *J Biol Chem*. 2010 Apr 30;285(18):13437–43.
18. Hu Q, D'Amora DR, MacNeil LT, Walhout AJM, Kubiseski TJ. The Oxidative Stress Response in *Caenorhabditis elegans* Requires the GATA Transcription Factor ELT-3 and SKN-1/Nrf2. *Genetics*. 2017 Jun 9; doi: 10.1534/genetics.116.198788.
19. Brenner S. The genetics of *Caenorhabditis elegans*. *Genetics*. 1974 May;77(1):71–94.
20. Lawrence KS, Chau T, Engebrecht J. DNA damage response and spindle assembly checkpoint function throughout the cell cycle to ensure genomic integrity. *PLoS Genet*. 2015 Apr;11(4):e1005150.
21. Dickinson DJ, Pani AM, Heppert JK, Higgins CD, Goldstein B. Streamlined Genome Engineering with a Self-Excising Drug Selection Cassette. *Genetics*. 2015 Aug;200(4):1035–49.
22. Ross AJ, Li M, Yu B, Gao MX, Derry WB. The EEL-1 ubiquitin ligase promotes DNA damage-induced germ cell apoptosis in *C. elegans*. *Cell Death Differ*. 2011 Jul;18(7):1140–9.
23. Hart A. Behavior. WormBook [Internet]. 2006; Available from: http://www.wormbook.org/chapters/www_behavior/behavior.html
24. Jensen VL, Gallo M, Riddle DL. Targets of DAF-16 involved in *Caenorhabditis elegans* adult longevity and dauer formation. *Exp Gerontol*. 2006 Oct;41(10):922–7.
25. Hu PJ. Dauer. Wormbook. 2007 Aug 8;1–19.
26. Kenyon C, Chang J, Gensch E, Rudner A, Tabtiang R. A *C. elegans* mutant that lives twice as long as wild type. *Nature*. 1993 Dec 2;366(6454):461–4.
27. Dorman JB, Albinder B, Shroyer T, Kenyon C. The age-1 and daf-2 genes function in a common pathway to control the lifespan of *Caenorhabditis elegans*. *Genetics*. 1995 Dec;141(4):1399–406.

28. An JH, Blackwell TK. SKN-1 links *C. elegans* mesendodermal specification to a conserved oxidative stress response. *Genes Dev.* 2003 Aug 1;17(15):1882–93.
29. Buck SH, Chiu D, Saito RM. The cyclin-dependent kinase inhibitors, *cki-1* and *cki-2*, act in overlapping but distinct pathways to control cell cycle quiescence during *C. elegans* development. *Cell Cycle Georget Tex.* 2009 Aug 15;8(16):2613–20.
30. van der Voet M, Lorson MA, Srinivasan DG, Bennett KL, van den Heuvel S. *C. elegans* mitotic cyclins have distinct as well as overlapping functions in chromosome segregation. *Cell Cycle Georget Tex.* 2009 Dec 15;8(24):4091–102.
31. Davies RG, Wagstaff KM, McLaughlin EA, Loveland KL, Jans DA. The BRCA1-binding protein BRAP2 can act as a cytoplasmic retention factor for nuclear and nuclear envelope-localizing testicular proteins. *Biochim Biophys Acta.* 2013 Dec;1833(12):3436–44.
32. Meneely PM, McGovern OL, Heinis FI, Yanowitz JL. Crossover distribution and frequency are regulated by *him-5* in *Caenorhabditis elegans*. *Genetics.* 2012 Apr;190(4):1251–66.
33. Doniach T. Activity of the Sex-Determining Gene *tra-2* Is Modulated to Allow Spermatogenesis in the *C. ELEGANS* Hermaphrodite. *Genetics.* 1986 Sep;114(1):53–76.
34. Emmons SW. Male development. *WormBook* [Internet]. 2005; Available from: http://www.wormbook.org/chapters/www_maleddevelopment/maleddevelopment.html
35. Okuyama T, Inoue H, Ookuma S, Satoh T, Kano K, Honjoh S, et al. The ERK-MAPK pathway regulates longevity through SKN-1 and insulin-like signaling in *Caenorhabditis elegans*. *J Biol Chem.* 2010 Sep 24;285(39):30274–81.
36. Qin Z, Hubbard EJA. Non-autonomous DAF-16/FOXO activity antagonizes age-related loss of *C. elegans* germline stem/progenitor cells. *Nat Commun* [Internet]. 2015 May 11;6. Available from: <http://www.ncbi.nlm.nih.gov/pmc/articles/PMC4432587/>
37. Lemmens BBLG, Johnson NM, Tijsterman M. COM-1 promotes homologous recombination during *Caenorhabditis elegans* meiosis by antagonizing Ku-mediated non-homologous end joining. *PLoS Genet.* 2013;9(2):e1003276.
38. Hsia MM, Callis J. BRIZ1 and BRIZ2 Proteins Form a Heteromeric E3 Ligase Complex Required for Seed Germination and Post-germination Growth in *Arabidopsis thaliana*. *J Biol Chem.* 2010 Nov 19;285(47):37070–81.
49. Gumienny TL, Savage-Dunn C. TGF- β signaling in *C. elegans*. *WormBook Online Rev C Elegans Biol.* 2013 Jul 10;1–34.
40. Maduzia LL, Gumienny TL, Zimmerman CM, Wang H, Shetgiri P, Krishna S, et al. *lon-1* regulates *Caenorhabditis elegans* body size downstream of the *dbl-1* TGF beta signaling pathway. *Dev Biol.* 2002 Jun 15;246(2):418–28.

41. Deng C-X. BRCA1: cell cycle checkpoint, genetic instability, DNA damage response and cancer evolution. *Nucleic Acids Res.* 2006;34(5):1416–26.
42. VanGompel MJW, Nguyen KCQ, Hall DH, Dauer WT, Rose LS. A novel function for the *Caenorhabditis elegans* torsin OOC-5 in nucleoporin localization and nuclear import. *Mol Biol Cell.* 2015 May 1;26(9):1752–63.

IV. Chapter 4

1. Li S, Ku C-Y, Farmer AA, Cong Y-S, Chen C-F, Lee W-H. Identification of a novel cytoplasmic protein that specifically binds to nuclear localization signal motifs. *J Biol Chem.* 1998;273(11):6183–6189.
2. Koon JC, Kubiseski TJ. Developmental Arrest of *Caenorhabditis elegans* BRAP-2 Mutant Exposed to Oxidative Stress Is Dependent on BRC-1. *J Biol Chem.* 2010 Apr 30;285(18):13437–43.
3. Hu Q, D'Amora DR, MacNeil LT, Walhout AJM, Kubiseski TJ. The Oxidative Stress Response in *Caenorhabditis elegans* Requires the GATA Transcription Factor ELT-3 and SKN-1/Nrf2. *Genetics.* 2017 Jun 9; doi: 10.1534/genetics.116.198788.
4. Blackwell TK, Steinbaugh MJ, Hourihan JM, Ewald CY, Isik M. SKN-1/Nrf, stress responses, and aging in *Caenorhabditis elegans*. *Free Radic Biol Med.* 2015 Nov;88(Pt B):290–301.
5. Rutkowski R, Dickinson R, Stewart G, Craig A, Schimpl M, Keyse SM, et al. Regulation of *Caenorhabditis elegans* p53/CEP-1-dependent germ cell apoptosis by Ras/MAPK signaling. *PLoS Genet.* 2011 Aug;7(8):e1002238.
6. Wang S, Teng X, Wang Y, Yu H-Q, Luo X, Xu A, et al. Molecular control of arsenite-induced apoptosis in *Caenorhabditis elegans*: roles of insulin-like growth factor-1 signaling pathway. *Chemosphere.* 2014 Oct;112:248–55.
7. Eberhard R, Stergiou L, Hofmann ER, Hofmann J, Haenni S, Teo Y, et al. Ribosome Synthesis and MAPK Activity Modulate Ionizing Radiation-Induced Germ Cell Apoptosis in *Caenorhabditis elegans*. *PLoS Genet* [Internet]. 2013 Nov 21;9(11). Available from: <http://www.ncbi.nlm.nih.gov/pmc/articles/PMC3836707/>
8. Davies RG, Wagstaff KM, McLaughlin EA, Loveland KL, Jans DA. The BRCA1-binding protein BRAP2 can act as a cytoplasmic retention factor for nuclear and nuclear envelope-localizing testicular proteins. *Biochim Biophys Acta BBA - Mol Cell Res.* 2013 Dec;1833(12):3436–44.
9. Fatima S, Wagstaff KM, Loveland KL, Jans DA. Interactome of the negative regulator of nuclear import BRCA1-binding protein 2. *Sci Rep.* 2015 Mar 30;5:9459.
10. Kim H-M, Colaiácovo MP. DNA Damage Sensitivity Assays in *Caenorhabditis elegans*. *Bio-Protoc* [Internet]. 2015;5(11). Available from: <http://www.ncbi.nlm.nih.gov/pmc/articles/PMC4723109/>
11. Pei B, Wang S, Guo X, Wang J, Yang G, Hang H, et al. Arsenite-induced germline apoptosis through a MAPK-dependent, p53-independent pathway in *Caenorhabditis elegans*. *Chem Res Toxicol.* 2008 Aug;21(8):1530–5.

12. He M, Zhou Z, Shah AA, Zou H, Tao J, Chen Q, et al. The emerging role of deubiquitinating enzymes in genomic integrity, diseases, and therapeutics. *Cell Biosci* [Internet]. 2016 Dec 20;6. Available from: <http://www.ncbi.nlm.nih.gov/pmc/articles/PMC5168870/>
13. Metzger MB, Pruneda JN, Klevit RE, Weissman AM. RING-type E3 ligases: Master manipulators of E2 ubiquitin-conjugating enzymes and ubiquitination. *Biochim Biophys Acta BBA - Mol Cell Res*. 2014 Jan;1843(1):47–60.
14. Kipreos E. Ubiquitin-mediated pathways in *C. elegans*. *WormBook* [Internet]. 2005; Available from: http://www.wormbook.org/chapters/www_ubiquitinpathways/ubiquitinpathways.html
15. Jensen VL, Gallo M, Riddle DL. Targets of DAF-16 involved in *Caenorhabditis elegans* adult longevity and dauer formation. *Exp Gerontol*. 2006 Oct;41(10):922–7.
16. Gumienny TL, Savage-Dunn C. TGF- β signaling in *C. elegans*. *WormBook Online Rev C Elegans Biol*. 2013 Jul 10;1–34.
17. Crittenden SL, Eckmann CR, Wang L, Bernstein DS, Wickens M, Kimble J. Regulation of the mitosis/meiosis decision in the *Caenorhabditis elegans* germline. *Philos Trans R Soc Lond B Biol Sci*. 2003 Aug 29;358(1436):1359–62.
18. Fonslow BR, Moresco JJ, Tu PG, Aalto AP, Pasquinelli AE, Dillin AG, et al. Mass spectrometry-based shotgun proteomic analysis of *C. elegans* protein complexes [Internet]. *WormBook*; 2005 [cited 2017 Jun 5]. Available from: <https://www.ncbi.nlm.nih.gov/books/NBK214455/>
19. Audhya A, Desai A. Proteomics in *Caenorhabditis elegans*. *Brief Funct Genomics*. 2008 May 1;7(3):205–10.
20. Zhang W, Xu J. DNA methyltransferases and their roles in tumorigenesis. *Biomark Res*. 2017;5:1.
21. Biegel JA, Busse TM, Weissman BE. SWI/SNF Chromatin Remodeling Complexes and Cancer. *Am J Med Genet C Semin Med Genet*. 2014 Sep;0(3):350–66.
22. Schott P, Singer SS, Kögler H, Neddermeier D, Leineweber K, Brodde O-E, et al. Pressure overload and neurohumoral activation differentially affect the myocardial proteome. *PROTEOMICS*. 2005 Apr;5(5):1372–81.
23. Imaizumi T, Ando M, Nakatochi M, Yasuda Y, Honda H, Kuwatsuka Y, et al. Effect of dietary energy and polymorphisms in BRAP and GHRL on obesity and metabolic traits. *Obes Res Clin Pract*. 2016 May 27;
24. Hsu P-C, Lin T-H, Su H-M, Juo S-HH, Lai W-T, Sheu S-H. Synergistic effect between BRAP polymorphism and diabetes on the extent of coronary atherosclerosis in the Chinese population. *Cardiology*. 2011;120(1):3–8.

25. Wu L, Xi B, Hou D, Zhao X, Liu J, Cheng H, et al. The single nucleotide polymorphisms in BRAP decrease the risk of metabolic syndrome in a Chinese young adult population. *Diab Vasc Dis Res*. 2013 May;10(3):202–7.
26. Hu X, Zhao Y, Wei L, Zhu B, Song D, Wang J, et al. CCDC178 promotes hepatocellular carcinoma metastasis through modulation of anoikis. *Oncogene*. 2017 Mar 20;
27. Deng C-X, Wang R-H. Roles of BRCA1 in DNA damage repair: a link between development and cancer. *Hum Mol Genet*. 2003 Apr 1;12 Spec No 1:R113-123.
28. Culetto E, Sattelle DB. A role for *Caenorhabditis elegans* in understanding the function and interactions of human disease genes. *Hum Mol Genet*. 2000 Apr 12;9(6):869–77.

Appendix

I. Loss of *hif-1* promotes resistance to the exogenous mitochondrial stressor ethidium bromide in *Caenorhabditis elegans*. BMC Cell Biol. 2016 Sep 13;17 Suppl 1:34. doi: 10.1186/s12860-016-0112-x.

Muntasir Kamal^{1,2}, Dayana R. D'Amora¹, and Terrance J. Kubiseski¹

1. Department of Biology, York University, Toronto, Ontario, Canada

2. Department of Molecular Genetics, University of Toronto, Toronto, Canada.

I contributed to this paper by performing qRT-PCR assays, ethidium bromide survival assays, worm culturing and preparation. I also edited the manuscript and final draft for publication.

II. The oxidative stress response in *C. elegans* requires the GATA transcription factor ELT-3 and SKN-1/Nrf2. Genetics. Jun 9 2017. doi: 10.1534/genetics.116.198788.

Queenie Hu^{1,2}, Dayana R. D'Amora¹, Lesley T. MacNeil³, Marian Walhout⁴ and Terrance J. Kubiseski¹

1. Department of Biology, York University, Toronto, Ontario, Canada
2. Sunnybrook Research Institute, Toronto, Ontario, Canada
3. Department of Biochemistry and Biomedical Sciences, Farncombe Family Digestive Health Research Institute, McMaster University, Hamilton, Ontario, Canada
4. Program in Systems Biology and Program in Molecular Medicine, University of Massachusetts Medical School, Worcester, MA

I contributed to this paper by performing worm lysates western blot, and whole worm antibody staining and quantification. I also edited the manuscript and final draft for publication.

Table 1: Worm strains used in this study. Strains were obtained from the *Caenorhabditis* Genetics Center (CGC), located at the University of Minnesota and the National Bioresource Project in Tokyo, Japan. Double mutant strains were generated using standard protocols and genotypes were verified using SW-PCR were applicable.

Strain	Genotype
CF1038	<i>daf-16(mu86) I</i>
CF1139	<i>daf-16(mu86) I</i> ; <i>muIs61</i>
DR466	<i>him-5(e1490) V</i>
DW102	<i>brc-1(tm1145) III</i>
KU25	<i>pmk-1(km25) IV</i>
MD701	<i>bcIs39 V [lim-7p::ced-1::GFP + lin-15(+)]</i>
PD9927	<i>ced-9(n2812) III/hT2 [bli-4(e937) let-?(q782) qIs48] (I;III); nIs106 X</i>
SD939	<i>mpk-1(gal11) unc-79(e1068) III</i>
VC204	<i>akt-2(ok393) X</i>
YF104	<i>brap-2(ok1492)/mIn 1 [MIs14dyp10 (e128)] II</i>
YF15	<i>brap-2(ok1492) II backcrossed 3X</i>
YF179	<i>brap-2(ok1492) II; ced-9(n2812) III/hT2 [bli-4(e937) let-?(q782) qIs48] (I;III); nIs106 X</i>
YF180	<i>brap-2(ok1492); bcIs39 [lim-7p::ced-1::GFP + lin-15(+)] V</i>
YF186	<i>akt-1(ok525) V; brap-2(ok1492) II</i>
YF188	<i>akt-2(ok393) X; brap-2(ok1492) I</i>
YF189	<i>brc-1(tm1145) III; daf-16(mu86) I</i>
YF19	<i>brap-2(ok1492) II; daf-16(mu86) I</i>
YF190	<i>brap-2(ok1492) II; daf-16(mu86) I; muIs61</i>
YF191	<i>brap-2(ok1492) II; phlp-2(tm7788) III</i>
YF192	<i>akt-1(ok525) V; phlp-2(tm7788) II</i>
YF193	<i>brc-1(tm1145) III; phlp-2 (tm7788) III</i>
YF195	<i>brap-2(ok1492) II; him-5(e1490) V</i>
YF197	<i>brap-2(ok1492) II; pmk-1(km25) IV</i>

YF198 *akt-1(ok525) V*
YF199 BRAP-2::GFP
YF200 *phlp-2(tm7788) III*
YF62 *cep-1(gk138) I*
YF63 *brap-2(ok1492) II; cep-1(gk138) I*
YF64 *brap-2(ok1492) II; brc-1(tm1145) III*
YF94 *brap-2(ok1492) II; mpk-1(ga111) unc-79(e1068) III*

Table 2: Forward and reverse primers for SW-PCR

Gene	Allele	Name	T_m (°C)	Sequence
<i>akt-1</i>	ok525	TK40	64.0	F: TATTGCTGACACCAGCGAAG
		TK41	63.6	R: TCGTTGTCTTCACTTGCTTCA
		TK42	63.8	F: ATTCGGATTTTCCCCAAGTC
<i>akt-2</i>	ok393	TK56	69.5	F: CGGCAGTACACAGAGTGTGAT
		TK57	70.1	R: CTCGTGTCCGTTTCAGACATCACAT
		TK58	63.8	F: GAGAGGGGTTATCACAACCTGAAG
<i>brap-2</i>	ok1492	olok14925	66.8	F: GTCAGCACCGAAAATGTGTCAG
		ok14923B	62.3	R: CAGACAACGTCGAATGATCTC
		ok14925	62.5	F: GAGTGTATTCGAGTTTGATTCCC
		ok1492N23	61.1	R: TTTGTTCTGCCTAGGAATAAGTG
<i>brc-1</i>	tm1145	<i>brc-1</i> N2For	65.0	F: AGAACCAGCCACAAAACAACC
		<i>brc-1</i> For	61.3	F: GTTCAATGCCCAATTTGTAGA
		<i>brc-1</i> Rev	60.3	R: CTAGTTTTTGGATTGGCTCAG
<i>cep-1</i>	gk138	<i>cep-1</i> For	70.0	F: GAAATTGTCCCGTTCCCGTGA
		<i>cep-1</i> N2 For	62.3	F: TAGGGGGTGGTGTAAAGAGAAA
		<i>cep-1</i> Rev	58.1	R: GTACAGCGACTTCTCTTCATC
<i>*daf-16</i>	mu86	MAM8	57.5	F: CTAGGAGGAAAAGCCATTTGT
		MAM9	59.5	F: CCAATAGCTGGAGAAACACGA
		MAM7	61.2	R: CGGTGACCATCTAGAGTCACA
<i>phlp-2</i>	tm7788	TK21	59.7	F: CTGTCCTCACTTCCCAAAC
		TK22	58.4	R: TCACCATAGGCACGCTTGTA
<i>pmk-1</i>	km25	pmk1N2For	60.3	F: CTGTTTGGTATGTCATTTCAACTG
		pmk1For	60.3	F: CAATCGATCTCAGATGTTCTTTTC
		pmk1Rev	58.4	R: CAGAATCAGTTTGACGTGCC

* Love et al.2010. PNAS Apr 20; 107(16):7413-8. doi: 10.1073/pnas.0911857107.

Table 3: Forward and reverse primers for qRT-PCR

Name	T_m (°C)	Sequence
<i>act-1</i>	63.9	F: GTCGGTATGGGACAGAAGGA
	64.1	R: GCTTCAGTGAGGAGGACTGG
<i>akt-1</i>	58.4	F: CCCGAAGATGCATTGGAGAT
	60.5	R: GCTTCTACTAGGCGGTGTCA
<i>ced-9</i>	64.0	F: AAATGATGGAATCCGTGGAA
	63.8	R: CCCACTTTTTTCAGCTTCTGC
<i>ced-13</i>	65.2	F: ACGGTGTTTGAGTTGCAAGC
	62.6	R: GTCGTACAAGCGTGATGGAT
<i>cki-1</i>	61.09	F: CCCAAGCTCTGCTGGATTCG
	60.53	R: GTTGGGATCCATCAGCGAGG
<i>cki-2</i>	63.7	F: ACCCGATCCAGAAGAGGTTT
	63.8	R: CTTCGGAAGCAGAAATCGAC
<i>ctl-1</i>	68.4	F: GTGTCGTTTCATGCCAAGGGA
	65.0	R: CCCAGTTACCCTCCTCGGTA
<i>cyb-1</i>	59.04	F: AAGAACTTCAAACAGGGGAAGC
	57.51	R: TTCCATTTCTGATGCGTCCA
<i>egl-1</i>	63.8	F: TCACCTTTGCCTCAACCTCT
	63.7	R: CATCGAAGTCATCGCACATT
<i>F08G5.6</i>	60.5	F: GTCCCACTGTCACAAGCTCA
	58.4	R: GTTTCGACCGAGAAATCGAG
<i>F35E12.6</i>	54.3	F: ACACAATCATTGCGATGGA
	58.4	R: GGTAGTCATTGGAGCCGAAA
<i>ins-7</i>	63.4	F: AGGTCCAGCAGAACCAGAAG
	64.2	R: GAAGTCGTCGGTGCATTCTT
<i>skn-1c</i>	66.6	F: TACTCACCGAGCATCCACCA
	66.8	R: TGATCAGCAGGAGCCACTTG

Table 4: Forward and reverse primers for cloning PHLP-2 into pCMV7.1 3xFLAG

Name	T_m (°C)	Sequence
<u>C-terminus</u>		
TK9	81.3	F:GGCCGCGAATTCATCGATAGATCTCAATTTAAGTT CAAACCGCCTGACAAG
PHLPP13xFLAG Rev	83.2	R:ACAGGGATGCCACCCGGGATCCTTAAATATTA GTAACCGTATTAGGAGGGCTCAA
<u>N-terminus</u>		
TK28	86.2	F:AGGATGACGATGACAAGCTTGCGGCCGCGATGGCT CCACTTGGCTACATAG
TK11	78.7	R:GCGGTTGAACTTAAATTGAGATCTTCCAGAAGCTC CAAAGAGCTG

Table 5: CRISPR-Cas9 primers used to generate BRAP-2::GFP strain

Name	T_m (°c)	Sequence
TK161	75.0	TTCAATTTTCTCGACGAGGGTTTTAGAGC TAGAAATAGCAAGT
<i>brap-2sgRNA</i>	53.0	TTCAATTTTCTCGACGAGG
<u>5'arm</u>		
TK2	94.0	AGTCACGACGTTGTAAAACGAGGCCAGTCGCCG GCAGGTGGAGACAAGCTTGAGGG
TK12	93.6	CATCGATGCTCCTGAGGCTCCCGATGCTCCCAAG GACTTTTTCTTCTTTCTGTTCAATTTTCTCGACGA TGATGACGACG
<u>3'arm</u>		
TK159	83.2	CGTGATTACAAGGATGACGATGACAAGAGATAA TTGGCATCTCAGGAGATCCATGTCC
TK160	79.5	GGAAACAGCTATGACCATGTTATCGATTTCAAA AATCGATAATCTTGGTTAGTGAGT

Table 6: Forward and reverse worm strain sequencing primers used in this study

Name	T_m (°C)	Sequence
<i>him-5</i>	58.3	F: ATGTCCAGAATTCGTTCTAATAAC
	72.1	R: GCGCGTTTTTTTTGGAATGCGGAATGACCAC
<i>mpk-1</i>	58.4	F: TCAATGCCTGATGGAGACTG
	58.4	R: TCTTGGATCAGCTCCTGGAT

Table 7: Antibodies and reagents for Western blot and immunostaining

Antibody	Company	Species	Dilution/Concentration
BRAP-2	Toronto Recombinant Antibody Centre	Rabbit	1:100
DAPI	Sigma	-	1 µg/mL
DAPI	VECTOR	-	1 µg/mL
FLAG-M2	Sigma	Mouse	1:5000
GAM HRP A555	Invitrogen	Mouse	1:1000
GAR HRP A488	Invitrogen	Rabbit	1:1000
GST	Cell Signal	Rabbit	1:5000
AKT-1 127/528	Gift from Dr. Brent Derry	Goat	1:1000
Phospho-p38 MAPK	Cell Signal	Rabbit	1:100 1:1000
RAD-51	Gift from Dr. Anton Gartner	Rabbit	1:100
Tubulin	Cell Signal	Mouse	1:2000

* Whole worm/gonad antibody staining